THÈSE

En vue de l'obtention du

DOCTORAT DE L'UNIVERSITÉ DE TOULOUSE

Délivré par :

Institut National Polytechnique de Toulouse (INP Toulouse)

Discipline ou spécialité :

Génie des Procédés et de l'Environnement

Présentée et soutenue par :

M. XINQIANG YOU

le lundi 7 septembre 2015

Titre :

APPROCHE THERMODYNAMIQUE POUR LA CONCEPTION ET L'OPTIMISATION DE LA DISTILLATION EXTRACTIVE DE MELANGES A TEMPERATURE DE BULLE MINIMALE (1.0-Ia)

Ecole doctorale :

Mécanique, Energétique, Génie civil, Procédés (MEGeP)

Unité de recherche :

Laboratoire de Génie Chimique (L.G.C.)

Directeur(s) de Thèse :

M. VINCENT GERBAUD

Rapporteurs :

M. JEAN-NOEL JAUBERT, INP DE NANCY

M. JEAN TOUTAIN, INP BORDEAUX

Membre(s) du jury :

Mme XUAN MI MEYER, INP TOULOUSE, Président

M. MICHEL MEYER, INP TOULOUSE, Membre

M. OLIVIER BAUDOIN, PROSIM SA, Membre

M. VINCENT GERBAUD, INP TOULOUSE, Membre

Title in English :

Thermodynamic Insight for the Design and Optimization of Extractive Distillation of 1.0-1a Class Separation

ABSTRACT

We study the continuous extractive distillation of minimum boiling azeotropic mixtures with a heavy entrainer (class 1.0-1a) for the acetone-methanol with water and DIPE-IPA with 2-methoxyethanol systems. The process includes both the extractive and the regeneration columns in open loop flowsheet and closed loop flowsheet where the solvent is recycled to the first column.

The first optimization strategy minimizes OF and seeks suitable values of the entrainer flowrate F_E, entrainer and azeotrope feed locations N_{FE}, N_{FAB}, N_{FReg}, reflux ratios R_1, R_2 and both distillates D_1, D_2. OF describes the energy demand at the reboiler and condenser in both columns per product flow rate. It accounts for the price differences in heating and cooling energy and in product sales. The second strategy relies upon the use of a multi-objective genetic algorithm that minimizes OF, total annualized cost (TAC) and maximizes two novel extractive thermodynamic efficiency indicators: total E_{ext} and per tray e_{ext}. They describe the ability of the extractive section to discriminate the product between the top and to bottom of the extractive section.

Thermodynamic insight from the analysis of the ternary RCM and isovolatility curves shows the benefit of lowering the operating pressure of the extractive column for 1.0-1a class separations. A lower pressure reduces the minimal amount of entrainer and increases the relative volatility of original azeotropic mixture for the composition in the distillation region where the extractive column operates, leading to the decrease of the minimal reflux ratio and energy consumption.

The first optimization strategy is conducted in four steps under distillation purity specifications: Aspen Plus or Prosim Plus simulator built-in SQP method is used for the optimization of the continuous variables: R_1, R_2 and F_E by minimizing OF in open loop flowsheet (step 1). Then, a sensitivity analysis is performed to find optimal values of D_1, D_2 (step 2) and N_{FE}, N_{FAB}, N_{FReg} (step 3), while step 1 is done for each set of discrete variables. Finally the design is simulated in closed loop flowsheet, and we calculate TAC and E_{ext} and e_{ext} (step 4). We also derive from mass balance the non-linear relationships between the two distillates and how they relate product purities and recoveries. The results show that double digit savings can be achieved over designs published in the literature thanks to the improving of E_{ext} and e_{ext}.

Then, we study the influence of the E_{ext} and e_{ext} on the optimal solution, and we run the second multiobjective optimization strategy. The genetic algorithm is usually not sensitive to initialization. It allows finding optimal total tray numbers N_1, N_2 values and is directly used with the closed loop flow sheet. Within Pareto front, the effects of main variables F_E/F and R_1 on TAC and E_{ext} are shown. There is a maximum E_{ext} (resp. minimum R_1) for a given R_1 (resp. E_{ext}). There exists an optimal efficiency indicator $E_{ext,opt}$ which corresponds to the optimal design with the lowest TAC. $E_{ext,opt}$ can be used as a complementary criterion for the evaluation of different designs. Through the analysis of extractive profile map, we explain why E_{ext} increases following the decrease of F_E and the increase of R_1 and we relate them to the tray numbers.

With the sake of further savings of TAC and increase of the environmental performance, double-effect heat integration (TEHI) and mechanical heat pump (MHP) techniques are studied. In TEHI, we propose a novel optimal partial HI process aiming at the most energy saving. In MHP, we propose the partial VRC and partial BF heat pump processes for which the coefficients of performance increase by 60% and 40%. Overall, optimal partial HI process is preferred from the economical view while full VRC is the choice from the environmental perspective.

Keywords

Extractive distillation, thermodynamic insight, reduced pressure, energy integration, multiobjective optimization, thermodynamic separation efficiency.

RÉSUMÉ

Nous étudions la distillation extractive continue de mélanges azéotropiques à temperature de bulle minimale avec un entraineur lourd (classe 1.0-1a) avec comme exemples les mélanges acétone-méthanol avec l'eau et DIPE-IPA avec le 2-méthoxyethanol. Le procédé inclut les colonnes de distillation extractive et de régénération de l'entraineur en boucle ouverte et en boucle fermée.

Une première stratégie d'optimisation consiste à minimiser la fonction objectif OF en cherchant les valeurs optimales du débit d'entraineur F_E, les positions des alimentations en entraineur et en mélange N_{FE}, N_{FAB}, N_{FReg}, les taux de reflux R_1, R_2 et les débits de distillat de chaque colonne D_1, D_2. OF décrit la demande en énergie par quantité de distillat et tient compte des différences de prix entre les utilités chaudes et froides et entre les deux produits. La deuxième stratégie est une optimisation multiobjectif qui minimise OF, le coût total annualisé (TAC) et maximise deux nouveaux indicateurs thermodynamiques d'efficacité de séparation extractive totale E_{ext} et par plateau e_{ext}. Ils décrivent la capacité de la section extractive à séparer le produit entre le haut et le bas de la section extractive.

L'analyse thermodynamique des réseaux de courbes de résidu ternaires RCM et des courbes d'isovolatilité montre l'intérêt de réduire la pression opératoire dans la colonne extractive pour les séparations de mélanges 1.0-1a. Une pression réduite diminue la quantité minimale d'entraineur et accroît la volatilité relative du mélange binaire azéotropique dans la région d'opération de la colonne extractive. Cela permet d'utiliser un taux de reflux plus faible et diminue la demande énergétique.

La première stratégie d'optimisation est conduite avec des contraintes sur la pureté des produits avec les algorithmes SQP dans les simulateurs Aspen Plus ou Prosim Plus en boucle ouverte. Les variables continues optimisées sont : R_1, R_2 et F_E (étape 1). Une étude de sensibilité permet de trouver les valeurs de D_1, D_2 (étape 2) et N_{FE}, N_{FAB}, N_{FReg} (étape 3), tandis l'étape 1 est faite pour chaque jeu de variables discrètes. Enfin le procédé est resimulé en boucle fermée et TAC, E_{ext} et e_{ext} sont calculés (étape 4). Les bilans matières expliquent l'interdépendance des débits de distillats et des puretés des produits. Cette optimisation permet de concevoir des procédés avec des gains proches de 20% en énergie et en coût. Les nouveaux procédés montrent une amélioration des indicateurs E_{ext} et e_{ext}.

Afin d'évaluer l'influence de E_{ext} et e_{ext} sur la solution optimale, la seconde optimisation multiobjectif est conduite. L'algorithme génétique est peu sensible à l'initialisation, permet d'optimiser les variables discrètes N_1, N_2 et utilise directement le shéma de procédé en boucle fermée. L'analyse du front de Pareto des solutions met en évidence l'effet de F_E/F et R_1 sur TAC et E_{ext}. Il existe un E_{ext} maximum (resp. R_1 minimum) pour un R_1 donné (resp. E_{ext}). Il existe aussi un indicateur optimal $E_{ext,opt}$ pour le procédé optimal avec le plus faible TAC. $E_{ext,opt}$ ne peut pas être utilisé comme seule fonction objectif d'optimisation mais en complément des autres fonctions OF et TAC. L'analyse des réseaux de profils de composition extractive explique la frontière du front de Pareto et pourquoi E_{ext} augmente lorsque F_E diminue et R_1 augmente, le tout en lien avec le nombre d'étage.

Visant à réduire encore TAC et la demande énergétique nous étudions des procédés avec intégration énergétique double effet (TEHI) ou avec des pompes à chaleur (MHP). En TEHI, un nouveau schéma avec une intégration énergétique partielle PHI réduit le plus la demande énergétique. En MHP, la recompression partielle des vapeurs VRC et bottom flash partiel BF améliorent les performances de 60% et 40% respectivement. Au final, le procédé PHI est le moins coûteux tandis que la recompression totale des vapeurs est la moins énergivore.

Mots clés

Distillation extractive, analyse thermodynamique, pression réduite, intégration énergétique, optimisation multiobjectif, indicateur thermodynamique d'efficacité de séparation.

ACKNOWLEDGMENTS

Firstly, let me give my deepest gratitude to my supervisor Mr. Vincent GERBAUD, for his constructive and illuminating guidances on my thesis. I deeply appreciate his high requirements and admire his great interest on research. His useful method, his wonderful personality, his high efficiency, his patience and persistence leave me the most profound impression. He is the perfect professor in my mind.

I should like to acknowledge the assistance and guidance given by Ms. Ivonne Rodriguez-Donis and Mr. Weifeng SHEN. Their helps and professional instructions are important for my research.

I am deeply indebted to prof. Jean-Noël JAUBERT, University of Lorraine, and prof. Jean TOUTAIN of Institut Polytechnique de Bordeaux. Both of them are reviewers of this thesis. I deeply thank them for spending time to give constructive suggestions and opinions, and kindly eliminate many of the errors in it, which are helpful and important for my thesis.

I really appreciate the presence of prof. Xuan MEYER, prof. Michel MEYER, and Dr. Olivier BAUDOUIN. All of them have graciously accepted to be a member of the jury. I would like to thank them for their constructive advices and important opinions for my thesis.

My gratitude also extends to my dear colleagues and friends: Philippe, René, Ségolène, Sofia, László, Antonio, Stephane, Ahmed, Jesus, Marco, Manuel, Maria, Anh and many others. I have passed a happy and wonderful life in Toulouse with all of them.

Last but importantly, my thanks would go to my family, especially to my wife for their supports during my study.

Xinqiang YOU

Le 08/09/2015 a Toulouse

CHAPTER CONTENTS

Title Page

Chapter 1. General Introduction 1

1. Introduction 2

1.1. Process feasibility 2

1.2. Process design and optimization 3

Chapter 2. State of The Art and Objectives 7

2. State of the art and objectives 8

2.1.1. Phase equilibrium model 8

2.1.2. Nonideality of mixture 9

2.2. Nonideal mixtures separation 10

2.2.1. Pressure-swing distillation 12

2.2.2. Azeotropic distillation 13

2.2.3. Reactive distillation 14

2.2.4. Generalized extractive distillation 15

2.2.4.1. Extractive distillation with solid salt or salt effect distillation 15

2.2.4.2. Extractive distillation with ionic liquid 16

2.2.4.3. Extractive distillation with low transition temperature mixtures (LTTMs) 17

2.2.4.4. Extractive distillation with hyperbranced polymers 17

2.2.4.5. Extractive distillation with pressurized carbon dioxide 17

2.3. Introduction of extractive distillation with liquid entrainer 18

2.3.1. Extractive distillation 18

2.3.2. Entrainer features 18

2.3.3. Relative volatility 19

2.3.4. Entrainer selectivity 20

2.3.5. Residue curve maps 21

2.3.6. Ternary VLE classification 22

2.4. Extractive distillation process feasibility 24
2.4.1. Thermodynamic insight on extractive distillation feasibility 24
2.4.1.1. Topological features of class 1.0-1a extractive distillation process 24
2.4.1.2. Product and limiting operating parameter for class 1.0-1a extractive distillation 26
2.4.1.3. Foregone feasibility research of our group 27
2.4.2. Feasibility assessed from intersection of composition profiles and differential equation 28
2.4.3. Extractive process feasibility from pinch points analysis 30
2.5. Research objectives 31
Chapter 3. Optimal Retrofits of ED, Acetone-Methanol with Water 33
3. Optimal retrofits of extractive distillation, acetone-methanol with water 34
3.1. Introduction 34
3.2. Optimal method and procedure 37
3.2.1. Extractive process feasibility 37
3.2.2. Optimal method 38
3.2.3. Extractive distillation process flow sheet 40
3.2.4. Objective function (OF) 41
3.2.5. Optimization procedure 42
3.3. Results and discussion 42
3.3.1. First step: continuous variables F_E, R_1, R_2 42
3.3.2. Second step: two distillates D_1 and D_2 43
3.3.3. Third step: three feed locations 43
3.3.4. Fourth step: closed loop corroboration 44
3.3.5. The final result and comparing with the design in literature 45
3.4. Conclusions 47
Chapter 4. Improved Design and Efficiency of Extractive Distillation 49
4. Improved design and efficiency of extractive distillation 50
4.1. Introduction 50
4.2. Back ground, methods and tools 50

4.2.1. Extractive process feasibility 50
4.2.2. Process optimization techniques 51
4.2.3. Objective function 52
4.3. Analysis of pressure and residue curve map 52
4.3.1. Pressure sensitivity of the azeotropic composition 52
4.3.2. Analysis of residue curve map 53
4.4. Optimization results 53
4.4.1. Continuous variables F_E, R_1, R_2 53
4.4.2. Distillates and three feed locations 54
4.4.3. Effect of entrainer purity on the process 55
4.4.4. Summary of optimal design parameters, product purity and recovery 56
4.5. Development of an extractive distillation process efficiency indicator 60
4.5.1. Extractive section efficiency 60
4.5.2. Comparison of efficiencies for extractive process design 60
4.6. Conclusions 63
Chapter 5. Design and Optimization of ED for separating DIPE-IPA 65
5. Design and Optimization of Extractive Distillation for Separating Diisopropyl ether and Isopropyl alcohol 66
5.1. Introduction 66
5.2. Steady state design 67
5.2.1. Extractive process feasibility 67
5.2.2. Pressure sensitivity of the azeotropic mixture 68
5.2.3. Analysis of residue curve map 69
5.2.4. Process optimization procedure 70
5.2.5. Objective function 70
5.3. Results and discussions 70
5.3.1. The relation of two distillate in extractive distillation 71
5.3.2. Choice of distillate flow rate for this chapter 72
5.3.3. Continuous variables F_E, R_1 and R_2 74
5.3.4. Selecting suitable feed locations 75

5.3.5. Closed loop design and optimal design parameters 76

5.3.6. Analysis from efficiency indicators and profile map in ternary diagram 79

5.4. Conclusions 80

Chapter 6. Influence of Thermodynamic Efficiency on Extractive Distillation 83

6. Influence of thermodynamic efficiency on extractive distillation acetone-methanol with water 84

6.1. Introduction 84

6.2. Optimal methods 84

6.2.1. Non-Sorted Genetic Algorithm as Process optimization technique 84

6.2.2. Advantages of NSGA for the design of extractive distillation process compared with SQP 85

6.2.3. Objective functions 85

6.3. Results and discussion 86

6.3.1. Problem setting 86

6.3.2. Pareto front of the optimal design solution 87

6.3.3. Insight on the Pareto front shape from the ternary map with extractive profile 89

6.3.4. Further improvement of GA optimal design 94

6.4. Results and discussion 98

Chapter 7. Reducing Process Cost and CO_2 Emissions 101

7. Reducing process cost and CO_2 emissions for extractive distillation by double-effect heat integration and mechanical heat pump 102

7.1. Introduction 102

7.2. Literature studies of extractive process with double-effect heat integration and heat pump 104

7.3. Evaluation method of heat pump performance and CO_2 emissions 107

7.3.1. Heat pump performance 107

7.3.2. Evaluation of CO_2 emissions for distillation column 108

7.3.3. Economic assessment 109

7.4. Extractive distillation with double-effect heat integration 109

7.4.1. Direct partial heat integration 109

7.4.2. Optimal partial heat integration 111

7.4.3. Optimal full heat integration 112
7.5. Extractive distillation with MHP heat pump 113
7.6. Evaluation of VRC heat pump assisted distillation process 114
7.6.1. VRC heat pump assisted extractive column 114
7.6.2. VRC heat pump assisted regeneration column 116
7.6.3. Full VRC heat pump process 117
7.6.4. Partial VRC heat pump process 118
7.7. Evaluation of BF heat pump assisted distillation process 119
7.7.1. BF heat pump assisted extractive column 119
7.7.2. BF heat pump assisted regeneration column 120
7.7.3. Full BF heat pump process 121
7.7.4. Partial BF heat pump process 122
7.7.5. Summary of mechanical heat pump 124
7.8. Comparison of OPHI and partial VRC 124
7.9. Conclusions 125
Chapter 8. Conclusions and perspectives 127
8. Conclusions and perspectives 128
8.1. Conclusions 128
8.2. Perspectives 131
Chapter 9. Appendix 133
9. Appendix 134
9.1. Cost data 134
9.2. Nomenclature 136
9.3. References 141

LIST OF TABLES

Table Page

Table 3.1 – Entrainer candidates for acetone-methanol separation with acetone as the distillate (from Kossack et al.,2008) ... 35

Table 3.2 – Entrainer candidates for acetone-methanol separation with methanol as the distillate (from Kossack et al.,2008) ... 35

Table 3.3 – Model binary parameters of acetone-methanol-water system ... 37

Table 3.4 – Experimental and predicted data of azeotropic point at 99.28 kPa ... 37

Table 3.5 – Step 1, optimal results of F_E, R_1 and R_2 ... 42

Table 3.6 – Optimal results of F_E, R_1, R_2, N_{FE}, N_{FF}, N_{FReg} under fixed D_1 and D_2 ... 44

Table 3.7 – Comparison of our optimal results with Luyben's design ... 45

Table 3.8 – Product purities from optimal results and Luyben's design ... 46

Table 4.1 – Acetone-methanol azeotropic temperature and composition at different pressures with UNIQUAC model ... 52

Table 4.2 – Optimized values of F_E, R_1 and R_2 for the extractive distillation of acetone – methanol with water under reduced pressure ... 54

Table 4.3 – Open loop optimal results of F_E, R_1, R_2, N_{FE}, N_{FAB}, N_{FReg} under fixed D_1 and D_2 for the extractive distillation of acetone – methanol with water ... 55

Table 4.4 – Optimal design parameters and cost data from closed loop simulation for the extractive distillation of acetone – methanol with water ... 56

Table 4.5 – Sizing parameters for the optimal designed columns and cost data from closed loop simulation for the extractive distillation of acetone – methanol with water ... 57

Table 4.6 – Product purities and recoveries for case 1, 2 and 3op designs ... 58

Table 4.7 – Efficiencies of per tray and total extractive section for the extractive distillation of acetone – methanol with water ... 60

Table 5.1 – DIPE-IPA azeotropic temperature and composition at different pressures with NRTL model ... 68

Table 5.2 – Relationship of distillates, purity and recovery for binary mixture for 100kmol/h binary mixture ... 72

Table 5.3 – Relationship of distillates, purity and recovery for DIEP-IPA 73

Table 5.4 – Optimized values of F_E, R_1, and R_2 for the extractive distillation of DIPE – IPA with 2-methoxyethanol 74

Table 5.5 – Open loop optimal results of F_E, R_1, R_2, N_{FE}, N_{FAB}, N_{FReg} under fixed D_1 and D_2 for the extractive distillation of DIPE – IPA with 2-methoxyethanol, P_1 = 0.4 atm and P_2 = 1 atm 75

Table 5.6 – Optimal design parameters and cost data from closed loop simulation for the extractive distillation of DIPE-IPA with 2-methoxyethanol 77

Table 5.7 – Product purities and recoveries for case Luo, case 1 and 2 designs 78

Table 5.8 – Efficiencies of per tray and total extractive section for the extractive distillation of DIPE – IPA with 2-methoxyethanol 80

Table 6.1 – Design parameters for G1-G6 belonging to the Pareto front, P_1 = 0.6 atm, P_2 = 1 atm 92

Table 6.2 – Sizing parameters for the columns and cost data of the design G1-G6 belonging to Pareto front 93

Table 6.3 – Final design results for acetone-methanol-water by NSGA and SQP 95

Table 6.4 – Sizing parameters for the columns and cost data of the design case 1, case G1 and case SQP 96

Table 6.5 – Product purities and recoveries for case NSGA and SQP designs 96

Table 7.1 – Temperature difference, TAC and OF2 of reboiler/condenser heat exchanger following P_2 .. 110

Table 7.2 – Design parameters of three double-effect heat integration extractive distillation processes, acetone-methanol with water 112

Table 7.3 – Sizing parameters and cost data of three double-effect heat integration extractive distillation processes, acetone-methanol with water 112

Table 7.4 – Cost data for extractive column with heat pump at different compressor outlet pressure 114

Table 7.5 – Comparison of extractive column with and without VRC heat pump 115

Table 7.6 – Cost data for extractive column with heat pump at different compressor outlet pressure 116

Table 7.7 – Comparison of regeneration column with and without heat pump 117

Table 7.8 – Cost data of the process without heat pump, full and partial VRC heat pump 118

Table 7.9 – Cost data for extractive column with BF heat pump at different throttle valve outlet pressure 120

Table 7.10 – Comparison of extractive column with and without BF heat pump 120

Table 7.11 – Cost data for regeneration column with BF heat pump at different throttle valve outlet pressure 121

Table 7.12 – Comparison of regeneration column with and without BF heat pump 121

Table 7.13 – Cost data of the process without heat pump, partial and full BF heat pump 123

Table 7.14 – Comparison of optimal partial HI, partial VRC processes 125

LIST OF FIGURES

Figure Page

Figure 1.1 – Onion model for energy efficiency improvement. 4

Figure 2.1 – Typical homogeneous mixtures with maximum boiling azeotrope water and formic acid, a negative deviation from Raoult's law 9

Figure 2.2 – Typical homogeneous mixtures with minimum boiling azeotrope methanol and chloroform, a positive deviation from Raoult's law 10

Figure 2.3 – Schematic diagram of various techniques for separation of azeotropic mixtures 11

Figure 2.4 – Indirect separation (a) and direct (b) azeotropic continuous distillation under finite for a 1.0-2 class mixture (from Gerbaud and Rodriguez-Donis, 2010) 14

Figure 2.5 – Azeotropic ternary mixture: Serafimov's 26 topological classes and Reshetov's statistics (Hilmen et al., 2002). (o) unstable node, (Δ) saddle, (●) stable 23

Figure 2.6 – Topological features of class 1.0-1a with heavy entrainer in extractive distillation process operation (adapted from Rodriguez-Donis et al., 2009a). 25

Figure 2.7 – Thermodynamic features of 1.0–1a mixtures. Separation of a minimum boiling azeotrope with a heavy entrainer. (adapted from Shen et al., 2012) 27

Figure 2.8 – Extractive distillation of acetone-methanol with water (1.0-1a class). Feed ratio as a function of the reflux ratio to recover 98% mol acetone. (adapted from Shen et al., 2012) 28

Figure 3.1 – T-xy and y-x experimentand predicted maps at 1 atm for acetone (A)-methanol (B)-water (E) system 36

Figure 3.2 – Extractive distillation column configuration and acetone – methanol – water 1.0-1a residue curve map at 1 atm with univolatility curves at 1 atm 38

Figure 3.3 – Closed loop (a) and open loop (b) flow sheet of the extractive distillation process 40

Figure 3.4 – Effects of D_1 and D_2 on OF with D_1, D_2, F_E, R_1 and R_2 as variables 43

Figure 3.5 – Temperature and composition profiles of extractive column for acetone – methanol with water (adapted from Luyben 2008) 45

Figure 3.6 – Our design: Temperature and composition profiles of extractive column for acetone – methanol with water 46

Figure 4.1 – Extractive distillation column configuration and acetone – methanol – water 1.0-1a residue curve map at 1 atm with univolatility curves at 0.6 and 1 atm 51

Figure 4.2 – Temperature and composition profiles of case 3opt extractive column for the extractive distillation of acetone – methanol with water..... 57

Figure 4.3 – Temperature and composition profiles of case 3opt regeneration column for the extractive distillation of acetone – methanol with water..... 58

Figure 4.4 – Liquid composition profiles for case 1(1atm),case 2(1atm) and 3(0.6atm) extractive distillation column designs for the extractive distillation of acetone – methanol with water 61

Figure 4.5 – Volatility profile of acetone vs methanol along the extractive column for the extractive distillation of acetone – methanol with water, case 1(1atm),case 2(1atm) and 3(0.6atm) 61

Figure 5.1 – Extractive distillation column configuration and DIPE – IPA –2-methoxyethanol class 1.0-1a residue curve map at 1atm with isovolatility curves at 0.4 and 1 atm. 68

Figure 5.2 – T-xy map of 2-methoxyethanol – DIPE 70

Figure 5.3 – Effects of D_1 and D_2 on OF with D_1, D_2, F_E, R_1 and R_2 as variables 73

Figure 5.4 – Temperature and composition profiles of case 2 extractive column for the extractive distillation of DIPE-IPA with 2-methoxyethanol 78

Figure 5.5 – Temperature and composition profiles of case 2 entrainer regeneration column for the extractive distillation of DIPE-IPA with 2-methoxyethanol 79

Figure 5.6 – Liquid composition profiles for case Luo (1atm), case 1(1atm) and case 2(0.4atm) extractive distillation column designs for the extractive distillation of DIPE-IPA with 2-methoxyethanol 80

Figure 6.7 – Pareto front of extractive distillation for acetone-methanol-water system, TAC versus E_{ext} and R_1, △ means G1 87

Figure 6.8 – Pareto front of extractive distillation for acetone-methanol-water system, E_{ext} versus R_1 and F_E, △ means G1..... 88

Figure 6.9 – Pareto front of extractive distillation for acetone-methanol-water system, TAC versus R_1 and F_E, △ means G1..... 89

Figure 6.10 – Relation map of E_{ext} and TAC for some designs from Pareto front 90

Figure 6.11 – Extractive section profile map for acetone-methanol-water, case G3 90

Figure 6.12 – Extractive section profile map for acetone-methanol-water, case G1 94

Figure 6.13 – Temperature and composition profiles of extractive column for the extractive distillation of acetone – methanol with water, case SQP 97

Figure 6.14 – Temperature and composition profiles of entrainer regeneration column for the extractive distillation of acetone – methanol with water, case SQP 98

Figure 7.1 – Mechanical heat pump flow sheet for extractive column (a) vapor compression (VC) (b) vapor recompression (VRC) (c) bottom flash (BF). 103

Figure 7.2 – Sketch for heat integration process 105

Figure 7.3 – Extractive distillation of acetone-methanol with water, case SQP in chapter 6 as base case . 106

Figure 7.4 – Effect of P_2 on TAC and OF2, the performance of direct partial heat integration process..... 110

Figure 7.5 – Relative volatility of methanol over water at different pressure 111

Figure 7.6 – Partial VRC heat pump for extractive distillation process. 114

Figure 7.7 – Total annual cost of extractive column following payback period with and without heat pump technique 116

Figure 7.8 – Total annual cost of regeneration column following payback period with and without heat pump technique 117

Figure 7.9 – Total annual cost of basic case, full and partial VRC heat pump processes following payback period..... 119

Figure 7.10 – Partial BF heat pump for extractive distillation process 122

Figure 7.11 – Total annual cost of basic case, full and partial BF heat pump processes following payback period..... 123

Figure 7.12 – Total annual cost of optimal partial HI and partial VRC process following payback period 124

Chapter 1. General Introduction

1.Introduction

Distillation is the most practical and hence the most widely used fluid mixture separation technology in many chemical and other industry fields like perfumery, medicinal and food processing (Olujić et al., 2009). The first clear evidence of distillation can be dated back to the first century AD. Being the leading process for the purification of liquid mixtures, distillation consumes large amounts of energy that are estimated to be more than 95% of the total energy used for separation processes in chemical process industries (Mahdi et al., 2015). Azeotropic and low relative volatility mixtures often occur in separating industry which separation cannot be realized by conventional distillation. Extractive distillation is then a suitable alternative process. Extractive distillation has been studied for many decades with rich literatures, some main subjects studied include: column with all possible configurations; process operation polices and strategy; process design, synthesis, optimization; determining separation sequencing; entrainer design and selection, feasibility studies and so on. Among those, process feasibility and process design and optimization are always the critical issues. It is necessary to assess process feasibility before making the design specifications, and the feasibility studies also contribute to a better understanding of complex unit operations. In the other view, process design and optimization which are more practical for industries are not only the aims of process feasibility studies, but also tools for the validation of process feasibility.

1.1.Process feasibility

Upon the feasibility study, the design of extractive distillation is connected to thermodynamics, in particular the volatility order. The residue curve maps analysis allows assessing the feasibility under infinite reflux conditions with the finding of the ultimate products under direct or indirect split conditions. However, under finite reflux conditions, finding which products are achievable and the location of the suitable feed composition region is more complicated because we must consider the dependency of composition profile on reflux and entrainer-to-feed ratio. That affects the range of composition available to each section profiles due to the occurrence of pinch points, which differ from the singular points of the residue curve map. The identification of possible cut under key parameters reflux, reboil ratio and entrainer flowrate has been the main challenge for an efficient separation of azeotropic mixtures.

For decades, the design of an extractive distillation process has relied upon a simple feasibility rule (Levy and Doherty, 1986; Andersen et al., 1991; Laroche et al., 1992): for the separation of a minimum (maximum) boiling azeotropic mixture A-B, one should add a heavy entrainer E that forms no new azeotrope. The corresponding ternary mixture A-B-E belongs to the (1.0-1a) class (Hilmen et al., 2002), which occurrence among all azeotropic ternary mixtures amounts to 21.6% (Kiva et al., 2003). Rodríguez-Donis et al., (2001) combined the knowledge of the thermodynamic properties of residue curve map and uni-volatility line, and expressed a general feasibility criterion for extractive distillation under infinite reflux. Residue curve maps

and uni-volatility line analysis allows assessing the feasibility under infinite reflux conditions and the finding of the ultimate products which is related to column configuration (direct or indirect split). Besides, isovolatility lines reflect the easiness of proposed separation system, especially for the regeneration column. However, distillation runs under finite reflux conditions and finding which products are achievable and the location of the suitable feed composition region is more complicated because we must consider the dependency of composition profiles on reflux as well as on entrainer flowrate (Lelkes et al., 1998a). Following the general feasibility criterion for extractive distillation, the use of heavy, light or intermediate boiling entrainers for the separation of minimum or maximum boiling azeotropic mixtures or of low relative volatility mixtures are feasible (Rodriguez-Donis et al., 2009a, 2009b, 2012a, 2012b). The total occurrence of suitable ternary mixtures classes for homogeneous extractive distillation reaches 53% in batch operation mode and can be extended to continuous operation as well (Shen et al., 2013; Shen and Gerbaud, 2013). The position of the uni-volatility curve in the residue curve map defines the product to be withdrawn as was first proposed by Laroche et al.,(1991). It also hints at the occurrence of limiting entrainer flow rate or the separation to be effective.

1.2. Process design and optimization

Upon the process design and optimization, following the definition of Figueirêdo et al. (2011), a well-designed extractive process means obtaining the lowest specific energy consumption and the least loss of solvent, taking into consideration the constraints imposed on the process. In the other hand, as global energy consumption continues to increase, global climate change has recently begun to affect human life. Many comprehensive energy reduction programs are being pursued to reduce energy usage and promote sustainable development for the near future (Gao et al., 2013). Studies on how to save energy cost during distillation operation is in urgent because distillation processes represent approximately 3% of the world energy consumption (Engelien and Skogestad, 2004) and it is ranked in a third of the total used energy in chemical industry (Linnhoff et al., 1983).

A systematic approach in saving energy consumption and improving the energy efficiency of industrial processes is the onion-model developed in industrial heat technology (Bruinsma and Spoelstra, 2010). The model is visualized in Figure 1.1.

In the first shell, the processes itself are optimized with respect to energy consumption and capital cost. It is done by an economic optimization in which energy and other operating cost are balanced with annualized investment cost for the equipments. In extractive distillation, the process means that both-columns are optimized with variables by minimizing the energy cost and total annual cost.

In the second shell, energy consumption can be saved further by heat integration using heat exchanger (HEX). There is a limitation for using heat integration technique because a temperature driving force is needed for heat exchangers. Preheating the feed stream by using the bottom stream is the basic heat

integration in stand-alone distillation columns. Further energy savings can be realized between condensers and reboilers of different distillation columns and applying side reboilers.

A great further reduction of energy consumption can be achieved in the third shell: the heat pump technique. Heat pump is a device that upgrades heat from a lower temperature source to a higher temperature. Interest to use heat pumps also for heating purposes increased with global awareness of the limited availability of fossil fuels in combination with the greenhouse effect. Vapor recompression (VRC) mechanical heat pump is the most studied heat pump technique.

In the last shell, the process utilities are also an aspect for saving energy cost. For extractive distillation, the entrainer is usually high boiling temperature, which means high pressure steam is needed for vaporizing the bottom liquid.

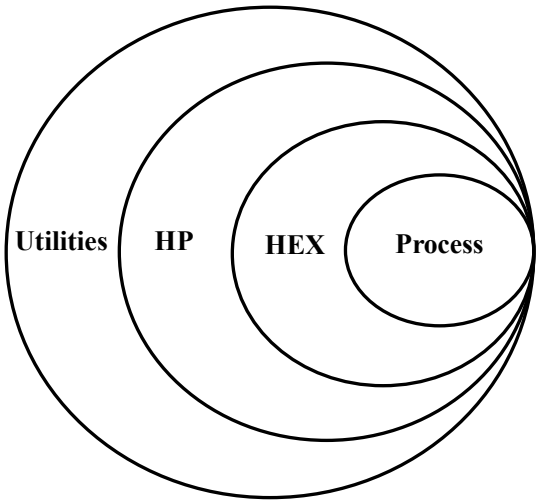

Figure 1.1 – Onion model for energy efficiency improvement.

The presentation of this work focuses on the following chapters:

Chapter 2 is a literature review to present the state of the art on the extractive distillation. This chapter introduces several issues related to our thesis: phase equilibrium, possible method to separate nonideal mixtures, the state of art on extractive distillation, entrainer selection, process feasibility. The objective and organization of the thesis are shown at the end of this chapter.

In chapter 3, we show the four steps procedure for the simultaneous optimization of the extractive column and entrainer regeneration column by using sensitivity analysis and Sequential quadratic programming (SQP) method built in Aspen plus software, and the results are verified with Prosim plus software. The procedure should be carried out based on good initial design from literature. The objective function OF (the energy consumption per product flow rate) is proposed and minimized under the constraints of product purity and recovery, and recycling entrainer purity. Given fixed two columns tray numbers, the process is optimized in

open loop flowsheet and process variables are reflux ratios and distillates of the two columns, three feed locations and the entrainer flowrate (It reflects entrainer-to-feed flowrate ratio). The effects of operating variables in the regeneration column on the extractive column and the total process are firstly qualified during optimization process. Then, the closed loop flowsheet is simulated with the variables got from the open loop flowsheet in order to make sure that the effect of impurity of recycling entrainer on the process is overcome. Total annual cost (TAC) for the process is calculated and worked as a complementary criterion for comparing different designs. A trade-off between the two columns variables is found and optimal parameters with lower energy consumption and TAC than literature results are found. The case study is provided with the extractive distillation separation of acetone-methanol with entrainer water (class 1.0-1a). Notice that the optimization procedure can treat the designs with different column tray number following TAC, but we keep the same column tray numbers as literatures for comparison in chapter 3, 4 and 5. Then we take them into account as variables in chapter 6 by using the genetic algorithm method.

In chapter 4, we show how thermodynamic insight can be used to improve the design of a homogeneous extractive distillation process and we define an extractive efficiency indicator to compare the optimality of different designs. Thermodynamic insight from the analysis of the ternary residue curve map and isovolatility curves shows that a lower pressure reduces the minimal amount of entrainer and increases the relative volatility of acetone – methanol in the extractive column. A 0.6 atm pressure is selected to enable the use of cheap cooling water in the condenser. The four steps procedure shown in Chapter 3 is used by minimizing the total energy consumption per product unit. The TAC is calculated for all processes. Double digit savings in energy consumption and in TAC are achieved compared to literature values. We then propose a novel efficiency indicator E_{ext} and e_{ext} that describes the ability per tray of the extractive section to discriminate the desired product between the top and the bottom of the extractive section. Shifting the feed trays locations improves the efficiency of the separation, even when less entrainer is used.

In chapter 5, in order to further demonstrate the effects of thermodynamic insight and extractive efficiency indicators on the homogeneous extractive distillation process itself, we show the optimization process of the separation of the diisopropyl ether (DIPE) – isopropyl alcohol (IPA) minimum boiling azeotrope with heavy entrainer 2-methoxyethanol aiming at finding the possible way to save energy cost and TAC. The four steps procedure and the thermodynamic insight from the analysis of the ternary residue curve map and isovolatility curves shows again that a lower pressure reduces the usage of entrainer and increases the relative volatility of DIPE – IPA for the same entrainer content in the extractive column. A 0.4 atm pressure is selected to enable the use of cheap cooling water in the condenser. We pay attention to explain the relationship of two distillates in extractive distillation process and the curious behaviors that the energy cost OF decreases following the increase of the distillate flowrate. Double digit savings in energy consumption have achieved while TAC is reduced. The efficiency indicator of extractive section is calculated for comparison and explanation of the energy savings.

In chapter 6, we consider thermodynamic efficiency indicator E_{ext} and e_{ext} for optimizing the extractive distillation in addition to energy cost OF and TAC. A two step optimization strategy for extractive distillation is conducted to find suitable values of the entrainer feed flowrate, entrainer feed and azeotropic mixture feed locations, total number of trays, reflux ratio, heat duty and condenser duty in both the extractive column and the entrainer regeneration column. The first strategy relies upon the use of a multi-objective genetic algorithm (GA) with four objective functions: OF, TAC, E_{ext} and e_{ext}. Secondly, results taken from the GA Pareto front are further optimized focusing on decreasing the energy cost by using the four steps procedure shown in chapter 3 with only OF as objective function. In this way, the most suitable design with relatively high efficiency and low cost are obtained. The final design is related to the thermodynamic insight and help understanding the process behaviors. We find that there is a maximum E_{ext} at given reflux ratio, and there is minimum reflux ratio for a given E_{ext}. There is an optimal efficiency indicator $E_{ext,opt}$ which corresponding the minimum TAC. In other word, $E_{ext,opt}$ can be a criterion for the comparison between different design for the same separating system.

In chapter 7, we show the double-effect heat integration and mechanical heat pump (MHP) technique for extractive distillation in order to further save energy cost and TAC. As extractive distillation is an energy intensive non-ideal liquid mixture separation process, reducing the total process cost and TAC is an interesting issue for the process itself as well as the environmental pollution reduction effort. Double-effect heat integration and mechanical heat pump technique are investigated for extractive distillation process and compared from the economical view by TAC and environmental aspect by CO_2 emissions. A novel optimal partial heat integration process is proposed and optimized through the new objective function OF2. The direct partial and full heat integration are regarded as the extremely conditions where (Q_{r1}-Q_{c2}) in OF2 taking the maximal value or the minimal value zero. Instead of the minimum TAC founded in the optimal full heat integration process as intuition, the optimal partial heat integration has the lowest TAC. Further, the mechanical heat pumps (VRC and BF) are evaluated and both economical and environmental aspects are taken into account. Based on the character of extractive distillation process that the temperature difference between the bottom of the extractive column and the top of the regeneration column is usually small, we proposed the new partial VRC and new partial BF process flowsheet in order to reduce the high initial capital cost of compressors. We find that Partial VRC process gives better performance from economical view while full BF process leads better performance in environmental aspect.

The last part chapter deals with conclusions and future studies that can be drawn. Appendixes collect the formulations for calculating the cost data of distillation column, some definitions of common terms of extractive distillation in this manuscript.

Chapter 2. State of The Art and Objectives

2.State of the art and objectives

2.1.Phase equilibrium

As the systems in extractive distillation are non-ideal, the phase equilibrium model and thermodynamic model used to describe the proposed system are fatal for all the works and the results should be validated by the experimental data.

2.1.1.Phase equilibrium model

Phase equilibrium behavior is the foundation of chemical mixture components separation by distillation. The basic relationship for every component in the vapor and liquid phases of a system at equilibrium is the equality of fugacity in all phases. In an ideal liquid solution the liquid fugacity of each component in the mixture follows Raoult' law and is directly proportional to the mole fraction of the component. However, because of the non-ideality in the liquid solution of the systems, activity coefficient which represents the deviation of the mixture from ideality methods is used to describe the liquid phase behavior. For the vapor phase, as the pressure is not high, ideal gas behavior is assumed and the gas fugacity equals to the partial pressure. Thus the basic vapor-liquid equilibrium equation (McCabe et al., 2004; Poling et al., 2001) is modified as:

$$f_i^l = x_i \gamma_i f_i^{*,l} = f_i^v = y_i P \tag{2.1}$$

γ_i is the liquid activity coefficient. With the liquid phase reference fugacity $f_i^{*,l}$ being calculated from:

$$f_i^{*,l} = \varphi_i^{*,v}(T, P_i^*) P_i^* \theta_i^* \tag{2.2}$$

Where $\varphi_i^{*,v}$ is the fugacity coefficient of pure component i at the system temperature (T) and saturated vapor pressure, as calculated from the vapor phase equation of state (for ideal vapor phase: $\varphi_i^{*,v} = 1$). P_i^* is the saturated vapor pressure of component i at the system temperature. θ_i^* is the Poynting correction for pressure $\exp(\frac{1}{RT}\int_{P_i^*}^{P} V_i^{*,l} dP)$.

At low pressures, the Poynting correction is near unity and can be ignored. Thus the overall vapor–liquid phase equilibrium (VLE) relationship for most of the mixture systems in the following chapters can be described as the following equation:

$$y_i P = x_i \gamma_i P_i^* \tag{2.3}$$

Equation (2.3) is the so-called Raoult-Dalton's Law. Calculation of the saturated vapor pressure for a pure component is needed in Equation (2.3) for the VLE relationship. The extended Antoine equation can be used to compute liquid vapor pressure as a function of the system temperature T:

$$\ln P_i^* = C_{1i} + \frac{C_{2j}}{T + C_{3i}} + C_{4i}T + C_{5i}\ln T + C_{6i}T^{C_{7i}} \tag{2.4}$$

Where C_{1i} to C_{7i} are the model parameters, model parameters for many components are available in the literature or from the pure component databank of the Aspen Physical Property System or from Simulis Thermodynamic.

2.1.2.Nonideality of mixture

In most distillation systems, the predominant nonideality occurs in the liquid phase because of molecular interactions. Equation (2.3) contains the liquid phase activity coefficient of the i component. When chemically dissimilar components are mixed together (for example, oil molecules and water molecules), there exists repulsion or attraction between dissimilar molecules. If the molecules repel each other, they exert a higher partial pressure than if they were ideal. In this case the activity coefficients are greater than unity (called a "positive deviation" from Raoult's law). If the molecules attract each other, they exert a lower partial pressure than if they were ideal. Activity coefficients are less than unity (negative deviations). Activity coefficients are usually calculated from experimental data or from the VLE models regressed on experimental data. Azeotropes occur in a number of nonideal systems. An azeotrope exists when the liquid and vapor compositions are the same ($x_i = y_i$) at a given azeotrope temperature. There are maximum boiling azeotrope (Figure 2.1) and minimum boiling azeotrope (Figure 2.2).

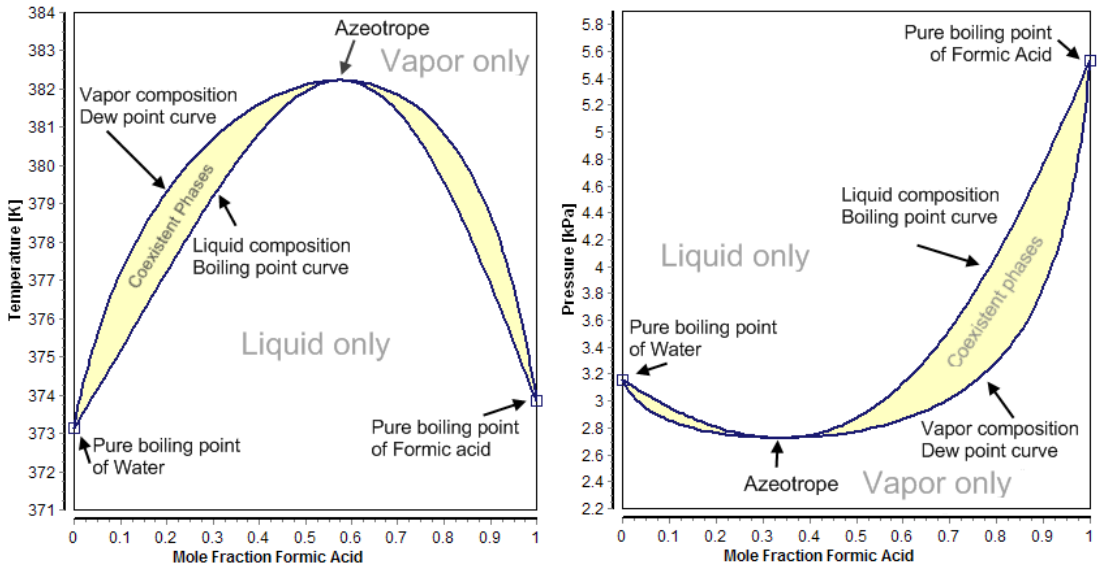

Figure 2.1 – Typical homogeneous mixtures with maximum boiling azeotrope water and formic acid, a negative deviation from Raoult's law

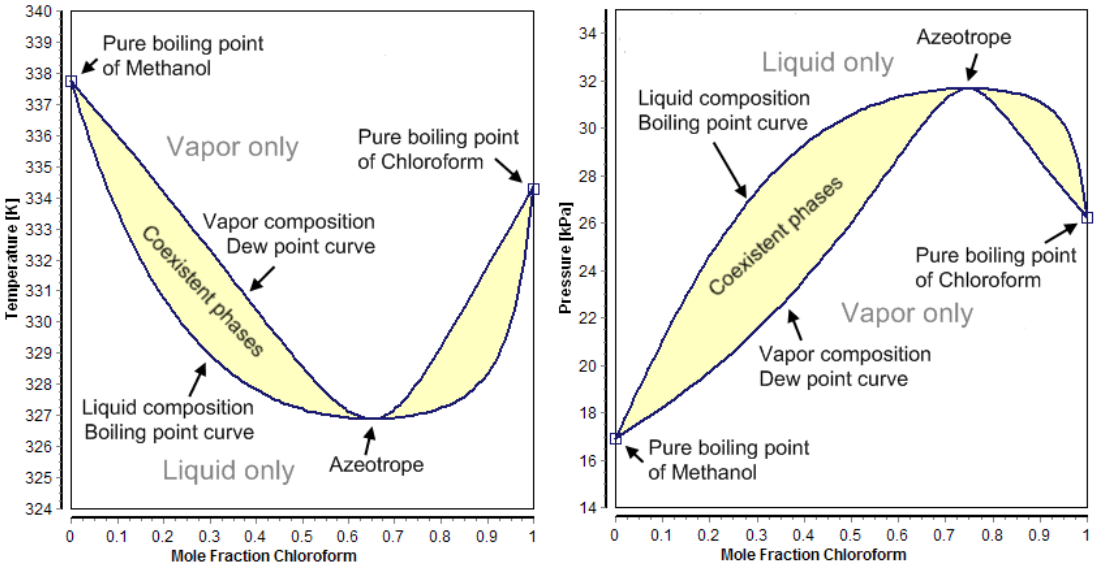

Figure 2.2 – Typical homogeneous mixtures with minimum boiling azeotrope methanol and chloroform, a positive deviation from Raoult's law

The Figure 2.1 and Figure 2.2 shows a combined graph of the bubble and dew temperatures, pressures and the vapor-liquid equilibrium phase map, which gives a complete representation of the VLE. Each of these diagrams uniquely characterizes the type of mixture. Negative deviations (attraction) can give a higher temperature boiling mixture than the boiling point of the heavier component, called a maximum-boiling azeotrope (Figure 2.1). Positive deviations (repulsion) can give a lower temperature boiling mixture than the boiling point of the light component, called a minimum boiling azeotrope (Figure 2.2).

2.2. Nonideal mixtures separation

For the separation of nonideal mixtures, advanced techniques are needed because nonideal mixtures can't be separated by conventional distillation. These technologies have been classified into three major categories: membrane processes, process intensification and enhanced distillation as shown in Figure 2.3 (Mahdi et al., 2015).

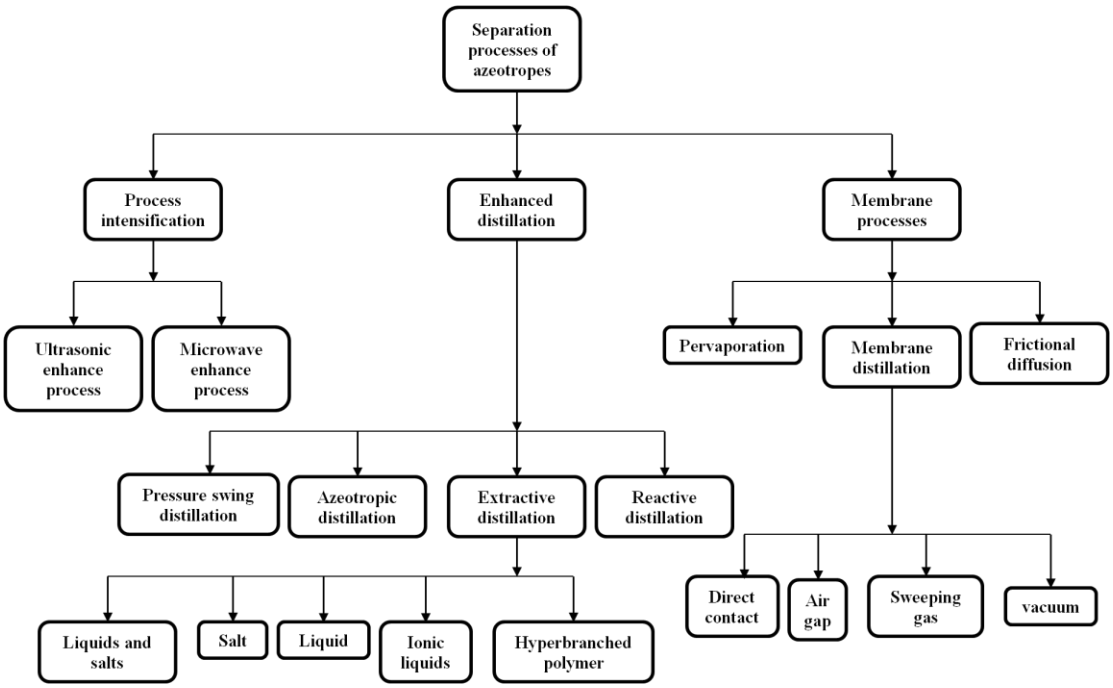

Figure 2.3 – Schematic diagram of various techniques for separation of azeotropic mixtures

First, membrane processes include pervaporation, frictional diffusion and membrane distillation. Pervaporation (PV) involves permeation of feed components through a membrane, followed by evaporation into the downstream in different rates. The driving force for the separation is the difference in the partial pressures of the components on the two sides of the membrane, and the main advantage of PV is that it is not limited by the vapor-liquid equilibrium because it is independent of the relative volatility of the mixture. Frictional Diffusion is a separation technology based on differences of diffusivities in a mass separating sweep gas or vapor mixtures. Its driving force is the gradient in the chemical potential. It has been shown to allow for the breaking azeotropes of alcohols and water mixtures (Breure et al., 2008; Selvi et al., 2007) aiming at increasing the energy efficiency and reducing the use of hazardous solvents. Comparing with conventional membrane processes such as microfiltration, nanofiltration, reverse osmosis and pervaporation, membrane distillation is an emerging thermally driven membrane process in which a hydrophobic microporous membrane separates a heated feed solution and a cooled receiving phase (Onsekizoglu, 2012). Membrane distillation includes four configurations: direct contact, air gap, sweeping gas and vacuum. The difference among them is the way in which the vapor is condensed in the permeate side. The temperature difference across the membrane results in a water vapor pressure gradient, causing water vapor transfer through the pores from high vapor pressure side to the low one. The key advantages of membrane distillation are relatively lower energy costs and lower operating pressure and temperature (Onsekizoglu, 2012). The main disadvantage of membrane distillation is the risk of membrane pores getting filled with liquid or wetted (Banat and Simandl, 1999). Generally speaking, the membrane processes are usable for breaking azeotrope. However, it has the drawbacks of low flow rate through the membrane, the swelling or shrinking of the

membrane materials caused by the feed mixtures and so on (Mahdi et al., 2015; Wang et al., 2005). Besides, they are limited in terms of industrial application because it is yet to be proven in large scale production.

Second, process intensifications include microwave enhanced process and ultrasonic enhanced process. Gao et al., (2013) studied the separation of benzene-ethanol mixture using microwave technology and demonstrated that the effect of VLE under a microwave field was significant, indicating that a strong dependence on the dielectric properties of the binary mixture might exist. Ripin et al., (2009) studied the effects of ultrasonic waves on the vapor-liquid equilibrium of methyl-tert-butyl-ether and methanol mixture, and proved that ultrasonic waves at different intensities and frequencies had potential to favorably manipulate the relative volatility of an azeotropic mixture. The main advantage of microwave and ultrasonic technology is that the azeotropic point can be shifted or eliminated by choosing suitable operating conditions. However, those studies are still in laboratory stage and more research attentions are needed before they are used in industrial separation processes.

Third, there are four enhanced distillation processes by modifying the process conditions and configurations: (1) Pressure-swing distillation (PSD), which consists in taking advantage of the binary azeotropic composition changing with the pressure (Knapp and Doherty, 1992; Phimister and Seider, 2000). (2) Azeotropic distillation (AD), in which a third component E is added to the feed. A or B components become either a residue curve stable or unstable node in the relevant distillation region, thus being removable as product by either an indirect or a direct split respectively (Widagdo and Seider, 1996). (3) Reactive distillation (RD), which uses chemical reaction to modify the composition of the mixture or, alternatively, uses existing vapor-liquid differences between reaction products and reactants to enhance the performance of a reaction. (4) Extractive distillation (ED), in which the third component is fed at another location than the main feed, giving rise to an extractive section (Pierotti, 1944; Lelkes et al., 1998b;). Usually but not always, the achievable product of extractive distillation is a residue curve saddle node in the relevant distillation region. For generalized extractive distillation, the separating agent can be a liquid solvent, dissolved salt (salt distillation), mixture of liquid solvents, mixture of dissolved salts, ionic liquids and hyperbranched polymers (Mahdi et al., 2015). As the industrial proven processes for separating azeotropic mixture, enhanced distillation processes are still the main technologies in large scale production.

2.2.1.Pressure-swing distillation

Pressure-swing distillation can be used for the binary pressure-sensitive azeotrope (Luyben, 2012; Modla and Lang, 2010) or pressure-insensitive azeotrope with an entrainer (Knapp and Doherty, 1992; Li et al., 2013) or ternary mixture with one, two or three binary azeotropes and at least one of them is pressure sensitive (Modla et al., 2010). In binary pressure-swing distillation, two columns operated in sequence at two different pressures if composition of the azeotrope changes significantly with pressure (Seader et al., 2010). Generally, the composition of component A (light in the azeotropic mixture) increases as pressure decreases, possibly until disappearance of the azeotrope allowing the use of a conventional distillation process.

For pressure insensitive azeotropes, Knapp and Doherty, (1992) proposed a new pressure-swing distillation to separate them with a suitable pressure-swing entrainer. This new technique uses varying pressure to move distillation boundaries that lie between the desired products which otherwise would make the separation impossible. The design and control of pressure-swing distillation for separating pressure insensitive maximum boiling azeotrope phenol-cyclohexanone using acetophenone as a heavy entrainer is shown by Li et al., (2013). In a ternary mixture separation, there may exist distillation boundaries involving azeotrope (s) as seen on residue curve maps. These boundaries can be crossed by changing the pressure because they vary with pressure along with the azeotrope composition. Between the boundaries at two different pressures, there is a region from where different products can be obtained at the different pressures. If all products obtained at different pressures are pure components or pressure sensitive binary azeotrope (s) this region is considered as the operating region of pressure-swing distillation (Modla et al., 2010).

2.2.2.Azeotropic distillation

Azeotropic distillation usually refers to the specific technique of adding another component along with the main feed. In some senses, adding an entrainer is similar to extractive distillation. Azeotropic distillation processes have been well studied and the feasibility assessment only relies upon residue curve map analysis whereas for extractive distillation, the volatility order region must be known as well (Gerbaud and Rodriguez-Donis, 2014). Consider the separation of a minimum boiling azeotrope AB with a light entrainer E forming no new azeotrope. The ternary diagram belongs to the 1.0-2 class (see Figure 2.4). Both A and B are stable node but they are located in different batch distillation regions. Residue curves begin at the unstable entrainer vertex (E) and end at the stable A or B. In batch, both azeotropic components can be distillated if the boundary is curved enough (Bernot et al., 1990; Doherty and Malone, 2001). In continuous only A or B is obtained from the column. Regarding continuous process, research has focused on advances in the methodologies for the synthesis, design, analysis and control of separation sequences involving homogeneous and heterogeneous azeotropic towers. Maps of residue curves and distillation lines were examined in a review article (Widagdo and Seider 1996), as well as geometric methods for the synthesis and design of separation sequences, trends in the steady-state and dynamic analysis of homogeneous and heterogeneous towers, the nonlinear behavior of these towers, and strategies for their control. Emphasis is placed on the methods of computing all of the azeotropes associated with a multicomponents mixture, on the features that distinguish azeotropic distillations from their non azeotropic counterparts, on the possible steady-state multiplicity, and on the existence of maximum and minimum reflux bounds. Important considerations in the selection of entrainers are examined (Foucher et al., 1991). For the synthesis of separation trains, when determining the feasible product compositions, the graphical methods are clarified, especially the conditions under which distillation boundaries can be crossed and bounding strategies under finite reflux (Gerbaud and Rodriguez-Donis, 2014). A recent update on azeotropic distillation was published by Arlt (2014).

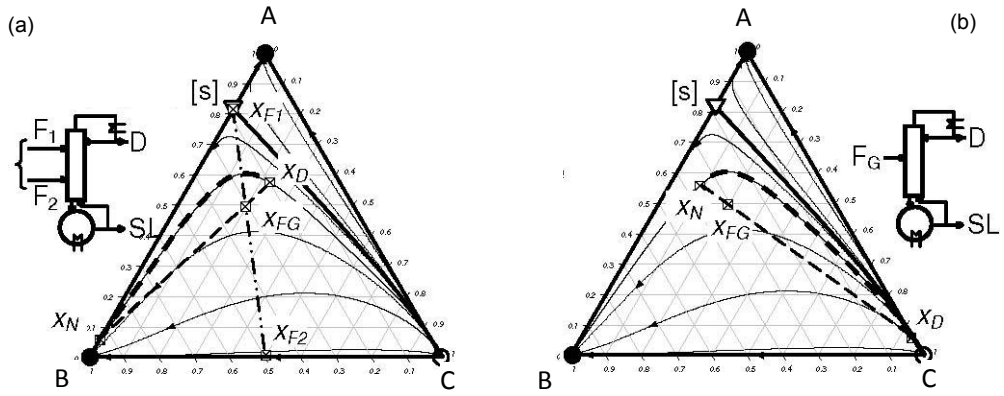

Figure 2.4 – Indirect separation (a) and direct (b) azeotropic continuous distillation under finite for a 1.0-2 class mixture (from Gerbaud and Rodriguez-Donis, 2010)

2.2.3.Reactive distillation

Reactive Distillation (RD) is a combination of reaction and distillation in a single vessel owing to which it enjoys a number of specific advantages over conventional sequential approach of reaction followed by distillation or other separation techniques (Hiwale et al., 2004). Harmsen, (2007) reported that more than 150 industrial scale reactive distillations which is operated worldwide at capacities of 100–3000 kiloton/year because it offers the advantage of improved selectivity, increased conversion, better heat control, effective utilization of reaction heat, scope for difficult separations and the avoidance of azeotropes. In RD, the entrainer reacts preferentially and reversibly with one of the original mixture components, the reaction product is distilled out from the non-reacting component and the reaction is reversed to recover the initial component. This can result in significant reductions in both energy and equipment in systems that have appropriate chemistry and appropriate vapor–liquid phase equilibrium. Besides, conversion can be increased far beyond what is expected by the equilibrium due to the continuous removal of reaction products from the reactive zone (Luyben and Yu, 2009).

Although invented in 1921, the industrial application of reactive distillation did not take place before the 1980. Being a relatively new field, research on various aspects such as modeling and simulation, process feasibility, column hardware design, non-linear dynamics and control is in progress. The suitability of RD for a particular reaction depends on various factors such as volatilities of reactants and products along with the feasible reaction and distillation temperature. A commentary paper (Malone and Doherty, 2000) on RD exposes an effective way of decomposing the design and development of reactive distillation involves four stages: (1) feasibility and alternatives, (2) conceptual design and evaluation, (3) equipment selection and hardware design, and (4) operability and control. The feasibility criteria for single-feed and double-feed continuous and batch reactive distillation systems are studied by Guo and coworkers (Guo et al., 2004; Guo and Lee, 2004) using graphical method and the phase and reaction equilibrium information. Brehelin et al., (2007) studied the catalytic reactive distillation process for the production of n-propyl acetate based on experiments and simulations. Pilot plant experiments were performed using a homogeneous strong acid catalyst in a packed column. Simulation results are in good agreement with experimental data. Filipe et al.,

(2008) investigated the multiobjectives design of complex reactive distillation columns through the use of feasible regions. A cost indicator reflecting energy usage and column size is introduced and used to build the Pareto surface describing the optimal combinations of cost and performance. Mo et al., (2011) studied the design and control of the RD for hydrolysis of methyl lactate based on the objective function of TAC. The effects of tray number of rectifying section, tray number of reactive section, and feed location on the TAC were investigated, and a dual-temperature control structure was proposed. Fernandez et al., (2013) presented a series of experiments for the production of ethyl acetate from esterification of acetic acid and ethanol in a reactive distillation pilot column. Predicted and measured results show good agreement and reveal a strong dependency of the structured packing catalyst activity on the pilot geometry and its operating conditions. The experimental validation is shown to be essential to provide realistic hydrodynamic parameters, to understand the sensitive parameters such as heat losses and to adapt values for the catalyst holdup as a function of the system. A recent update on reactive distillation was published by Keller (2014).

2.2.4.Generalized extractive distillation

Extractive distillation is a powerful and widely used technique for separating azeotropic and low relative volatility mixtures in pharmaceutical and chemical industries. Given an azeotropic mixture A-B (with A having a lower boiling temperature than B), an entrainer E is added to interact selectively with the original components and alter their relative volatility, thus enhancing the original separation. Compared with azeotropic distillation, some energy saving is expected in extractive distillation because the amount of entrainer is usually less, leading to the energy saving in entrainer regeneration column (Lang, 1992; Lei et al., 2003). The main distinction between extractive distillation and azeotropic distillation is that: the entrainer is fed at a different location than the main mixture, bringing an additional extractive section in the column, between the usual stripping and/or the rectifying sections (Gerbaud and Rodriguez-Donis, 2014). We will introduce the extractive distillation following the separating agent: solid salt, combination of liquid solvent and solid salt, ionic liquid and hyperbranched polymers. Notice that the extractive distillation processes with a liquid entrainer are the main part of this work and will be introduced emphatically in the next part.

2.2.4.1. Extractive distillation with solid salt or salt effect distillation

In salt effect distillation, a salt is dissolved in the mixture of azeotropic or zeotropic liquids mixtrures and alters the relative volatilities sufficiently so that the separation becomes possible. The salt is fed into the distillation column at the top of the column at a steady rate. It dissolves in the liquid phase, and since it is non-volatile, flows out with the heavier bottoms stream. The bottoms are partially or completely evaporated to recover the salt for reuse. The simulate and optimization of a saline extractive distillation process for dehydration of ethanol have been studied by using four saline agents (NaCl,KCl,KI,$CaCl_2$) (Pinto et al., 2000).

Compared to the liquid agent, solid salt is more effective and requires a much smaller salt ratio, thus leading to a high production capacity and a low energy consumption (Gil et al., 2008). Besides, the product at the top

of the column is free from salt impurities since solid salt is not volatile. However, salt effect distillation has the disadvantages of dissolution, reuse and transport of the salt, corrosion of equipment. Thus its application in industry is limited (Lei et al., 2005).

In order to overcome the disadvantages of salt effect distillation, Lei et al., (2002) studied the use of N,N-dimethylformamide (DMF) as a solvent to separate C4 mixture by adding a small amount of solid salt to DMF and achieved an improvement in the relative volatilities of C4. They also described the relationship between microscale salt coefficients and macroscale relative volatilities at infinite dilution by using the scaled particle theory. Gil et al., (2008) analyzed an extractive distillation process for azeotropic ethanol dehydration with ethylene glycol and calcium chloride mixture as entrainer, and obtained a substantial reduction in the energy consumption. Dhanalakshmi et al., (2014) investigated the salt effect of four inorganic salts on the vapor liquid equilibria of the binary methyl acetate–methanol system at 1 atm and they observed that the bivalent cation salts had greater salting out effect than uni-valent cation. They also found that zinc nitrate is more effective than the other nitrate salts of calcium and magnesium even at lower salt concentrations, which leads to energy saving in reboiler. However, because of the equipment corrosion caused by salts and the decomposition of salts at high temperatures, the suitable solid salts are available only in a narrow range.

2.2.4.2. Extractive distillation with ionic liquid

The use of ionic liquids (ILs) as separating agents in the extractive distillation process is a recent strategy and has received considerable attention due to their unique advantages of negligible vapor pressure at room temperature (Earle et al., 2006). Besides, extractive distillation with the ILs has the following advantages: (1) Absence of product impurities at the top of the column as ILs are not volatile. (2) A wide using temperature range. (3) Facile recovery and reuse of ILs. (4) High stability when the operations of extractive distillation in terms of thermal and chemical conditions (Mahdi et al., 2015). Dhanalakshmi et al., (2013) studied the separation of methyl acetate-methanol and ethyl acetate-ethanol with 13 cations and 27 anions as entrainers to identify suitable ILs using the conductor-like screening model for realistic salvation (COSMO-RS) model. They reported that the shorter alkyl chain of the cation favors the azeotrope separation, and the anion plays an important role and decides the solubility of ionic liquid in alcohols by which methyl acetate and ethyl acetate are removed from the alcohol solutions. Ramírez-Corona et al., (2015) presented a design method for distillation systems aided by ILs based on tray-by-tray calculations with the ethanol dehydration as case study. They found that the most important design parameter is the IL concentration, and that the separation process can be intensified with the use of a single column.

Nevertheless, extractive distillation with ILs has some disadvantages such as the long time required to prepare ILs, the high cost of synthesis specialty components, difficult to manage due to the separation of viscous solutions, and moisture sensitivity of ILs (Lei et al., 2005; Pereiro et al., 2012). Such disadvantages have slowed down the application of this process in industry.

2.2.4.3. Extractive distillation with low transition temperature mixtures (LTTMs)

LTTMs are commonly defined as mixtures of two or more solid compounds, which have much lower melting point than the initial components due to hydrogen bonding. Originally, LTTMs were called deep eutectic solvents (DESs), but this name does not cover the complete class of solvents because many mixtures do not show an (eutectic) melting point, but a glass transition instead (Rodríguez et al., 2015). LTTMs have some common properties that make them suitable as entrainers for extractive distillation: low vapor pressure, wide liquid range, water compatibility, biodegradability, non-flammability and easy and cheap preparation by mixing natural and readily starting materials (Francisco et al., 2013). Oliveira et al., (2013) studied three different DESs for the separation of azeotropic mixture heptane plus ethanol and found that DESs surpass the performance of existing extraction solvents ILs, leading to an increase in efficiency and a reduction in energy consumption of the overall process. Rodríguez et al., (2015) measured the vapor–liquid equilibrium data for the pseudo-binary mixtures of water–LTTM and ethanol–LTTM and found that the ethanol–water azeotrope can be broken by LTTMs such as lactic acid–choline chloride 2:1, malic acid–choline chloride 1:1 (MC 1:1) and so on. Rodriguez and Kroon, (2015) considered two different LTTMs as potential entrainers for the azeotropic mixture of isopropanol and water and reported that the given LTTMs cannot break the azeotrope at given concentrations. However, the azeotrope was displaced to a much higher isopropanol concentration. LTTMs are recently discovered as potential entrainer for the extractive distillation and more basic researches are needed before it can be applied into industries.

2.2.4.4. Extractive distillation with hyperbranced polymers

Hyperbranched polymers represent highly branched, polydisperse macromolecules with a treelike topology and a large number of functional groups. Seiler et al. (2003) seems the pioneers who suggested the use of hyperbranched polymers as entrainers for extractive distillation. They found that the commercially available hyperbranched polyesters and hyperbranched polyesteramides can be capable of breaking the ethanol-water and THF-water azeotrope. Later, the author (Seiler et al., 2004) simulated the extractive distillation with hyperbranced polymers based on thermodynamic studies of the influence of hyperbranched polymers on the vapor–liquid and liquid–liquid equilibrium of the azeotropic ethanol–water and THF–water systems and showed the potential of hyperbranched polymers as selective solvent in terms of feasibility and energetic efficiency compared with conventional process. However, all the works are limited to laboratory stage and more efforts are needed to put forward the industrial application of hyperbranced polymer.

2.2.4.5. Extractive distillation with pressurized carbon dioxide

In 1957, Baker and Anderson (1957) found that homogeneous aqueous solutions of alcohols (ethanol) can be split into two liquid phases by pressurized gases CO_2. The vapor−liquid phase equilibrium behavior of CO2 + liquid can be tuned into a vapor−liquid−liquid phase equilibrium behavior by pressurizing CO2, and the transition occurs at the lower critical solution pressure. Ye et al., (2013) studied the separation of azeotropic mixture acetonitrile−water system by tuning the phase behavior using pressurized CO2 as a tunable solvent

and showed that it has significant potential to reduce the separation costs up to 30.5% compared with the conventional pressure-swing distillation process. However, few research attentions are focused on it and more basic studies are needed for this process.

2.3. Introduction of extractive distillation with liquid entrainer

2.3.1. Extractive distillation

Extractive distillation has been studied for many decades with very rich literatures, some main subjects studied include: column with all possible configurations; feasibility studies; process operation polices and strategy; process design, synthesis, optimization; determining separation sequencing; entrainer design and selection, and so on (Shen, 2012). Among those, process feasibility is a critical issue as before making the separation mission and find the optimal design, the designer should know that it is possible or not. Feasibility studies also contribute to a better understanding of complex unit operations such as the batch and continuous extractive distillation. Optimal design is another important issue in extractive distillation process since all the studies on the separation of azeotrope is aimed to make the separating process come true in industry.

Extractive distillation is considered as a promising distillation process compared with azeotropic distillation when the mixtures which are azeotropic or close-boiling because of saving energy, especial under the global background of energy use reduction and emissions reduction. Extractive distillation is suitable for the separation of non ideal mixtures, including minimum or maximum boiling azeotropes and low relative volatility mixtures (Luyben and Chien, 2010; Petlyuk, 2004). The main tools for the feasibility study of extractive distillation are residue curve map and uni-volatility line.

Entrainer selection and process optimal design are always the important issues in the design of extractive distillation. The entrainer selection issue is strongly related to the process feasibility. Feasibility rules have been published for batch (Lang et al., 1999; Lelkes et al., 1998a; Rodriguez-Donis et al., 2009a, 2009b, 2012a, 2012b) and continuous process (Botía et al., 2010; Knapp and Doherty, 1994; Laroche et al., 1991; Li and Bai, 2012; Luyben, 2008; Petlyuk, 2004; Shen et al., 2013; Shen and Gerbaud, 2013) for the separation of minimum or maximum boiling azeotropes or low relative volatility mixtures with heavy, light or intermediate entrainers, giving rise to extractive separation classes (Gerbaud and Rodriguez-Donis, 2014). Once an extractive separation class is considered, the process optimal design is undertaken by simulation and optimization, based on the calculation of the total annual cost, a trade-off between capital cost and operating cost. Energy consumption and solvent losses are included in the operating costs.

2.3.2. Entrainer features

The effectiveness of an extractive distillation process relies on the choice of the extractive agent (Kossack et al., 2008) because it affects the feasibility and efficiency of the processes since the processes synthesis and design is evidently based on the thermodynamic properties of the mixture to be separated: residue curve map topology and equi-volatility. In the choice of solvent, many qualitative heuristic methods have been developed. After that, a more effective method for selecting solvents is computer-aided molecular design

(CAMD) (Pretel et al., 1994). Van Dyk and Nieuwoudt, (2000) proposed a method for design solvent of extractive distillation based on CAMD, and used UNIFAC model to estimate the relative volatilities. The boiling and freezing points are estimated by Joback's group contribution methods, and they reported that the predicted solvents for extractive distillation agree well with the solvent currently used in industry. The entrainer for extractive distillation should possess suitable features on thermodynamics and process operation (Gerbaud and Rodriguez-Donis, 2014).

First, features of thermodynamics such as boiling point, critical properties (Marrero and Gani, 2001). The entrainer boiling temperature sets the ternary residue curve map topology, the most appropriate column configuration, and the product cut sequence. For decades, the unique standard for selecting entrainer is having the highest boiling point in the proposed system and not forming new azeotropes with the original components. However, when the azeotropic components are heat sensitive or have a high boiling temperature, the light or intermediate entrainer or reduced pressure distillation are recommended, so the selectivity of the entrainer should not be the unique concern. Second, features of process operation such as entrainer-feed flow ratio, selectivity and solvency (Yang and Song, 2006). Entrainer-feed flow rate ratio is one of the important process operation parameters for extractive distillation as it directly affects the process feasibility (Kim et al., 2004). It can be partly predicted from the thermodynamic insight, involving the properties of residue curve map and uni-volatility curves. Selectivity is usually assessed via the relative volatility of A versus B ($\alpha_{A,B}$) and the ratio of activity coefficients of A and B at infinite dilution in the entrainer. Solvency refers to the total or partial miscibility of the entrainer with components A or B, which will lead to homogeneous or heterogeneous distillation. Besides, other features for entrainer selection e.g. corrosion, price, toxicity, thermal stability, environmental waste and so on (Weis and Visco, 2010) should also be taken into consideration.

2.3.3.Relative volatility

The relative volatility of the components i and j in a given binary mixture with ideal vapor phase is defined by

$$\alpha_{ij} = \frac{y_i / x_i}{y_j / x_j} = \frac{\gamma_i p_i^0}{\gamma_j p_j^0} \tag{2.5}$$

Where x and y are the molar fractions in the liquid and vapor phase, γ is the activity coefficient and p^0 the pure component vapor pressure.

The relative volatility is well-known characteristics of the vapor–liquid equilibrium and the base of distillation. The relative volatility is a very convenient measure of the ease or difficulty of separation in distillation. The relative volatility characterizes the ability of component i to transfer (evaporate) into the vapor phase compared to the ability of component j. Component i is more volatile than component j if $\alpha_{ij}>1$, and less volatile if $\alpha_{ij}<1$. For ideal and nearly ideal mixtures, the relative volatilities for all pair of

components are nearly constant in the whole composition space. The situation is different for non-ideal and in particular azeotropic mixtures where the composition dependence can be complex.

Heuristics in distillation state that a large value of relative volatility α implies that components i and j can be easily separated in a distillation column. Values of α_{ij} close to 1 imply that the separation will be very difficult, requiring a large number of trays and high energy consumption. For binary systems, the relative volatility of light to heavy component is simply called α:

$$\alpha = \frac{y/x}{(1-y)/(1-x)} \tag{2.6}$$

$$y = \frac{\alpha x}{1+(\alpha-1)x} \tag{2.7}$$

Where x and y are the mole fractions of the light component in the liquid and vapor phases respectively. Rearrangement of equation (2.6) leads to the very useful y-x relationship equation (2.7) that can be employed when α is constant in a binary system. If the temperature dependence of the vapor pressure of both components is the same, relative volatility α will be independent of temperature. This is true for many components over a limited temperature range, particularly when the components are chemically similar. Short-cut distillation columns are frequently designed assuming constant relative volatility because it greatly simplifies the VLE calculations. Relative volatilities usually decrease somewhat with increasing temperature in most systems.

Uni-volatility line diagrams can be used to sketch the VLE diagrams and represent the geometry of the simple phase transformation trajectories. The qualitative characteristics of the relative volatility functions are typical approaches for the thermodynamic topological analysis. Kiva et al (2003) considered the behavior of these functions for binary mixtures. The composition dependency of the distribution coefficients is qualitative and quantitative characteristics of the VLE for the given mixture. The patterns of these functions determines not only the class of binary mixture (zeotropic, minimum-or maximum-boiling azeotrope, or biazeotropic), but also the individual behavior of the given mixture.

The relative volatility features can be represented by isovolatility lines. Then the system of uni-volatility lines where $\alpha_{ij} = 1$ was proposed. It is evident that the point of a binary azeotrope A_{zij} gives rise to a α_{ij} uni-volatility line and that the point of a ternary azeotrope gives rise to the three uni-volatility lines (Kiva et al. 2003). For the illustration of a binary azeotrope uni-volatility line, see Figure 3.2 in chapter 3 for acetone-methanol with water system.

2.3.4.Entrainer selectivity

In the extractive distillation, the entrainer is introduced to enhance the relative volatility of the original mixtures in order to make the azeotropes disappear. Following equation 2.5, the ratio P_i^0/P_j^0 is constant for a

given temperature; the solvent only affects the ratio of the activity coefficients γ_i/γ_j. In the presence of a solvent S, this ratio is called selectivity S_{ij}

$$S_{ij} = \left(\frac{\gamma_i}{\gamma_j} \right)_S \tag{2.8}$$

The activity coefficients depend on the liquid phase composition. Since the effect of the entrainer tends to increase with concentration in the mixture, it is common practice to evaluate the selectivity at infinite dilution. The definition of selectivity given before then becomes

$$S_{ij}^{\infty} = \left(\frac{\gamma_i^{\infty}}{\gamma_j^{\infty}} \right) \tag{2.9}$$

Which also represents the maximum possible selectivity.

Another proposed measure to assess the suitability of an entrainer is the capacity (Kossack et al., 2008), which is determined by $C^{\infty}_{j,entrainer} = 1/\gamma_i^{\infty}$, where j denotes the solute. The smaller the value of the activity coefficient γ_i^{∞}, the stronger are the interactions between component j and the entrainer, which results in a larger capacity $C^{\infty}_{j,entrainer}$.

S_{ij}^{∞} can only provide a preliminary guidance for the selection of entrainer as the selectivity may change following the increasing of the solute concentration. Jork et al (Jork et al., 2005) stated that highly selective ionic liquid entrainer often possess a low capacity. Kossack et al (Kossack et al., 2007, 2008) found that selectivity alone was not a good criterion for ranking entrainers, instead, $S_{ij}^{\infty}C^{\infty}_{j,entrainer}$ agrees well with the total annualized cost of optimized process for screening entrainer. They also noted that $S_{ij}^{\infty}C^{\infty}_{j,entrainer}$ can only serve as a rule of thumb and it is limited to the screening of entrainer alternatives since minimum entrainer flowrates and reflux bounds are not available.

2.3.5.Residue curve maps

A residue curve map (RCM) is a collection of the liquid residue curves in a simple one-stage batch distillation originating from different initial compositions (Doherty and Perkins, 1978). The RCM technique is considered as a powerful tool for the flowsheet development and preliminary design of conventional multi-component separation processes since the synthesis and design of extractive or azeotropic distillation is based on the analysis of multicomponent residue curve maps (Doherty and Malone, 2001). It has been extensively studied since 1900. Using the theory of differential equations, Doherty and colleagues explored the topological properties of RCM which are summarized in two articles (Hilmen et al. 2002; Kiva et al. 2003). The simple RCM was modeled by the set of differential equations.

$$\frac{dx_i}{dh} = x_i - y_i^* \tag{2.10}$$

Where h is a dimensionless time describing the relative loss of the liquid in the still-pot and $dh = dV/L$. x_i is the mole fraction of species i in the liquid phase, and y_i is the mole fraction of species i in the vapor phase. The y_i values are related with the x_i values using equilibrium constants K_i. Such residue curves are considered to be a good approximation of the tray column liquid composition profiles under the condition of infinite reflux ratio. In practice, the reflux ratio of distillation column is finite, so Van Dongen and Doherty, (1985) use difference mass balance equations to calculate column liquid composition profiles under finite reflux conditions.

The singular points of differential equation are checked by computing the associated eigenvalues. Within a non-reactive residue curve map, a singular point can be a stable or an unstable node or a saddle, depending on the sign of the eigenvalues related to the residue curve equation.

2.3.6.Ternary VLE classification

The study of the thermodynamic classification of liquid-vapor phase equilibrium diagrams for ternary mixtures and its topological interpretation has a long history. Considering a ternary diagram A-B-E formed by a binary mixture A-B with the addition of an entrainer E, the classification of azeotropic mixtures in 113 classes was first proposed by (Matsuyama;Nishimura, 1977, 1978), then it was extended to 125 classes (Foucher et al., 1991). After the work of Hilmen et al., (2002), it became known that a more concise classification existed since the 70's: Serafimov classification. As explained by Hilmen (2000), Serafimov extended the work of Gurikov and used the total number of binary azeotropes M and the number of ternary azeotropes T as classification parameters. Serafimov's classification denotes a structure class by the symbol "M.T" where M can take the values 0, 1, 2 or 3 and T can take the values 0 or 1. These classes are further divided into types and subtypes denoted by a number and a letter. As a result of this detailed analysis, four more feasible topological structures, not found by Gurikov, were revealed. Thus Serafimov's classification includes 26 classes of feasible topological structures of VLE diagrams for ternary mixtures. Both the classifications of Gurikov and Serafimov consider topological structures and thus do not distinguish between antipodal (exact opposite) structures since they have the same topology. Thus, the above classifications include ternary mixtures with opposite signs of the singular points and opposite direction of the residue curves (antipodal diagrams). Serafimov's classification is presented graphically in Figure 2.5. The transition from one antipode to the other (e.g.changing from minimum-to maximum-boiling azeotropes) can be made by simply changing the signs of the nodes and inverting the direction of the arrows and the correspondence between Matsuyama and Serafimov's classification is detailed in Kiva et al., (2003) and Hilmen (2000).

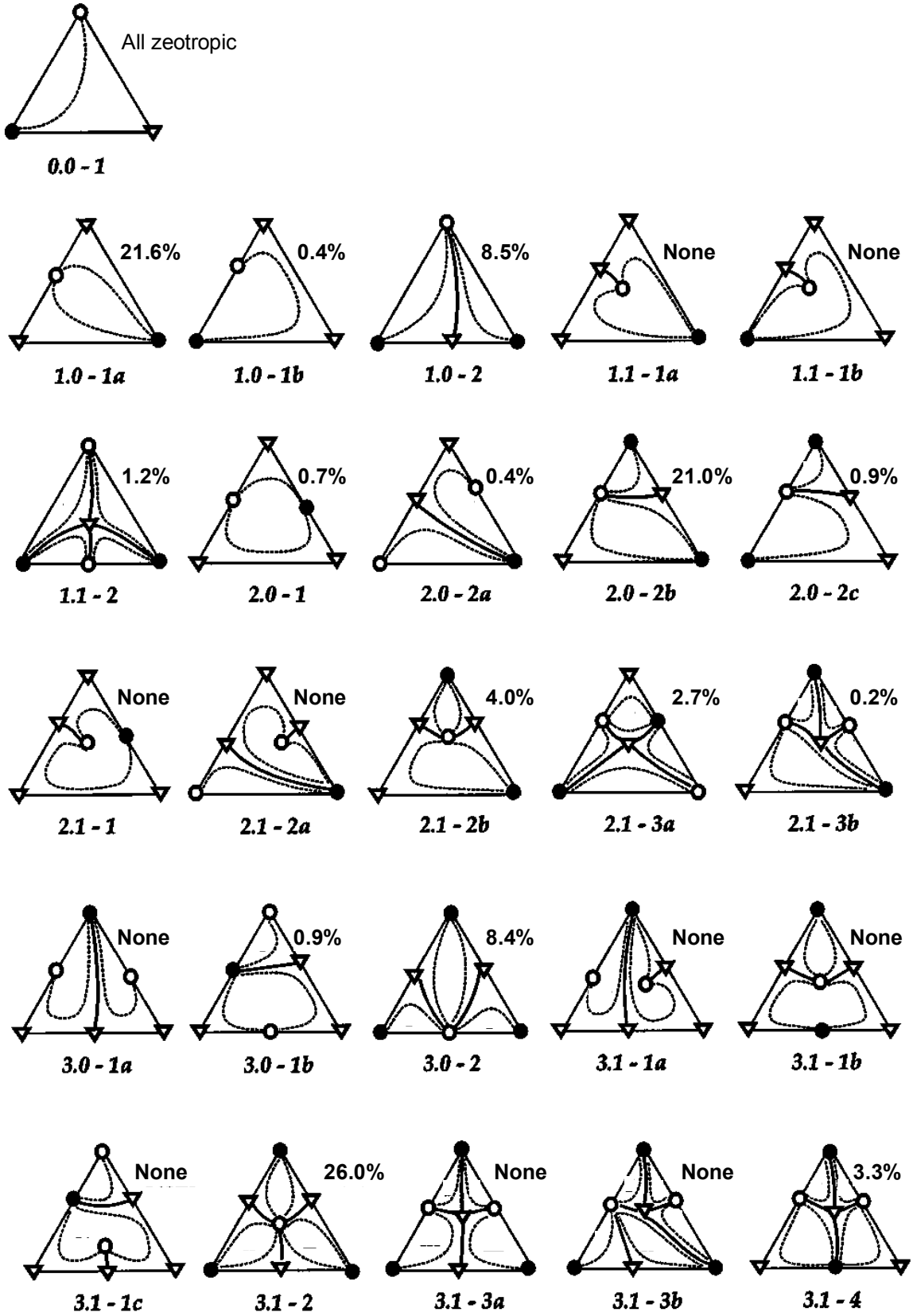

Figure 2.5 – Azeotropic ternary mixture: Serafimov's 26 topological classes and Reshetov's statistics (Hilmen et al., 2002). (o) unstable node, (Δ) saddle, (●) stable

The studies on the frequency of occurrences of different types of phase diagrams for ternary azeotropic and zeotropic mixtures were presented by (Reshetov and Kravchenko, 2007). All 26 Serafimov's classes are topologically and thermodynamically feasible but their occurrence is determined by the probability of certain combinations of molecular interactions. The statistics on the physical occurrence of these 26 classes were provided to Kiva et al. by Dr. Reshetov but the original source is not available. The hereafter called "Reshetov's statistics" are based on thermodynamic data for 1609 ternary systems from which 1365 are azeotropic. The database covers data published from 1965 to 1998. The results in Figure 2.5 show that 16 out of the 26 Serafimov's classes were reported in the literature. Although Reshetov's statistics do not necessarily reflect the real occurrence in nature they can be used as an indicator of common azeotropic classes that worthy further investigation.

2.4. Extractive distillation process feasibility

2.4.1. Thermodynamic insight on extractive distillation feasibility

Almost all the literature relied upon the feasibility rule that a heavy entrainer forming new azeotrope was suitable to separate a minimum boiling azeotrope. The corresponding ternary diagram belongs to the 1.0-1a Serafimov's class (occurrence 21.6%). As (Laroche et al., 1991; Laroche et al., 1992) showed for the 1.0-1a class, knowledge of the residue curve map and of the location of the uni-volatility curve $\alpha_{AB} = 1$ can help assess which product is removed in the distillate when using a light, intermediate or heavy entrainer. With a heavy entrainer, A (or B) can be distillated using a direct sequence if the uni-volatility curve intersects the A-E edge (the B-E edge). Those two intersection subcases helped to explain some counterintuitive observation that sometimes the intermediate boiling compound B within the A-B-E mixture is removed in the distillate.

Completion and extension of thermodynamic insight to other mixture classes was published by Rodriguez-Donis et al (2009a, 2009b, 2012a, 2012b) who combined knowledge of the thermodynamic properties of residue curve maps and of the uni-volatility line location. They expressed a general feasibility criterion for extractive distillation under infinite reflux,

"***homogeneous extractive distillation of a A-B mixture with entrainer E feeding is feasible if there exists a residue curve connecting E to A or B following a decreasing (a) or increasing (b) temperature direction inside the region where A or B are the most volatile (a) or the heaviest (b) component of the mixture***".

The volatility order is set by the uni-volatility curves which knowlege is therefore critical. An illustrative example will be discussed in Chapter 4.

2.4.1.1. Topological features of class 1.0-1a extractive distillation process

The general feasibility criterion enounced by Rodriguez-Donis and coworkers (Gerbaud and Rodriguez-Donis, 2014; Rodríguez-Donis et al., 2009a; Shen et al., 2013) strictly holds for infinite reflux operation. For finite reflux, things are more complicated and can only be exhaustively studied from the computation of extractive singular points (Frits et al., 2006; Petlyuk et al., 2015). Figure 2. displays the qualitative

topological features of the class 1.0-1a diagram reproduced here from the literature (Rodríguez-Donis et al., 2009) because it will be used in the discussion section.

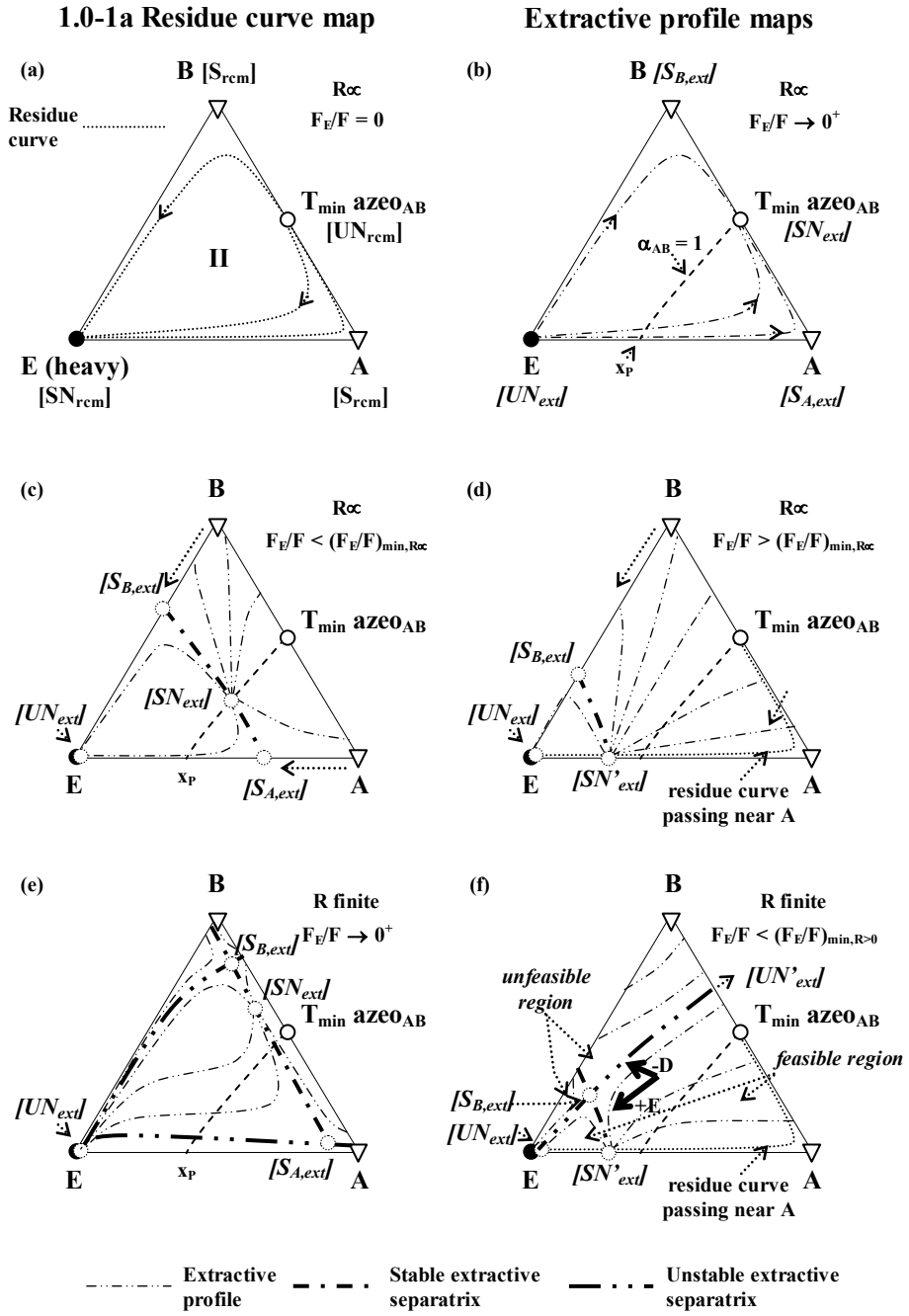

Figure 2.6 – Topological features of class 1.0-1a with heavy entrainer in extractive distillation process operation (adapted from Rodriguez-Donis et al., 2009a).

Feasible and unfeasible regions for the composition in the extractive section of the column are deduced from the analysis of the extractive composition profile map, similarly to residue curve map (rcm) analysis. The feasible composition regions are the search space for the extractive section composition profile during the optimization of extractive distillation with GA method. Those regions are bounded by extractive stable and unstable separatrices crossing at saddle extractive singular points (Knapp and Doherty, 1994). For the class

1.0-1a, the pinch point of the extractive composition profiles is a stable extractive node SN_{ext} issued from the original minimum boiling azeotrope. Saddle extractive points $S_{i,ext}$ are emerged from the rcm saddle points (A and B vertices). An extractive unstable node UN_{ext} is located near the entrainer vertex.

At infinite reflux while F_E/F increases (Figure 2.c), SN_{ext} moves along $\alpha_{AB} = 1$, $S_{A,ext}$ and $S_{B,ext}$ moves along the binary edges (A-E and B-E, respectively), toward the vertex (E), which is the entrainer. Extractive stable separatrices that link SN_{ext}-$S_{A,ext}$- $S_{B,ext}$ move inside the composition triangle toward E with no effect on feasibility because of infinite reflux ratio.

Close to a limiting value $F_E/F_{min,R\infty}$, SN_{ext} and $S_{A,ext}$ merge and the extractive composition profiles are attracted to a new extractive stable node SN_{ext}' located below the A-E edge. $F_E/F_{min,R\infty}$ is defined as the value for which the process becomes feasible: Extractive composition profiles ending at SN_{ext}' cross a rectifying profile that can reach the vicinity of the expected product (A) (see Figure 2.d).

At finite reflux as F_E/F increase, the extractive unstable separatrix UN_{ext}-$S_{A,ext}$-UN_{ext}' near the A-E edge holds (see Figure 2.e) until SN_{ext} and $S_{A,ext}$ merge at $F_E/F_{min,R>0} > F_E/F_{min,R\infty}$, giving rise to SN_{ext}' (Figure 2.f). In the meantime (Figure 2.f), $S_{B,ext}$ moves toward the vertex E inside the triangle. Consequently, the extractive unstable separatrix UN_{ext}-$S_{B,ext}$-UN_{ext}' remains and now sets unfeasible composition regions located above it (see Figure 2.f) that prevent the total recovery of component A from the column. Knowledge of this unstable separatrix location will help us in the analysis of the optimization results. Besides, the extractive stable separatrix also remains, joining $S_{B,ext}$ to SN_{ext}' and SN_{ext}'' located outside the ternary composition space through the B-E edge. Notice that there exists a minimum reflux ratio R_{min} at a given F_E/F. When $R < R_{min,}$ there is no feasible region for extractive section profile. The size of the unfeasible region increases as R_{min} decreases.

So finite reflux operation is feasible if $F_E/F > F_E/F_{min,R>0}$ and $R>R_{min}$. Now, the more component E is fed to the column, the closer is SN_{ext}' to component E and away from the distillate that is close to component A (see Figure 2.f). For a proper extractive distillation design, it is necessary to enable the extractive section composition at the entrainer feed tray location to reach SN_{ext}'. It allows the connection with a rectifying section that can reach a high purity distillate near A, following approximately a residue curve shape.

2.4.1.2. Product and limiting operating parameter for class 1.0-1a extractive distillation

Figure 2.7 displays the essential features of the 1.0–1a class, corresponding to the separation of a minimum boiling azeotropic mixture A-B with a heavy entrainer E. The univolatility curve $\alpha_{AB} = 1$ and the residue curve map features are also shown.

With a heavy entrainer, the light original component A and the heavy original component B are both residue curve map (rcm) saddle points and form a minimum boiling azeotrope T_{min} $azeo_{AB}$, which is a rcm unstable node. The heavy entrainer E is a rcm stable node. The univolatility curve $\alpha_{AB} = 1$ switches the volatility order of its concerned compounds, and volatility orders are ABE or BAE (see in Figure 2.7) depending on the side (Kiva et al., 2003). In Figure 2.7a (resp.Figure 2.7b), the $\alpha_{AB} = 1$ curve intersects the binary side A-E (resp.

B-E) at the so-called point x_P. Then, A (resp. B) is the expected product in the distillate because it is the most volatile in the region where it is connected to E by a residue curve of decreasing temperature from E to A (resp. B). This matches the general feasibility criterion under infinite reflux ratio for extractive distillation (Rodríguez-Donis et al., 2009). The point x_P will give us information about the minimum content of entrainer ($F_E/(F+F_E)$) (see section 4.2.1). Below this value, the terminal point of the extractive section profiles, SN_{ext}', lies on the univolatility curve. Above this value, SN_{ext}' leaves the univolatility curve to lie near the [x_P; E] segment (Frits et al., 2006; Knapp and Doherty, 1994; Rodríguez-Donis et al., 2009; Shen et al., 2013). Then the extractive profile can cross a rectifying profile, which is approximated by a residue curve under infinite reflux ratio and which reaches the vicinity of the product, ex. A (resp. B).

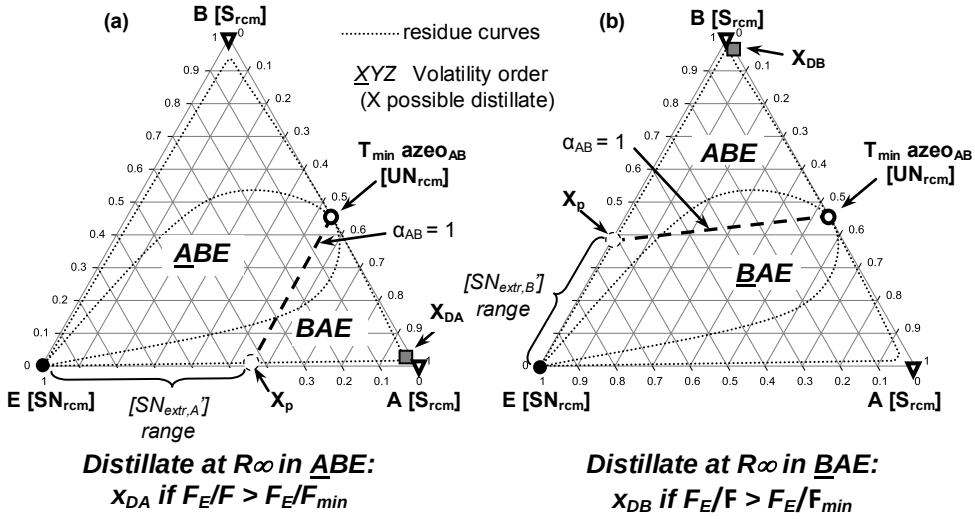

Figure 2.7 – Thermodynamic features of 1.0–1a mixtures. Separation of a minimum boiling azeotrope with a heavy entrainer. (adapted from Shen et al., 2012)

2.4.1.3. Foregone feasibility research of our group

Using illustrative examples covering all subcases, but exclusively operated in batch extractive distillation, Rodriguez-Donis and colleagues found that Serafimov's classes covering up to 53% of azeotropic mixtures were suited for extractive distillation : 0.0-1 (low relative volatility mixtures), 1.0-1a, 1.0-1b, 1.0-2 (azeotropic mixtures with light, intermediate or heavy entrainers forming no new azeotrope), 2.0-1, 2.0-2a, 2.0-2b and 2.0-2c (azeotropic mixtures with an entrainer forming one new azeotrope). For all suitable classes, the general criterion under infinite reflux could explain the product to be recovered and the possible existence of limiting values for the entrainer flow rate for batch operation: a minimum value for the class 1.0-1a, a maximum value for the class 1.0-2, etc. The behavior at finite reflux could be deduced from the infinite behavior and properties of the residue curve maps, and some limits on the reflux were found. However precise finding of the limiting values of reflux or of the entrainer flow rate required other techniques.

Shen et al (2013a, 2013b) extended the general feasibility criterion from batch to continuous mode of minimum- and maximum-boiling azeotropic mixtures with a heavy entrainer belonging to class 1.0-1a and

1.0-2 ternary diagrams. They assessed the feasible product and feasible ranges of the operating parameters reflux ratio (R) and entrainer/feed flow rate ratio for continuous (F_E/F) and batch (F_E/V) operation. Class 1.0-1a processes allow the recovery of only one product because of the location of the univolatility line above a minimum value of the entrainer/feed flow rate ratio for both batch and continuous processes. A minimum reflux ratio R also exists.

Figure 2.8 emphasizes the universal behaviors of all 1.0-1a class mixtures. It refers to the separation of the acetone-methanol minT azeotropic mixture with heavy water (1.0-1a). The column specifications are given by Knapp et al., (1990). Calculations are done with $x_{DAcetone} = 0.98$ as acetone (A) is the product because $\alpha_{AB} = 1$ reaches the A-E side. For this mixture, the minimal reflux increases a significant 2.5 fold for the continuous process at R = 20: the batch process is feasible for $F_E/V = 0.13$ (equivalent to $F_E/F = 2.5$), whereas the continuous process is feasible above $F_E/F = 4.5$. For more detail, see Shen et al., (2012)

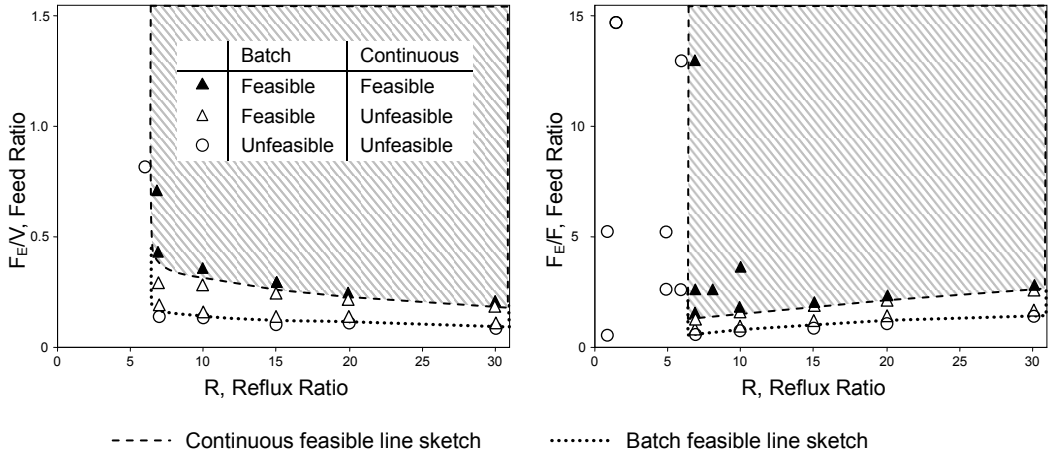

Figure 2.8 – Extractive distillation of acetone-methanol with water (1.0-1a class). Feed ratio as a function of the reflux ratio to recover 98% mol acetone. (adapted from Shen et al., 2012)

For identical target purity, the minimum feed ratio is higher for the continuous process than for the batch process, for the continuous process where stricter feasible conditions arise because the composition profile of the stripping section must intersect that of the extractive section. Class 1.0-2 mixtures allow either A or B to be obtained as a product, depending on the feed location. Then, the univolatility line location sets limiting values for either the maximum or minimum of the feed ratio F_E/F. The feasible range of operating parameters for the continuous process is again smaller than that for the batch process.

2.4.2.Feasibility assessed from intersection of composition profiles and differential equation

The feasibility assessment always relies upon intersection for composition profiles in the various column sections (rectifying, extractive, stripping), joining the top and bottom composition, whatever the operation parameter values (reflux, flow-rates...) (Frits et al., 2006).The process is feasible if the specified product compositions at the top (x_D) and the bottom (x_W) of the column can be connected by a single or by a composite composition profile.

A single composition profile belongs to one column section and a composite composition profile is composed by two or three column section composition profiles connected at some punctual composition. The number of section depends on the column configuration. The column section profiles are described by the general finite differential model of (Lelkes et al., 1998a):

$$\frac{dx_i}{dh} = \pm \frac{V}{L} \cdot \left[y(x) - y_i^* \right] \tag{2.11}$$

Where V and L are the vapor and liquid flow-rates within the column, the vapor composition y* in equilibrium with x is computed by the liquid-vapor equilibrium relation and the actual vapor composition y is computed from the mass balance in each column section, depending on the chosen column configuration (Rodriguez-Donis et al., 2007).

This differential equation is an initial value problem that should be solved by starting the computation from a known liquid composition. The double sign ± shown in equation (2.11) is to be actualized according to the direction (top down or bottom up) considering that column height h is equal to zero at the top. Therefore, equation (2.11) must be used in computing the liquid composition profile of a rectifying, extractive and stripping column section with an adequate definition of the initial point for x, and the direction of the solution and the mass balance equation for y. The driving force applied in equation (2.11) is to be understood at a given column height h. This is valid even at the very top of the column. The composition of the vapor emerging from the column top, and the imagined vapor composition that would be in equilibrium y* with the countercurrent liquid x_0 are in the same relation. Therefore, the composition of this countercurrent liquid x_0 is a good candidate to be an initial point for the higher (rectifying or extracting) column section and the equation is solved top down. Otherwise, if the bottom composition x_W is known then it can be directly applied as the initial value, and equation (2.11) is solved bottom up in the lowest (stripping) column section keeping a negative sign.

Thus, computation of the top (rectifying or extractive) column section composition profile should be started from the composition of the liquid flowing on the top of the column if there are at least two column sections. This is called 'the top liquid composition', and denoted by x_0. The top liquid composition x_0 is identical to the composition of the reflux stream x_R if there is not external feed mixed with the liquid reflux. This x_R, in turn, is identical to the distillate composition x_D if there is no decanter (homogeneous extractive case). If there is a liquid phase distribution then, the composition of the reflux stream x_R is determined by the compositions x_D and the distributed liquid phases, and the reflux ratio R, together. Besides, if there is some external liquid feed sent to the top of the column then it should be accounted as a feed mixed to the reflux stream. The top liquid composition x_0 is then determined by the mass balance of mixing the external feed stream to the reflux stream. Finally, if there are three sections in the column then the rectifying and stripping composition profiles begin at x_R and x_W, respectively, whereas for exploring the range of potentially valid extractive composition profiles (the intermediate column section) a series of composition profiles should be

computed started from several points in the composition triangle. The more detailed relation of equation 2.11 for the rectifying, stripping and extractive section, please refer Gerbaud and Rodriguez-Donis, (2014) for both batch and continuous mode.

2.4.3.Extractive process feasibility from pinch points analysis

In 1985, Levy and coworkers (Levy et al., 1985; Levy and Doherty, 1986) proposed an algebraic trial-and-error tangent pinch points procedure for determining the minimum reflux ratio without the necessity of lengthy iteration schemes involving column profile calculations. The method consisted in finding the value of reflux which makes the feed pinch point, the saddle pinch point, and the controlling feed composition collinear but was restricted to ternary mixtures. (Knapp and Doherty, 1990, 1994) used bifurcation theory to analyze the separating behaviors of the acetone – methanol azeotrope with water belonging to the 1.0-1a class and related the feasibility to the appearance of saddle-node bifurcation points and branching points. Feasible processes required that a ternary saddle originating from a pure component exists whereas the appearance of a ternary unstable node on the pinch branch originating at the azeotrope led to an unfeasible separation. Once the minimal value was known, some heuristics to set the operational values of R and F_E is also shown. For the same 1.0-1a mixture as in the study of Knapp and Doherty, (1994), Frits et al., (2006) used an interval arithmetic-based branch-and-bound optimizer to find limiting flows based on the existence and location of singular points and separatrices in profile maps for batch extractive distillation. They found a feasible process under infinite reflux above a minimal entrainer flow rate which corresponded to the merging of a stable pinch point originating from the azeotrope with a saddle point originating from a pure component, this point agrees with the study of (Knapp and Doherty, 1994) . Finite reflux analysis showed that the pinch points moved inside the composition triangle and brought unfeasible regions.

Brüggemann and Marquardt (2004) exploited a fully-automated shortcut design procedure to determine the limit value. The method is based on the approximation of all column profiles by so-called rectification body method (RBM) which is constructed from nonlinear analysis of the pinches of each section (Bausa et al., 1998). Like Knapp and Doherty (1994), they also set some operational constraint to determine the quasi-optimal values once the minimal values of R and F_E are known. All was incorporated into a general algorithm for the determination of the optimal values of the entrainer flow rate and the reflux ratio. Kossack et al., (2008) then used the RBM method as a second screening criterion for evaluating the extractive distillation entrainer candidates. Fast and efficient, the method bears some critics when the profiles are highly curves because each rectification body has straight boundaries (Lucia et al., 2008).

Most recently, Petlyuk et al., (2015) described a general method *infinitely sharp splits* for the search and identification of possible splits of extractive distillations in any ternary azeotropic mixture. In an extractive column at infinite height and finite reflux, this method can find all feasible product compositions. Limiting parameters of the entrainer flow rate and the reflux ratio are determined fast and robustly from the local *K*-values (vapor–liquid distribution coefficients) of all three components along the sides of the concentration triangle. Besides, the method can determine the required number of trays in all the column sections for a

given product specifications. Therefore, both operating and capital costs can be analyzed without cumbersome simulations.

2.5. Research objectives

Azeotropic and close boiling components are commonly encountered in fine-chemical and specialty industries. Extractive distillation is the widely used process for separating azeotropic and close boiling mixture, but its high-energy consumption is a major main disadvantage, which requires dispatching (Van Duc Long and Lee, 2013). In other hand, global climate change has recently begun to affect human life as global energy consumption continues to increase (Gao et al., 2013). Therefore, researches on how to save energy and capital cost during extractive distillation process would provide not only economical benefits but also environmental benefits. Following the *onion* model mentioned before, extractive distillation process itself and process integration are the two main aspects. Extractive distillation process itself includes the column retrofitting and process optimal design. Process integration includes heat integration, heat pump and utilities. Entrainer selection affects both process itself and process integration, and also the environmental benefits.

First, we focus on the entrainer selection from the literatures for the separation of acetone-methanol minimum azeotropic mixture as it is one of the most studied examples in literature. Then aiming at energy saving and environmental benefits, we introduce a two-step optimization procedure with case study and do the column retrofitting (keep the column tray number as literature) because column retrofitting is performed more often than the installation of new equipment since distillation requires large capital investment (Gadalla et al., 2003).

Second, we show how thermodynamic insight can be used to improve the design of a homogeneous extractive distillation process based on the knowledge of process feasibility and univolatility line. The analysis of the ternary residue curve map and isovolatility curves shows that the column operating pressure has a strong effect on the minimal entrainer amount and the relative volatility. We define a novel extractive efficiency indicator to compare the optimality of different designs and explain why the energy cost and TAC is reduced since the efficiency indicator E_{ext} describes the ability of the extractive section to discriminate the desired product between the top and the bottom of the extractive section. In order to further demonstrate that thermodynamic insight can work as a guideline for process optimal design, we study another case with the same methodology.

Third, focusing on the process optimal design, a two step optimization strategy for extractive distillation is introduced in order to completely consider the effects of the thermodynamic efficiency indicator E_{ext} and e_{ext} on the extractive distillation process as well as OF and TAC.

Fourth, in order to further reduce the energy cost and environmental pollution, double-effect heat integration and heat pump technology are taken into account for extractive distillation process and compared from the

economical view by total annual cost and environmental aspect by CO_2 emissions. Based on the character of extractive distillation, we propose a novel optimal partial heat integration process, and a new partial VRC and new partial BF process in order to reduce the high initial capital cost of compressors.

Chapter 3. Optimal Retrofits of ED, Acetone-Methanol with Water

Results in this chapter have been published in

Congress ESCAPE 24: You, X., Rodriguez-Donis, I., Gerbaud, V., 2014. Extractive Distillation Process Optimisation of the 1.0-1a Class System, Acetone - methanol with Water, in: Computer Aided Chemical Engineering. Elsevier, pp. 1315–1320.

3.Optimal retrofits of extractive distillation, acetone-methanol with water

3.1.Introduction

Process retrofitting has proved to be a beneficial option for improving energy efficiency and reducing CO_2 emissions (Mahmoud et al., 2009). Avoiding inefficient use of energy through better operating practice or improved process design can decrease energy consumption and gas emissions. A wide range of process improved design and process integration concepts for saving energy have been developed and successfully applied to improve the energy efficiency of existing process sites (Gharaie et al., 2015). In this chapter, we will introduce a four step optimization procedure for the process retrofitting of the extractive distillation aiming at saving energy.

For decades, the separation of acetone-methanol azeotropic mixture is an hot topic in extractive distillation (Laroche et al., 1991; Knapp and Doherty, 1994; Hilal et al., 2002; Frits et al., 2006; Kossack et al., 2008; Luyben, 2008; Gil et al., 2009; Botía et al., 2010; Orchillés et al., 2012; You et al., 2014, 2015). The acetone-methanol mixture is the main components in the aqueous product obtained from hydrocarbon syntheses by the Fischer-Tropsch process. Acetone and methanol are extensively applied in chemical engineering. Acetone is used as crude material for the production of epoxy resin, polycarbonate and so on, and as good solvent for coating and cement, and as extractant in industries such as oil production industry. Methanol is used as solvent in petroleum industry, and as reagent for organic products and so on. For azeotropic mixture, the description of the vapor-liquid equilibrium is the crucial issue.

Both acetone and methanol can be distillates depending on the location of univolatility line toward the AE or BE side (Rodriguez-Donis et al., 2009a; Shen et al., 2013). The polar entrainer associate with methanol and produce acetone as the distillate product in the extractive column, while the nonpolar entrainer binds with acetone and produces high purity methanol as the distillate product in the extractive column, even though methanol is the intermediate-boiling component in the original mixture (Kossack et al., 2008). Several entrainer candidates can be found: (Laroche et al., 1991) suggest water, ethanol, isopropanol and chlorobenzene, while (Lei et al., 2003) add ethylene glycol as entrainer candidate. Kossack et al. (2008) reported more entrainer by using computer-aided molecular design (CAMD) method, as shown in Table 3.1 and Table 3.2.

After comparing the results from rectifying body method (RBM) and mixed integer non-linear programming (MINLP), Kossack et al. (2008) concluded that selectivity should not be used alone to predict entrainer performance, and that DMSO and chlorobenzene should be the entrainer, but water is probably more preferable since it is environmentally friendly and only induces a moderate economic penalty. Notice that when water is used as entrainer, Kossack could only obtain the methanol purities at 98.2% mol instead of

99.5% mol, whereas (Luyben, 2008) obtained 99.5% mol product purities for both acetone and methanol by using the same thermodynamic model Uniquac and the same built-in binary parameters from Aspen plus software. Therefore, we will study the separation of acetone-methanol mixture using water as entrainer with Luyben's design as initial value and for comparison, and try to explain why some author can't obtain high purity methanol.

Table 3.1 – Entrainer candidates for acetone-methanol separation with acetone as the distillate (from Kossack et al.,2008)

Entrainer	T_{boil}/K	S_{ij}^{∞} Unifac	S_{ij}^{∞} Uniquac
Water	373.15	4.81	2.42
Ethylene glycol	470.45	2.99	4.19
Ethanol	351.44	1.76	1.65
DMSO	464.0	1.47	2.89
Isopropanol	355.41	1.3	1.72

Table 3.2 – Entrainer candidates for acetone-methanol separation with methanol as the distillate (from Kossack et al.,2008)

Entrainer	T_{boil}/K	S_{ij}^{∞} Unifac	S_{ij}^{∞} Uniquac
chlorobenzene	404.87	5.51	5.84
Ethylbenzene	409.35	4.59	1.04
p-xylene	411.51	4.40	2.32
m-xylene	412.27	4.40	---
o-xylene	417.58	4.40	---
Mesitylene	437.89	3.75	---
1,2,4-trimethylbenzene	442.53	3.59	---
1,2,3-trimethylbenzene	449.27	3.59	---
Benzyl ethyl ether	458.15	2.53	--

According to Gmehling and Bölts (1996) from experimental data, acetone forms a minimum-boiling azeotrope with methanol at 99.28 kPa with an azeotropic temperature of 54.7℃ and azeotropic composition of 78.63 % mol acetone. Just as recommended by Gil and coworkers (Gil et al., 2009, Botia et al., 2010), compared with Wilson and NRTL model, the UNIQUAC physical property model is the most suitable one to predict VLE of acetone-methanol with water system following the experimental data. Thus, UNIQUAC model is used to describe the non-ideality of the liquid phase and the vapor phase is assumed to be ideal gas. The UNIQUAC model binary parameters of this system are taken from Aspen Plus as shown in Table 3.3.

The reliability of the binary parameters is proved through two aspects: one is comparing T-xy map and y-x map with the liquid-vapor data from DECHEMA (Gmehling and Onken, 1977), and the other one is comparing the azeotropic temperature and composition of the azeotropic point with the experimental data.

Figure 3.1 demonstrates that the model fits the experimental data well and the binary parameters are valid. With UNIQUAC model, the predicted azeotropic temperature and azeotropic composition (at 99.28kPa) are shown in Table 3.4. The predicted result agrees very well with experimental data.

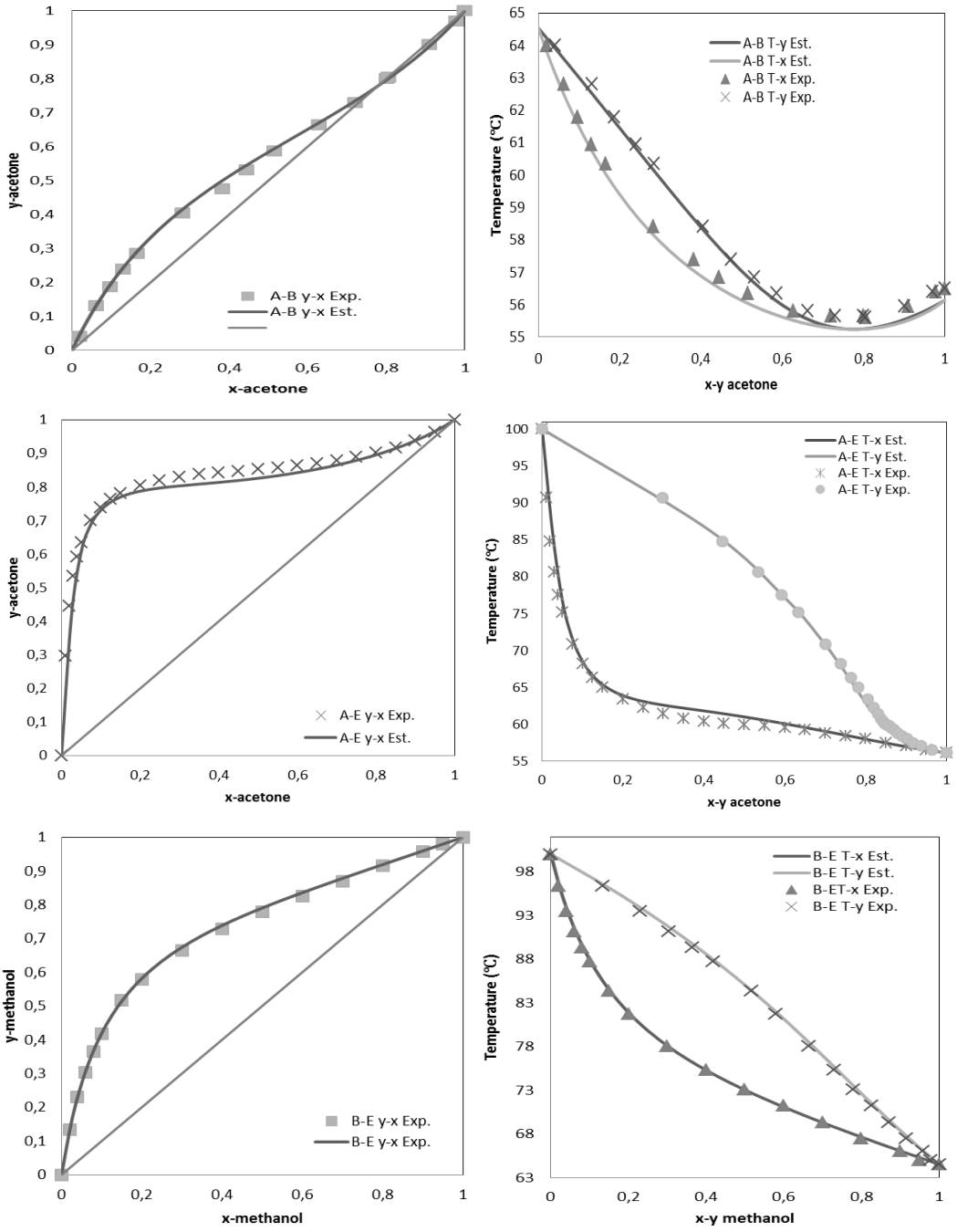

Figure 3.1 – T-xy and y-x experimentand predicted maps at 1 atm for acetone (A)-methanol (B)-water (E) system

Table 3.3 – Model binary parameters of acetone-methanol-water system

Component i Component j	Acetone Methanol	Acetone Water	Methanol Water
aij	0	8.6051	-1.0662
aji	0	-4.8338	0.6437
bij	-225.153	-3122.58	432.8785
bji	52.7705	1612.196	-322.131

Table 3.4 – Experimental and predicted data of azeotropic point at 99.28 kPa

Azeotropic data	Pressure /kPa	Temperature/^{0}C	Composition/ mol %	
			acetone	methanol
Experiment	99.28	54.7	78.63	21.37
Predict value	99.28	54.67	78.05	21.95
	101.325	55.20	77.74	22.26

3.2. Optimal method and procedure

3.2.1. Extractive process feasibility

Inspired by works of Laroche and coworkers (Laroche et al., 1991; Lionel Laroche et al., 1992) and others(Knapp and Doherty, 1994; Lelkes et al., 1998a; Stéger et al., 2005), our team published a general feasibility criterion for extractive distillation under infinite reflux ratio (Rodríguez-Donis et al., 2009a). In ternary map, the volatility order is set by the univolatility curves. They found that Serafimov's classes covering up to 53% of azeotropic mixtures were suited for extractive distillation: 0.0-1 (low relative volatility mixtures) (Rodriguez-Donis et al., 2009b), 1.0–1a, 1.0–1b, 1.0–2 (minimum or maximum boiling azeotropic mixtures with light, intermediate or heavy entrainers forming no new azeotrope) (Rodriguez-Donis et al., 2009a, 2012a, 2012b; Shen et al., 2013; Shen and Gerbaud, 2013), 2.0-1, 2.0-2a, 2.0-2b and 2.0-2c (azeotropic mixtures with an entrainer forming one new azeotrope) (Gerbaud and Rodriguez-Donis, 2014). For all suitable classes the general feasibility criterion could explain which product can be recovered under infinite reflux ratio, which direct or indirect split configuration is required and the possible existence of limiting values for the entrainer flow rate. The behavior at finite reflux ratio could be deduced from the infinite value behavior and from the properties of the extractive profile maps. Limits on the reflux ratio were described for the most frequent classes (Li and Bai, 2012; Shen et al., 2013; Shen and Gerbaud, 2013).

The univolatility curve α_{AB} = 1, 2 and 3 intersects the binary side A-E as shown on Figure 3.2 displaying also the residue curve map.

Combining the general feasibility criterion and Figure 3.2, we know that acetone is the only possible distillate with water as entrainer, the process configuration is direct split and there is minimum entrainer flow rate, which can be calculated from the point x_p with the following equation 3.1 and 3.2.

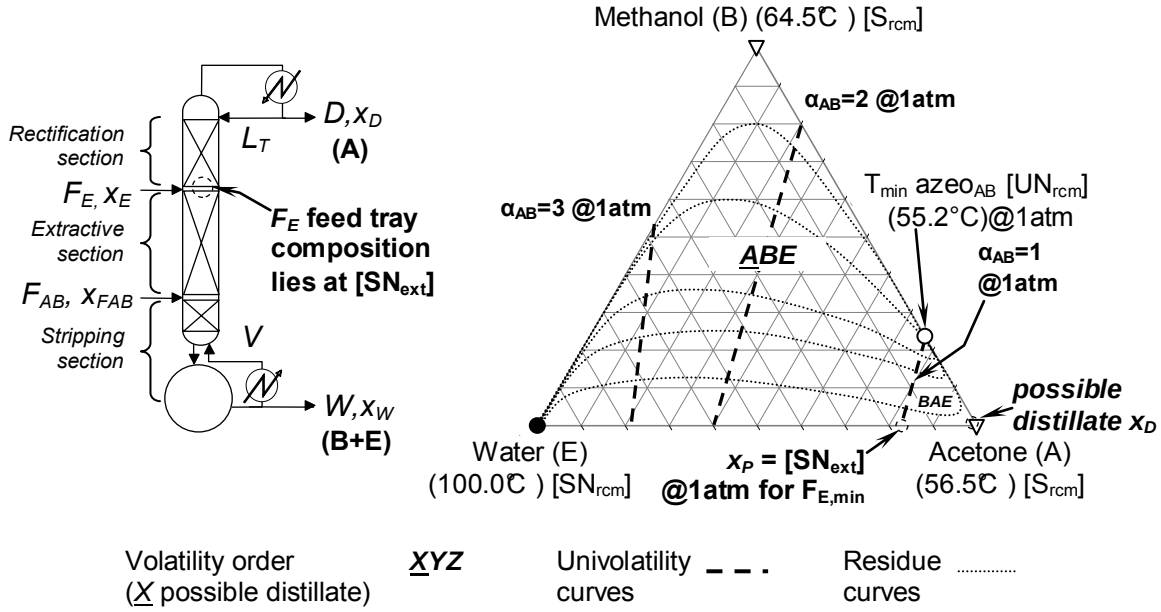

Figure 3.2 – Extractive distillation column configuration and acetone – methanol – water 1.0-1a residue curve map at 1 atm with univolatility curves at 1 atm

The batch minimum entrainer flow rate F_E/V depending on the vapor flow rate V produced at the boiler is defined by the equation 3.1 (Lelkes et al., 1998a):

$$\left(\frac{F_E}{V}\right)_{\min,R\infty} = \frac{(x_P - y^*_P)}{(x_E - x_P)} \tag{3.1}$$

Where y^*_P is the entrainer amount in the vapor phase in equilibrium with x_P and x_E is the entrainer composition. It can be transposed to a minimum entrainer flow rate for continuous operation F_E/F_{AB} with the following equation (Gerbaud and Rodriguez-Donis, 2014; Shen et al., 2013; Shen and Gerbaud, 2013).

$$\left(\frac{F_E}{F_{AB}}\right) = (R+1)\cdot\left(\frac{F_E}{V}\right)\cdot\left(\frac{D}{F_{AB}}\right) \tag{3.2}$$

The [SN_{ext}] point location is critical to the process understanding because it describes approximately the composition in the column on the entrainer feed tray location, where the extractive section and the rectifying section connect together. By considering the locations of the [SN_{ext}] and the liquid composition at the main feed tray, we show how the design of an extractive distillation process based on the values published by (Luyben, 2008) can be further improved in chapter 3 and 4.

3.2.2.Optimal method

Compared with a simple conventional distillation, the difficulties of the extractive distillation process design lie on a greater number of degrees of freedom and the recommended recycling of the entrainer with impurity. The entrainer flowrate and entrainer feed location are all the additional degrees of freedom. The optimization of extractive distillation is usually considered as a large size problem because of the solving of a significant

number of strongly nonlinear equations. Besides, good initial values are needed for solving the nonlinear programming subproblems (Vázquez-Ojeda et al., 2013). For the optimization methods of extractive distillation, there are sensitivity analysis (Gil et al., 2009; Luyben, 2008), sequential iterative optimization (Wang et al., 2012), Sequential Quadratic Programming (SQP) (Figueirêdo et al., 2011; Kiss and Suszwalak, 2012), mixed-integer nonlinear programming (MINLP) (García-Herreros et al., 2011; Kossack et al., 2008), genetic algorithm (GA) (Gutérrez-Antonio et al., 2011; Leboreiro and Acevedo, 2004) and so on. Besides, the the common procedure for optimizing extractive distillation process is that: first, optimizing the extractive column and then the entrainer regeneration column. In this chapter, we will show the importance of optimizing the two columns together.

For a detailed process design, an economic trade-off must be found between the investment and operating costs. For the extractive distillation process both the extractive column and the entrainer regeneration column should be included and connected with the solvent recycle stream. For finding optimal parameters for the acetone – methanol separation with water, some authors have run a sensitivity analysis over the process variables, namely the reflux ratio, the entrainer–feed flow rate ratio, the number of trays in each of the rectifying, extractive, stripping column sections and the distillate flow rate (Gil et al., 2009; Hilal et al., 2002; Langston et al., 2005; Luyben, 2008). Luyben, (2008) performed a sensitivity analysis of the effect of reflux ratio and solvent flow rate on the acetone purity. He concluded that a solvent – feed flow rate ratio of 2.06 was needed to achieve the desired 99.5 mol% acetone purity. However, the procedure is tedious and may fail to find the best solution. Caballero et al., (2005) presented a superstructure-based optimization algorithm that combines the capabilities of commercial process simulators and generalized disjunctive programming. With the proposed method, the rigorous design of distillation columns in which operational conditions (reflux and reboil ratios, recoveries etc.) and the structural parameters (number of trays, location of feed and product streams etc.) are simultaneously optimized, but it requires good initial values and bounds to converge. Kiss and Suszwalak, (2012) used the Aspen built-in SQP method to optimize the extractive distillation process for the separation of ethanol-water with ethylene glycol as entrainer in both a two-column classic sequence and an extractive dividing-wall column. Several authors formulated a MINLP problem to optimize simultaneously both the continuous variables (reflux, entrainer flow rate) and the discrete variables (total number of tray, feed tray location). Kossack et al., (2008) used a successive relaxed MINLP (SR-MINLP) procedure to reduce the influence of the initial guess on the final result. García-Herreros et al., (2011) looked at the ethanol extractive dehydration with glycerol as entrainer and solved the MINLP problem through a two-level strategy that combines stochastic and deterministic algorithms.

In this chapter, we fixed the two column tray numbers due to two aspects: the column retrofitting in industry and comparison our design with literatures. We use optimizing procedure as (Figueirêdo et al., 2011): basing on an SQP scheme built in Aspen plus simulator for optimizing the continuous variables and a sensitivity analysis over the feed locations. Unlike Figueiredo's work and following Kossack et al., (2008), we consider the two column sequence of extractive distillation process as in Figure 3.3. The two columns are strongly

coupled: The entrainer-feed flow rate ratio F_E/F_F and composition x_{FE} are key optimization variables, along with the reflux ratio R_1. But as F_E/F_F and x_{FE} impact the liquid residue which feeds the entrainer regeneration column, they also affect the reflux ratio of the entrainer regeneration column R_2. Besides, the entrainer recycle purity and flow rate from the regeneration column affect the extractive column separating effect, possibly preventing to achieve the distillate purity as specified. Notice that the pressure drop is neglected in this chapter.

3.2.3.Extractive distillation process flow sheet

The traditional process flow sheet of extractive distillation process is presented in Figure 3.3 as it is set in Aspen Plus. Notice that the simulation is run by using the MESH rigorous model *Radfrac* in Aspen Plus, and that the tray number is counted from top to bottom of the column, and condenser is considered as the first tray in all of the manuscript. Simulation flowsheets have been tested in Prosim plus and the same results were achieved.

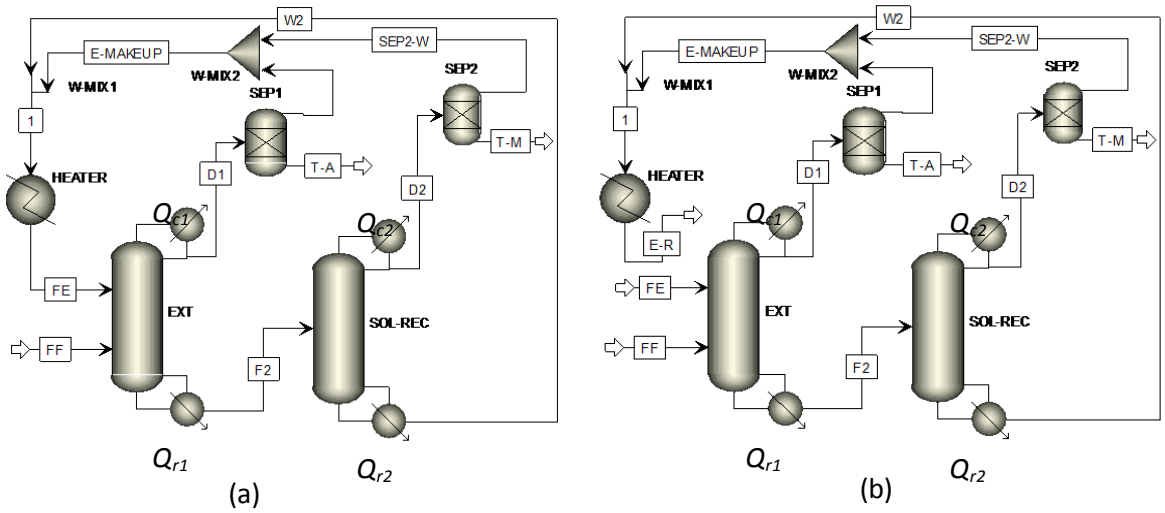

Figure 3.3 – Closed loop (a) and open loop (b) flow sheet of the extractive distillation process

The extractive column is fed with entrainer and azeotropic mixture, where the product A (acetone) is recovered from the distillate and the mixture B+E is fed to the entrainer regeneration column. This second column removes product B (methanol) from the distillate and recycles the entrainer (water) from the bottom. The recycled entrainer is cooled before entering the extractive column to a temperature preset at 320 K, matching Luyben's process value for the sake of comparison

The process needs a make-up entrainer to compensate losses with the products. As the flow rate of make-up entrainer is not known beforehand, we equal it to the entrainer losses combined after sharp splits on the two product distillates.

The open loop flow sheet in Figure 3.3b is used during the optimization procedure with a pure entrainer feed because it allows more robust convergence of the simulation. It is systematically checked with the closed loop flow sheet that corresponds to the industrial plant, where the entrainer is recycled. But then the recycled entrainer contains some impurities that will affect the operation of the extractive column.

3.2.4.Objective function (OF)

For a process optimization, the importance of defining a suitable objective function is obvious. (Figueirêdo et al., 2011) used the ratio of the reboiler heat duty of extractive distillation column and the specified production flowrate (Q_R/D) as objective function. The condenser heat duty is then neglected despite its impact on the process cost; and the regeneration column is not taken into account. Furthermore, it discards the differences of the two products' prices. Arifin and Chien, (2008) used the total annual cost (TAC) including capital cost and operating cost as objective function. They showed that it exhibits a minimal value vs the total number of trays for the extractive process sequence columns.

Inspiration of the work above, we define a novel objective function and do some improvements. Our objective function for the optimization of variables is:

$$\begin{aligned} \min OF &= \frac{Q_{r1} + m \cdot Q_{c1} + Q_{r2} + m \cdot Q_{c2}}{k \cdot D_1 + D_2} \\ subject\ to &: x_{acetone,D1} \geq 0.995 \\ & x_{acetone,W1} \leq 0.001 \\ & x_{methanol,D2} \geq 0.995 \\ & x_{water,W2} \geq 0.9999 \end{aligned} \tag{3.3}$$

Constraints 1 and 3 concern the products purity in D_1 and D_2. Constraint 2 in bottom W_1 aims at keeping high the main product recovery. Constraint 4 focuses on the recycling entrainer purity. Q_{r1} and Q_{c1}: extractive column reboiler and condenser duty, Q_{r2} and Q_{c2}: entrainer regeneration column reboiler and condenser duty, D_1 and D_2 extractive column and entrainer regeneration column distillate flow rate, k = 5.9: product price factor for acetone vs methanol, m = 0.036: energy price difference factor for condenser vs reboiler. Update of k and m is done by using chemicals prices and (Douglas, 1988) costs method with Marshall and Swift inflation index corrections. Compared with previous works where the optimization is done by minimizing only reboiler duty (Li and Bai, 2012; Luyben, 2008), or by Qr/D with the cost of condenser been neglected (Figueirêdo et al., 2011), our OF accounts for both columns energy demands, but also reflects the weight coefficient of the two product prices k and reboiler vs condenser cost price m. Then our OF reflects the operation of the entrainer regeneration column. The meaning of *OF* is the energy consumption used per product unit flow rate (kJ/kmol). *OF* is sensitive to the variables F_E/F_F, R_1, R_2, D_1, D_2 and the three feed location as well.

Finally the *TAC* is calculated for each optimal solution. We use the *TAC* formula of Li and Bai (2012) with Douglas' costs correlations. The payback period is considered as 3 years and Douglas' cost formulas (Douglas, 1988) are used with Marshall and Swift inflation 2011 index (M & S = 1518.1) (Marshall & Swift, 2011).

$$TAC = \frac{capital\ cost}{payback\ \ period} + operating\ costs \tag{3.4}$$

The capital cost includes column shell, tray and heat exchanger costs; the operating cost group the reboiler and condenser energy cost. To emphasize the effect of the entrainer flow rate recycle on the process, the heat exchanger annual cost is taken into account. The energy cost of the reboiler is 3.8 $ per GJ, after consulting a chemical company in Chongqing China. Other costs such as the liquid delivery pumps, pipes, valves are neglected at the conceptual design stage that we consider. Details of calculation are given in Appdix.

3.2.5.Optimization procedure

- Step 1, minimizing *OF* by optimizing continuous variable F_E, R_1 and R_2 under fixed stage numbers N_{Ext} and N_{Reg} and feed positions N_{FE}, N_{FF}, N_{FReg}.
- Step 2, minimizing *OF* by optimizing D_1, D_2, F_E, R_1 and R_2 as variables.
- Step 3, minimizing *OF*, taking N_{FE}, N_{FF}, N_{FReg}, F_E, R_1 and R_2 as variable with to get optimal value while keeping better values of D_1 and D_2.
- Step 4, corroborating the optimal values by simulation and calculating TAC.

3.3.Results and discussion

We keep Luyben's total number of trays of the extractive column (N_{Ext} = 57) and of the entrainer regeneration column (N_{Reg} = 26). We also keep the same product purity specifications (0.995 molar fraction) for both acetone and methanol, and the same equimolar feed (F_{AB} = 540 kmol/h) at 320 K and preheat the entrainer to 320K as well. In this chapter, the extractive column operating pressure is 1 atm.

3.3.1.First step: continuous variables F_E, R_1, R_2

Table 3.5 displays the optimized F_E, R_1, R_2 while the other variables are kept constant. Results are compared to Luyben's (2008) results that were taken for initializing the procedure. N_{Ext} = 57, N_{Reg} = 26, N_{FE} = 25, N_{FF} = 40, N_{FReg} = 14, equimolar F_F = 540 kmol/h.

Table 3.5 – Step 1, optimal results of F_E, R_1 and R_2

variable	Optimized value			
	Luyben (2008)	F_E	F_E and R_1	F_E R_1 and R_2
F_E, kmol/h	1100	809.0	922.7	883.3
R_1	3.44	3.44	3.228	3.277
R_2	1.6	1.6	1.6	1.491
OF, kJ/kmol	36194.4	35564.1	34864.7	34421.7

We observe (1) a *OF* significant decrease as more variables are taken into account. (2) A 4.9 % energy consumption saving if F_E, R_1 and R_2 are optimized at the same time. (3) that optimizing the regeneration column together with the extractive column improves further the *OF*: when R_2 is taken into account, R_1 becomes bigger, F_E decreases and R_2 gets smaller, If less entrainer is fed to the extractive column, a greater

R_1 is needed to get the same separation effect. Meanwhile the concentration of entrainer fed to the regeneration column decreases due to mass balance, and less energy (R_2 decrease) is used to recycle the entrainer.

3.3.2.Second step: two distillates D_1 and D_2

As the effect of D_1 and D_2 on the product purity is strongly non-linear, the simulation cannot converge steadily, so D_1 and D_2 are varied with a discrete step of 0.1 kmol/h from 270 kmol/h (recovery = 99.5 %) to 271.3 kmol/h (recovery = 99.98 %) and the SQP optimization is run for F_E, R_1 and R_2. The results are shown in Figure 3.4.

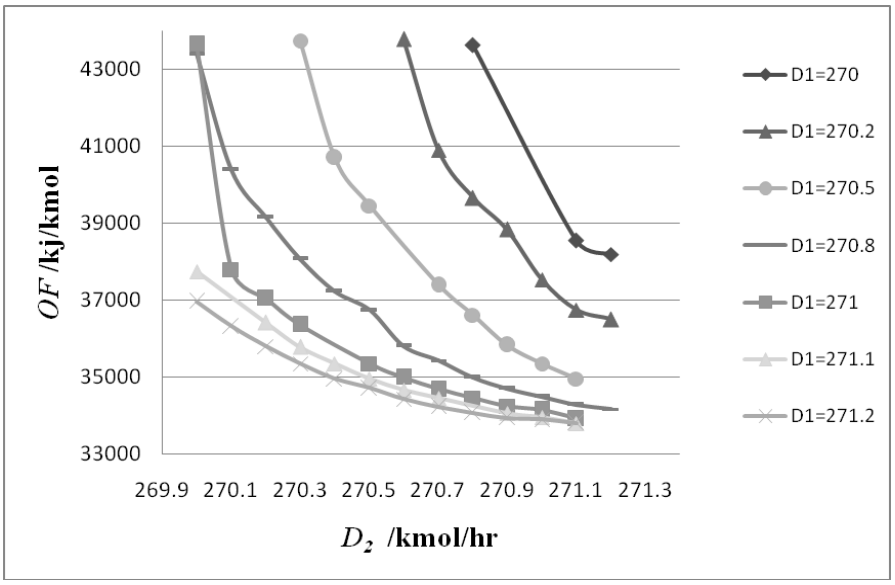

Figure 3.4 – Effects of D_1 and D_2 on OF with D_1, D_2, F_E, R_1 and R_2 as variables

From Figure 3.4, we observe that D_2 in the regeneration column has effect on the total process energy cost, and D_1 = 270.7 kmol/h and D_2 = 271.1 kmol/h published in Luyben's results are not optimal values for our OF. Also, OF decreases with the increase of D_2 (resp. D_1) when D_1 (resp. D_2) is fixed. As we will optimize other variables such as N_{FE}, N_{FF}, N_{FReg}, N_{Ext} and N_{Reg} in the subsequent steps, we select D_1 = 271 kmol/h and D_2 = 271.1 kmol/h; those values corresponding to a product recovery high enough but not too high so as to make the flow sheet convergence difficult. The corresponding OF value is 33911.2 kJ/kmol, with F_E = 901.5 kmol/h, R_1 = 3.255 and R_2 = 1.406.

3.3.3.Third step: three feed locations

The variables N_{FE}, N_{FF} and N_{FReg} are varied through sensitivity analysis and F_E, R_1, R_2 are optimized while D_1 and D_2 are fixed. N_{FE}, N_{FF}, N_{FReg} impact the OF not independently of each other. Thus, the sensitivity analysis over the three feed positions is done with the initial value from Luyben's design. For each group of N_{FE}, N_{FF} and N_{FReg} values (a, b, c) with (a_0=25, b_0=40, c_0=14), the total 27 designs with ranges [a_0-1, a_0, a_0+1] for N_{FE}, [b_0-1, b_0, b_0+1] for N_{FF}, [c_0-1, c_0, c_0+1] for N_{FReg} were optimized simultaneously so as to avoid local minimum. The results were ranked by minimizing OF value in order to obtain the new group of (a_1, b_1, c_1).

Then repeat the process to get (a_2, b_2, c_2) until OF can be minimized further, the corresponding (a_n, b_n, c_n) are the final results for three feed locations. Meanwhile, the three continuous variables F_E, R_1, R_2 are obtained. The key results are in Table 3.6.

Table 3.6 – Optimal results of F_E, R_1, R_2, N_{FE}, N_{FF}, N_{FReg} under fixed D_1 and D_2

N_{FE}	N_{FF}	N_{FReg}	F_E	R_1	R_2	OF kJ/kmol
25	40	14	901.5	3.255	1.406	33911.2
25	40	15	911.8	3.246	1.340	33541.9
29	44	16	847.3	2.934	1.264	31618.6
29	46	17	776.3	2.910	1.216	31104.6
30	44	16	904.0	2.871	1.289	31589.9
31	44	17	927.7	2.866	1.344	31917.1
31	48	15	846.0	2.760	1.321	31145.3
31	48	16	810.8	2.791	1.254	30851.4
31	48	17	806.3	2.797	1.230	30741.4
31	49	18	802.3	2.816	1.258	30962.9
32	48	18	845.1	2.758	1.295	30994.7
32	49	17	838.0	2.776	1.244	30789.0
32	49	18	845.9	2.766	1.295	31031.5

From Table 3.6, we observe that (1) F_E, R_1 and R_2 are changing as the three feed stages change. The impact on *OF* is nonlinear, highlighting again the coupling of all variables and the necessity to consider the regeneration column as well. (2) The best *OF* value is 30741 kJ/kmol, a 9.3 % decrease compared to step 2 and 15.1 % decrease compared to the *OF* for Luyben's design. (3) Compared with line 1 and 2 design results, we see that one tray increase of N_{FReg} will cause the increase of F_E, and decrease of R_1 and R_2, giving a 1.1% reduction of OF. It demonstrates the effect of N_{FReg} in the regeneration column on the process and shows the importance of optimizing the two columns together. (4) The minimum value of *OF* is found for a greater number of trays in the extractive section than Luyben. This point agrees with Rodriguez-Donis et al., (2009a) who have explained for the (1.0-1a) class separation that this is needed to keep the methanol content as low as possible in the extractive section stable node composition. It can be seen in Figure 3.6 that the methanol content is very low at the entrainer feed location where is the extractive section stable node.

3.3.4.Fourth step: closed loop corroboration

All the optimization procedure was done with an open loop flowsheet (Figure 3.3b) where F_E is pure water. As the product purities are constrained in the objective function, they are satisfied. For example, we obtain $x_{acetone,D1}$ = 0.995002 with optimal values from step 3. However when simulating the extractive process flowsheet with a closed recycle loop as in practice, we obtain $x_{acetone,D1}$ = 0.99484 with the optimal values from step 3. This happens because the recycled entrainer purity is then 99.98 % and not pure water and show the importance of the purity of recycled entrainer.

Increasing R_2 would seem at first relevant to improve the recycled entrainer purity, but it is not efficient here because that purity is already very high: a small increase of R_2 to 1.495 to get $x_{water,W2}$ = 0.99999 affects the *OF* that increases from 30741 to 32142 kJ/kmol. Increasing R_1 from 2.797 to 2.823 keeps *OF* low and raises $x_{acetone,D1}$ from 0.99484 to 0.99500 in the closed loop simulation.

3.3.5.The final result and comparing with the design in literature

The final results are shown in Table 3.7 and Table 3.8. For practical implementation, we have ultimately rounded up the optimal values: F_E = 807 kmol/h, R_1 = 2.880, D_1 = 271 kmol/h, R_2 = 1.231, D_2 = 271.1 kmol/h, N_{FE} = 31, N_{FF} = 48, N_{FReg} = 17. The temperature and composition profile maps of extractive column for Luyben's design and our design are shown in Figure 3.5 and Figure 3.6

Table 3.7 – Comparison of our optimal results with Luyben's design

variable	F_E	R_1	R_2	D_1	D_2	N_{FE}	N_{FF}	N_{FReg}	*OF* kJ/kmol	TAC 10^6\$
This work	807	2.880	1.231	271	271.1	31	48	17	30916.6	3.069
Luyben	1100	3.44	1.61	270.7	271.1	25	40	14	36194.8	3.489

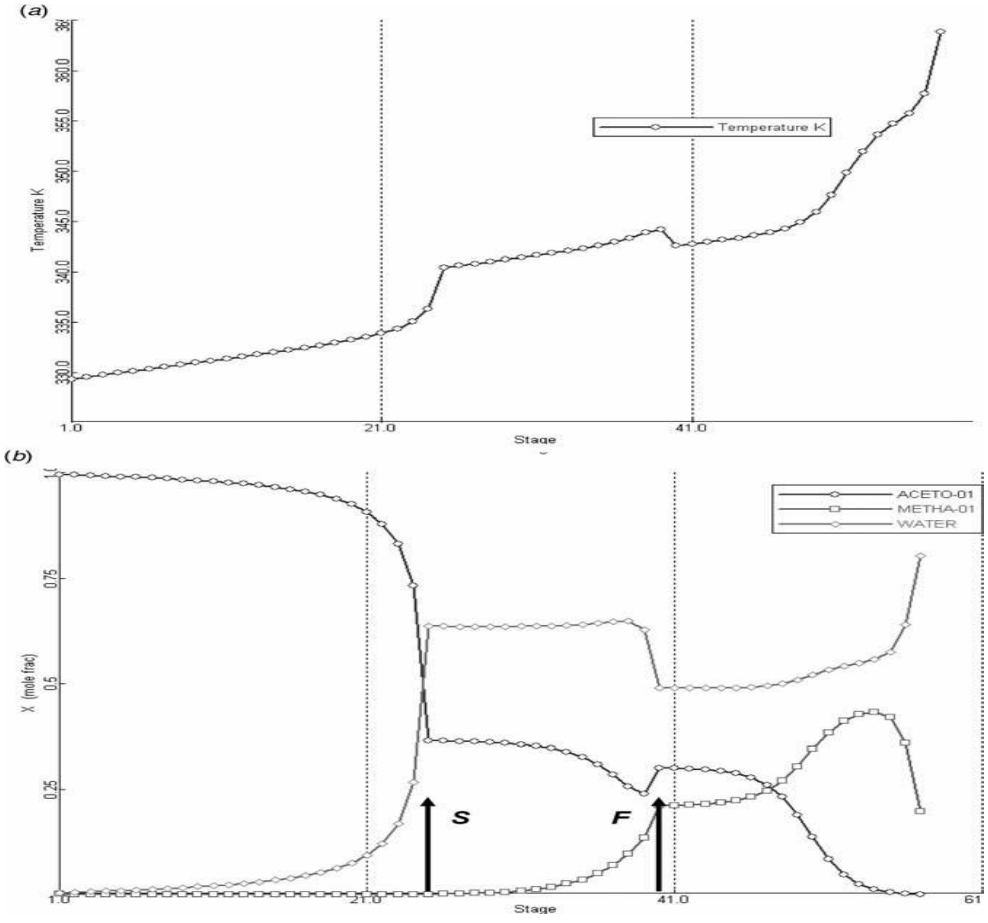

Figure 3.5 – Temperature and composition profiles of extractive column for acetone – methanol with water (adapted from Luyben 2008)

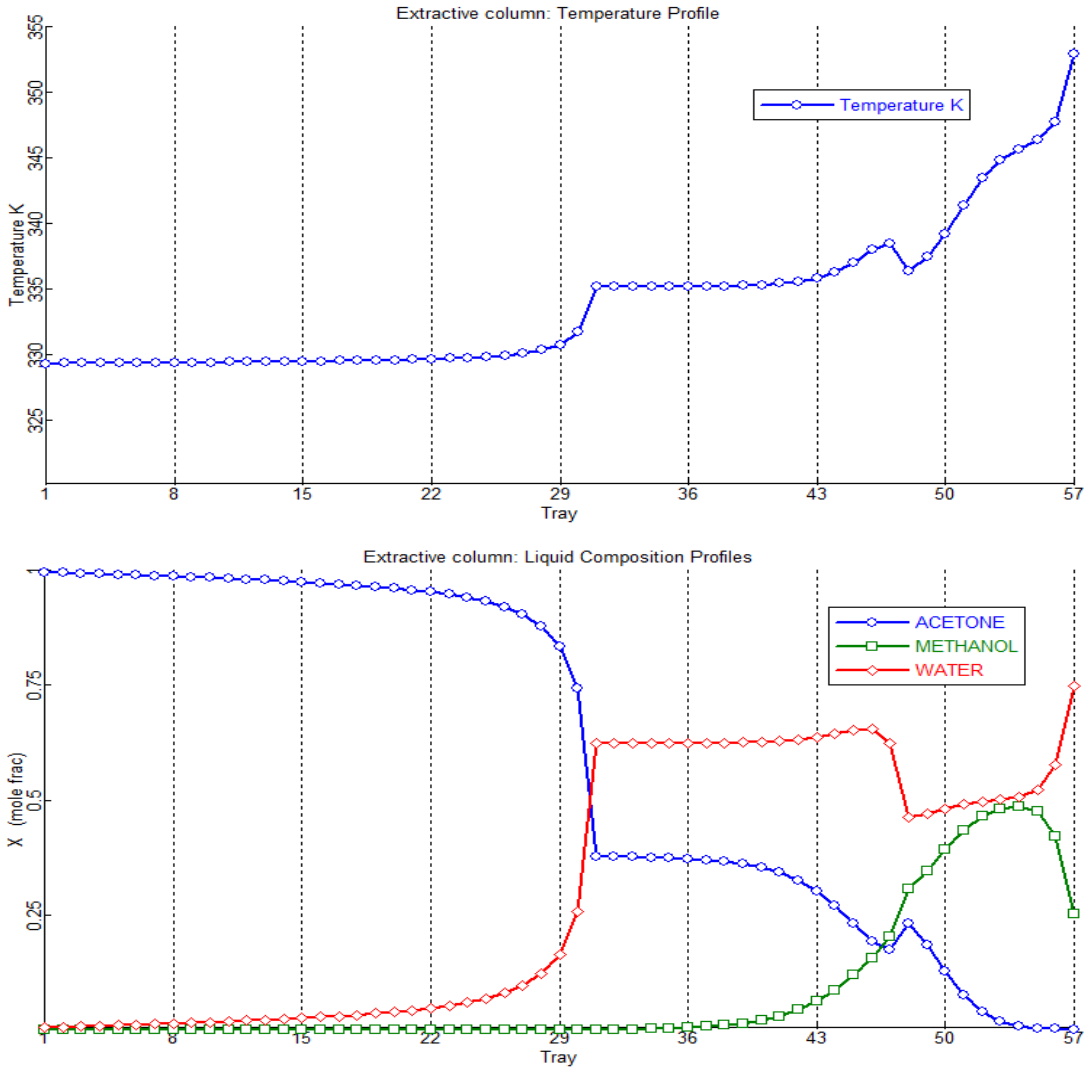

Figure 3.6 – Our design: Temperature and composition profiles of extractive column for acetone – methanol with water

Table 3.8 – Product purities from optimal results and Luyben's design

mole fraction	Mole Frac	D_1	D_2	W_2=*water*	$W_1=F_2$	*recovery*
This work	Acetone	0.99516	0.00115	1.88E-12	0.00029	99.88%
	Methanol	0.00066	0.99529	9.84E-05	0.25084	99.93%
	Water	0.00418	0.00356	0.999901	0.74887	
Luyben	Acetone	0.99573	0.00168	9.51E-15	0.00033	99.83%
	Methanol	0.00017	0.99578	5.64E-06	0.19715	99.98
	Water	0.00410	0.00254	0.999994	0.80252	

From Table 3.7 and Table 3.8, we can see (1) a 14.5 % energy consumption reduction compared to Luyben's design based on the same stage number of columns (N_{Ext} = 57, N_{Reg} = 26). (2) A 12.0 % saving in TAC. (3) A greater production (D_1) while maintaining the product purity and using less both energy and total annual cost.

(4) The recovery of acetone is greater though the recovery of methanol is smaller as the weigh coefficient of acetone is higher than methanol.

Comparing Figure 3.5 with Figure 3.6, we know that (1) The top temperature are very closed, but the entrainer and main feed tray temperature in Luyben's design are higher than our design, it demonstrates that more entrainer water is used, leading to a high water content and a relatively high temperature. (2) From tray number 40 to 45 in Figure 3.5, the temperature and composition just have a little changes, it hints the unnecessary trays are used in stripping section. (3) In our design, two more trays are used in extractive section which is important for extractive column. It agrees with the fact that the extractive section should have enough trays in order to reach the stable node of the extractive section SN_{Ext}, as suggested by earlier works (Lelkes et al., 1998a; Rodríguez-Donis et al., 2009a). (4) 6 extra trays are used in rectifying section in our design that account for reducing R_1 from 3.44 to 2.88, which leads the significant decrease of the condenser and reboiler duties reflected by OF we proposed.

3.4. Conclusions

We have obtained optimal parameters for an extractive distillation process for separating the minimum boiling azeotropic mixture acetone-methanol with water (class 1.0-1a) as entrainer, taking into account the both extractive distillation and the entrainer regeneration columns and compared it with Luyben's design at 1 atm under the constraint of 0.995 mole fraction acetone and methanol products. In a MINLP scheme we have combined SQP optimization for the continuous variables F_E, R_1, R_2, and sensitivity analysis for D_1, D_2, N_{FE}, N_{FF}, N_{FReg}. We have proposed a new objective function accounting for all the energy consumption of per product flow rate value. Compared with Luyben's design in literature, the total annual cost and energy consumption are reduced by 12.0 % and 14.5 % respectively based on the same column stage numbers. It can be predict that more energy and total annual cost will be saved if the column stage numbers are changed and optimized follow the optimization process mentioned in this work.

Chapter 4. Improved Design and Efficiency of Extractive Distillation

Results in this chapter have been published in

Article: You, X., Rodriguez-Donis, I., Gerbaud, V., 2015. Improved Design and Efficiency of the Extractive Distillation Process for Acetone–Methanol with Water. Ind. Eng. Chem. Res. 54, 491–501.

4.Improved design and efficiency of extractive distillation

4.1.Introduction

Following the definition of (Figueirêdo et al., 2011), a well-designed extractive process means obtaining the lowest specific energy consumption and the least loss of solvent, taking into consideration the constraints imposed on the process. In this chapter, we consider the extractive distillation of the minimum boiling azeotrope acetone (A) – methanol (B) with a heavy entrainer E, belonging to the 1.0-1a-m1 extractive separation class (Gerbaud and Rodriguez-Donis, 2014). The acetone-methanol azeotrope is also pressure-sensitive and could be broken by pressure-swing distillation. However, Luyben reported that pressure-swing distillation has a 15% higher total annual cost than extractive distillation for the ternary system acetone – methanol with water as entrainer (Luyben, 2008).

The purpose of this chapter is first to improve the design of a continuous extractive distillation process proposed in the literature and our design in chapter 3. This is done first by getting some thermodynamic insight from the residue curve map and isovolatility curves that lead to an operating pressure decrease, then secondly by optimizing the extractive process sequence, including the entrainer regeneration column, with regards to the energy consumed per unit product output flow rate. The second purpose is to get some insight on the column performance and to define an efficiency criterion for the extractive process that would characterize the optimality of the design. It is related to the extractive section ability to segregate the product between the column top rectifying section and the bottom stripping section. The pressure drop is neglected in each column that operates at constant pressure.

4.2.Back ground, methods and tools

4.2.1.Extractive process feasibility

The separation of a minimum boiling azeotrope with a heavy entrainer gives rise to a ternary diagram A-B-E that belongs to the 1.0–1a Serafimov's class, one of the most common among azeotropic mixtures with a reported occurrence of 21.6% (Hilmen et al., 2002). In our case, the separation of the minimum boiling azeotropes acetone A (56.1°C) – Methanol B (64.5°C) ($x_{azeo,A}$ = 0.78 @55.2°C) with heavy entrainer water E (100.0°C) belongs to the 1.0-1a-m1 extractive separation class. The univolatility curve $\alpha_{AB} = 1$ intersects the binary side A-E as shown on Figure 4.1 displaying also the residue curve map. The vapor-liquid equilibrium of the system acetone-methanol with water is described with the UNIQUAC thermodynamic model. The reliability of the VLE model used to compute Figure 4.1 residue curve has been assessed by Botia et al (Botía et al., 2010) using vapor-liquid equilibrium experimental data under atmospheric and vacuum pressure and was discussed in Chapter 3. That model was also used in Luyben's work (Luyben, 2008) and our design in chapter 3, to which we intend to compare our improved process design. In this work, we focus on the

analysis of residue curve map and univolatility line based on the knowledge of thermodynamic insight of the process and doing a primary evaluation, aiming at finding the possibility to save energy cost.

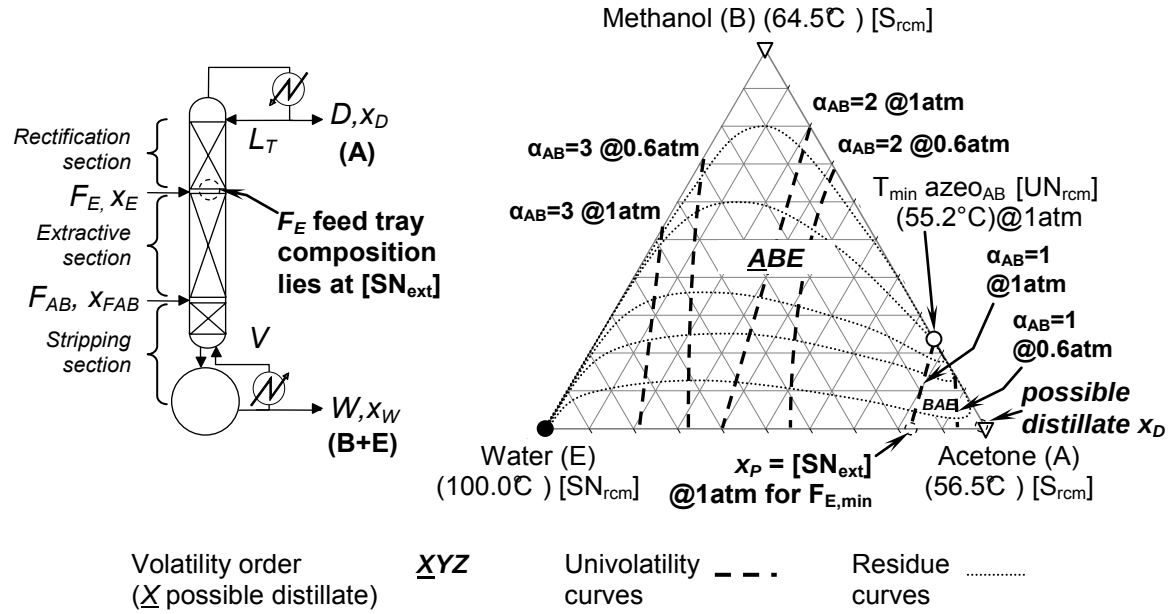

Figure 4.1 – Extractive distillation column configuration and acetone – methanol – water 1.0-1a residue curve map at 1 atm with univolatility curves at 0.6 and 1 atm

For the extractive separation class 1.0-1a-m1, the feasibility criterion is satisfied in the volatility order region *ABE*. Component A acetone is a residue curve map saddle [S_{rcm}] and cannot be obtained by azeotropic distillation. Thanks to the entrainer feeding F_E at a different location than the main feed F_{AB} an extractive section in the column occurs. A can be obtained as distillate product by a direct split configuration, above a minimum entrainer flow rate value. For this minimum value and for batch operation, the stable node of the extractive section in the distillation column [SN_{ext}] is located at the intersection point x_P of the univolatility curve $\alpha_{AB} = 1$ and the A-E side (Rodríguez-Donis et al., 2009). The x_P location also describes the minimal amount of entrainer for which the azeotrope $azeo_{AB}$ is no longer effective. Above that amount, the relative volatility α_{AB} is always greater than one. This explains why the feasibility criterion is verified in the *ABE* volatility order region.

4.2.2.Process optimization techniques

In this chapter, we keep fixed the total number of trays for each column of the two columns extractive distillation sequence in order to match Luyben's process design to which we compare. It is also the same values as in a previous design by Knapp and Doherty who ran a sensitivity analysis on the total number of tray (Knapp and Doherty, 1994, 1990). The four steps procedure described in chapter 3 is used for process optimization and significant reductions of TAC and energy consumption are obtained due to a low operating pressure. This work also showed that a 1.49 entrainer – feed flow rate ratio was sufficient to obtain 99.5% acetone and methanol, compared to Luyben's 2.06 value. Notice that in this chapter we focus on the benefit of low pressure on the process.

4.2.3.Objective function

The objective function OF and TAC in chapter 3 are used here. Notice that a vacuum pump is needed to produce 0.6 atm (see section 4.3.1) while the process is under start-up. After that, the operating pressure of the column is controlled by the condenser heat duty. The condenser heat transfer area increase in order to overcome the decrease of temperature driving force due to the low pressure. For a close to 1 atm vacuum pump, there is no significant increase in the purchased cost compared with liquid delivery pump. Thus, we have neglected its cost at the conceptual design stage.

4.3.Analysis of pressure and residue curve map

4.3.1.Pressure sensitivity of the azeotropic composition

With the purpose of changing the operating pressure to improve the extractive distillation sequence, we report in Table 4.1 the acetone – methanol azeotropic composition change with pressure. We used the same VLE model than to compute Figure 4.1's residue curve map.

Table 4.1 – Acetone-methanol azeotropic temperature and composition at different pressures with UNIQUAC model

P /atm	$T_{b\ Acetone}$ /°C	$T_{b\ Methanol}$ /°C	$T_{b\ azeo}$ /°C	Azeotrope acetone mol fraction
10.0	143.6	137.3	134.4	0.3748
5.0	112.3	112.0	107.1	0.5070
2.5	85.6	89.8	83.0	0.6306
1.0	56.1	64.5	55.2	0.7774
0.8	49.7	59.0	49.1	0.8101
0.6	41.9	52.1	41.5	0.8502
0.5	37.2	47.9	36.9	0.8745

Table 4.1 shows that the acetone-methanol azeotrope is sensitive enough to pressure change. Notice that the mixture exhibits a Bancroft point near 5 atm, meaning that their volatility order is reversed. The related temperature near 112°C is in agreement with the experimental Bancroft point measured at 111.97 °C (Kamath et al., 2005). PSD should be feasible but we do not consider this option here as preliminary results corroborated Luyben's ones(Luyben, 2008). He found that the TAC of the PSD process was 15% higher than the extractive distillation process. Table 4.1 also shows that the content of acetone in the azeotropic mixture increases when the pressure decreases, as seen in Figure 4.1 for P_1 = 1 atm and P_1 = 0.6 atm. As recalled in section 4.2.1, it means that a lower entrainer amount is needed to break the azeotrope, which could reduce the capital cost. Besides a lower operating pressure implies lower boiling temperatures and possible energy cost savings. If we assume that the extractive column distillate is almost pure acetone and consider a conservative value of 40°C as the minimum allowed temperature in the condenser to use cheap cooling water, Table 4.1 shows that we could use an operating pressure greater or equal to 0.6 atm as the acetone boiling point is then computed at 41.93°C.

4.3.2.Analysis of residue curve map

The 1.0-1a class RCM for the acetone – methanol – water ternary system at 1 atm is shown in Figure 4.1. Figure 4.1 also displays univolatility curves $\alpha_{AB} = 1$ and $\alpha_{AB} = 2$ and $\alpha_{AB} = 3$ at 1 atm and 0.6 atm. From $\alpha_{AB} = 1$ intersection x_P with the A-E edge, we can use equation 3.1 to compute the minimum entrainer/feed flow rate ratio under infinite reflux ratio $F_E/V_{min,R\infty} = 0.07$ at 0.6 atm; lower than $F_E/V_{min,R\infty} = 0.17$ at 1 atm. The univolatility curves indicate that the acetone – methanol relative volatility α_{AB} increases more rapidly for lower pressures when the entrainer content increases. Therefore for the same amount of entrainer, the entrainer will increase more α_{AB} under vacuum pressure, making the separation easier and inducing costs saving. We will use $P_1 = 0.6$ atm in the extractive distillation column from now.

As is well known, the binary mixture water – acetone equilibrium curve exhibit a pinch near pure acetone. This hints that a significant number of trays are necessary in the rectifying section to reach high purity acetone.

4.4.Optimization results

We aim at improving the extractive distillation sequence design proposed by Luyben (Luyben, 2008), referred to as case 1 in the text, by reducing the operating pressure at $P_1 = 0.6$ atm. We keep Luyben's total number of trays of the extractive column ($N_{Ext} = 57$) and of the entrainer regeneration column ($N_{Reg} = 26$). Those values also match Knapp and Doherty's design (Knapp and Doherty, 1990). We also keep the same product purity specifications (0.995 molar fraction) for both acetone and methanol, and the same thermodynamic model as Luyben that was also used to draw Figure 4.1. We also use Luyben's equimolar feed ($F_{AB} = 540$ kmol/h) at 320 K and preheat the entrainer to 320K as well. Other design parameters are obtained from simulation with the open loop flow sheet. They are marginally different from Luyben's article that showed closed loop results.

The four steps optimization procedure described in section 4.2.2 is used. Our design parameters under $P_1 = 1$ atm in chapter 3 are used as initial point of the optimization under $P_1 = 0.6$ atm. Notice D_1 and D_2 is taken from chapter 3 since the effects of distillates on the process is the same as Figure 3.4 in chapter 3.

4.4.1. Continuous variables F_E, R_1, R_2

Table 4.2 displays the optimized F_E, R_1, R_2 while the other variables are kept constant. Case 1 is our closed loop simulation results by using the design parameters of Luyben at 1 atm (Luyben, 2008). Case 2a and 2b represent results in chapter 3 keeping $P_1 = 1$ atm. The difference between case 2a and 2b is that the three feed locations of case 2a are the same as case 1, and that of case 2b is taken from our previous work (You et al., 2014). Case 2b is taken as the initial point for the SQP problem. Case 3 is new results with the extractive column operating at 0.6 atm and regeneration column operating at 1 atm.

Case 2a and 2b already showed that for the same operating pressure the design based on Luyben's parameters (case 1) could be improved by reducing the entrainer flow rate, even when the feed location was

kept unchanged (Case 2a). They also showed that changing the feed tray location brought additional savings (case 2b).

Table 4.2 – Optimized values of F_E, R_1 and R_2 for the extractive distillation of acetone – methanol with water under reduced pressure

Variables	Initial design *Case 1	Designs from chapter 3		Designs in this chapter		
		Case 2a	Case 2b	F_E Case 3a	F_E and R_1 Case 3b	F_E R_1 and R_2 Case 3c
N_{Ext}	57	57	57	57	57	57
N_{FE}	25	25	31	31	31	31
N_{FAB}	40	40	48	48	48	48
F_E kmol/h	1100	883	807	376	779	567
F_{AB} kmol/h	540	540	540	540	540	540
P_1 atm	1	1	1	0.6	0.6	0.6
R_1	3.44	3.28	2.83	2.83	2.47	2.48
N_{Reg}	26	26	26	26	26	26
N_{FReg}	14	14	17	17	17	17
P_2 atm	1	1	1	1	1	1
R_2	1.61	1.49	1.24	1.24	1.24	1.14
OF kJ/kmol	36247.5	34421.7	30916.2	30302.0	29526.8	28597.2

* Closed loop based on Luyben, 2008

Table 4.2 shows that further reducing the pressure to $P_1 = 0.6$ atm (case 3) enables an additional 7.5% reduction of the energy consumption materialized by the objective function OF decrease. This represents a 21% savings over case 1 design. This goes along with our intuition based on the analysis of the ternary map and univolatility curves at different pressures discussed in section 3.2. We also observe the close interrelation between F_E, R_1 and R_2. First the lowest F_E is achieved when only that variable is optimized. But a smaller OF value can be obtained when R_1 is optimized simultaneously. Furthermore, the OF value gets even smaller when the regeneration column reflux R_2 is taken into account: R_1 increases slightly, F_E decreases drastically and R_2 gets smaller. This highlights the importance of optimizing the regeneration column together with the extractive column. We also conclude that if less entrainer is fed to the extractive column, a greater R_1 is needed to achieve the same product purity. Meanwhile the concentration of entrainer fed to the regeneration column decreases due to mass balance, and less energy is used to recycle the entrainer, leading to a decrease of R_2. Case 3 entrainer – feed flow rate value is almost half of Luyben's value.

4.4.2. Distillates and three feed locations

In chapter 3, we ran a sensitivity analysis on the distillate D_1 and D_2 flow rates and selected $D_1 = 271$ kmol/h (99.86% acetone recovery) and $D_2 = 271.1$ kmol/h (99.90% methanol recovery), close to Luyben's values. Such very high recovery values are debatable since we are aware that they depend on the thermodynamic

model used and should be validated with experimental data. We do not optimize them further and find relevant to postpone their optimization to the availability of pilot plant experimental data.

On the contrary the variables N_{FE}, N_{FAB} and N_{FReg} are worth optimization at the process design step. The method stated in chapter 3 is used here. For each set of values, F_E, R_1, R_2 are optimized while D_1 and D_2 are fixed. As shown by You's case 2a and 2b results for P_1 = 1 atm and recalled in Table 4.2, there is a strong incentive to shift the feed locations and improve the process efficiency. Table 4.3 shows the results considering now P_1 = 0.6 atm.

Table 4.3 – Open loop optimal results of F_E, R_1, R_2, N_{FE}, N_{FAB}, N_{FReg} under fixed D_1 and D_2 for the extractive distillation of acetone – methanol with water

N_{FE}	N_{FAB}	N_{FReg}	F_E	P_1	R_1	P_2	R_2	OF kJ/kmol
31	48	17	567.0	0.6	2.48	1	1.14	28597.2
30	49	17	476.3	0.6	2.54	1	1.11	28507.9
31	47	18	519.4	0.6	2.50	1	1.10	28372.5
31	48	18	483.7	0.6	2.51	1	1.09	28269.4
32	47	18	535.3	0.6	2.48	1	1.11	28363.4
32	48	18	507.6	0.6	2.48	1	1.09	28217.7
32	48	19	501.8	0.6	2.48	1	1.10	28262.8
32	49	16	502.7	0.6	2.49	1	1.15	28567.0
33	47	18	558.8	0.6	2.46	1	1.11	28327.9
33	48	18	543.5	0.6	2.45	1	1.12	28275.8
33	49	17	531.8	0.6	2.46	1	1.12	28341.5

From Table 4.3, we can infer that (1) Decreasing the pressure P_1 allows using a lower reflux ratio R_1, as seen by comparing case 2b with all the cases at P_1 = 0.6 atm. Indeed we discussed earlier that the univolatility curves shown in Figure 4.1 were more favorable for the separation process at low pressure. (2) The feed location of entrainer moves down the column from 25 in case 1 to 32 for the lowest OF design exemplifies the well-known fact that increasing the number of trays in the rectifying section allows using a lower reflux ratio R_1. (3) The minimum value of OF is found with one extra number of trays in the extractive section than Luyben's parameter-based case 1. This number difference is not significant itself but is related to the efficiency of the extractive section that is discussed in a later section. (4) The lowest energy cost for per unit product OF is 28217.7 kJ/kmol. It represents a decrease of 22% compared to Luyben's parameter-based case 1 see Table 4.2. The decrease is only 1.3 % compared to step 1 case 3c, mostly due to a lower entrainer flow rate F_E. It hints that case 3c bore already many of the features that we now observe for a proper design.

4.4.3.Effect of entrainer purity on the process

All the optimization procedure done above for case 3 was run with an open loop flow sheet (Figure 3.3b) where F_E is pure water. However, the real process should implement an entrainer recycle stream bearing some impurities. Based on the optimized results N_{FE} = 32, N_{FAB} = 48, N_{FReg} = 18, F_E = 507.6 kmol/h, R_1 = 2.48

and R_2 = 1.09 for which OF = 28217.7 kJ/kmol, a simulation is ran by using the closed loop flow sheet displayed in Figure 3.3a, with Wegstein tear method used for convergence. It happens that the entrainer purity converges to 0.9998. Although very close to 1, that affects the distillate acetone purity that becomes 0.9949, below the 0.995 specification. Methanol purity in the regeneration column remains above 0.995.

To solve this problem, we adjust R_1 and R_2 for the closed loop simulation and obtain the final design of the process labeled case 3opt with R_1 = 2.49 and R_2 = 1.10 for which OF = 28318.5 kJ/kmol. We did not chose to adjust the entrainer flow rate because analysis of the rectifying section profile above the entrainer feed tray (Figure 4.2) shows that the methanol content is very low, a consequence of an extractive stable node that should lie very close to the water – acetone edge as discussed in section 3.2.

4.4.4.Summary of optimal design parameters, product purity and recovery

The design and operating variables are shown in Table 4.4, referring to the flow sheet notations in Figure 3.3. Table 4.5 provides the cost data in the supporting information file. Table 4.6 displays the product purity and recovery values. The temperature and composition profiles in the two columns of case 3opt are shown in Figure 4.2 and Figure 4.3.

Table 4.4 – Optimal design parameters and cost data from closed loop simulation for the extractive distillation of acetone – methanol with water

	Case 1	Case 2b	Case 3opt
N_{Ext}	57	57	57
P_1 /atm	1	1	0.6
W_2 / kmol/h	1098.2	804.9	505.9
$E_{make\text{-}up}$ / kmol/h	1.8	2.1	2.1
F_E / kmol/h	1100.0	807.0	508.0
D_1 / kmol/h	270.7	271.0	271.0
N_{FE}	25	31	32
N_{FAB}	40	48	48
R_1	3.44	2.83	2.49
Q_C / MW	9.87	8.51	7.98
Q_R / MW	10.89	9.26	8.14
N_{Rreg}	26	26	26
P_2 / atm	1	1	1
D_2 / kmol/h	271.1	271.1	271.1
N_{FReg}	14	17	18
R_2	1.61	1.24	1.10
Q_C / MW	6.92	5.94	5.57
Q_R / MW	7.33	6.29	6.09
TAC / 10^6\$	3.469	3.030	2.918
OF / kJ/kmol	36247.5	30916.2	28318.5

Table 4.5 – Sizing parameters for the optimal designed columns and cost data from closed loop simulation for the extractive distillation of acetone – methanol with water

	Case 1		Case 2b		Case 3opt	
column	C_1	C_2	C_1	C_2	C_1	C_2
Diameter / m	2.88	1.92	2.66	1.77	2.88	1.72
Height / m	33.53	14.63	33.53	14.63	33.53	14.63
I_{CS} / 10^6\$	1.164	0.389	1.069	0.356	1.164	0.346
A_C / m^2	601	284	518	244	679	229
A_R / m^2	551	371	469	319	412	309
I_{HE} /10^6\$	1.166	0.807	1.055	0.731	1.118	0.709
$Cost_{cap}$ / 10^6\$	2.576	1.252	2.341	1.137	2.528	1.102
$Cost_{ope}$ / 10^6\$	1.290	0.869	1.097	0.746	0.967	0.722
$Cost_{CA}$ / 10^6\$	2.148	1.287	1.877	1.125	1.809	1.089
Q_{HA} / MW	1.24		0.91		0.58	
$Cost_{HA}$ /10^6\$	0.035		0.028		0.021	

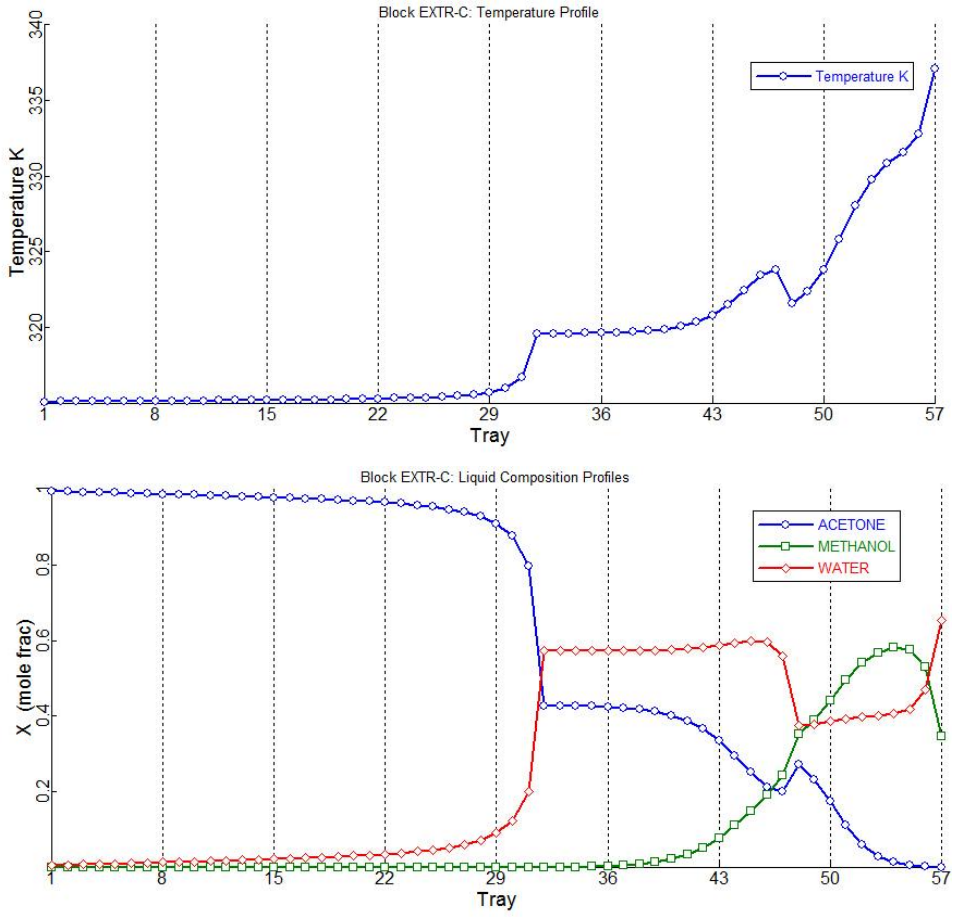

Figure 4.2 – Temperature and composition profiles of case 3opt extractive column for the extractive distillation of acetone – methanol with water

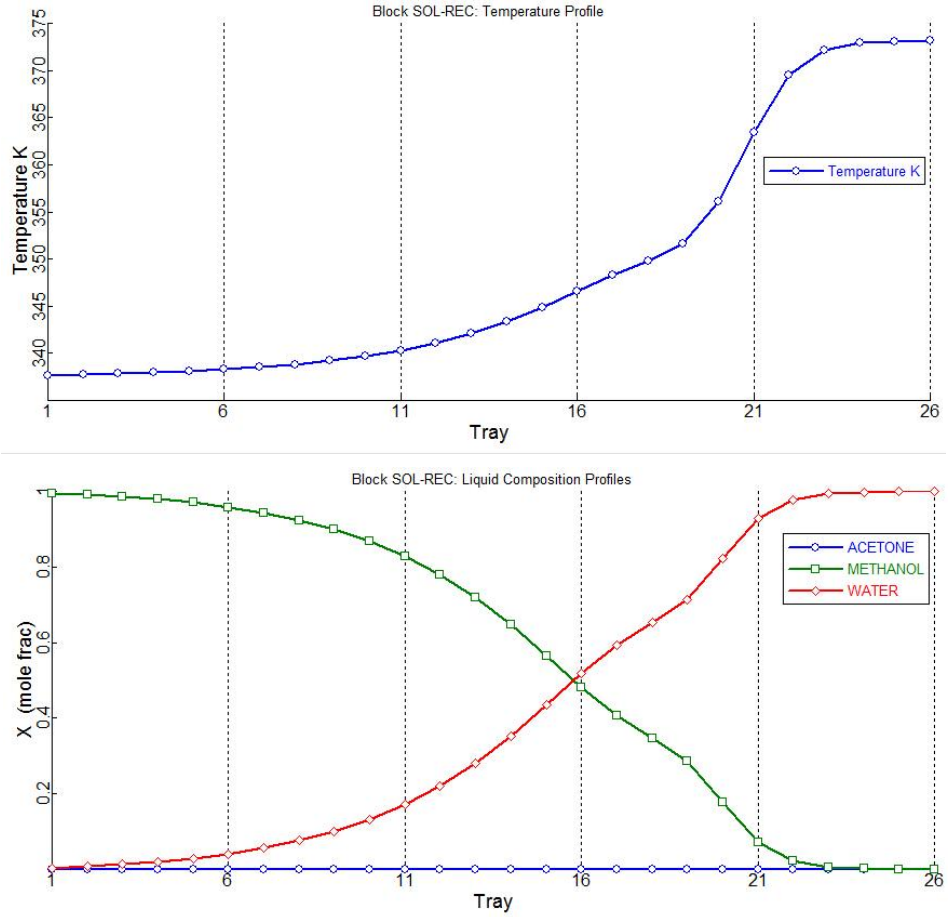

Figure 4.3 – Temperature and composition profiles of case 3opt regeneration column for the extractive distillation of acetone – methanol with water

Table 4.6 – Product purities and recoveries for case 1, 2 and 3op designs

Mole fraction		D_1	D_2	W_2=water	$W_1=F_2$	recovery
Case 1	Acetone	0.99573	0.00168	9.51E-15	0.00033	99.83%
	Methanol	0.00017	0.99578	5.64E-06	0.19715	99.98
	Water	0.00410	0.00254	0.999994	0.80252	
Case 2b	Acetone	0.99516	0.00115	1.88E-12	0.00029	99.88%
	Methanol	0.00066	0.99529	9.84E-05	0.25084	99.93%
	Water	0.00418	0.00356	0.999901	0.74887	
Case 3opt	Acetone	0.99500	0.00131	1.88E-12	0.00045	99.87%
	Methanol	0.00029	0.99565	8.42E-05	0.34743	99.97%
	Water	0.00471	0.00304	0.999916	0.65212	

Table 4.4 shows that Luyben's parameter based case 1 initial design could be improved, while keeping the same number of trays in the extractive and regeneration columns. In summary, (1) the entrainer flow rate decreased drastically from 1100 kmol/h in case 1 to 807 kmol/h in case 2b, showing that improvement was possible due principally to a combination of a lower reflux ratio and a shift of feed locations. The extra reduction to 508 kmol/h for case 3opt proved the usefulness of decreasing the pressure in the extractive

column, as deduced from the pressure dependency of the azeotrope composition and the isovolatility curves. (2) Energy consumption underlying the OF value is reduced by 21.9% and 8.4% compared to case 1 and 2, respectively. It is mostly attributed to the reduction in entrainer flow rate. (3) Meanwhile, TAC savings reach 16% and 3.7% due to the decrease of entrainer flow rate, column diameters and heat exchanger areas in the second column. (4) If we just take the extractive column in case 2 and case 3opt into account, the decrease of the pressure leads to an increase of the column diameter, and an increase of the condenser heat exchanger area due to the decrease of condenser temperature. However, the decrease of the pressure results in the decrease of reboiler duty by 12%, and the benefit of decreasing pressure overcomes the punishment as the annual cost of extractive column is reduced from 1.877 to 1.809 (10^6\$). Besides, the increase of the temperature difference (driving force) in the reboiler due to the pressure decrease will lead to lower pressure of steam used. This aspect is not taken into account as we assume the same temperature driving force in all case and the same price for the used steam.

Table 4.4 also shows the importance of adjusting the feed tray locations to reduce the process energy consumption. Luyben explained that the feed tray locations of the column were found empirically by finding what locations give minimum energy consumption in their study. In our work, the two columns are taken into account and the feed location is optimized by give minimum OF using the four steps procedure described in chapter 3. This point is evidenced by comparing the total heat duty of case 1 (18.22 MW) and case 2b (15.55 MW): a 14.6 % total heat duty is saved. Further decrease of the pressure allows an additional saving of 8.5% in heat duty between case 2b and case 3opt (14.23 MW).

Meanwhile, we notice that more acetone product (0.3kmol/h) is obtained in case 2b and 3 despite lower energy consumption than in case 1. This phenomenon is counterintuitive: normally, the more products at specified purity are obtained, the more energy (reboiler duty) should be used. The reasonable interpretation is that our optimization is conducted following OF, which reflects the energy consumption per unit product. The optimization resulted in balancing the energy consumption more evenly between the extractive column and regeneration column with a reboiler duty ratio of 1.486 in case 1, 1.472 in case 2b and 1.337 in case 3opt.

Regarding the TAC we have used Douglas's method with M&S 2011 index = 1511. Case 1 value (3.469E06 \$) is close to Luyben's value (3.750E06 \$) where he used different *k* and *m* factors, and energy consumption price. Case 3opt value (2.918E06 \$) which corresponds to 508 kmol/hr of entrainer is close to Knapp and Doherty's TAC (2.750E06 \$) obtained with a 540 kmol/hr of entrainer and submitted in jan 1990 (Knapp and Doherty, 1990). If we use the 1989 M&S index = 895.1, the TAC of case 3opt design equals 2.414E06 \$.

Regarding product recovery, Table 4.6 shows that the recoveries are high and comparable for all three cases. Also for the temperature profile, the extractive section temperature is above 320K which was the preset temperature of the entrainer feed, not further considered for optimization because we wanted to compare to Luyben's design.

4.5. Development of an extractive distillation process efficiency indicator

4.5.1. Extractive section efficiency

In line with the discussion about the tray location, we have noticed that the composition profiles in the extractive section have similar shapes for all cases 1, 2 and 3opt, but they differ significantly when looking at the composition values on the feed trays. This prompts us to define a novel efficiency indicator for the extractive section by the following equation:

$$E_{ext} = x_{P,H} - x_{P,L} \tag{4.5}$$

Where E_{ext}: the total efficiency indicator of extractive section, $x_{P,H}$: product mole fraction at one end of extractive section, $x_{P,L}$: product mole fraction at another end of extractive section. Here, we use the entrainer feed and the main feed trays locations as ends of the extractive section.

For different designs of extractive distillation, different of F_E/F and tray number in extractive section will have effect on E_{ext}, so the efficiency indicator per tray in extractive section is needed:

$$e_{ext} = \frac{E_{ext}}{N_{ext}} \tag{4.6}$$

Where e_{ext}: efficiency indicator per tray, N_{ext}: tray number of extractive section.E_{ext} and e_{ext} describe the ability of the extractive section to discriminate the desired product between the top and the bottom of the extractive section.

4.5.2. Comparison of efficiencies for extractive process design

The efficiency indicator per tray and total efficiency indicator of the extractive section are shown in Table 4.7 for the case 1, 2 and 3opt, along with the acetone composition at the feed trays. Knapp and Doherty and Gil's values are discussed afterwards. Figure 4.4 also displays the extractive column composition profiles in a ternary map.

Table 4.7 – Efficiencies of per tray and total extractive section for the extractive distillation of acetone – methanol with water

	Pressure /atm	Acetone composition		N_{ext}	E_{ext} /10^{-3}	e_{ext} /10^{-3}
		E feed tray (SN_{ext})	Feed tray			
Case 1 $	1	0.358	0.303	15	55.4	3.69
Case 2b £	1	0.372	0.234	17	138	8.13
Case 3opt	0.6	0.428	0.272	16	156	9.72
Knapp and Doherty, 1990 *	1	0.52	0.36	13	160	12.3
Gil et al., 2009 *	1	0.525	0.40	16	125	7.8

* estimated from Fig. 9 in their work ¤ estimated from Fig. 22 in their work
$ Closed loop based on Luyben, 2008 £ Closed loop from You et al., 2014

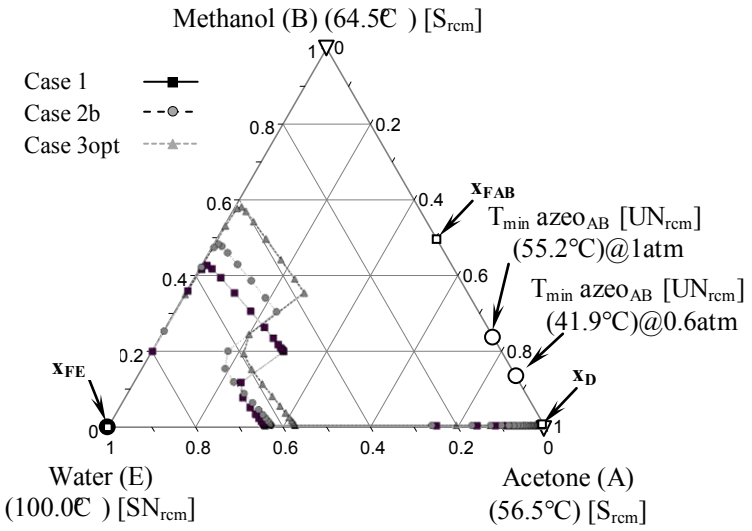

Figure 4.4 – Liquid composition profiles for case 1(1atm),case 2(1atm) and 3(0.6atm) extractive distillation column designs for the extractive distillation of acetone – methanol with water

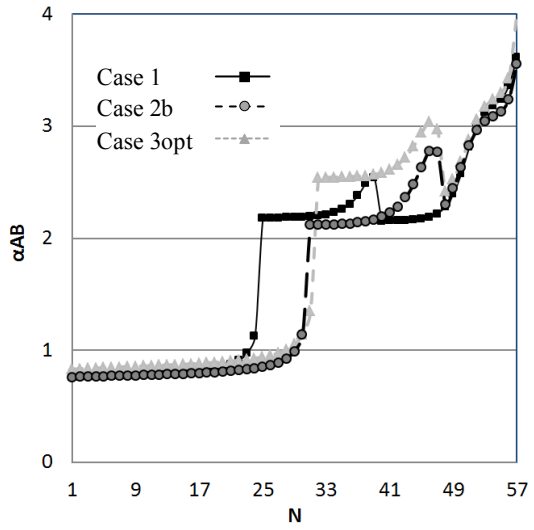

Figure 4.5 – Volatility profile of acetone vs methanol along the extractive column for the extractive distillation of acetone – methanol with water, case 1(1atm),case 2(1atm) and 3(0.6atm)

We remark: (1) A lower entrainer flow rate as in case 2b and case 3opt operating at low pressure is beneficial for reducing the energy consumption in both columns. This is why the OF in case 3opt decreases by 8.4% and 21.9% compared with case 2b and case 1 respectively.

(2) For case 3opt, with the lowest entrainer flow rate, SN_{ext} is closer to the product vertex, which may hint at a shorter rectifying section to reach the product purity specification.

(3) As discussed in section 4.3.2 and in earlier works (Lelkes et al., 1998a; Rodríguez-Donis et al., 2009), the extractive section should have enough tray so that the composition at the entrainer feed tray should be near to the stable node of the extractive section SN_{Ext}. As shown in Figure 4.4, the SN_{Ext} location is near the product

– entrainer edge depends on the reflux and on the entrainer flow rate (Gerbaud and Rodriguez-Donis, 2014; Rodríguez-Donis et al., 2009a). This point is also in agreement with the sensitivity analysis performed by Lang for the same separating system (Lang, 1992).

(4) Extra trays used in stripping section in case 1 are needed to keep acetone from entering bottom liquid. For case 2b, the better efficiency of the extractive section to discriminate results in less trays needed in the stripping section. Case 3opt operating at another pressure, cannot be rightfully discussed here.

(5) The total efficiency indicator E_{ext} and the efficiency indicator per tray in extractive section e_{ext} increase by 2.5 and 2.2 times in case 2b compared to case 1. It demonstrates the importance of finding a suitable extractive section position by moving the feed tray locations. For case 3opt, operating at a lower pressure which was shown in section 3.2 to be beneficial thanks to more favorable isovolatility curves and SN_{ext} location, E_{ext} and e_{ext} are even better. Although one less tray than case 2b is used in the extractive section, E_{ext} increases further by 13% compared to case 2b, and boosts e_{ext} by 19%. Case 3opt is therefore regarded as the most efficient design, as shown by the OF value that in case 3opt decreases by 8.4% and 21.9% compared with case 2b and case 1 respectively.

(6) The acetone – methanol relative volatility α_{AB} profile along the extractive distillation column (Figure 4.5) confirms the efficiency ranking. α_{AB} rises sharply at the entrainer feed tray and drops at the main feed tray. In the extractive section of case 2b, the increase in α_{AB} is larger than in case 1. This is a remarkable achievement since the entrainer usage decreases by 26.6%, enabling to reduce the energy consumption as OF decrease by 14.7%. Case 3opt brings additional savings translated into a better efficiency as it operates at a higher level of relative volatility. This is because at lower pressure the volatility is higher as discussed in section 3.2.

We compare our design with the earlier works of (Gil et al., 2009; Knapp and Doherty, 1990; Luyben, 2008). The extractive efficiency for their design is reported in Table 4.7. Luyben's design corresponds to our case 1.

Knapp and Doherty's design has a larger efficiency. We interpret it as a consequence of a smaller reflux ratio. However, when we simulated Knapp and Doherty's flow sheet we could recover 98.79 % of the acetone and 98.74% of the methanol. This is attributed to the Van Laar thermodynamic model used by Knapp and Doherty that overestimated the relative volatility compared to our UNIQUAC model Notice that those authors separated also an equimolar feed in 99.5%mol pure acetone and methanol with a reflux ratio equal to 0.55 and to 1. They also optimized additional parameters, like the feed quality and temperature, which we set fixed. Relaxing them, as in a future work in preparation could lead us to improve further our design.

Gil and coworkers' design was done with the same UNIQUAC model. It does not exhibit an extractive efficiency as high as we do. But they used a rather high reflux ratio equal to 5 to separate an azeotropic feed rather than an equimolar feed. They also recovered a 99.0%mol acetone distillate in a 52 trays column with entrainer and main feed streams entering the column at trays 22 and 48 respectively.

4.6.Conclusions

We have looked at improving the design a homogeneous extractive distillation process for the separation of the acetone – methanol minimum boiling azeotrope with water. The process flow sheet includes both the extractive distillation column and the entrainer regeneration column. By using insight from the analysis of the ternary residue curve map and isovolatility curves, we have noticed the beneficial effect of lowering the pressure in the extractive distillation column for a 1.0-1a-m1 extractive separation class. A lower pressure reduces the minimal amount of entrainer and increases the relative volatility of acetone – methanol for the composition in the distillation region where the extractive column operates. A 0.6 atm pressure was selected to enable the use of cheap cooling water in the condenser.

Then we have run an optimization aiming at minimizing the total energy consumption per product unit as objective function OF. OF includes both products and both columns energy demands at boiler and condenser and accounts for the price difference in heating and cooling energy and for the price difference in product sales. Rigorous simulations in closed loop flow sheet were done in all cases. For the sake of comparison we have kept the total number of trays identical to literature works of Luyben and of Knapp and Doherty. Other variables have been optimized; entrainer flow rate, reflux ratios, entrainer feed location and main feed location. The total annualized cost (TAC) was calculated for all processes.

Double digit savings in energy consumption and in TAC have been achieved compared to literature values thanks to the optimization scheme helped with thermodynamic insight analysis. Two important issues have emerged. First the reduction of pressure is beneficial to the separation by extractive distillation. Second, we have proposed a novel function expressing the efficiency of the extractive section and found it correlated with the best design. The efficiency of the extractive section describes the ability of the extractive section to discriminate the desired product between the top and the bottom of the extractive section. We have shown that a high E_{ext} is correlated to a well-designed extractive distillation process. We have noticed that a suitable shift of the feed trays locations improves the efficiency of the separation, even when less entrainer is used and related that to thermodynamic insight gained from the ternary diagram analysis. Comparison with literature design confirms that the total extractive efficiency and the extractive efficiency per tray functions are a relevant criterion to assess the performance of an extractive distillation process design.

Next chapter deals with the optimization process including the efficiency indicator as a secondary objective function to design extractive distillation processes. Additional optimization variable like the total number of tray will be included.

Chapter 5. Design and Optimization of ED for separating DIPE-IPA

Results in this chapter have been submitted to

Article: You, X., Rodriguez-Donis, I., Gerbaud, V., 2015. Optimisation of Low Pressure Extractive Distillation for Separating Diisopropyl ether and Isopropyl alcohol. AIChE Journal.

5.Design and Optimization of Extractive Distillation for Separating Diisopropyl ether and Isopropyl alcohol

5.1.Introduction

Diisopropyl ether (DIPE) has become an important gasoline additive over the past decade. DIPE can not only be used as an octane-enhancing components, but also improve the combustion of gasoline and reduce emissions (Lladosa et al., 2008). DIPE is also widely used in many other fields, such as tobacco production and synthetic chemistry. Isopropyl alcohol (IPA) is extensively used in medicine industry as a chemical intermediate and solvent (Wang et al., 2008). IPA can be produced by using solid acid or liquid acid as catalytic agent, with DIPE as a coproduct (Logsdon and Loke, 2000). The separation of DIPE/IPA is the key downstream process that determines the entire process economic benefits. However, IPA and DIPE can't be separated by conventional distillation process because they form a binary minimum boiling homogeneous azeotrope. Hence, other types of distillation methods such as extractive distillation or pressure-swing distillation are necessary for this separation.

Extractive distillation is the common method for the separation of azeotropic mixture or close boiling mixture in large scale productions (Doherty and Malone, 2001; Luyben and Chien, 2010; Petlyuk, 2004). Based on the analysis of residue curve map, univolatility line and univolatility order regions, the thermodynamic feasibility of extractive distillation process can be predicted by using the general feasibility criterion without any systematic calculations of composition profiles. Here the thermodynamic feasibility of extractive distillation process includes knowing which component will be withdrawn in the first distillate cut, what the adequate column configuration is, and whether it exists some limiting operating parameter value or not (Rodríguez-Donis et al., 2009). Subsequent calculation of composition profiles can then help refine the reflux ratio and entrainer feed flow rate range (Petlyuk et al., 2015).

Pressure-swing distillation can be used for separating pressure-sensitive azeotrope (Luyben, 2012; Modla and Lang, 2010) or pressure-insensitive azeotrope with an entrainer (Knapp and Doherty 1992; Li et al., 2013). According to Lladosa et al., (2007), the azeotrope of DIPE and IPA is very sensitive to pressure following the equilibrium diagrams of them based on experimental data. Therefore, the azeotrope can be separated by pressure-swing distillation. The author also reported that 2-methoxyethanol is an excellent solvent to break the azeotrope based on the vapor-liquid equilibrium experimental data. In 2014, Luo et al., (2014) compared the pressure-swing distillation and extractive distillation with 2-methoxyethanol for the separation of DIPE and IPA. The results show that the fully heat-integrated pressure-swing distillation system offers a 5.75% reduction in the total annual cost and 7.97% savings in energy consumption as compared to the extractive distillation process.

In order to find the possible way to save energy cost and total annual cost for extractive distillation process, we showed in chapter 4 that a suitable decrease of pressure in extractive distillation column for the separation of the 1.0-1a class acetone-methanol minimum boiling azeotrope with water system followed by an optimization of the extractive column and regeneration column process allowed double digit saving in TAC and energy cost. This was conducted with the help of thermodynamic insight and was analyzed in terms of novel efficiency indicators of extractive section E_{ext} and per stage in extractive section e_{ext} that described the ability of the extractive section to discriminate the desired product between the top and the bottom of the extractive section.

In this chapter, we perform a similar study for the extractive distillation of the DIPE-IPA minimum boiling azeotrope with 2-methoxyethanol system and compared it with designs in literature based on the feasibility analysis of residue curve, isovolatility line and ternary map. In addition to what was done in chapter 3 and 4, we also dicuss the issue of selecting suitable distillate flowrate based on the non-linear relation between distillate flowrates, product purities and recovery yields of the two columns. The two-step procedure as stated in chapter 3 is used as optimization method and the effects of the main parameters on the process and efficiency indicators are investigated. Based on the general feasibility criterion, the extractive distillation process feasibility after reducing the operating pressure on the process, is discussed in order to find the possibility to save the energy cost and TAC for the separation process itself instead of heat integration ((Luo et al., 2014) or dividing wall column (Dejanović et al., 2010). Besides, the two efficiency indicators are calculated to explain how the low pressure in extractive distillation gives benefit to the separation process.

5.2.Steady state design

5.2.1.Extractive process feasibility

In our case, the separation of the minimum boiling azeotropes DIPE A (68.5°C) – IPA B (82.1°C) ($x_{azeo,A}$ = 0.78 @66.9°C) with heavy entrainer 2-methoxyethanol E (124.5°C) belongs to the 1.0-1a-m1 extractive separation class (Gerbaud and Rodriguez-Donis, 2014). The univolatility curve $\alpha_{AB} = 1$ intersects the binary side A-E as shown on Figure 5.1 displaying also the residue curve map. The vapor-liquid equilibrium of the system is described with the nonrandom two-liquid (NRTL) thermodynamic model (Renon and Prausnitz, 1968), while the vapor phase is assumed to be ideal. The binary parameters of the model are the same as (Luo et al., 2014), who got the values by regressing from the experimental data (Lladosa et al., 2008).

In fact, for the extractive separation class 1.0-1a-m1, the feasibility criterion is satisfied in the volatility order region ABE. Component A DIPE, is a residue curve map saddle [S_{rcm}] and cannot be obtained by azeotropic distillation. Thanks to the entrainer feeding FE at a different location than the main feed FAB an extractive section in the column occurs. A can be obtained as distillate product by a direct split configuration, above a minimum entrainer flow rate value. For this minimum value and for batch operation, the stable node of the extractive section in the distillation column [SN_{ext}] is located at the intersection point x_P of the univolatility curve $\alpha_{AB} = 1$ and the A-E side (Rodríguez-Donis et al., 2009). The x_P location also describes the minimal

amount of entrainer for which the azeotrope is no longer effective. Above that amount, the relative volatility α_{AB} is always greater than one.

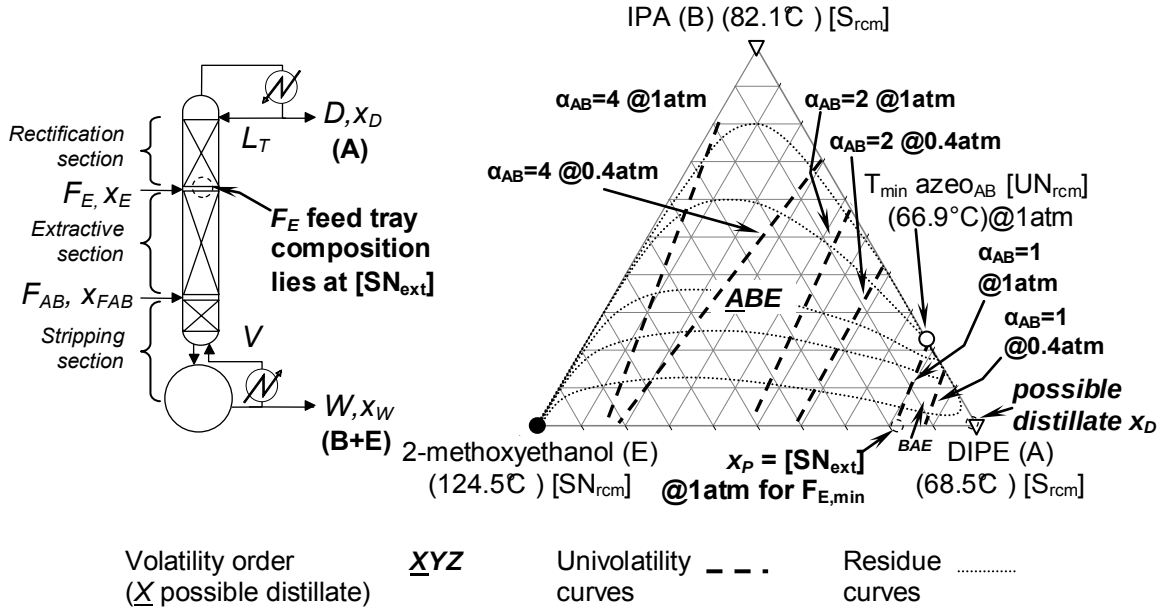

Figure 5.1 – Extractive distillation column configuration and DIPE – IPA –2-methoxyethanol class 1.0-1a residue curve map at 1atm with isovolatility curves at 0.4 and 1 atm.

5.2.2.Pressure sensitivity of the azeotropic mixture

With the purpose of changing the operating pressure to improve the extractive distillation sequence, we report in Table 5. the DIPE – IPA azeotropic composition change with pressure. We used the same VLE model than to compute Figure 5.1's residue curve map.

Table 5.1 – DIPE-IPA azeotropic temperature and composition at different pressures with NRTL model

P /atm	$T_{b\ DIPE}$ /°C	$T_{b\ IPA}$ /°C	$T_{b\ azeo}$ /°C	Azeotrope DIPE mol fraction
10.0	161.8	155.72	154.6	0.2957
5.0	128.1	129.5	123.7	0.5551
4.0	118.4	121.9	114.6	0.6004
2.5	99.7	107.1	96.9	0.6732
1.0	68.5	82.1	66.9	0.7745
0.8	61.7	76.6	60.4	0.7950
0.6	53.4	69.8	52.4	0.8200
0.5	48.4	65.7	47.5	0.8351
0.4	42.5	60.9	41.8	0.8531

Table 5. shows that the DIPE/IPA azeotrope is sensitive enough to pressure change. Notice that the boiling temperature of IPA is lower than that of DIPE when pressure is high enough. That means the mixture exhibit a Bancroft point (Elliott and Rainwater, 2000) near 5.8 atm with temperature close to 134.8°C, where their volatility order is reversed. Considering the pressure sensitivity of the azeotrope, the PSD process is feasible

for the mixture and this was investigated by Luo et al., (2014). Table 5. also shows that the content of DIPE in the azeotropic mixture increases when the pressure decreases. As seen in Figure 5.1 for P_1 = 1 atm and P_1 = 0.4 atm this also prompts the univolatility curve to intersect the A-E edge nearer the DIPE vertex. As cited in the literature survey and discussed in the next section, it means that a lower entrainer amount is needed to break the azeotrope, which could reduce the capital cost. Besides a lower operating pressure implies lower boiling temperatures and possible energy cost savings. In particular, if we assume that the extractive column distillate is almost pure DIPE and consider a conservative value of 40°C as the minimum allowed temperature in the condenser to use cheap cooling water, Table 5. shows that we could use an operating pressure greater or equal to 0.4 atm as the DIPE boiling point is then computed at 42.5°C.

5.2.3.Analysis of residue curve map

The 1.0-1a class residue curve map (RCM) for the DIPE – IPA – 2-methoxyethanol ternary system at 1 atm was shown in Figure 5.1. Figure 5.1 also displays isovolatility curves α_{AB} = 1 and α_{AB} = 2 and α_{AB} = 4 at 1 atm and 0.4 atm, respectively. According to the general feasibility criterion (Rodríguez-Donis et al. 2009a), the region ABE in Figure 5.1 satisfies it, so we can expect that (1) DIPE will be the distillate in extractive column as A is the most volatile component in the region and there is residue curve linked AE following the increase of temperature. (2) The column configuration is a direct split as the component cut is the most volatile one.(3) There is minimum entrainer-to-feed flow rate ratio $(F_E/F)_{min}$ as α_{AB} = 1 reaches AE side at x_P. When F_E/F is lower than $(F_E/F)_{min}$, the process for achieving a high purity distillate is impossible because the stable node of extractive section SN_{ext} is located on the α_{AB} = 1 curve. Indeed, the point x_P intersection of the univolatility curve with the triangle edge gives us the information to calculate the $(F_E/V)_{min}$ by the method shown in (Lelkes et al., 1998a) and then transfer $(F_E/V)_{min}$ to $(F_E/F)_{min}$ by using the equation 3.2 shown in chapter 4.

In addition to the aforementioned reduction of the minimum entrainer feed ratio as the pressure is decreased to 0.4 atm, the isovolatility curves α_{AB} = 2 and α_{AB} = 4 in Figure 5.1 indicate that the DIPE – IPA relative volatility α_{AB} increases more rapidly for lower pressures when the entrainer content increases. This will make the separation easier and inducing costs saving at low pressure. We will use P_1 = 0.4 atm in the extractive distillation column from now.

Finally, we have drawn in Figure 5.2 the liquid – vapor equilibrium curve for the binary mixtures 2-methoxyethanol – DIPE. It exhibits a pinch point near pure DIPE. This hints that a significant number of trays are necessary in the rectifying section to reach high purity DIPE. This point is proved by our design below.

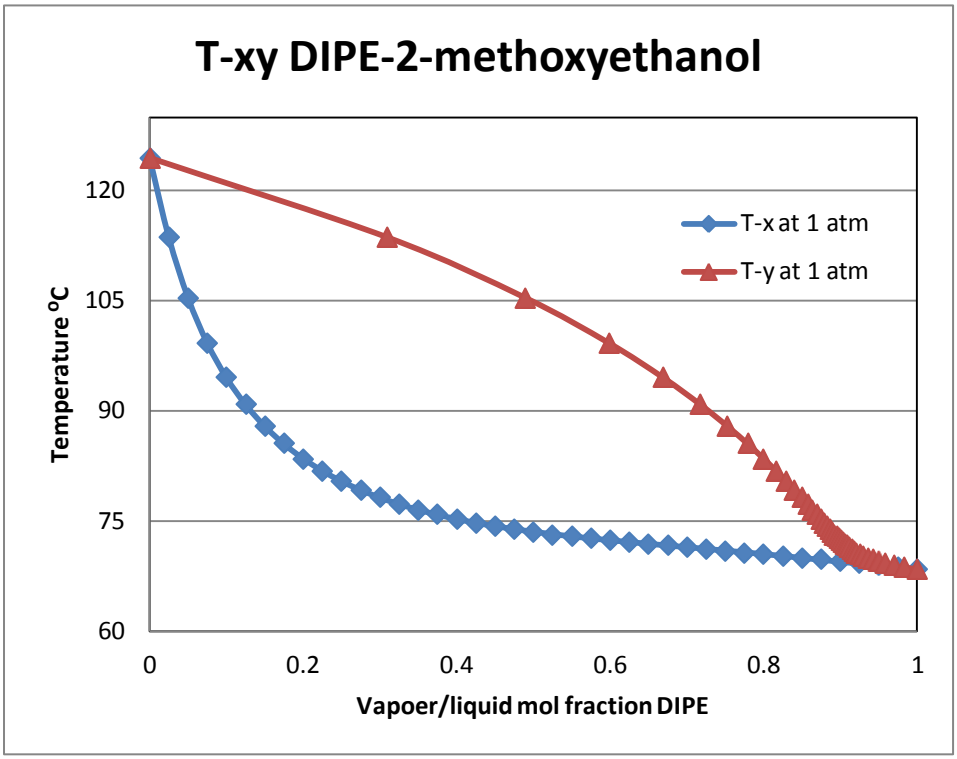

Figure 5.2 – T-xy map of 2-methoxyethanol – DIPE

5.2.4.Process optimization procedure

In this chapter, we keep fixed the total number of trays for each column of the two columns extractive distillation sequence and the value is taken from Luo's design for the same separating system. The optimization problem is the same as in chapter 3 and 4.

5.2.5.Objective function

The objective function OF and TAC in chapter 3 are used here. Notice that $k = 3.9$ (product price index) is used as it describes the price differences between products DIPE and IPA, and the energy price index m is the same. The pressure drop of per tray is assumed as 0.0068 atm as (Luo et al., 2014). When calculating TAC, the tray efficiency is set at 85% (Figueiredo et al., 2014).

5.3.Results and discussions

Aiming at saving energy cost for the extractive distillation sequence of DIPE-IPA with 2-methoxyethanol, the operating pressure of extractive column is adjusted to $P_1 = 0.4$ atm, which gives top temperature near 42.5°C enabling to use cheap cooling water at condenser. Intending to revisit Luo's design, we keep his proposed total number of trays in the extractive column ($N_{Ext} = 66$) and in the entrainer regeneration column ($N_{Reg} = 40$). We use the same feed as Luo's ($F_{AB} = 100$ kmol/h, 0.75 (DIPE): 0.25 (IPA)) and preheat the entrainer to 328.15K as they did. We select new product purity specifications equal to 0.995 molar fraction for both DIPE and IPA. Other design parameters are obtained from simulation with the open loop flow sheet. The two step optimization procedure described before is used and the Luo's design under 1 atm is used as the

initial point of the optimization under 0.4 atm. Notice that the optimization for continuous variables (step 1) is neglected here since it is conducted in step 2 and 3.

5.3.1. The relation of two distillate in extractive distillation

For a given separation, the product purities and recovery are the important specification for the design process. For extractive distillation, the condition is a little complicated because the binary azeotropic mixture are obtained as two columns distillates for a direct split and there is inherent relationship between them. We will show the relation below. For binary azeotropic mixture AB in direct split with flow rate F and content $x_{F,A}$, $x_{F,B}$, the product purities and process recovery are $x_{D1,A}$, $x_{D2,B}$ and ψ_A, ψ_B, so

$$\psi_A = \frac{D_1 x_{D1,A}}{F x_{F,A}} \Leftrightarrow D_1 = \frac{F x_{F,A} \psi_A}{x_{D1,A}} \tag{5.1}$$

$$\psi_B = \frac{D_1 x_{D1,B}}{F x_{F,B}} \Leftrightarrow D_2 = \frac{F x_{F,B} \psi_B}{x_{D1,B}} \tag{5.2}$$

But, we can also write the mass balance for A (equation 5.3) and B (equation 5.4) and use equations 5.1 and 5.2 to obtain the relation influence of one component recovery on the other distillate flow rate:

$$D_2 = \frac{F x_{F,A} - D_1 x_{D1,A}}{1 - x_{D2,B} - x_{D2,E}} = \frac{F x_{F,A} - (\frac{F x_{F,A} \psi_A}{x_{D1,A}}) x_{D1,A}}{1 - x_{D2,B} - x_{D2,E}} = \frac{F x_{F,A}(1-\psi_A)}{1 - x_{D2,B} - x_{D2,E}} > \frac{F x_{F,A}(1-\psi_A)}{1 - x_{D2,B}} \tag{5.3}$$

$$D_1 = \frac{F x_{F,B} - D_2 x_{D2,B}}{1 - x_{D1,A} - x_{D1,E}} = \frac{F x_{F,B} - (\frac{F x_{F,B} \psi_B}{x_{D2,B}}) x_{D2,B}}{1 - x_{D1,A} - x_{D1,E}} = \frac{F x_{F,B}(1-\psi_B)}{1 - x_{D1,A} - x_{D1,E}} > \frac{F x_{F,B}(1-\psi_B)}{1 - x_{D1,A}} \tag{5.4}$$

Where $x_{D1,E}$ and $x_{D2,E}$ are the entrainer content in the two distillate.

From these equations we observe that the distillate D_2 (resp. D_1) is controlled not only by the recovery and product purity of B (resp. A), but also the recovery of A (resp. B). So an unreasonable choice of distillate flow rate will lead to product quality (satisfy the purity specification or not), as well as product recovery (related the difficulty of separation). Based on the equation above, we test the DIPE-IPA system at low purity and recovery. The results are shown in Table 5.2 below.

From theTable 5.2, we know that (1) Following equation 5.1 and 5.2, the range value of A-rich distillate D_1 and B-rich distillate D_2 is easy to calculate from ψ_1 and ψ_2 respectively, but it is not strict enough. If we check with equation 5.3 that describes the influence of the recovery of A ψ_A on the B-rich distillate D_2, ψ_A has to be within a very narrow range; otherwise D_2 can't reach the reasonable range value. Similarly from equation 5.4, ψ_B has to be within a very narrow range, otherwise D_1 can't reach the expected range value. But in that case the B recovery is low and not acceptable. In other words, for the binary mixture of AB with

100kmol/h and $x_{F,A} = 0.75$, if the two products specifications are set at 98%, we should choose a recovery of A between 99.3197% < ψ_A < 99.333% which will ensure that the recovery of B is within 98% < ψ_B < 100%.

Table 5.2 – Relationship of distillates, purity and recovery for binary mixture for 100kmol/h binary mixture

Feed composition		Purity specification	
$x_{F,A}$	0.75	$x_{D1,A}$	0.98
$x_{F,B}$	0.25	$x_{D2,B}$	0.98
Range of distillate (equation 5.1 and 5.2)			
D_1 /kmol/h	75.00 (ψ_A=98%)	76.53 (ψ_A=100%)	
D_2 /kmol/h	25.00 (ψ_B=98%)	25.51(ψ_B=100%)	
Range of distillate (equation 5.3 and 5.4)			
D_1 /kmol/h	>76.53 (ψ_B=93.877%)	>75.00 (ψ_B=94%)	
D_2 /kmol/h	>25.51 (ψ_A=99.3197%)	>25.00 (ψ_A=99.333%)	

These relations also indicate that the choice of distillate impacts the necessary entrainer feed flow rate. For example, if $D_1 = 75$ equation 5.1 gives $\psi_A = 0.98$ for a purity of $x_{D1,A} = 0.98$. Thus there will be 75 ×(1-0.98) = 1.5 kmol/h of A entering the second regeneration column. As D_2=25 kmol/h, the purity of B will be not higher than $x_{D2,B}$ = (1-1.5/25) = 0.94 if neglect the loss of A in the recycled entrainer stream W2. On the other hand, if we want to achieve $x_{D2,B}$=0.98, the maximum value of A that should reach in D_2 is 0.5 kmol/h (25×(1-0.98)). Subtracted from the 1.5 kmol/hr entering column 2, 1 kmol/h A has to be recycled with the entrainer recycle stream W_2. That impurity in the recycle entrainer implies that the entrainer flow rate has to be over 1000(1÷(1-0.999)) kmol/h in order to guarantee our specification of 0.999mol% pure entrainer recycled to column 1. This corresponds to a very large entrainer-to-feed flow rate ratio (F_E/F = 10), leading to large energy cost. A more reasonable example is to assume D_1 = 76.1 kmol/h. Then with $x_{D1,A}$ = 0.98 equation 5.1 gives ψ_A = 0.99437 and 76.1 × (1-0. 0.99437) = 0.428 kmol/h of A will enter the second column. Being below the maximum 0.5 kmol/hr of A to enter column 2, the purities of B and recycling entrainer can be met and the entrainer-to-feed flow rate ratio does not have to very high.

In summary, D_1 and D_2 strongly interact each other and with the recycled entrainer-riche stream. Also, a suitable increase of D_1 from 75 to 76.1 did not increase the separation cost but rather can result in energy cost savings.

5.3.2.Choice of distillate flow rate for this chapter

With the new product purity specification, we use equations 5.1 to 5.4 to select suitable distillate flow rate, as shown in Table 5.3.

Table 5.3 shows that the recovery of DIPE should be at least higher than 99.83% and that the recovery of IPA should be above 99.5%. Our final design overcomes these values. Also, we can explain that Luo' design that fixed D_1 = 75.44 kmol/h prevented him to reach a purity of 0.9950 for DIPE since it is above the 75.37 kmol/h limit value for that purity. He obtained 0.9930 which corresponds to a ψ_A = 99.88% from equation 5.1.

Table 5.3 – Relationship of distillates, purity and recovery for DIEP-IPA

Feed composition		Purity specification	
x_1	0.75	$x_{D1,A}$	0.995
x_2	0.25	$x_{D2,B}$	0.995
Range of distillate (equation 5.1 and 5.2)			
D_1 /kmol/h	75.00 (ψ_A=99.5%)	75.37 (ψ_A=100%)	
D_2 /kmol/h	25.00 (ψ_B=99.5%)	25.12 (ψ_B=100%)	
Range of distillate (equation 5.3 and 5.4)			
D_1 /kmol/h	>75.37 (ψ_B=98.493%)	>75.00 (ψ_B=98.50%)	
D_2 /kmol/h	>25.12 (ψ_A=99.8325%)	>25.00 (ψ_A=99.833%)	

A side effect of the strongly nonlinear dependency of D_1 and D_2 on the product purity is that the simulation cannot be converged steadily when we directly treat the distillates as an optimized variable in the SQP method. So D_1 is varied with a discrete step of 0.05 kmol/h from 75 kmol/h (ψ_A = 99.5%) to 75.35 kmol/h (ψ_A = 99.96%) and D_2 is varied with a discrete step of 0.03 kmol/h from 25 kmol/h (ψ_B = 99.5 %) to 25.12 kmol/h (ψ_B = 99.98 %), and the SQP optimization is ran to obtain F_E, R_1 and R_2. The results shown in Figure 5.3 display the value of the objective function OF vs D_1 and D_2.

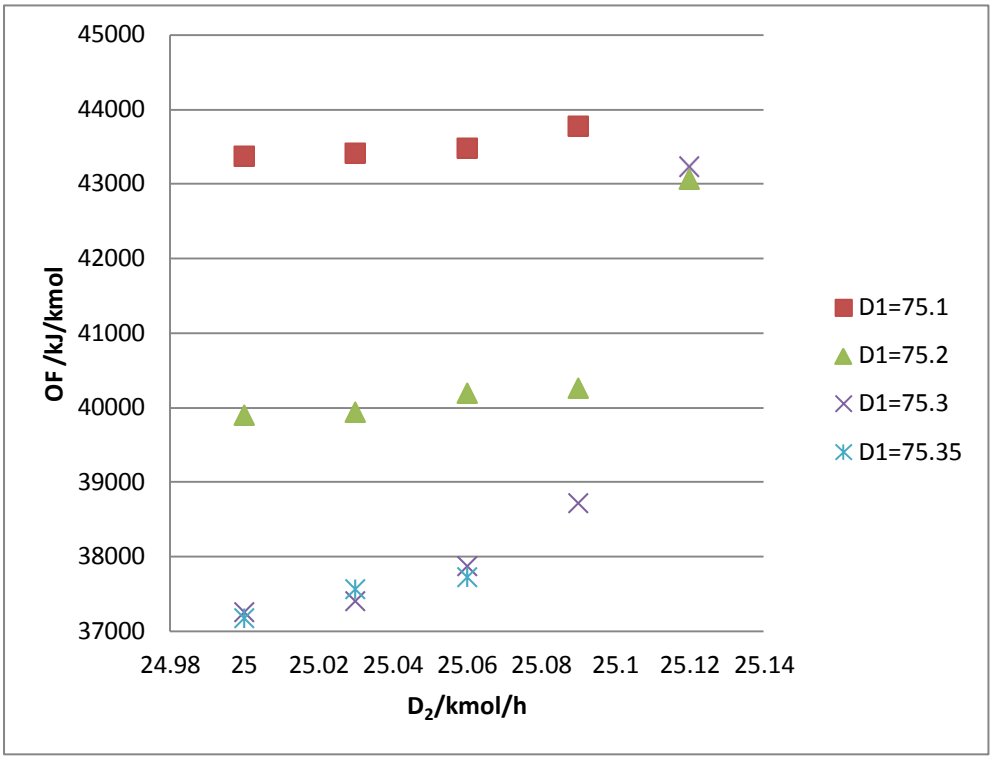

Figure 5.3 – Effects of D_1 and D_2 on OF with D_1, D_2, F_E, R_1 and R_2 as variables

From Figure 5.3, we observe that OF describing the total energy demand per product flow rate decreases quickly with the increase of D_1. The same statement was made in our previous study for the acetone-

methanol-water system. Also this phenomenon is counterintuitive: normally, the more products at specified purity are obtained, the more energy (reboiler duty) should be used. But as explained in section 2.4, fewer products (e.g. a distillate D_1 of 75 kmol/h) induced a large entrainer feed – main feed ratio in column 1 to meet the purity specifications. Besides, seeking a larger D_1 DIPE-rich distillate increases the separation difficulty in the extractive column but eases the separation in the entrainer regeneration column as less DIPE impurity enters it, here inducing global energy savings. Obviously, our objective function OF accounting for both columns can describe quantitatively the trade-off between the two columns. Meanwhile, Figure 5.3 shows that an increase in D_2 increases the OF value. Notice that for D_1 is lower than 75.1 kmol/h, the OF value is very high above 45000 kJ/kmol because of too much DIPE entering regeneration column, leading to high energy cost. This point agrees with the relation of two distillate mentioned before. Thus D_1 lower than 75.1 kmol/h cannot be considered further as suitable and not shown in Figure 5.3.

As we will optimize other variables such as N_{FE}, N_{FF}, N_{FReg}, N_{Ext} and N_{Reg} in the subsequent steps, we select $D_1 = 75.35$ kmol/h and $D_2 = 25$ kmol/h; those values correspond to a product recovery of 99.96% for DIPE-rich distillate and 99.5% for IPA-rich distillate, respectively. The corresponding *OF* value is 37174.9 kJ/kmol, with $F_E = 96.9$ kmol/h, $R_1 = 1.85$ and $R_2 = 1.80$ at $P_1 = 0.4$ atm.

5.3.3.Continuous variables F_E, R_1 and R_2

The optimized F_E, R_1, R_2 value are shown in Table 5.4 while the other variables are kept constant. Notice that the initial values of the three feed locations in case A and case B are taking from Luo's design (Luo et al., 2014).

Table 5.4 – Optimized values of F_E, R_1, and R_2 for the extractive distillation of DIPE – IPA with 2-methoxyethanol

	Case A	Case B
P_1 /atm	1	0.4
P_2 /atm	1	1
N_1	66	66
N_2	40	40
D_1 kmol/h	75.35	75.35
D_2 kmol/h	25	25
N_{FE}	30	30
N_{FAB}	56	56
N_{FReg}	10	10
F_E /kmol/h	96.9	84.6
R_1	1.85	1.70
R_2	1.80	1.33
OF /kJ/kmol	37174.9	30639.9

We observe (1) under lower pressure (case B), the values of F_E, R_1, R_2 in case B are lower and OF decreases by 17.6%. It materializes the benefit of the pressure reduction that was anticipated through the analysis of

residue curve map and univolatility line for a 1.0-1a class mixture. (2) The reduction in R_2 is more pronounced that in R_1. If less entrainer is fed to the extractive column, a greater R_1 is needed to get the same separation effect. Meanwhile the concentration of entrainer fed to the regeneration column decreases due to mass balance, and less energy (R_2 decrease) is used to recycle the entrainer. Overall, these observations agree with those in chapter 4 for the separation of acetone-methanol-water system. These results also show the benefit of optimizing both columns together to improve further the OF.

5.3.4.Selecting suitable feed locations

The method stated in chapter 3 is used here. For each set of values, F_E, R_1, R_2 are optimized while D_1 and D_2 are fixed. Table 5.5 shows the results considering now P_1 = 0.4 atm and P_2 = 1 atm as in case B above

Table 5.5 – Open loop optimal results of F_E, R_1, R_2, N_{FE}, N_{FAB}, N_{FReg} under fixed D_1 and D_2 for the extractive distillation of DIPE – IPA with 2-methoxyethanol, P_1 = 0.4 atm and P_2 = 1 atm

N_{FE}	N_{FAB}	N_{FReg}	F_E	R_1	R_2	OF kJ/kmol
26	58	13	75.1	1.76	1.20	30292.8
27	59	14	75.0	1.75	1.17	30081.9
28	58	13	75.1	1.76	1.17	30144.8
28	59	15	74.1	1.77	1.16	30110.5
28	60	15	75.0	1.74	1.17	30042.9
28	60	16	74.0	1.77	1.16	30122.2
28	61	15	74.0	1.78	1.15	30213.2
29	55	9	80.0	1.73	1.37	30827.4
30	56	10	84.6	1.70	1.33	30639.9
30	57	11	84.4	1.66	1.34	30410.7
31	55	10	86.5	1.67	1.39	30740.8
31	56	11	86.6	1.65	1.38	30619.0

As a whole, the shifting of the three feed locations improves further the OF value by 1.9% but also impacts the process efficiency that will be discussed in section 4.5. A few statements can be made from Table 5.5: (1) OF is moderately sensitive to small changes of the three feed locations when F_E, R_1, *and* R_2 are optimized. (2) In conventional distillation an increase of the number of trays in the rectifying section allows to use a lower reflux ratio R_1, but here for an extractive column, the opposite is found as feed location of entrainer moves up the column from 30 to 28 for the lowest OF design. The reason was stated in Lelkes et al.[31]: too much trays in the rectifying section is not recommended in extractive distillation for the 1.0-1a class because the pure product DIPE is a saddle in the RCM. (3) The minimum value of OF is found with six extra number of trays in the extractive section than Luo's design. As discussed earlier, a key factor to achieve the extractive separation is to reach the extractive section stable node SN_{ext} near the DIPE-2methoxyethanol edge. This can be achieved by more trays in the extractive section. Another consequence is that the efficiency of the extractive section that will be discussed in section 4.5 is improved. (4) The lowest energy cost for per unit

product OF is 30042.9kJ/kmol with N_{FE} = 28, N_{FAB} = 60 and N_{FReg} = 15. It represents a further 1.9% reduction in energy cost compared the design with N_{FE} = 30, N_{FAB} = 56 and N_{FReg} = 10.

5.3.5.Closed loop design and optimal design parameters

The optimal design is re-simulated in closed loop flowsheet in order to make sure the product purity is achieved and that the effect of impurity in recycling entrainer on the process is accounted for. Case 2 under P_1 = 0.4 atm corresponds to the open loop design of case B. It is compared to case 1 that corresponds to our best closed loop design under P_1 = 1 atm. Indeed case A (P_1 = 1 atm) in Table 5.4 that corresponded to a design with Luo's feed locations did not allowed under closed loop simulation to reach the targeted purity for the distillates and cannot be used for comparison.

The design and operating variables and the cost data are shown in Table 5.6, referring to the flow sheet notations in Figure 3.3 in chapter 3. Table 5.7 displays the product purity and recovery values. Figure 5.4 and Figure 5.5 show the temperature and composition profiles of the extractive and entrainer regeneration columns for the best case, case 2, where ME notation holds for 2-methoxyethanol.

Table 5.6 confirms that a process design operating at 1 atm like case 1 can be improved further, while keeping the same number of trays in the extractive and regeneration columns. In summary, (1) the entrainer flow rate decreased drastically from 100 kmol/h in case 1 to 75 kmol/h in case 2, showing that improvement was possible due principally to a combination of a shift of feed locations and pressure reduction, as deduced from the pressure dependency of the azeotrope composition and isovolatility curves. (2) The energy consumption underlying the OF value in case 2 is reduced by 18.3% compared to case 1. It is mostly attributed to a reduction in the entrainer flow rate allowed by the reduced pressure. (3) Meanwhile, TAC savings reach 3.4% mainly due to the decrease of the entrainer flow rate and reflux ratio in the second regeneration column. (4) If we just take into account the extractive column in case 1 and case 2, the decrease of the pressure leads to an increase of the column diameter, and an increase of the condenser heat exchanger area due to the decrease of condenser temperature. However, the decrease of the pressure results in the decrease of reboiler duty by 11.6%, and the benefit of decreasing pressure overcomes the punishment as the annual cost of extractive column is slightly reduced from 1.293 to 1.284 (10^6\$). Regarding Luo's design, his sequential approach based in sensitivity analysis was to achieve the lowest TAC. But Table 5.6 shows that his design's TAC is higher than case 1's TAC at the same pressure. Luo's design OF is lower that case 1 value, but recall that as seen in Table 5.7, Luo's design does not meet our molar purity specification on the DIPE distillate. To meet that specification, case 1 result show that R_1 must be increased and the condenser heat duty as well. This latter increases the OF value.

Table 5.6 – Optimal design parameters and cost data from closed loop simulation for the extractive distillation of DIPE-IPA with 2-methoxyethanol

	Case Luo*		Case 1		Case 2	
column	C_1	C_2	C_1	C_2	C_1	C_2
N_{Ext}	66		66		66	
P_1 / atm	1		1		0.4	
F_{AB} / kmol/h	100		100		100	
F_E / kmol/h	100		100		75	
D_1 / kmol/h	75.44		75.35		75.35	
N_{FE}	30		29		28	
N_{FAB}	56		59		60	
R_1	1.54		1.86		1.83	
Q_C / MW	1.553		1.746		1.838	
Q_R / MW	2.279		2.205		1.948	
N_{Rreg}		40		40		40
P_2 / atm		1		1		1
D_2 / kmol/h		25.03		25		25
N_{FReg}		10		12		15
R_2		1.93		1.88		1.18
Q_C / MW		0.823		0.811		0.614
Q_R / MW		0.748		0.737		0.658
column	C_1	C_2	C_1	C_2	C_1	C_2
Diameter / m	1.44	0.78	1.37	0.69	1.66	0.65
Height / m	46.33	28.05	46.33	28.05	46.33	28.05
I_{CS} / 10^6\$	0.720	0.251	0.683	0.220	0.838	0.207
A_C / m^2	66	23	74	22	164	18
A_R / m^2	116	38	112	38	99	34
I_{HE} /10^6\$	0.347	0.172	0.354	0.170	0.443	0.151
$Cost_{cap}$ / 10^6\$	1.184	0.449	1.145	0.412	1.426	0.378
$Cost_{ope}$ / 10^6\$	0.938	0.313	0.911	0.308	0.809	0.274
$Cost_{CA}$ / 10^6\$	1.333	0.462	1.293	0.445	1.284	0.399
Q_{HA} / MW	0.407		0.407		0.305	
$Cost_{HA}$ /10^6\$	0.016		0.016		0.013	
TAC / 10^6\$	1.810		1.754		1.696	
OF / kJ/kmol	35098.7		37230.7		30398.9	

* Luo's process distillate molar purity for DIPE-rich product is below our specifications

Table 5.7 – Product purities and recoveries for case Luo, case 1 and 2 designs

Mole fraction		D_1	D_2	W_2	W_1	recovery
Case Luo	DIPE	0.99350	0.00202	4.67E-27	0.00041	99.93%
	IPA	0.00044	0.99637	0.00028	0.20044	99.64%
	ME	0.00606	0.00161	0.99972	0.79915	
Case 1	DIPE	0.99504	0.00096	5.67E-26	0.00019	99.97%
	IPA	0.00076	0.99772	0.00034	0.20033	99.78%
	ME	0.00420	0.00132	0.99966	0.79948	
Case 2	DIPE	0.99501	0.00105	1.39E-23	0.00026	99.96%
	IPA	0.00090	0.99730	0.00042	0.25044	99.73%
	ME	0.00409	0.00165	0.99958	0.74930	

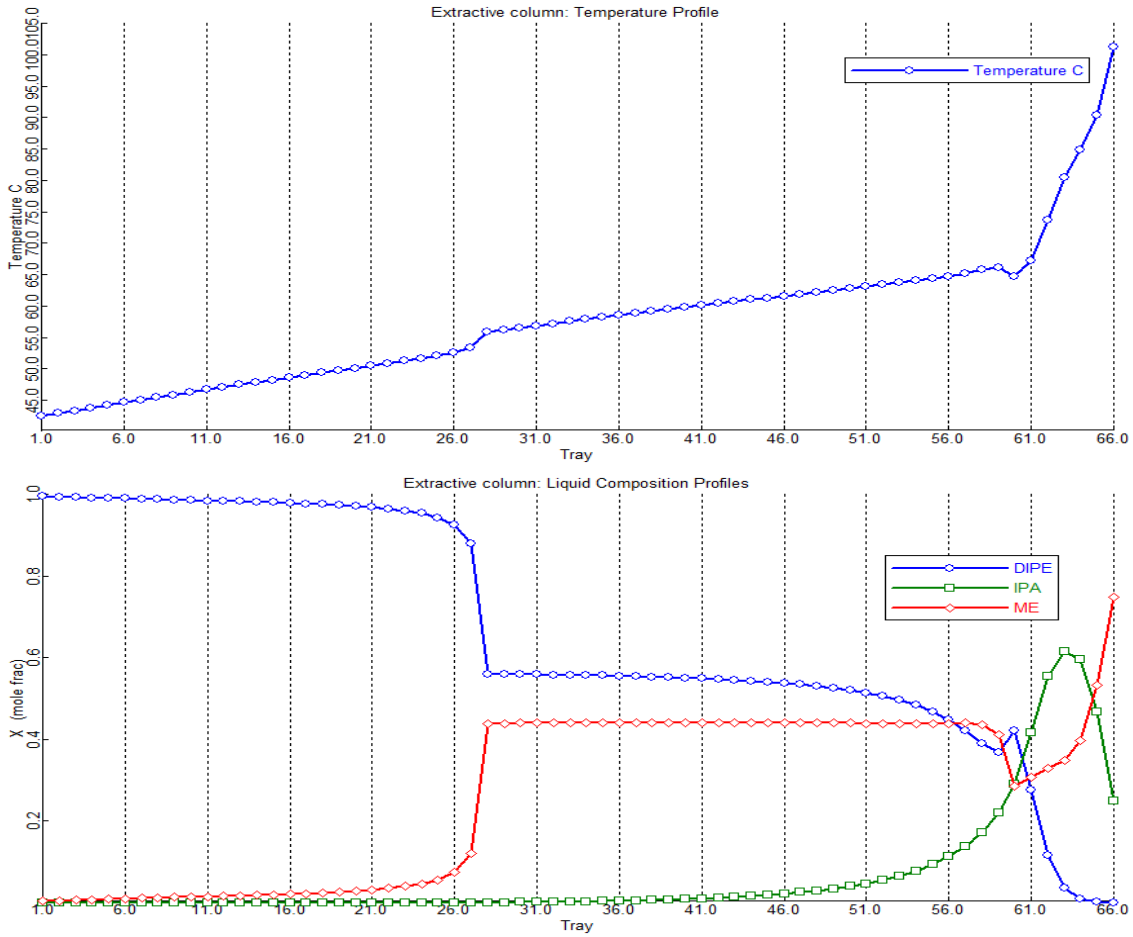

Figure 5.4 – Temperature and composition profiles of case 2 extractive column for the extractive distillation of DIPE-IPA with 2-methoxyethanol

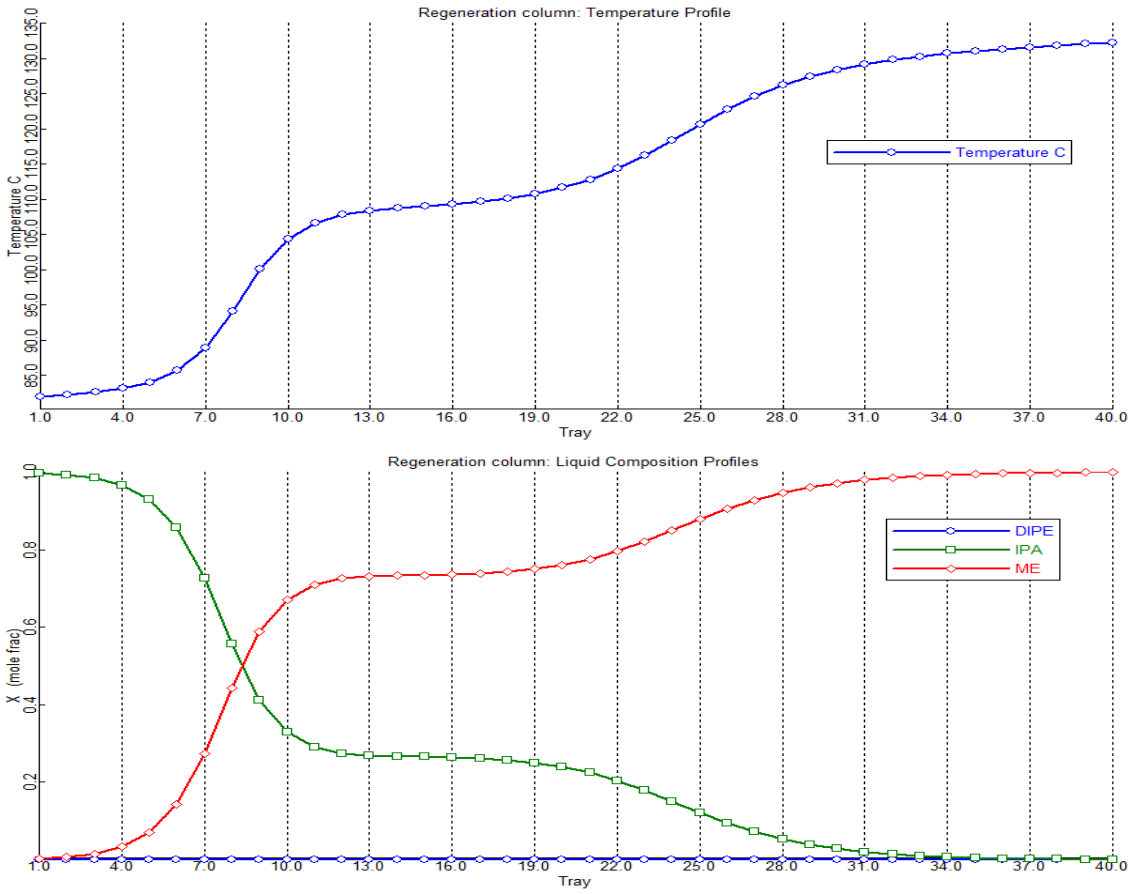

Figure 5.5 – Temperature and composition profiles of case 2 entrainer regeneration column for the extractive distillation of DIPE-IPA with 2-methoxyethanol

Table 5.6 also shows that shifting the feed tray locations and running a new optimization improves the OF and thus reduces the process energy consumption. This point is evidenced by comparing the total reboiler heat duty of case 1 (2.942 MW) and case 2 (2.606 MW): a 11.4 % total heat duty is saved. Regarding product purity and recovery, Table 5.7 shows that purity targets are met and that recoveries are high and in agreement with the relationship between the two distillate flow rates from the mass balances discussed in section 5.2.4.

5.3.6.Analysis from efficiency indicators and profile map in ternary diagram

The efficiency indicator per tray e_{ext} and total efficiency indicator of the extractive section E_{ext} are shown in Table 5.8 for the case 1 and 2, along with the DIPE composition at the feed trays. Figure 5.6 displays the extractive column composition profiles in a ternary map.

From Table 5.8 and Figure 5.6, we remark that (1) Luo's design efficiency indicators are negative, stating that the extractive section is not able to improve the DIPE purity. (2) A lower entrainer flow rate as in case 2 operating at low pressure allows the top end of the extractive section SN_{ext} to lie closer to the product vertex. (3) The efficiency indicators are slightly higher for case 2 than for case 1. Indeed the lower operating

pressure leads to more favorable isovolatility curves and SN_{ext} location as shown in Figure 5.1 and Figure 5.6, which directly affect the efficiency indicators E_{ext} and e_{ext}.

Compared to Luo's design, both case 1 and case 2 show positive and evidently higher efficiency indicators. Their absolute value is comparable to those observed for the acetone – methanol extractive distillation process with water in chapter 4. Also case 2 with a lower TAC has a higher efficiency than case 1. But we cannot conclude that the design with the highest efficiency indicator is the more economical. However, there is optimal efficiency indicator $E_{ext,opt}$ which corresponds the optimal design. The calculation method of $E_{ext,opt}$, and related process will be shown in chapter 6.

Table 5.8 – Efficiencies of per tray and total extractive section for the extractive distillation of DIPE – IPA with 2-methoxyethanol

	Pressure /atm	DIPE composition		N_{ext}	E_{ext} /10^{-3}	e_{ext} /10^{-3}
		Entrainer feed tray (SN_{ext})	Feed tray			
Case Luo	1	0.463	0.492	27	-	-
Case 1	1	0.501	0.393	31	108	3.48
Case 2	0.4	0.560	0.422	33	138	4.18

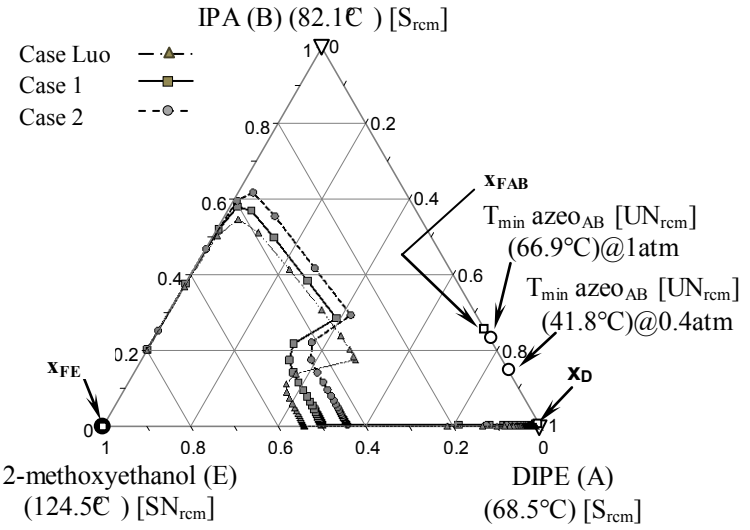

Figure 5.6 – Liquid composition profiles for case Luo (1atm), case 1(1atm) and case 2(0.4atm) extractive distillation column designs for the extractive distillation of DIPE-IPA with 2-methoxyethanol

5.4. Conclusions

Aiming at finding the possible way to save energy cost and total annual cost, we have optimized the design of a homogeneous extractive distillation process for the separation of the DIPE – IPA minimum boiling azeotrope with heavy entrainer 2-methoxyethanol. The process flow sheet includes both the extractive distillation column and the entrainer regeneration column. By using insight from the analysis of the ternary residue curve map and isovolatility curves, we have noticed the beneficial effect of lowering the pressure in the extractive distillation column for a 1.0-1a-m1 extractive separation class. A lower pressure reduces the usage of entrainer and increases the relative volatility of DIPE – IPA for the same entrainer content in the

distillation region where the extractive column operates. A 0.4 atm pressure was selected to enable the use of cheap cooling water in the condenser.

Then we have run an optimization aiming at minimizing the total energy consumption per product unit as objective function OF. OF includes both products and both columns energy demands at boiler and condenser and accounts for the price difference in heating and cooling energy and for the price difference in product sales. Rigorous simulations in closed loop flow sheet were done in all cases. The total number of trays identical to literature works of Luo et al. Other variables have been optimized; two distillates, entrainer flow rate, reflux ratios, entrainer feed location and main feed location. The total annualized cost (TAC) was calculated for all processes.

Thanks to the optimization scheme helped with thermodynamic insight analysis, double digit savings in energy consumption has been achieved while TAC is also reduced. Three important issues have emerged. First the reduction of the pressure is beneficial to the separation by extractive distillation. Second, the energy cost function OF decreases when the distillate flow rate increases at constant purity. This phenomenon has been explained by the relationship of two distillates through mass balance. Third, efficiency indicators of the extractive section that describes the ability of the extractive section to discriminate the desired product between the top and the bottom of the extractive section are relevant criterions to assess the performance of an extractive distillation process design. We have shown that pressure reduction is a possible way to save energy cost and total annual cost based on the thermodynamic insight gained from the ternary diagram analysis. Further investigation of assessing the relation of the efficiency indicators on the process TAC and total energy consumption will be shown in chapter 6.

Chapter 6. Influence of Thermodynamic Efficiency on Extractive Distillation

Results in this chapter have been submitted to:

Aarticle: You, X., Rodriguez-Donis, I., Gerbaud, V., 2015. Influence of thermodynamic efficiency indicator as an optimization criterion for extractive distillation acetone-methanol-water class 1.0-1a as case study. Ind. Eng. Chem. Res.

6.Influence of thermodynamic efficiency on extractive distillation acetone-methanol with water

6.1.Introduction

As a common method applied in industry for separating azeotropic or low relative volatility liquid mixtures, extractive distillation is becoming a more and more important separation method in petrochemical engineering because of the saving both energy cost and capital cost (Doherty and Knapp, 1993; Luyben, 2006).

In this chapter, the configuration of continuous extractive distillation enabling a direct split suitable for the acetone-methanol minimum boiling azeotrope mixture separation with a heavy entrainer water (class 1.0-1a) (Gerbaud and Rodriguez-Donis, 2014) is used shown in Figure 3.3a in chapter 3

In chapter 4, we intended to assess the engineering and physical meaning of an optimal extractive distillation design based on the knowledge of thermodynamic insights from the residue curve map and univolatility line for extractive distillation. We ran the optimization by using the four steps procedure (You et al., 2015). The optimization process led to significant savings in energy consumption and TAC compared to literature values thanks to the low pressure in extractive column and optimization scheme helped with thermodynamic insight analysis. Comparing with literature design, we defined and analyzed them based on the total extractive efficiency and the extractive efficiency per tray that describe the ability of the extractive section to discriminate the product between the top and bottom of that section. For comparison, we fixed the total number of trays as they were proposed in Luyben's design. (Luyben, 2008, 2006).

In this chapter, we investigate if the optimization of extractive distillation can be run satisfactorily with the thermodynamic efficiency indicator E_{ext} and e_{ext}, and no need the good initial value. A multi-objectives genetic algorithm is used with energy cost, TAC, E_{ext} and e_{ext}.

6.2.Optimal methods

6.2.1.Non-Sorted Genetic Algorithm as Process optimization technique

Compared with other methods mentioned in section 6.1, the genetic algorithms are attractive in solving optimization problems with modular process simulators due to the following characteristics. First, the knowledge of initial feasible points is not required and the initial points do not influence the final solution as the search for optimal solution in genetic algorithm is not limited to one point but rather it relies on several points simultaneously (Leboreiro and Acevedo, 2004). Second, in Non-Sorted Genetic Algorithm (NSGA), it is not necessary to have explicit information of the mathematical model or its derivatives because the algorithms are based on a direct search method.

NSGA has been implemented in Excel with visual basic for applications (VBA) programming by our colleagues (Gomez et al., 2010), named genetic algorithm library MULTIGEN. It can handle multi-objective constrained optimization problems involving mixed variables (boolean, integer, real) and some of these problems can be related to process structural optimization. Constraints as well as Pareto domination principles can be handled by the algorithms. Non-Sorted Genetic Algorithm II (NSGAII) is the method we used. NSGAII is based on a ranking procedure, where the rank of each solution is defined as the rank of the Pareto front to which it belongs. The diversity of non-dominated solutions is guaranteed by using a crowding distance measurement, which is an estimation of the size of the largest cuboids enclosing a given solution without including any other. This crowding sorting avoids the use of the sharing parameter used in the previous version of the NSGA algorithm (Gomez et al., 2010).

The stable link between Excel and Aspen Plus was coded in VBA, as was done by (Vázquez-Ojeda et al., 2013). The node of variables such as tray number of column, reflux ratio and so on, are found by Aspen plus tools named *variable explorer*. The simulation is run by using the MESH model *Radfrac* in Aspen Plus.

For NSGA method, a set of optimal designs called Pareto front will be obtained as the results instead of only one optimal design by other methods. As stochastic optimization methods, NSGA is generally robust numerical tools and it presents a reasonable computational effort in the optimization of multivariable functions (Bravo-Bravo et al., 2010). Besides, it can be applicable to unknown structure problems, requiring only calculations of the objective function, and also can be used with all models without problem reformulation (Teh and Rangaiah, 2003).

6.2.2. Advantages of NSGA for the design of extractive distillation process compared with SQP

Compared with SQP optimization solver, NSGA brings advantages. First, there is no need to found a good initial value to guarantee the optimization process to be converged successfully. Second, we no longer have to choose two important aspects in extractive distillation: the choice of distillate flow rates, and the choice of open loop or closed loop flow sheet. (1) Earlier, we chose the two distillate flow rates by sensitivity analysis (You et al., 2015, 2014) because their effects on the achievable product purity are strongly non-linear. (2) The open loop flow sheet does not connect the recycled entrainer and the fresh entrainer feed. However, the closed loop flow sheet can be directly used in NSGA, and the effect of impurity in the recycled entrainer on the product purity is readily handled.

6.2.3.Objective functions

We minimize the total process energy consumption by using the objective function OF as in chapter before. With the use of OF, the two columns in the extractive distillation process are evaluated simultaneously. Only the two product purities are regarded as constraints, and not the recycling entrainer purity thanks to the use of NSGA in closed loop flow sheet, see Figure 3.3 in chapter 3.

$$\begin{aligned} &\min OF = \frac{Q_{r1} + m \cdot Q_{c1} + Q_{r2} + m \cdot Q_{c2}}{k \cdot D_1 + D_2} \\ &subject\ to: \\ &\quad x_{acetone,D1} \geq 0.995 \\ &\quad x_{methanol,D2} \geq 0.995 \end{aligned} \tag{6.1}$$

The TAC is used as the second objective function for the comparison of the different designs. The calculation of TAC is the same as chapter before, and the tray efficiency of 85% is used (Figueiredo et al., 2014).

The efficiency indicator of extractive section E_{ext} (equation 4.3) and the efficiency indicator of per tray in extractive section e_{ext} (equation 4.4) are the third and fourth objective functions. The definition of the efficiency indicators is the same as in part 4.5. Efficiency indicator per tray e_{ext} is supplementary to E_{ext} for dealing the different designs with different entrainer-to-feed flow rate ratio, different reflux ratio and different tray number in the extractive section. E_{ext} and e_{ext} describe the ability of the extractive section to discriminate the desired product between the top and the bottom of the extractive section.

6.3. Results and discussion

6.3.1. Problem setting

This work uses the extractive section efficiency indicator E_{ext} and e_{ext} for the first time as objective functions for the optimization of extractive distillation process, along with OF and TAC. Notice that energy cost OF and total annual cost are minimized, while the efficiency indicator for extractive section E_{ext} and per tray e_{ext} are maximized. For selecting the parameters of GA, the tuning process is done: several tests are conducted with different values of individual, crossover and mutation fraction. After tuning, we choose 300 individuals, 270 generations, 0.8 for crossover fraction, and 0.1 for mutation fraction.

As in chapter 3 and 4, the main feed flow rate is 540 kmol/h (equimolar acetone versus methanol) at 320K. The ten variables of the processes are tray number of the two column N_1 and N_2, distillates and reflux ratios of the two column D_1, D_2 and R_1, R_2, the feed locations of entrainer, main feed and regeneration column N_{FE}, N_{FAB}, N_{FR}, and the entrainer flow rate F_E (It reflects F_E/F). Notice that the operating pressures of extractive column and entrainer generation column are set at 0.6 atm and 1 atm. We showed in chapter 4 that a 0.6 atm leads to a lower $(F_E/F)_{\min}$ and enhances the relative volatility between A and B in the presence of E. The pressure drop of per tray is now assumed as 0.005 atm which was neglected in chapter 3 and 4.

The Pareto front of the process is obtained as the result of the NSGA optimization: a set of nondominated, optimal designs that satisfy the specification of the product purities. A design reported in the Pareto front means that it can't be improved through one objective function without worsening the other objectives.

The procedure of the NSGAⅡ method works as follows: first, the variables of the initial populations are generated randomly within the given value range in Excel. The variables of each individual are sent one by one to Aspen Plus software to run the simulation that gives back the product purities and other information

for calculating objectives to Excel. Generally speaking, no feasible design that satisfies the constraints (product purities) is obtained in the first generation. For such meaningless designs, for example no extractive section exist or the number of feed location over the number of column stage, the product purities are set directly to zero without sending to Aspen. For the case that Aspen simulation is not converged or with error, the Aspen run state parameter is used to avoid this situation. Second, based on the number of satisfied constraints, the population is divided in subpopulation. In our case, the better individuals are those that satisfy the 2 constraints (2 products purities), then that satisfy only one products purities, and that satisfy no product purities. The individuals in subpopulation are ranked according to fitness function. Thanks to the different subpopulation, the GA can optimize the four objective functions, and meanwhile, minimizes the difference between the required and obtained product purities. Finally, the Pareto fronts are obtained as the results of the optimization of extractive distillation process.

6.3.2.Pareto front of the optimal design solution

Although four objectives are used for the optimization, the optimal design that we select is the one with the minimum TAC. The energy cost OF decreases with the increase of the column tray number, and it is useful for finding the minimum energy cost of each design. Regarding e_{ext}, it is used to avoid the situation that only maximizing E_{ext} will result in too many trays used in extractive section.

Figure 6.7 shows the Pareto front of the acetone-methanol-water system extractive distillation, TAC versus E_{ext} and R_1, and Figure 6.8 show the Pareto front of TAC versus R_1 and F_E, and Figure 6.9 show the Pareto front of TAC versus e_{ext} and E_{ext}.

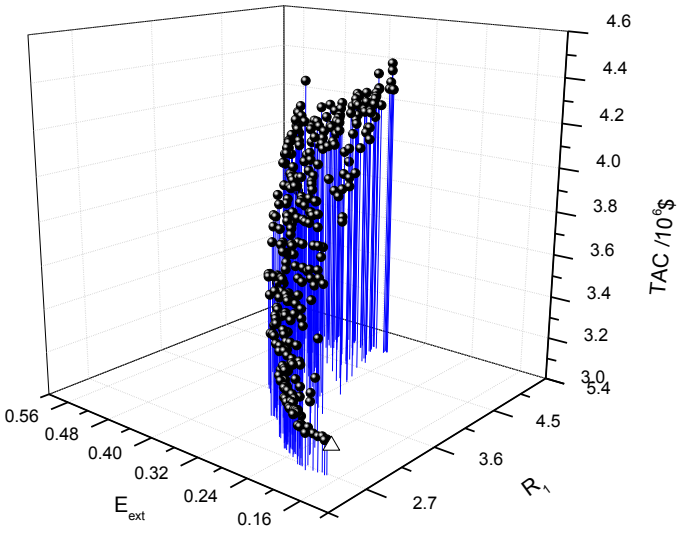

Figure 6.7 – Pareto front of extractive distillation for acetone-methanol-water system, TAC versus E_{ext} and R_1, ∆ means G1

The lowest TAC design is shown as a triangle and later called G1 in Figure 4, 5 and 6. Notice that for all the 300 designs in the Pareto front, the product purities are satisfied. The recycling entrainer purity is not a constraint for the optimization process but remains very high as will be seen later.

From Figure 6.7, we know that (1) the optimal design is not the one with maximum E_{ext}. Along with the decrease of E_{ext} and R_1, TAC decreases. Evidently, a low R_1 is related to a low heat duty and the operating cost and the TAC decreases. (2) A consequence is that E_{ext} that we have thought to be maximized can't be the unique criterion for optimizing the process. (3) The shape of the front shows that there is a maximum E_{ext} for a given reflux ratio, and there is a minimum R_1 for a given E_{ext}. (4) Following the decrease of R_1, the value of E_{ext} decreases, and meanwhile, the value range of E_{ext} gets narrower. We can infer that a suitable design should correspond to an optimal efficiency $E_{ext,opt}$, for which the minimum reflux ratio R_1 exists. Such a minimum feasible reflux ratio was already pointed out in the literatures (Knapp and Doherty 1994; Shen et al., 2013a)

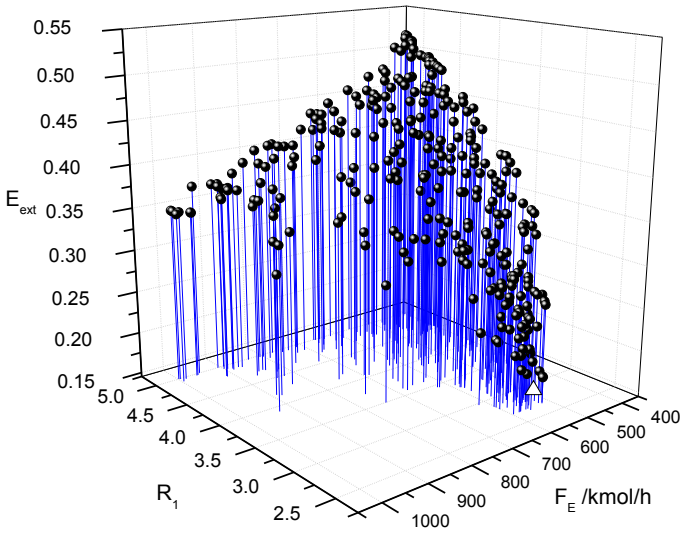

Figure 6.8 – Pareto front of extractive distillation for acetone-methanol-water system, E_{ext} versus R_1 and F_E, Δ means G1

From Figure 6.8, we know that (1) the highest efficiency indicator is located at highest reflux ratio and lowest entrainer flow rate. (2) The efficiency indicator increases at fixed reflux ratio while following the decrease of F_E. Recall from Figure 2. that R_1 and F_E impact the unstable separatrix and that the stable node of extractive section $SN_{ext,A}$' is close to the x_p intersection of $\alpha_{AB} = 1$ with the AE edge when F_E/F decreases. Then, the content of acetone in $SN_{ext,A}$' increases, and so does the efficiency indicator E_{ext}. (3) The efficiency indicator decreases at fixed F_E/F following the decrease of R_1. The reason is that as the reflux ratio decreases, the unstable separatrix moves toward the distillate composition and narrows down the feasible region (see Figure 2.). So E_{ext} is likely to decrease following the meaning of E_{ext}. From another view, as the reflux ratio

decreases for a fixed distillate, the liquid flow rate from column top to the main feed tray decrease, leading to the acetone content on the main feed tray to increase relatively, so E_{ext} decreases following its definition.

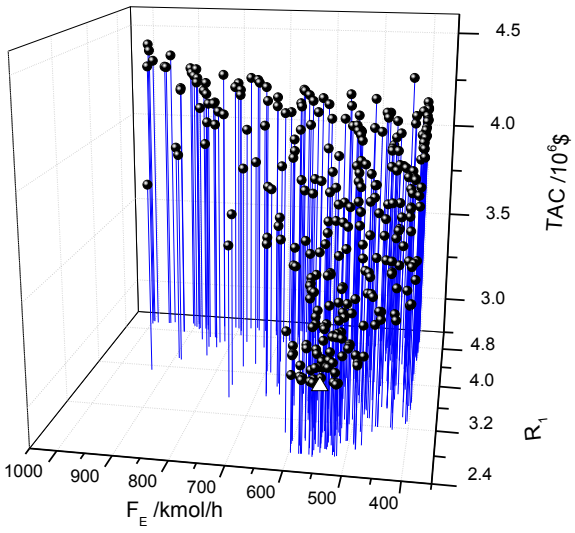

Figure 6.9 – Pareto front of extractive distillation for acetone-methanol-water system, TAC versus R_1 and F_E, Δ means G1

From Figure 6.9, we know that (1) there are only a few points belonging to the Pareto front in the region of reflux ratio R_1 lower than 4 and entrainer flow F_E higher than 700 kmol/h. At a relatively high entrainer flow rate, the separating cost in regeneration column increases. Then, TAC increases compared with the design at a more suitable entrainer flow rate, leading to fewer designs in this region to be ranked in the Pareto front. (2) At low F_E (400-500 kmol/h) and reflux ratio (2.4-2.8), no design is ranked. For these values, the specification of product purities is difficult to achieve for finite tray number. (3) Finally for the value P_1 = 0.6 atm that we chose, an economical feasible value range of the entrainer flow rate is (450 – 650 kmol/h), namely (0.83 - 1.2) for F_E/F.

6.3.3.Insight on the Pareto front shape from the ternary map with extractive profile

In order to further understand the effect of the efficiency indicator E_{ext} on the process, we extract from Figure 6.7 the relation map of E_{ext} and TAC and analyze some designs from Pareto front, namely G1-G6, as shown in Figure 6.10. G1, G3, G4 and G6 are chosen on the upper border of the Pareto front. G2 has a TAC close to that of G3 but exhibits a lower thermodynamic efficiency E_{ext}. G5 has the same E_{ext} than G4 but a much higher TAC. Table 6.1 shows the design variables of G1-G6 and Table 6.2 provides the sizing parameters and cost data.

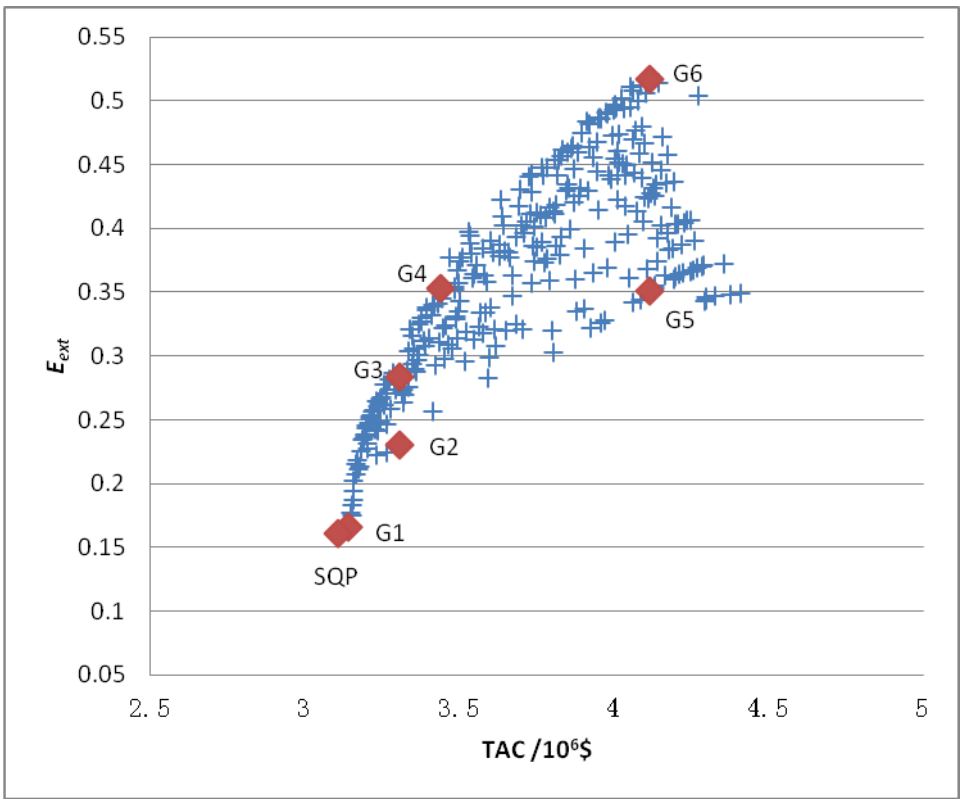

Figure 6.10 – Relation map of E_{ext} and TAC for some designs from Pareto front

We question the reasons for the occurrence of the upper border of the Pareto front and we display the extractive section profile map of G3 at 0.6 atm and 1 atm and the simulating composition profile in Figure 6.11.

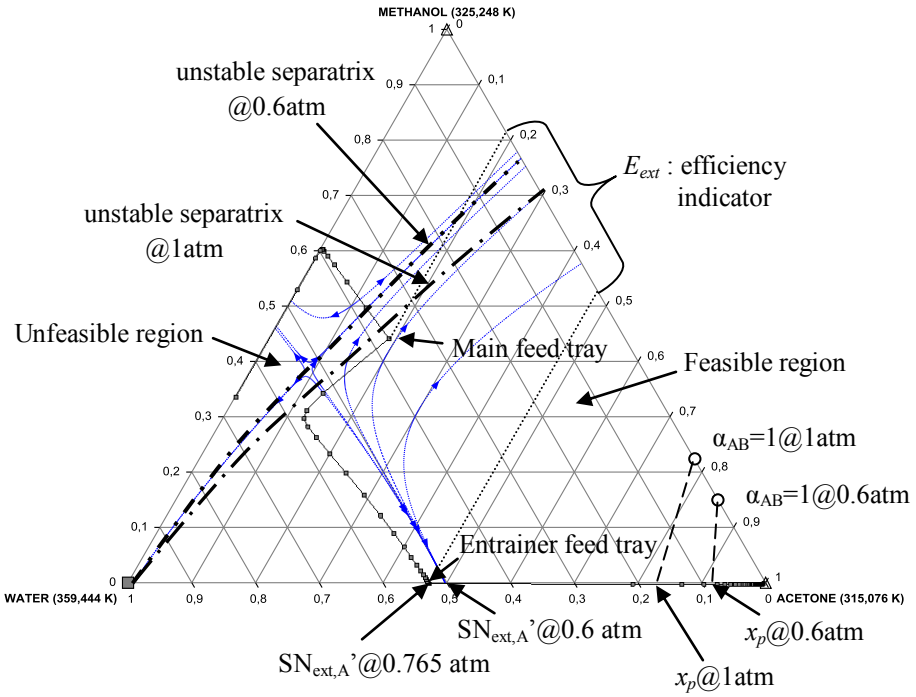

Figure 6.11 – Extractive section profile map for acetone-methanol-water, case G3

Following the physically meaning of E_{ext}, we can infer that the efficiency indicator will be the highest at low F_E/F ratio when the stable node of the extractive section is more close to x_p and when the extractive section profile nears the unstable extractive separatrix. The second condition is nearly achieved for G3 design as shown in Figure 6.11.

The use of the approximate differential extractive profile map derived from mass balance and assuming an infinite number of trays is relevant as Figure 2.7 show that the approximate profile shape agrees with the simulated one, which is calculated with rigorous MESH equations at given tray number for each section. We observe that at point G3, the first condition for maximizing the thermodynamic efficiency is not achieved. Indeed, the process is feasible as the stable node of the extractive section $SN_{ext,A}$' is closed to AE side but as the F_E/F (0.98) is bigger than the minimum value 0.19 and the reflux ratio 3.00 is bigger than the minimum value 2.00, $SN_{ext,A}$' lies far from x_p. Figure 6.11 also shows that as the extractive unstable separatrix moves inside the diagram, giving rise to a shrinking unfeasible composition region when the reflux ratio decreases, the composition's location of main feed stage should be at the lower side of the unstable separatrix, otherwise the process will be unfeasible as the extractive profiles no longer reaches $SN_{ext,A}$' and acetone is no longer the distillate. Besides, when the reflux ratio increases, the separatrix is closer to the BE side, giving a bigger feasible region for extractive distillation in the diagram and leading to bigger efficiency indicator. This point was observed in Figure 6.8 and agrees with the statement about the feasibility of extractive distillation (Rodriguez-Donis et al., 2009a; Shen et al., 2013). However, increasing R_1 is not always a good way to obtain a higher E_{ext} as the energy cost and TAC will increase. A better way to improve the design is to change F_E/F and the suitable feed location to increase the average relative volatility as shown in chapter 4.

In Table 6.1, the G1 design exhibits the lowest TAC and represents our so called optimal design from the NSGA optimization. Comparing the designs of G2 and G3 point with the same total column numbers and nearly the same reflux ratio, OF and TAC, we notice that G3 shows a higher E_{ext} than G2 due to a lower F_E/F but G2 has a higher e_{ext} than G3 because G2 extractive section is shorter than G3 (16 trays vs 22). We may infer that for the same TAC and OF, lowering the entrainer feed flow rate (G3) can be compensated by a higher efficiency per tray (G2).

Comparing G4 and G5, (1) G5 TAC is much higher than G4's because the much larger F_E/F and a large reflux ratio for G5 induce larger reboiler and condenser duties and raise OF and TAC. This evidences that a decrease of the entrainer flow rate and R_1 due to more suitable feed locations N_{FAB} and N_{FE} in the design of G4 greatly reduces OF and TAC. This point proves the importance of increasing the tray number in extractive section as 24 trays for the design of G4 and 13 trays for the design of G5. As discussed in earlier works (Lelkes et al., 1998a; Rodríguez-Donis et al., 2009; You et al., 2015), the extractive section should have enough trays so that the composition at the entrainer feed tray lies near the stable node of the extractive section SN_{ext}' that should be as close as possible to the product – entrainer edge. This point is also in agreement with the sensitivity analysis over the tray number performed by Lang for the same separating

system (Lang, 1992). (2) G5 design shows that a high thermodynamic extractive efficiency per tray e_{ext} doesn't always mean low OF and TAC. Compared to G4, the increase of e_{ext} in G5 by decreasing the tray number in the extractive section requires F_E/F and R_1 to be increased in order to get the same E_{ext} for both G4 and G5. This leads to the increase of TAC due to the increase of the energy cost in extractive column and the separation in entrainer recovery column.

Table 6.1 – Design parameters for G1-G6 belonging to the Pareto front, $P_1 = 0.6$ atm, $P_2 = 1$ atm

	G1	G2	G3	G4	G5	G6
Extractive column						
N_1	65	65	65	61	64	65
F_{AB}, kmol/h	540.0	540.0	540.0	540.0	540.0	540.0
W_2, kmol/h	545.3	616.3	525.7	431.4	864.8	400.4
E_{makeup}/kmol/h	1.7	1.6	1.9	1.3	1.5	1.3
F_E /kmol/h	547.0	617.9	527.6	432.7	866.3	401.7
$N_{F,E}$	34	37	33	26	31	25
$N_{F,AB}$	53	52	54	49	43	55
D_1 /kmol/h	271.3	271.3	271.3	271.3	271.3	271.3
R_1	2.66	2.98	3.00	3.44	4.64	4.98
Q_C/MW	8.38	9.10	9.15	10.17	12.91	13.92
Q_R/MW	8.71	9.49	9.47	10.41	13.49	13.69
Regeneration column						
N_2	35	35	35	35	35	35
D_2 /kmol/h	270.4	270.3	270.6	270.0	270.2	270.0
N_{FR}	26	24	28	27	26	25
R_2	1.02	1.05	1.05	1.04	1.20	1.03
Q_C/MW	5.32	5.41	5.43	5.39	5.82	5.35
Q_R/MW	5.70	5.81	5.80	5.72	6.34	5.66
OF /kJ/kmol	28657.5	30429.8	30368.2	32111.7	39431.6	38964.8
TAC/10^6\$	3.140	3.305	3.304	3.438	4.115	4.117
E_{ext} /10^{-3}	166	230	284	353	351	517
e_{ext} /10^{-3}	8.3	14.4	12.9	14.7	27.0	16.7

Comparing the designs of G3 and G4, both on the upper frontier of the Pareto front, the higher E_{ext} for G4 is due to the decrease of F_E that moves $SN_{ext,A}$' closer to x_p and to the increase of R_1 that approaches the unstable separatrix closer to the BE edge.

Finally, G6 and G1 display the best and the worst thermodynamic efficiency. G6 very high TAC shows that maximizing the total efficiency, by getting the main feed tray composition near the unstable extractive separatrix and by looking for the lowest entrainer flow rate, is not leading to the lowest OF and TAC design. On the contrary, the best design G1 shows the lowest E_{ext} but it is still larger than the one for Luyben's

design, E_{ext} = 55×10^{-3}, and close to that of Knapp and Doherty's design (Knapp and Doherty, 1990), E_{ext} = 160×10^{-3}, as we discussed in chapter 4.

Table 6.2 – Sizing parameters for the columns and cost data of the design G1-G6 belonging to Pareto front

	G1	G2	G3	G4	G5	G6
	Extractive column					
Diameter /m	2.825	2.954	2.962	3.135	3.564	3.679
Height /m	45.72	45.72	45.72	42.68	44.50	45.72
I_{CS} /10^6\$	1.462	1.533	1.538	1.546	1.833	1.937
A_C /m^2	878	954	959	1066	1353	1435
A_R /m^2	441	480	479	527	683	704
I_{HE} /10^6\$	1.257	1.328	1.330	1.421	1.668	1.720
$Cost_{cap}$ /10^6\$	3.044	3.210	3.218	3.323	3.954	4.147
$Cost_{ope}$ /10^6\$	1.033	1.125	1.124	1.236	1.600	1.652
$Cost_{CA}$ /10^6\$	2.048	2.195	2.196	2.344	2.918	3.034
	Regeneration column					
Diameter /m	1.614	1.626	1.630	1.625	1.689	1.618
Height /m	23.78	23.78	23.78	23.78	23.78	23.78
I_{CS} /10^6\$	0.477	0.480	0.482	0.480	0.500	0.478
A_C /m^2	183	185	186	185	200	184
A_R /m^2	289	294	294	290	321	286
I_{HE} /10^6\$	0.648	0.656	0.656	0.652	0.691	0.647
$Cost_{cap}$ /10^6\$	1.196	1.208	1.210	1.203	1.268	1.`96
$Cost_{ope}$ /10^6\$	0.675	0.689	0.687	0.678	0.750	0.671
$Cost_{CA}$ /10^6\$	1.074	1.091	1.091	1.079	1.173	1.069
Q_{HA}/MW	0.67	0.76	0.65	0.53	1.06	0.491
$Cost_{HA}$ /10^6\$	0.018	0.019	0.017	0.015	0.024	0.014

Figure 6.12 displays the extractive section profile map and the simulation composition profile for G1. The beginning point of the extractive section (at main feed tray) in the design of G1 (see Figure 6.12) is not as close to the unstable separatrix as would have been expected from the design of G3 (see Figure 6.11) and E_{ext} is consequently lower. The reasonable explanation is that during optimization procedure of NSGA with maximizing E_{ext}, the effect of reflux ratio (R_1) is a dominant variable to reduce OF and TAC. When E_{ext} is closer to its optimal value $E_{ext,opt}$, the effect of R_1 become weak, and meanwhile the effect of other variables (entrainer flow rate, entrainer and main feed locations) become more obvious, leading to that a design with much lower TAC and the beginning point away from unstable separatrix. This phenomenon proves that finding an optimal design can't only upon the sole maximization of E_{ext}, but that optimization is much needed for a given R_1 and F_E.

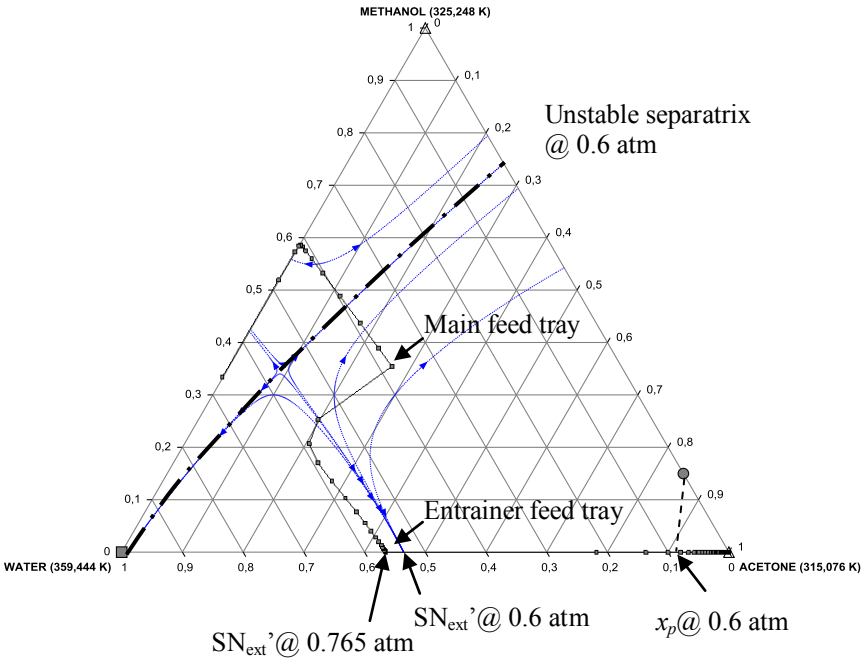

Figure 6.12 – Extractive section profile map for acetone-methanol-water, case G1

This answers our initial question and tempers our optimism displayed in our previous work: we cannot use the thermodynamic efficiency indicator alone to optimize the extractive distillation process for the 1.0-1a class and there likely exist an optimal $E_{ext,opt}$ near G1's values that we now verify.

6.3.4.Further improvement of GA optimal design

The results shown in Pareto front are obtained through the optimization of the four objective functions, but in practice the design with the lowest TAC is the most favorable one. So we select the design of G1 which has the lowest TAC as initial design to run a further optimization by SQP method in order to appreciate the ability of the NSGA to find an optimal solution. The results are shown in Table 6.3 namely case SQP. Besides, in order to compare fairly with our previous design in chapter 4 ($N_1 = 57$, $N_2 = 26$) namely *case 3opt* where a 100% tray efficiency was assumed and the pressure drop per tray was neglected, we now optimize it as *case 3opt'* under 85% tray efficiency and a 0.005 atm pressure drop per tray.

The four-step procedure stated in chapter 4 is used. The single objective function for the SQP optimization is OF and is based on the same column tray number ($N_1 = 57$, $N_2 = 26$) for Case 3opt' and ($N_1 = 65$, $N_2 = 35$) for Case SQP. The other 8 variables are optimized by SQP through minimizing OF. TAC and two efficiency indicators are calculated afterwards. The design and operating variables are shown in Table 6.3 and Table 6.4, referring to the flow sheet notations in Figure 3.3 in chapter 3. Table 6.5displays the product purity and recovery values.

With the same number of trays than Luyben and Knapp and Doherty's design but with stricter product purity constraints, Table 6.3 shows that Case 3opt in chapter 4 represented a great improvement over Luyben's

design with a double digit saving in OF and TAC and reached OF = 28318.5 kJ/kmol and TAC = 2.918×10^6\$. By taking into account the tray efficiency and the pressure drop Case 3opt' OF and TAC increase now to OF = 30119.8 kJ/kmol and TAC = 3.153×10^6\$ respectively, mostly because of the decrease of the tray efficiency. The pressure drop slightly affects the relative volatility which decreases when the pressure increases. Therefore the separation is more demanding and TAC and OF are slightly larger.

From Table 6.3, we also know that (1) the G1 design reduces OF by 4.8% over case 3opt'. A suitable increase of tray number proposed by the NSGA optimization in the columns allows a lower entrainer flow rate to be used and decreases the energy cost in both columns. (2) The G1 design from NSGA with 4 objective functions is marginally improved through the SQP method that only minimizes OF. At the design step of the process, the improvement is not significant. (3) The SQP method runs faster than NSGA but requires a good initialization that the NSGA results can propose. (4) Compared with case G1, two more trays are used in the extractive section of case SQP design, resulting in a small decrease of the reflux ratio in extractive column. (5) For the acetone-methanol equimolar mixture separation with water, $E_{ext,opt}$ should be at 0.161±3% for extractive column operating at 0.6 atm. It is greater than Luyben's figure and similar to Knapp and Doherty's estimate (see Table 4.7 in chapter 4).

Table 6.3 – Final design results for acetone-methanol-water by NSGA and SQP

	Case 1	Case G1	Case SQP
Extractive column			
N_{Ext}	57	65	65
F_{AB} /kmol/h	540	540.0	540.0
W_2 /kmol/h	636.1	545.3	557.9
E_{makeup} /kmol/h	2.1	1.7	2.1
F_E /kmol/h	638.2	547.0	560.0
N_{FE}	32	34	34
N_{FAB}	48	53	55
D_1 /kmol/h	271.0	271.3	271.1
R_1	2.74	2.66	2.59
Q_C/MW	8.55	8.38	8.21
Q_R/MW	8.93	8.71	8.56
Regeneration column			
N_{Reg}	35	35	35
D_2 /kmol/h	271.1	270.4	271.0
N_{FR}	19	26	25
R_2	1.18	1.02	1.00
Q_C/MW	5.78	5.32	5.30
Q_R/MW	6.21	5.70	5.68

Table 6.4 – Sizing parameters for the columns and cost data of the design case 1, case G1 and case SQP

	Case 1	Case G1	Case SQP
	Extractive column		
Diameter /m	2.857	2.825	2.796
Height /m	39.63	45.72	45.72
I_{CS} /10^6\$	1.319	1.462	1.446
A_C /m^2	896	878	861
A_R /m^2	452	441	434
I_{HE} /10^6\$	1.276	1.257	1.242
$Cost_{cap}$ /10^6\$	2.882	3.044	3.008
$Cost_{ope}$ /10^6\$	1.059	1.033	1.016
$Cost_{CA}$ /10^6\$	2.020	2.048	2.018
	Regeneration column		
Diameter /m	1.683	1.614	1.609
Height /m	17.68	23.78	23.78
I_{CS} /10^6\$	0.393	0.477	0.475
A_C /m^2	198	183	182
A_R /m^2	315	289	288
I_{HE} /10^6\$	0.685	0.648	0.647
$Cost_{cap}$ /10^6\$	1.234	1.196	1.192
$Cost_{ope}$ /10^6\$	0.736	0.675	0.673
$Cost_{CA}$ /10^6\$	1.114	1.074	1.071
Q_{HA}/MW	0.77	0.67	0.69
$Cost_{HA}$ /10^6\$	0.020	0.018	0.018
OF /kJ/kmol	30119.8	28657.5	28326.3
TAC	3.153	3.140	3.107
E_{ext} /10^{-3}	153	166	161
e_{ext} /10^{-3}	9.0	8.3	7.3

Table 6.5 – Product purities and recoveries for case NSGA and SQP designs

Mole fraction		D_1	D_2	W_2=water	W_1=F_2	recovery
Case 1	Acetone	0.99502	0.00129	8.10E-11	0.00039	99.87%
	Methanol	0.00055	0.99540	0.00009	0.29753	99.95
	Water	0.00443	0.00331	0.99991	0.70208	
Case G1	Acetone	0.99502	0.00019	1.43E-12	6.22E-05	99.98%
	Methanol	0.00053	0.99799	0.000143	0.33089	99.95%
	Water	0.00445	0.00182	0.999857	0.66905	
Case SQP	Acetone	0.99505	0.00090	9.58E-13	0.00029	99.91%
	Methanol	0.00023	0.99608	4.36E-05	0.32568	99.98%
	Water	0.00472	0.00302	0.999956	0.67403	

Table 6.5 shows that case 3opt', G1 and SQP optimized in closed loop flowsheet achieve the product purities for both distillates. We also notice that the water content in recycled entrainer is very high for all cases but lower than 99.99% in case G1 obtained with the NSGA optimization. In chapter 4 and 5, based on a SQP optimization with an open loop flow sheet assuming a pure entrainer feed to the extractive column, we had to run an additional closed loop simulation to overcome the effects of the impurities in recycled entrainer on the product purity. This is no longer necessary with the NSGA method optimizing directly the closed loop flowsheet.

The temperature and composition profiles in the two columns of case SQP are shown in Figure 6.13 and Figure 6.14. When displayed on a ternary diagram, the case SQP composition profile looks very similar to the one for G1 displayed in Figure 6.12.

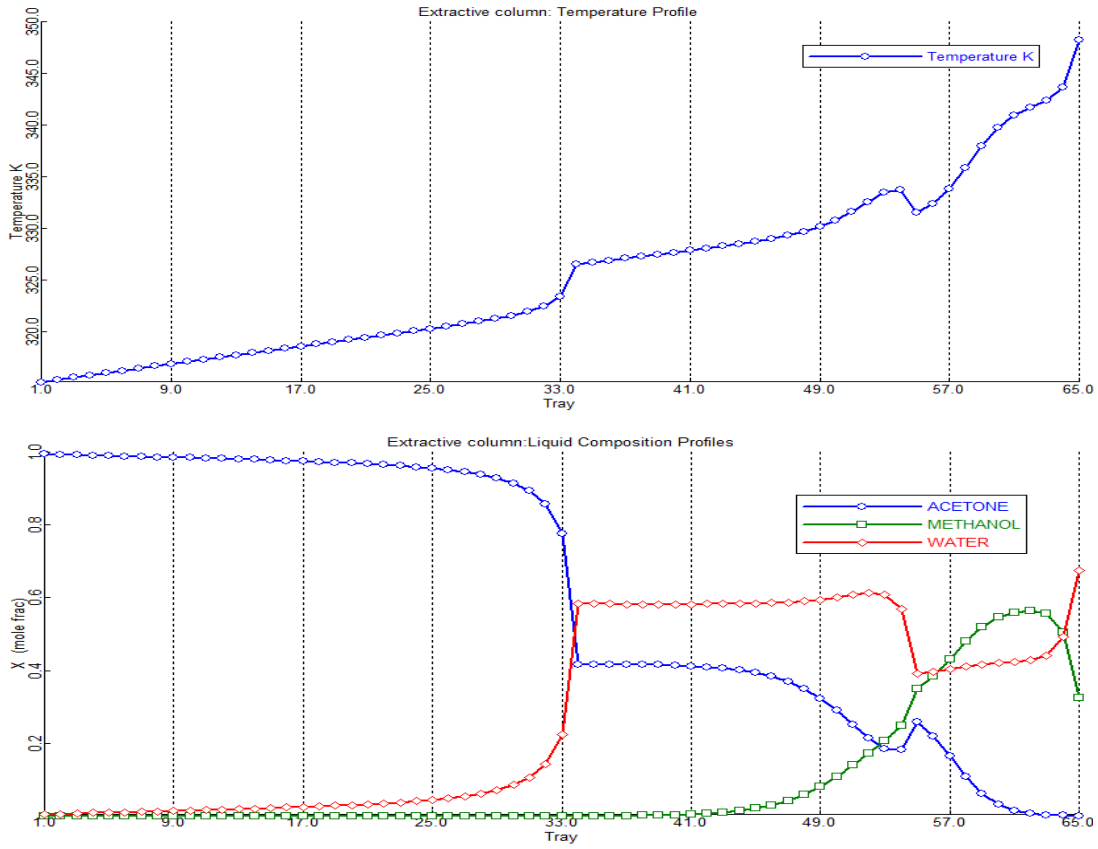

Figure 6.13 – Temperature and composition profiles of extractive column for the extractive distillation of acetone – methanol with water, case SQP

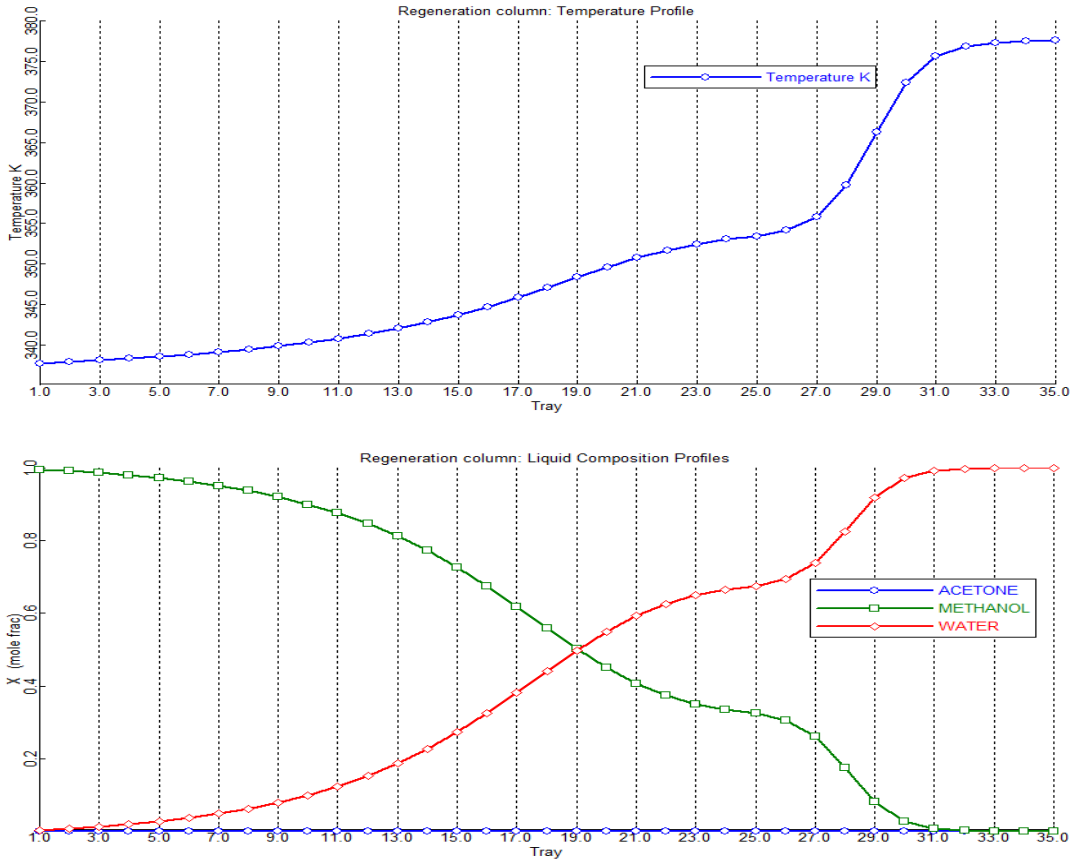

Figure 6.14 – Temperature and composition profiles of entrainer regeneration column for the extractive distillation of acetone – methanol with water, case SQP

From Figure 6.13, there is a temperature decrease in the temperature profile map of extractive column as the main feed temperature was fixed at 320K during the optimization the same as in chapter 4 and 5. We can also notice in Table 6.5 that most of the impurity in distillate (D_1) is the high-boiling temperature water because the rectifying section profile reaches x_{D1} on the acetone-water mixture side where there is a pinch point at the high acetone content side. Its effect is that more than half of the trays (34 out of 65) are used in rectifying section in extractive column for separating the acetone from water. Besides, the content of methanol in the rectifying section is very low (see Figure 6.13) which proves that the extractive section pinch point (SN_{ext}') was able to come very close to the AE side.

6.4. Results and discussion

The optimization of the extractive distillation process including the extractive and entrainer regeneration columns for the separation of acetone-methanol minimum azeotropic mixture with heavy entrainer water was investigated. Based on our study in chapter 4, the operating pressure of extractive column was set at 0.6 atm because it takes the benefit of low pressure for enhancing the relative volatility and the separation as well as the use of cheap cooling water. Not needing good initial value and allowing the optimization of both continuous (reflux ratio, entrainer and distillate flowrates) and discrete (column tray number and feed locations) variables, a multi-objective NSGA method coded in Excel is used as optimization method and it is linked with Aspen plus software through programming in VBA. Aiming at investigating the influences of a

thermodynamic efficiency indicator to find an optimal design, we run the optimization with four objective functions: extractive efficiency indicator E_{ext} and e_{ext} are maximized meanwhile TAC (economic view) and OF (energy cost per unit product) are minimized while 99.5% products purities in the distillates are set as constraints.

Through the analysis of Pareto front, the effects of the main variables entrainer-to-feed ratio and reflux ratio on TAC and efficiency indicator are discussed. The results show that there is a maximum E_{ext} for a given reflux ratio, and there is a minimum R_l for a given E_{ext}. There also exists an optimal efficiency indicator $E_{ext,opt}$ which corresponds the optimal design defined as the one with the lowest TAC and $E_{ext,opt}$ can be used as a criterion for the evaluating of different design for the same system. For acetone-methanol with water system, $E_{ext,opt}$ equals to 0.161±3% at 0.6 atm. Indeed we have to conclude that although the thermodynamic efficiency indicators can't be used as an optimization criterion alone, it is worth combining it with usual criteria such as TAC and OF as near its $E_{ext,opt}$ value the design is still very sensitive to the entrainer feed flow rate and reflux ratio parameters that have a dominant impact on OF and TAC. Through the analysis of extractive profile map, we explain the reasons that efficiency indicator increase following the decrease of entrainer flow rate and the increase of reflux ratio.

The SQP method is used to further improve the design following the decrease of TAC with the good initial values from NSGA method. A competitive design is shown with marginal improvement showing that NSGA optimization with the four criteria described above is able to find a consistent and performance design for the extractive process concerning the 1.0-1a class mixture.

Based on the view of total new design, an optimization procedure NSGA plus SQP is demonstrated for extractive distillation. The advantage of both methods are taken into account: NSGA method can avoid the local optimal and supply a good initial design for SQP method meanwhile the optimal design can be obtained more quickly.

Chapter 7. Reducing Process Cost and CO_2 Emissions

Results in this chapter have been submitted to:

Article: You, X., Rodriguez-Donis, I., Gerbaud, V., 2015. Reducing process cost and CO2 emissions for extractive distillation by double-effect heat integration and mechanical heat pump. Applied energy.

7.Reducing process cost and CO_2 emissions for extractive distillation by double-effect heat integration and mechanical heat pump

7.1.Introduction

Distillation is one of the most widely used separation methods in the chemical and petrochemical industry. It is commonly known in chemical industry that distillation process is ranked in a third of the total used energy in chemical industry (Linnhoff et al., 1983). High quality energy in distillation is used to create the vapour flow in reboiler and the vapour flow is cooled down in condenser, meanwhile, it becomes low quality energy. Two approaches are commonly used to improve the energy efficiency of distillation process: double-effect heat integration and heat pumps technology. The interest to use double-effect heat integration and heat pump for heating purposes in distillation column also increase with global awareness of the limited availability of fossil fuels in combination with the greenhouse effect (Bruinsma and Spoelstra, 2010). Carbon dioxide as the main greenhouse gas plays a vital role in global warming since it is responsible for about two-thirds of the enhanced greenhouse effect Gadalla et al. (2005).

Gutiérrez-Guerra et al., (2009) studied the conventional and thermally coupled extractive distillation for the separation of zeotropic and azeotropic mixtures, and showed that thermally coupled extractive distillation can achieve significant reductions of CO_2 emissions due to the energy saving. Jana, (2010) gave a review on the heat integrated distillation operation and pointed out that the main challenges for heat integrated distillation are high investment cost, complex equipment design and control, and lack of experimental data at sufficiently large scale to verify the theoretical predictions. Harwardt and Marquardt, (2012) studied the internally heat-integrated distillation columns (HIDiC) and vapour recompression technique (VRC) for the binary, multicomponent, and nonideal mixtures based on rigorous optimization. They pointed out that excepting rare situation, VRC design are typically superior over HIDiC design with respect to energy and cost savings. Fonyo and Benkö, (1998) analyzed various heat pump assisted continuous distillation configurations including several mechanical heat pump arrangements (vapour compression (VC), vapour recompression (VRC) and bottom flash (BF)) and absorption heat pump arrangements. Bruinsma and Spoelstra, (2010) gave a comprehensive review of different kinds of heat pumps and they focused on two conventional ways to integrate heat pump and distillation columns: the vapor compression column (VC) and vapor recompression column (VRC) as shown in Figure 7.1 (a,b and c).

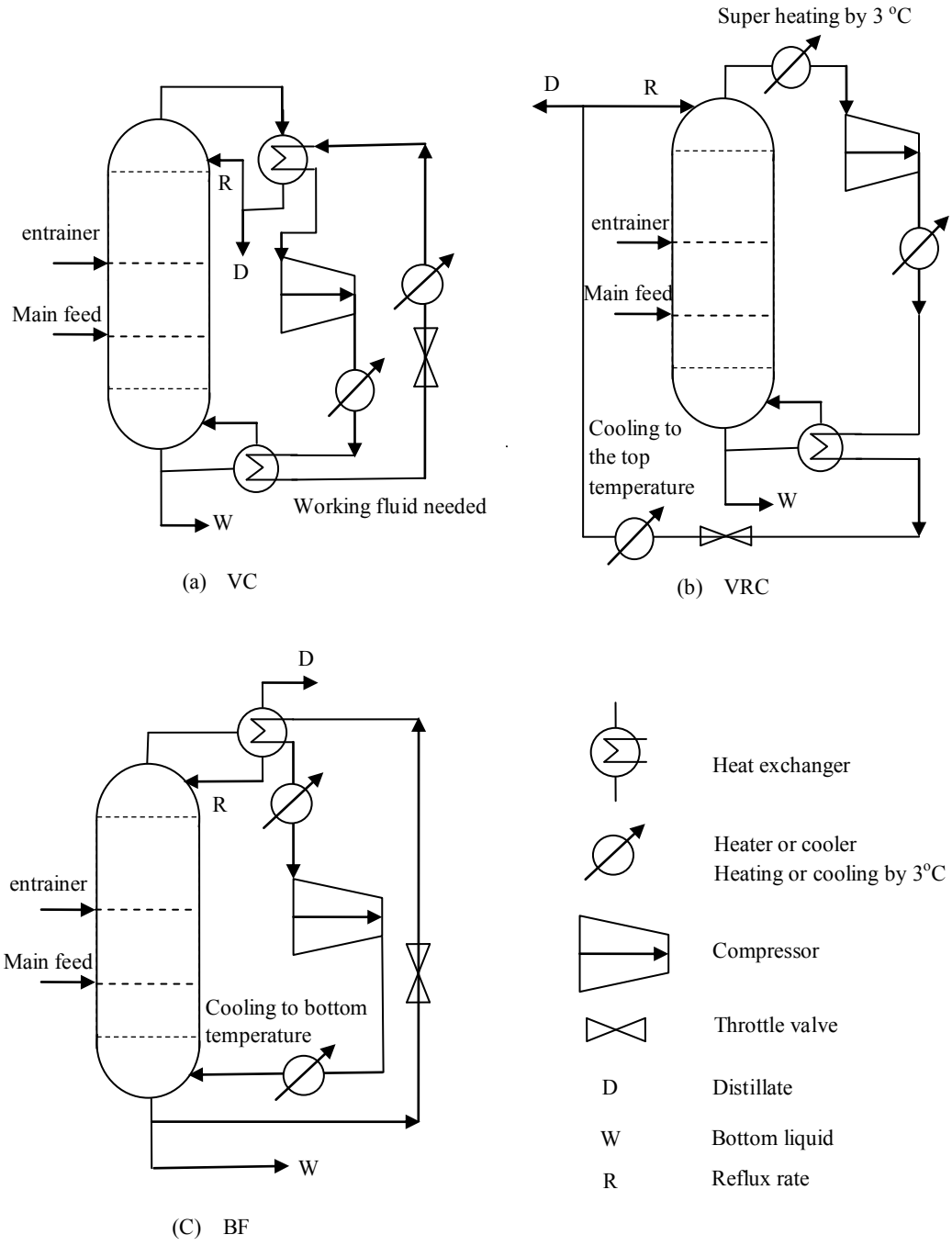

Figure 7.1 – Mechanical heat pump flow sheet for extractive column (a) vapor compression (VC) (b) vapor recompression (VRC) (c) bottom flash (BF).

The advantage of VC is that it can be used for the process that the distillate vapor can't be compressed. In VC, a working fluid is used to absorb the heat from condenser by evaporating, and then it is compressed to a higher (saturation) temperature, give off the heat by liquefying, and then it is cooled down to a temperature below the condenser by expansion over a throttle valve. In VRC, the working fluid is the top vapor flow. It is directly compressed and condensed in the reboiler, after reducing pressure by valve. Then it is partially refluxed to the column top and the other is taken out as distillate. In order to balance the heat input mainly

generating by the compressor, a small condenser is needed. The advantage of VRC over VC is that smaller condenser heat transfer area and lower temperature lift can be used because the heat is exchanged only once. Kiss et al., (2012b) proposed a practical selection scheme of energy efficient distillation technologies with a special focus on heat pump. Using the scheme, process designers can effectively narrow down the number of technology alternatives that can deliver significant energy savings considering the particular process conditions. Modla and Lang (2013) studied the VC, VRC and VRC with external heat exchanger in batch distillation for the separation of low relative volatility mixture. They concluded that for the VRC system in the minimal payback period point, the batch operation time was significantly longer than that of the conventional batch distillation but the payback times was considerable reduced by applying an external heat exchanger.

On the other hand, the bottom flash column (BF) (Figure 7.1c) is an alternative process to VC and VRC (Fonyo and Benkö, 1998). In BF, the bottom liquid is cooled down by expansion over a throttle valve to a temperature below the condenser, it is evaporated at the condenser to cool down the top vapor. Then it is compressed to a higher pressure to reenter the column as bottom vapor flow. Díez et al., (2009) analyzed several distillation assisted heat pump process including VRC and BF for close boiling mixture i-butane and n-butane, and showed that more than 30% energy cost and 9% total cost reductions compared with conventional distillation. Gao et al. (2013) compared VRC and BF heat pump for the separation of n-butanol and isobutanol. VRC heat pump performances were found a little better than BF heat pump and TAC decreased by more than 70% compared with conventional distillation.

Until now, heat pump technique is still not applied as widely as it could be, because of high investment costs and difficulties in system design and integration (Chua et al., 2010). As pointed out by (Fonyo and Mizsey, 1994), when designing heat pump assisted distillation, all three types of MHP processes (VC,VRC and BF) should be considered since there is no unanimous thermodynamic reason to prefer VRC despite its seemingly lower TAC and energy demand.

7.2. Literature studies of extractive process with double-effect heat integration and heat pump

The zeotropic and azeotropic mixtures are mostly encountered in petrochemical engineering and chemical industries. As one of the effective method for separating azeotropic mixture which can't be separated by conventional distillation, extractive distillation is commonly applied in industry, and is becoming a more and more important separation method (Lei et al., 2003). In extractive distillation, entrainer is used to alter the relative volatility of the components to be separated. Thermodynamic insight gained from analysis of residue curve map and volatility order region allows one to assess which component will be withdrawn as product, what the adequate column configuration is, and whether it exists some limiting operating parameter value or not (Rodriguez-Donis et al., 2009a; Rodríguez-Donis et al., 2009b). Therefore, one pure component is attained at the top (resp. bottom) of the extractive column while the other one with the solvent obtained at the

bottom (resp. top) are send to a secondary distillation column by using a direct (resp. indirect) split process configuration (Shen et al., 2013; Shen and Gerbaud, 2013).

The double-effect heat integration extractive distillation flowsheet is shown in Figure 7.2.

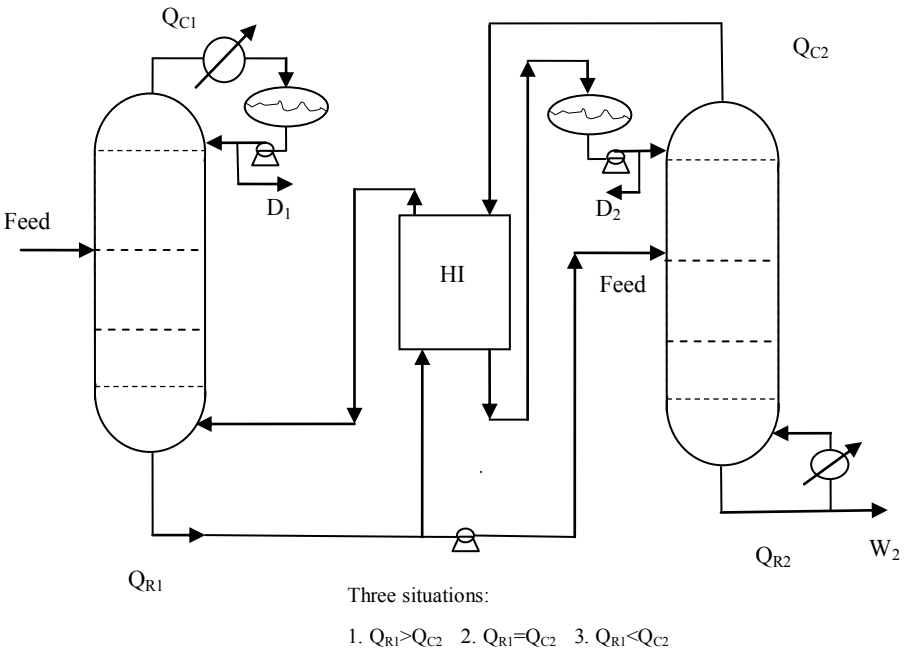

Figure 7.2 – Sketch for heat integration process

The double-effect heat integration implemented in the extractive column was considered by many researchers. In 1990, Knapp and Doherty (1990) systematically studied the thermal integration (double-effect) of the extractive distillation for acetone-methanol-water system. They concluded that the energy cost decreases significantly even though there was no big decrease in TAC. Luyben, (2008) studied the double-effect heat integration distillation process for the same acetone-methanol-water system and obtained 20.5% reduction in TAC compared with conventional extractive distillation process. But we showed in chapter 4 and 6 that Luyben's conventional extractive distillation design could be further optimized to get a lower TAC. Therefore, the expected TAC reduction of double-effect heat integration process over an optimized conventional process may be less. Kravanja et al. (2013) studied the heat integration of biochemical ethanol production from straw by process simulation and pinch point analysis. They showed an improved design through modifying the pressure and heat load, and obtained a 15% reduction of the utility compared to the base case. Palacios-Bereche et al., (2015) investigated the ethanol dehydration extractive distillation process with double-effect heat integration and the results showed that there was no significant difference in total annual cost between conventional process and the double-effect heat integration process. In contrary, Luo et al., (2014) studied the separation of Diisopropyl ether and isopropyl alcohol and found that double-effect heat-integrated extractive distillation increase the TAC instead of decrease compared with conventional

extractive distillation. However, the double-effect heat integrations mentioned above are all direct partial double-effect heat integration and the calculation of TAC is based on 3 year payback period. Is it the same situation for full double-effect heat integration? Is there an optimal heat duty to be integrated that contributes the minimum TAC for extractive distillation process and how to find it? What is the influence of the payback period? These problems will be addressed in this chapter.

There are also many works investigating the continuous extractive distillation process assisted with heat pump. Kiss et al., (2012a) proposed a selection scheme of energy efficient distillation technologies, with a special focus on the choice of heat pump for binary distillation technologies. Van de Bor and Ferreira, (2013) presented a performance map for mechanical heat pumps by using the available temperature glide increases performance, and succeeded in reducing the payback period. They also pointed out that the mechanical heat pumps are able to achieve better economical results over their technical life time due to improving the performance although they require higher initial investment. Gao et al., (2015) studied a coupled separation system involving a mechanical vapor recompression heat pump and double effect distillation for N,N-dimethylacetamide and water two components system, and found that the double-effect distillation with mechanical vapor recompression heat pump has great advantages in terms of both energy and TAC savings. Luo et al., (2015) proposed a heat pump assisted extractive dividing-wall column distillation process, where the top vapor stream is recompressed and used to drive the side reboiler.

Based on the character of extractive distillation process, we will show the possible way for arranging heat pump process in order to save TAC as well as the CO_2 emissions. Our basic case design used for comparison is shown in Figure 7.3.

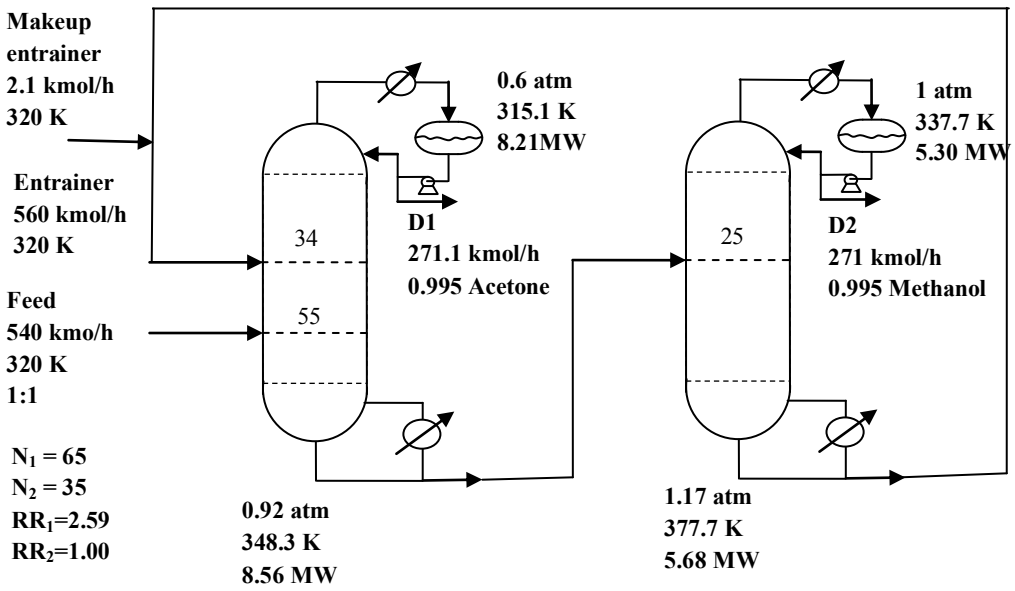

Figure 7.3 – Extractive distillation of acetone-methanol with water, case SQP in chapter 6 as base case

The base case is an extractive distillation process optimized in chapter 6 by focusing on the energy saving of the process itself for the separation of the minimum azeotropic mixture acetone-methanol with heavy entrainer water. That typical 1.0-1a class extractive separation is favored in energy cost at low operating pressure of the extractive column and the P = 0.6 atm is chosen in order to use cooling water for the condenser.

In this chapter, the possible double-effect heat integration process and mechanical heat pumps process are investigated for further energy and capital cost savings as well as the assessment of the effect of process on environment. Since the top vapor components of the two columns are compressed, the VC heat pump will not be considered in this study due to additional heat exchanger capital cost compared with the VRC heat pump process. The goals of this paper are (1) to compare double-effect heat integration processes and find the suitable heat duty to be integrated between extractive and regeneration columns. (2) To study two mechanical heat pumps process (VRC, BF) for continuous extractive distillation, and propose new mechanical heat pump sequences for the reduction of TAC and initial capital cost. (3) To simulate and optimize the heat integration and heat pump systems within the continuous extractive distillation including the solvent regeneration column. (4) Aiming at energy cost and capital cost reduction, to estimate the costs and payback times of these systems and the environmental assessment though CO_2 emissions.

7.3. Evaluation method of heat pump performance and CO_2 emissions

7.3.1. Heat pump performance

Bruinsma and Spoelstra, (2010) give a detail derivation of the coefficient of performance (COP) in order to evaluate the heat pump technique in distillation process. For heating application, it is the ratio of the heat rejected at high temperature to the work input:

$$COP = \frac{Q_h}{W} \tag{7.1}$$

The upper theoretical value of COP obtainable in a heat pump is COPc, related to the Carnot cycle:

$$COP_C = \frac{T_H}{T_H - T_L} \tag{7.2}$$

Where, the temperature lift (T_H-T_L) is the sum of the temperature difference over the column and the temperature difference over the heat exchanger.

(Pleşu et al., 2014) provide an easy way to check whether or not the use of a heat pump can provide a more sustainable distillation process decreasing its energy requirements in the early stages of design. The simplified equation is as follow:

$$COP_S = \frac{Q}{W} = \frac{1}{\eta} = \frac{T_C}{T_R - T_C} \tag{7.3}$$

Where Q is the reboiler duty of column, W the work provided, η the Carnot efficiency, T_R and T_C temperature (K) of reboiler and condenser. They also pointed out that when the Q/W ratio exceeds 10, a heat pump is clearly recommended, between 5 and 10 it should be evaluated more detail, and if it is lower than 5, using a heat pump technique should not bring any benefits.

7.3.2.Evaluation of CO_2 emissions for distillation column

In 1991, Smith and Delaby (1991) have related energy targets to the resulting flue gas emissions from the utility system for a given process with fixed process conditions by considering the typical process industry utility devices such as boilers, furnaces and turbines; the emitting gas being CO_2, SO_2 and NO_2. Based on their works, Gadalla et al. (2005) proposed a simple model for the calculation of CO_2 emissions for heat-integrated distillation system. The model for calculating CO_2 emissions is as follow, based on the assumption that no carbon monoxide is formed during combustion since the air is regarded as in excess.

$$[CO_2]_{emiss} = Q_{fuel} \bullet Fuel_{factor} \tag{7.4}$$

Where Q_{fuel} is the amount of fuel burnt, reflecting the heating device, and $Fuel_{factor}$ is the fuel factor, reflecting the types of the fuel. It is defined as follow:

$$Fuel_{factor} = \left(\frac{\alpha}{NHV}\right) \bullet \left(\frac{C\%}{100}\right) \tag{7.5}$$

Where α (= 3.67) is the molar masses content of carbon in CO_2, NHV(kJ/kg) means the net heating value of a fuel with a carbon content of C%. $Fuel_{factor}$ takes the effect of the fuel on the process in terms of C%, NHV and α. In this study, assume heavy fuel oil is used and NHV = 39771 kJ/kg, C% = 86.5% (Gadalla et al., 2005).

In distillation system, steam is used for heating in reboiler. The steam is produced by boiler from the combustion of fuel. The theoretical flame temperature and the stack temperature are assumed as 1800 ^{O}C and 160 ^{O}C. so Q_{Fuel} can be calculated from following equation:

$$Q_{fuel} = \frac{Q_{proc}}{\lambda_{proc}} \bullet (h_{proc} - 419) \bullet \frac{T_{FTB} - T_0}{T_{FTB} - T_{stack}} \tag{7.6}$$

Where λ_{proc} (kJ/kg) and h_{proc} (kJ/kg) are the latent heat and enthalpy of steam delivered to the process, respectively, while T_{FTB} (^{O}C), T_{stack} (^{O}C) and T_0 (^{O}C) are the flame temperature, the stack temperature and the ambient temperature. The boiler feedwater is assumed to be at 100 ^{O}C with an enthalpy of 419 kJ/kg (Gadalla et al., 2005). The equation 7.6 is obtained from a simple steam balance around the boiler to relate the amount of fuel necessary in the boiler to provide a heat duty of Q_{proc}. The CO_2 emissions for the electricity power of a compressor is take as 51.1 kg CO_2 /GJ (Waheed et al., 2014), that is 184 kg CO_2/hr for 1000 kW power which we use in this study.

7.3.3.Economic assessment

The total annualized cost TAC is used for the comparison of the different designs and its calculation formulas are the same as before. The price of electricity is assumed the same as that of the one used for the column reboiler duty. Notice that we will take the payback period into account in order to give a fair comparison.

7.4.Extractive distillation with double-effect heat integration

Hereafter, the base case will be used as initial value of the design, as shown in Figure 7.3. The bottom temperature of extractive column is 348.3 K at 0.6 atm and the condenser temperature of entrainer regeneration column is 337.7 K at 1 atm. The heat integration is therefore impossible as there is no temperature difference. Hence, the operating pressure of regeneration column P_2 is adjusted to a pressure to give a heat integration feasible condenser temperature.

Aiming at optimizing the two columns together, we use the objective function OF for extractive distillation process as shown in chapters 3, 4 and 5. Based on OF, OF2 is used for the double-effect heat integration extractive distillation process and it is as follow:

$$\begin{aligned} &\min OF2 = \frac{(Q_{r1} - Q_{c2}) + Q_{r2} + m \cdot Q_{c1}}{k \cdot D_1 + D_2} \\ &subject\ to: x_{acetone,D1} \geq 0.995 \\ &\qquad x_{acetone,W1} \leq 0.001 \\ &\qquad x_{methanol,D2} \geq 0.995 \\ &\qquad x_{water,W2} \geq 0.9999 \end{aligned} \tag{7.7}$$

The meanings of the variables are the same as before. In OF2, the direct partial and full heat integration could be regarded as the extremely conditions where (Q_{r1}-Q_{c2}) taking the maximal value and the minimal value zero, respectively.

7.4.1.Direct partial heat integration

Direct partial heat integration (DPHI) of extractive distillation means that the design variables of extractive column are taken from Figure 7.3, just adjusting the operating pressure of the regeneration column from 1 atm to P_2 atm and increasing R_2 to make methanol product satisfy the purity specification. The reboiler/condenser heat exchanger is sized by using an overall heat transfer coefficient with the value of 0.00306 GJ $h^{-1}m^{-2}K^{-1}$ (Luyben and Chien, 2010). The effect of P_2 on the process TAC and OF2 of direct partial heat integration is shown in Figure 7.4 and Table 7.1 shows the TAC, OF2 and the temperature difference (TD) of the reboiler/condenser heat exchanger.

Table 7.1 – Temperature difference, TAC and OF2 of reboiler/condenser heat exchanger following P_2

P_2 / atm	1(base case)	2	3	3.5	4	5
TD / K	-10.6	8.1	20.2	25.1	29.4	36.8
OF / kJ/kmol	28326.3	18556.2	19100.1	19329.4	19541.9	19970.2
TAC / 10^6\$	3.04	2.583	2.508	2.503	2.506	2.521

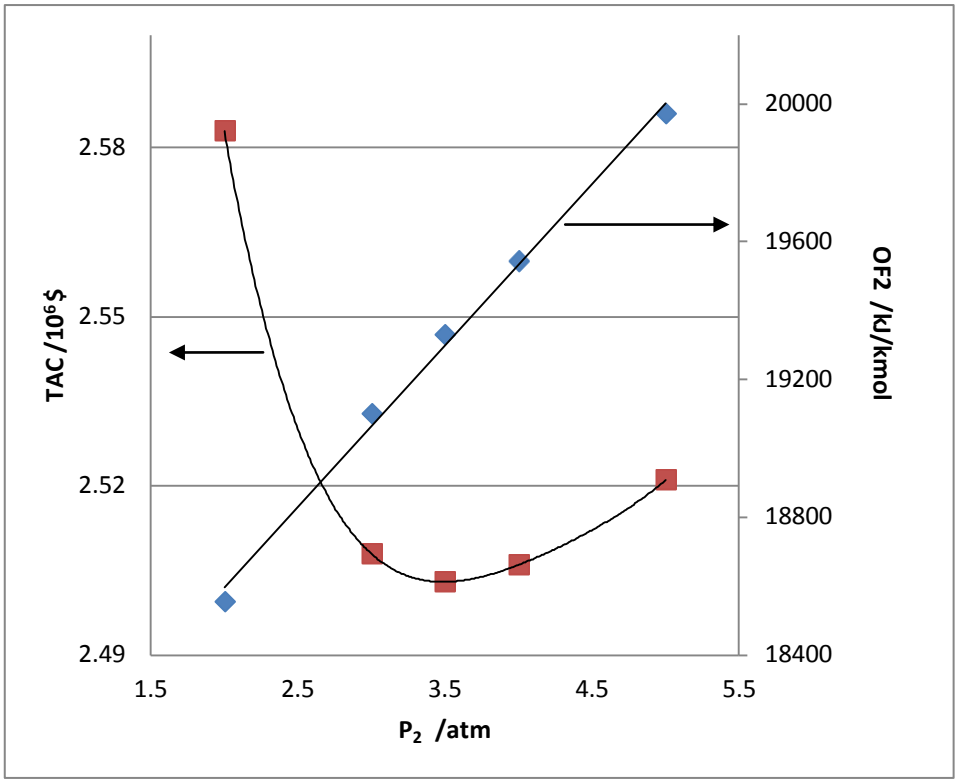

Figure 7.4 – Effect of P_2 on TAC and OF2, the performance of direct partial heat integration process

From Figure 7.4 and Table 7.1, we know that (1) when heat integration is taken into account, both TAC and energy cost per unit product flow rate OF2 decrease drastically, up to more than 15% and 30%, respectively. It shows the strong interest to consider heat integration of the process. (2) OF2 increases linearly following the increase of P_2. This is because the separation of methanol and water in regeneration column becomes more and more difficult as shown in Figure 7.5, the relative volatility of methanol-water at different pressure. (3) TAC firstly decreases quickly and then increases when P_2 increases above 4 atm. For the reboiler/condenser heat exchanger, the heat transfer area decreases quickly as the temperature difference increase from its small value, leading to the decrease of its capital cost and the TAC of the whole process. When TD is high enough (29 K for P_2 = 4 atm), the benefit of the increase of TD on the process is lessened, meanwhile, the cost penalty in the regeneration column caused by the increase of operating pressure becomes more obvious and overcomes the benefit from the heat exchanger smaller. (4) As the value with minimal TAC, P_2 = 3.5 atm is used hereafter which will give the reductions of TAC and OF by 19.4% and 31.8%. The heat exchanger duty for heat integration is 6.04 MW and the corresponding heat transfer area is

283 m^2. (5) The differential temperature driving force is 25.1 K. The results agree with the fact that the reasonable differential temperature driving force is more than 20K (Luyben and Chien, 2010).

Based on the feasibility and univolatility analysis that led us to select P_1 = 0.6 atm, the choice of a lower pressure allows us to choose P_2 = 3.5 atm instead of P_2 = 5 atm as used in Luyben's heat integrated design for the separation systems, our design with P_1 = 0.6 atm and P_2 = 3.5 atm results in 16% TAC saving and 27.6% OF (energy consumption per unit product flow rate) saving compared to Luyben's heat integrated design with P_1 = 0.6 atm and P_2 = 3.5 atm.

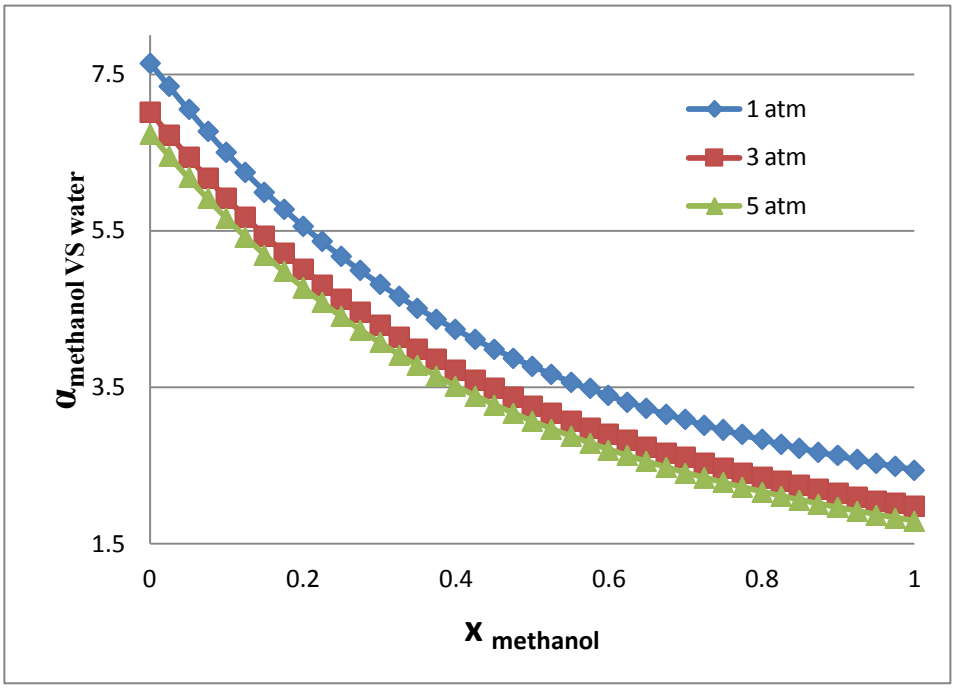

Figure 7.5 – Relative volatility of methanol over water at different pressure

7.4.2. Optimal partial heat integration

Optimal partial heat integration (OPHI) of extractive distillation process means all the design variables are being optimized with objective function OF after the operating pressure of regeneration column is changed to 3.5 atm from above results.

The four-step optimization procedure in chapter 3 for extractive distillation is used since we keep fixing the two columns stage number as base case. The results after recheck in closed loop flow sheet are shown as OPHI in Table 7.2 and Table 7.3. There is a small decrease of OF when more variables are taken into account. The optimal values of F_E, R_1, D_1 D_2, N_{FE} and N_{FF} are almost similar to the DPHI case. Differences are seen in the R_2 and N_{FR} values. Indeed, the new regeneration column design leads to a more suitable heat exchange duty for heat integration and reduces the operating cost and the capital cost, giving rise to the drops of TAC by 6%.

7.4.3.Optimal full heat integration

In optimal full heat integration (OFHI) of extractive distillation, the reboiler heat duty of extractive column equals to the condenser heat duty of regeneration column. The process is achieved in Aspen Plus by using *design specification* with the Q_{r1}-Q_{c2} = 0 as specification and the reflux ratio of regeneration column R_2 as variable. In order to do a fair comparison, the variable of F_E, R_1, R_2 (keep Q_{r1}-Q_{c2} = 0), D_1 D_2, N_{FE}, N_{FF}, and N_{FREG} are also optimized by four steps procedure (chapter 3). After recheck in closed loop flow sheet, the design parameters and the cost data of three double-effect heat integration extractive distillation processes are shown in Table 7.2 and Table 7.3.

Table 7.2 – Design parameters of three double-effect heat integration extractive distillation processes, acetone-methanol with water

	Case DPHI	Case OPHI	Case OFHI
N_E	65	65	65
N_R	35	35	35
P_1 /atm	0.6	0.6	0.6
P_2 /atm	3.5	3.5	3.5
F/kmol/h	540	540	540
F_E/kmol/h	560	552	574.3
R_1	2.59	2.56	2.53
R_2	1.46	1.78	2.44
D_1/ kmol/h	271.1	270.9	270.7
D_1/ kmol/h	271.0	271.1	271.1
N_{FE}	34	35	36
N_{FF}	55	56	55
N_{FR}	25	19	20

Table 7.3 – Sizing parameters and cost data of three double-effect heat integration extractive distillation processes, acetone-methanol with water

	Case DPHI		Case OPHI		Case OFHI	
Diameter/m	2.796	1.335	2.782	1.425	2.769	1.596
Height /m	45.72	23.78	45.72	23.78	45.72	23.78
I_{CS} /10^6\$	1.446	0.389	1.439	0.417	1.431	0.471
Q_C	8.21	0	8.14	0	8.06	0
Q_R	2.52	7.23	1.66	8.00	0	9.67
A_R /m^2	128	366	84	345	0	490
A_C /m^2	861	0	854	0	845	0
I_{HE} /10^6\$	0.976	0.435	0.920	0.418	0.749	0.525
$Cost_{cap}$/10^6\$	2.742	0.877	2.676	0.894	2.495	0.996
$Cost_{ope}$/10^6\$	0.323	0.829	0.224	0.782	0.034	1.109
$Cost_{CA}$/10^6\$	1.237	1.122	1.116	1.080	0.865	1.464
Q_H/ MW	1.18		1.16		1.22	
$Cost_{HA}$/10^6\$	0.021		0.021		0.022	
Q_{HE}/ MW	6.04		6.82		8.42	
A_{HE} /m^2	284		318		395	
$Cost_{HE}$/10^6\$	0.123		0.132		0.153	
TAC/10^6\$	2.503		2.349		2.504	
CO_2 emissions /kg/h	3146.2		3117.2		3120.4	
OF2 /KJ/kmol	19329.4		19162.8		19178.4	

From Table 7.2 and Table 7.3, we know that (1) comparing heat integration process with no heat integration base case, TAC and energy cost for per unit product decreases by 31.8% and 19.4% respectively. (2) A counter-intuitive result is obtained: compared with direct partial heat integration, optimal full heat integration is not recommended because it gives a little increase in TAC although the energy cost decreases a little. The reason is that in order to achieve full heat integration, R_2 increases a lot to make the condenser duty in regeneration column match the reboiler duty in extractive column, leading to the increase of heat exchanger area and the capital cost that overcome the operating cost reduction in the extractive column. Besides, as R_2 goes up, so does the reboiler duty of regeneration column Q_{R2} and the operating cost accordingly. (3) The optimal partial heat integration proposed in this study remains competitive because it gives a 6.2% reduction in TAC compared with direct partial or optimal full heat integration, and also a little decrease in energy cost following OF2. It demonstrates that there exists an optimal heat duty to be integrated in the extractive distillation process. Besides, more high price steam is needed in case OFHI as more reboiler duty is needed in regeneration column and the bottom temperature (414 K) in regeneration column is higher than that (348 K) in extractive distillation. (4) The total columns reboiler heat duties (9.66 MW) in the heat integration case OPHI studied in this work has a 32.2 % saving compared with base case (14.24 MW) without heat integration. Compared with the partial heat integration design in Luyben's book (Luyben and Chien, 2010), a 28.4% reduction in the total columns reboiler heat duties is obtained for the same design purity objective. (5) OF proves suited as the objective function for extractive distillation to deal with partial or full heat integration as full heat integration can be regarded as the (Q_{r1}-Q_{c2}) equal to zero. (6) With the lowest TAC, case OPHI also shows a little less CO_2 emissions and energy consumption per unit product.

7.5.Extractive distillation with MHP heat pump

For the base case with no heat integration of the separation of acetone-methanol with water shown in Figure 7.3, the COP_S values for extractive column and regeneration column calculated from equation 3 are 9.5 and 8.4, respectively. They are in the value range where a heat pump assisted process should be evaluated in detail according to Plesu et al. (Pleşu et al., 2014).

We notice that the temperature difference (10.6 K) between the top of the regeneration column and the bottom of the extractive column is much smaller than that (40 K) between the top and the bottom of the regeneration column which is commonly true for extractive distillation, such a high temperature difference between the top and the bottom of the column is adverse to the performance of the heat pump process. So we propose a new flow sheet sequence shown in Figure 7.6 that one part of the extractive column reboiler duty is heated by the top vapor of the regeneration column with heat pump 2, and the left part is supplied by the top vapor of the extractive column with heat pump 1. Auxiliary condenser is needed to cooling the other part of the top vapor of the extractive column.

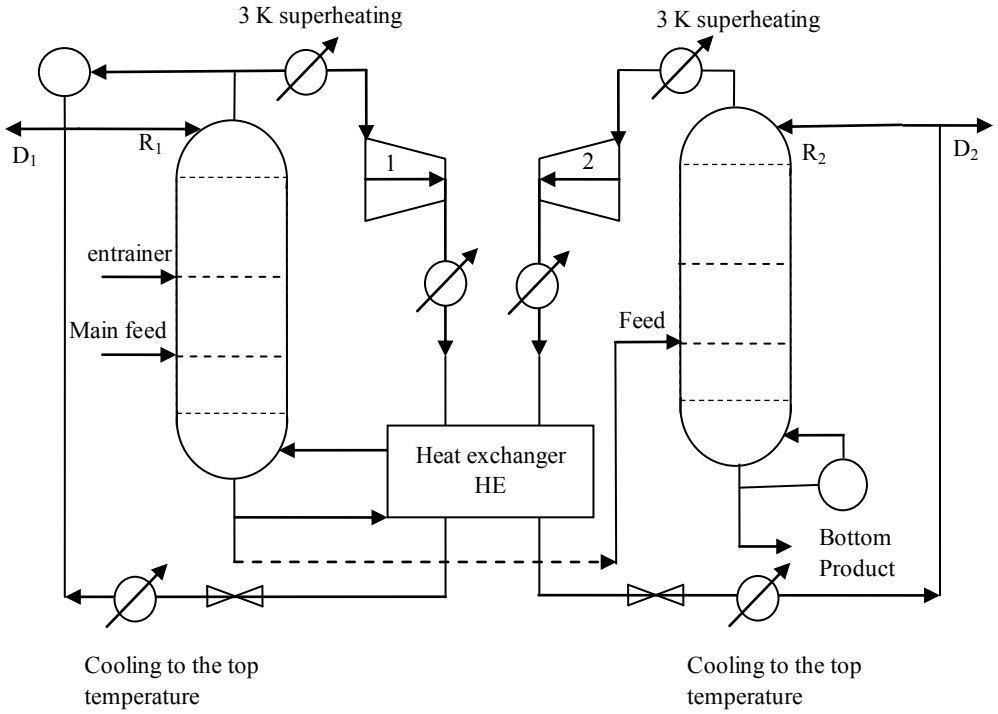

Figure 7.6 – Partial VRC heat pump for extractive distillation process.

7.6.Evaluation of VRC heat pump assisted distillation process

In order to respectively show the cost saving of the extractive and regeneration columns, we compared them separately with their corresponding heat pump assisted process.

7.6.1.VRC heat pump assisted extractive column

For the heat pump assisted column, the choice of compression ratio (the ratio of outlet and inlet pressure of compressor) reflects whether the temperature driving force is enough to heat up the column reboiler or not. In this study, the outlet pressure of compressor (OPC_1) for extractive column is regarded as variable to evaluate the performance of compressor as the inlet pressure of top vapor distillate is 0.6 atm that chosen from thermodynamic insight in chapter 4. The results are shown in Table 7.4 for a payback period of 3 years and corresponding temperature difference.

Table 7.4 – Cost data for extractive column with heat pump at different compressor outlet pressure

OPC_1/atm	2	2.5	3	4	5
TD /K	2.7	10.5	17.1	28.1	37.1
Energy cost /10^6\$	0.199	0.234	0.266	0.319	0.365
Capital cost /10^6\$	8.543	7.728	7.968	8.578	9.125
TAC at PP = 3 /10^6\$	3.046	2.81	2.921	3.178	3.406

As OPC_1 increases, so does the temperature driving force, and the energy cost increases due to a greater of compressor work, but the capital cost and TAC with 3 years payback period of extractive column with heat

pump decrease first and then increase. The high values of capital cost and TAC at OPC_1 = 2 atm is because the temperature driving force is too small, leading to a big heat exchanger area and capital cost. So OPC_1 = 2.5 atm is used hereafter and the comparison of extractive column with and without heat pump are shown in Table 7.5.

From Table 7.5 and Figure 7.7, we know that (1) there remains a condenser duty in VRC heat pump process. The reason is that after being compressed and heat exchanged, the top vapor becomes high pressure liquid, it is partial vaporized after throttle valve and it needs to be cooled to the top temperature before being refluxed into the column. (2) The energy cost in extractive column is reduced by 77.0% as most of the condenser duty is reused for heating up reboiler thanks to the heat pump. (3) The capital cost increases 2.5 times as the compressor's cost is much higher than that of the heat exchanger and column shell. The heat transfer area in the process with heat pump increases by 20% more than that without heat pump. (4) Then for a 3 year payback period, the VRC HP process is not competitive for the extractive column. However, the TAC for the process with VRC heat pump drops below the no heat pump process if the payback period is greater than 6 years. The 10 year total cost for the process with VRC heat pump (10.07×10^6\$) is reduced by 23.5% compared with that of the process without heat pump (13.17×10^6\$). (5) CO_2 emissions (kg/h) for the process with VRC heat pump is only 15.3% of that without heat pump.

Table 7.5 – Comparison of extractive column with and without VRC heat pump

Heat pump	no	Yes
Q_C /MW	8.21	1.63
Q_R /MW	8.56	0.42
Q_{HE} /MW	0	8.14
A_C /m^2	861	171
A_R /m^2	434	22
A_{HE} /MW	0	1365
Compressor work/MW	no	1.559
COP	-	5.2
Capital cost of compressor /10^6\$	0	4.608
Energy cost per year /10^6\$	1.016	0.234
Capital cost /10^6\$	3.008	7.728
CO_2 emissions /kg/h	2762.3	422.3
TAC at PP = 3 /10^6\$	2.018	2.810
TAC at PP = 10 /10^6\$	1.317	1.007

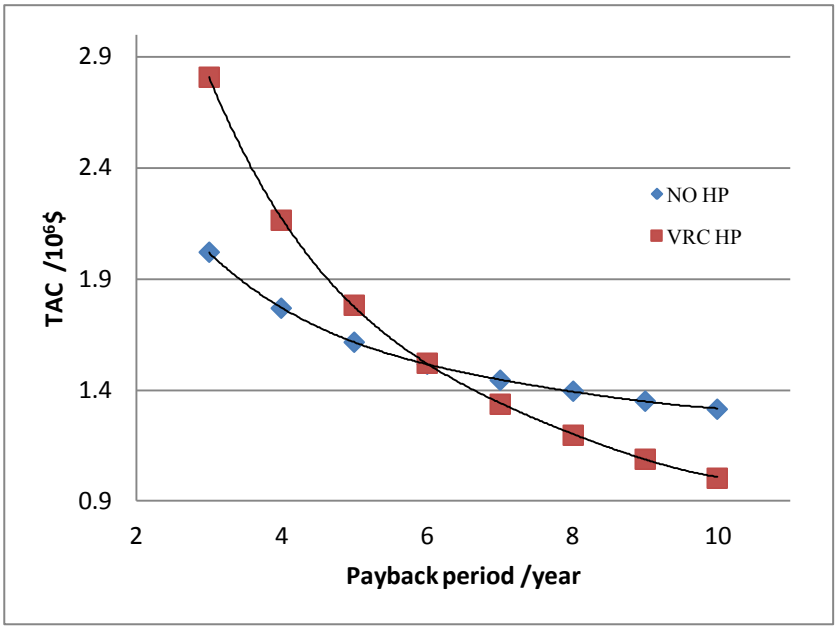

Figure 7.7 – Total annual cost of extractive column following payback period with and without heat pump technique

7.6.2.VRC heat pump assisted regeneration column

The outlet pressure of compressor for regeneration column (OPC_2) is regarded as variable to evaluate the performance of compressor with the top vapor distillate at atmosphere. The results are shown in Table 7.6.

Table 7.6 – Cost data for extractive column with heat pump at different compressor outlet pressure

OPC_2/atm	4.5	5	5.5	6	7
TD /K	3.8	7.3	10.6	13.7	19.2
Energy cost /10^6\$	0.141	0.149	0.156	0.164	0.178
Capital cost /10^6\$	5.489	5.169	5.147	5.202	5.384
TAC at PP = 3 /10^6\$	1.970	1.872	1.872	1.898	1.972

As OPC_2 increases, so does the temperature driving force and the energy cost due to a greater compressor work while the capital cost and TAC with 3 years payback period of extractive column with heat pump decreases first and then increases. The high values of capital cost and TAC at OPC_2 = 4.5 atm is because the temperature driving force is relatively small, causing a big heat exchanger area and capital cost. So OPC_2 = 5 atm is used hereafter and the comparison of the regeneration column with and without heat pump are shown in Table 7.7 and Figure 7.8.

From Table 7.7 and Figure 7.8, we know that (1) the energy cost in regeneration column with heat pump is reduced by 77.8% while the capital cost increases 4.3 times. For a 3 year payback period, the VRC heat pump is again not competitive. However, the CO_2 emissions is reduced a lot, and the TAC for the VRC heat pump assisted regeneration column gets competitive when the payback period is over 8 year. The 10 year total cost for the process with heat pump (6.66×10^6\$) is reduced by 16.0% compared with that of the process without heat pump (7.93×10^6\$).

Table 7.7 – Comparison of regeneration column with and without heat pump

Heat pump	no	Yes
Q_C /MW	5.30	0.75
Q_R /MW	5.68	0.15
Q_{HE} /MW	0	5.53
A_C /m^2	182	26
A_R /m^2	288	8
A_{HE} /MW	0	1334
Compressor work/MW	no	1.117
COP	-	4.9
Capital cost of compressor /10^6\$	0	3.506
Energy cost per year /10^6\$	0.673	0.149
Capital cost /10^6\$	1.192	5.169
CO_2 emissions /kg/h	1832.9	253.9
TAC at PP = 3 /10^6\$	1.071	1.872
TAC at PP = 10 /10^6\$	0.793	0.666

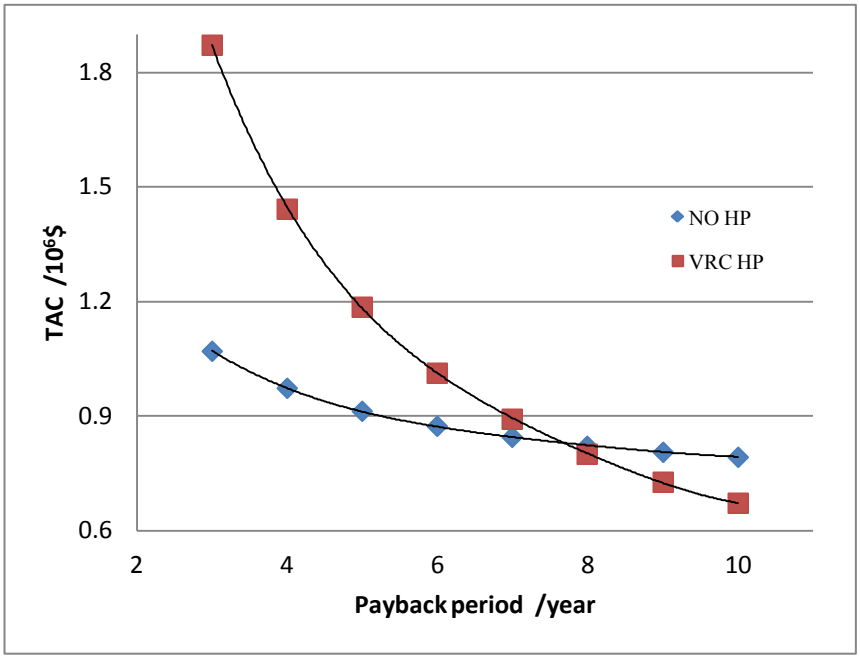

Figure 7.8 – Total annual cost of regeneration column following payback period with and without heat pump technique

7.6.3.Full VRC heat pump process

Full VRC heat pump process means that both column reboilers are heated up through heat pump as shown in Figure 7.1(b). The outlet pressures of compressors are 2.5 atm and 5 atm taking from above. The cost data of the process full VRC are shown in Table 7.8. Again it is better to use heat pump for both extractive and the

regeneration column from the economic and environmental views after payback period is greater than 6.5 years.

7.6.4.Partial VRC heat pump process

After validation, the outlet pressure of compressor 2 is 2 atm due to the decrease of temperature difference, and much reduction in capital cost for heat pump is possible. The cost data of the process without heat pump, and partial VRC are shown in Table 7.8 and the TAC at different payback periods are shown in Figure 7.9.

From Figure 7.9 and Table 7.8, we know that (1) the VRC heat pump process for a 3 year payback period is much higher than the process without heat pump. Compared with the process without heat pump, the total heat transfer area ($A_C + A_R + A_{HE}$) in full heat pump process and partial heat pump process increases by 1.65 times and 1.48 times instead of decrease. Indeed, the condenser area A_C is spared by the VRC heat pump technique, but this is overweighed by the increase of the heat transfer area A_{HE} for heat exchanger due to the small temperature driving force (7.3K). Another reason is that the capital cost of the necessary compressor is huge and increase quickly following the increase of compression ratio. (2) On the other hand, the energy cost per year decreases by 2.1 times in the process with partial VRC heat pump, and 4.4 times in the process with full VRC heat pump. The CO_2 emissions in partial VRC and full VRC heat pump process reduce by 2.3 and 6.8 times compared the process without heat pump. (3) Hence, the capital cost payback periods are 6.8 years and 5 years for full VRC process and partial VRC process. The 10 years total capital and energy cost are reduced by 20.7% and 21.6%, from (21.16×10^6\$) to (16.77×10^6\$) with full VRC and (16.77×10^6\$) with partial VRC. (4) The initial capital cost decrease by 33.4% in the proposed partial VRC process compared with full VRC process because the process coefficient of performance (COP) increase from 5.1 to 8.2.

Table 7.8 – Cost data of the process without heat pump, full and partial VRC heat pump

VRC Heat pump	no	partial	full
Q_C /MW	13.51	5.96	2.38
Q_R /MW	14.24	5.68	0.56
Q_{HE} /MW	0	8.56	13.68
A_C /m^2	1043	606	197
A_R /m^2	722	288	28
A_{HE} /MW	0	1720	2683
Compressor work/MW	no	1.048	2.676
COP	-	8.2	5.1
Capital cost of compressor /10^6\$	0	3.763	8.113
Energy cost per year /10^6\$	1.692	0.799	0.384
Capital cost /10^6\$	4.244	8.612	12.932
CO_2 emissions /kg/h	4595.1	2025.7	673.0
TAC at PP = 3 /10^6\$	3.107	3.670	4.695
TAC at PP = 10 /10^6\$	2.116	1.660	1.677

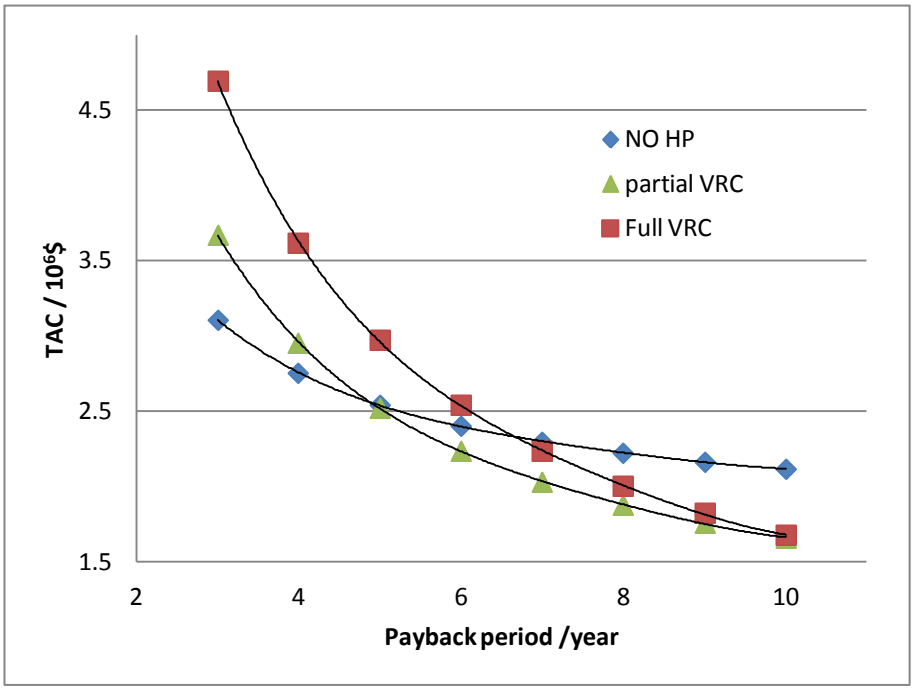

Figure 7.9 – Total annual cost of basic case, full and partial VRC heat pump processes following payback period

In summary, from the view of economic, the partial VRC heat pump process is the preferred choice, but from the environmental aspect, the full VRC heat pump process is better than the partial VRC as the CO_2 emissions are reduced by almost 3 times from 2025.7 to 673.0 kg/h.

7.7.Evaluation of BF heat pump assisted distillation process

The key parameter in the BF heat pump process is the outlet pressure of the throttle valve since it determines whether or not there is enough temperature driving force to remove the condenser heat duty. So the outlet pressure of throttle valve (OPT) is used as the variable for the evaluation of BF heat pump assisted distillation process. Notice that the operating pressures of the base case are 0.6 atm for the extractive column and 1 atm for regeneration column, so the outlet pressure of throttle valves will be lower than 1 atm.

7.7.1.BF heat pump assisted extractive column

For the extractive column, the bottom liquid is the mixture of non-product component and entrainer instead of high purity product stream. So the saturated vapor pressure of that mixture will determine the feasibility of the BF heat pump process. As the entrainer is usually a heavy boiling component with a low saturated vapor pressure, it will give benefit to use BF heat pump in the extractive distillation process.

The effect of throttle outlet pressures (OPT_1) is shown in Table 7.9, starting from 0.07 atm to provide enough temperature difference.

Table 7.9 – Cost data for extractive column with BF heat pump at different throttle valve outlet pressure

OPT_1 /atm	0.07	0.09	0.1	0.11
TD /K	13.6	8.8	6.5	3.8
Energy cost	0.305	0.272	0.258	0.246
Capital cost	9.550	9.116	9.038	9.238
TAC at PP = 3 /10^6\$	3.489	3.311	3.271	3.325

As OPT_1 increases, the bubble point and dew point of the bottom liquid mixtures increase, leading to the decrease of the temperature driving force to remove the condenser duty. Meanwhile, the energy cost decreases as the compressor duty decreases. However, the capital cost decreases until $OPT_1 = 0.1$ atm, after that the capital cost increase due to the increase of heat exchanger cost overwhelms the benefit caused by the decrease of the compressor duty. The TAC at 3 year payback period quantitatively shows the effect of OPT_1 on the extractive column. So $OPT_1 = 0.1$ atm is used hereafter and the comparison of extractive column with and without BF heat pump are shown in Table 7.10.

Table 7.10 – Comparison of extractive column with and without BF heat pump

Heat pump	no	Yes
Q_C /MW	8.21	1.87
Q_R /MW	8.56	0
Q_{HE} /MW	0	8.15
A_C /m^2	861	43
A_R /m^2	434	0
A_{HE} /MW	0	1472
Compressor work/MW	no	2.183
COP	-	3.7
Capital cost of compressor /10^6\$	0	6.072
Energy cost per year /10^6\$	1.016	0.258
Capital cost /10^6\$	3.008	9.038
CO_2 emissions /kg/h	2762.3	401.6
TAC at PP = 3 /10^6\$	2.018	3.271
TAC at PP = 10 /10^6\$	1.317	1.162

Just like the process with VRC heat pump, the BF heat pump process also increases the total heat transfer area instead of decrease. The energy cost per year decreases by 3.9 times but the capital cost increases by 3 times. In summary, the 10 year total cost is saved by 11.8% and the CO_2 emissions is reduced by 6.8 times. Over the long term, the benefits of the BF heat pump assisted extractive distillation column are obvious in both economic cost and environmental impact.

7.7.2.BF heat pump assisted regeneration column

The effect of the outlet pressures of throttle for regeneration column (OPT_2) is regarded as the main variable of the process and the results are shown in Table 7.11.

Table 7.11 – Cost data for regeneration column with BF heat pump at different throttle valve outlet pressure

OPT_2 /atm	0.1	0.15	0.2	0.22
TD /K	18.5	10.3	4.2	2.1
Energy cost	0.212	0.172	0.146	0.137
Capital cost	6.201	5.579	5.494	5.934
TAC at PP = 3 /10^6\$	2.279	2.032	1.977	2.115

Again, as OPT_2 increases, the temperature driving force for removing the condenser duty decreases, and the energy cost decrease as the compressor duty decrease. At OPT_2 = 0.22 atm, the cost for heat exchanger increases quickly leading to the increase of capital cost. Considering the TAC at 3 year payback period, OPT_2 = 0.2 atm is chosen hereafter for regeneration column with BF heat pump and the results are shown in Table 7.12.

Table 7.12 – Comparison of regeneration column with and without BF heat pump

Heat pump	no	Yes
Q_C /MW	5.30	1.01
Q_R /MW	5.68	0
Q_{HE} /MW	0	5.46
A_C /m^2	182	16
A_R /m^2	288	0
A_{HE} /MW	0	1526
Compressor work/MW	no	1.230
COP	-	4.4
Capital cost of compressor /10^6\$	0	3.794
Energy cost per year /10^6\$	0.673	0.146
Capital cost /10^6\$	1.192	5.494
CO_2 emissions /kg/h	1832.9	226.3
TAC at PP = 3 /10^6\$	1.071	1.977
TAC at PP = 10 /10^6\$	0.793	0.695

The energy cost per year for the regeneration column with BF heat pump decreases by 4.6 times, and the capital cost increases by 4.6 times. Generally speaking, the 10 year total cost is reduced by 12.4% and the CO_2 emissions are reduced from 1832.9 kg/h to 226.3 kg/h. Again, over the long term, the benefits of BF heat pump for the entrainer regeneration column than base case is obvious in both economic and environment aspect.

7.7.3.Full BF heat pump process

Full BF heat pump process means that both column condensers are cooled down by the vaporization of the bottom liquid streams after throttle valve. The flow sheet is shown in Figure 7.1(c). The outlet pressures of the two throttle valves are 0.1 atm and 0.2 atm taking from above.

7.7.4.Partial BF heat pump process

Again, in order to reduce the capital cost of full BF heat pump process, a new partial BF heat pump flow sheet is proposed as shown in Figure 7.10. The condenser in the regeneration column is cooled down by vaporizing of partial bottom liquid in extractive column, and the other part is used to move heat from the condenser of the extractive column.

After validation, the OPT_2 is 0.3 atm due to the decrease of temperature difference, leading to much reduction in capital cost for heat pump.

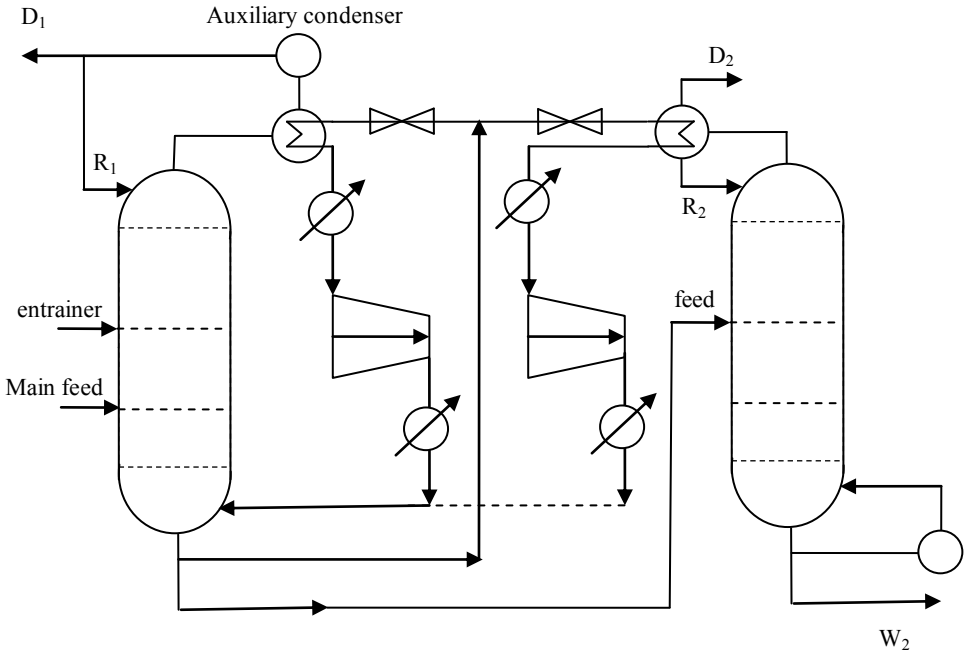

Figure 7.10 – Partial BF heat pump for extractive distillation process

The cost data of the process without heat pump, full and partial BF heat pump are shown in Table 7.13 and the TAC at different payback periods are shown in Figure 7.11.

From Figure 7.11 and Table 7.13, we know that (1) compared with the process without heat pump, the total heat transfer area in full and partial BF heat pump process increase by 1.73 times and 1.28 times. (2) The energy cost per year dramatically by 2.0 times in the process with partial BF heat pump, and 4.2 times in the process with full BF heat pump. The CO_2 emissions in partial BF and full BF heat pump process reduce by 2.2 and 7.3 times compared the process without heat pump. This is the main advantages of heat pump technique. (3) Meanwhile, the total capital cost increase dramatically due to the cost of compressors. (4) The capital cost payback periods are 8.0 years and 6.2 years for full and partial BF process. (5) The 10 years total capital and energy cost are reduced by 7.3 % and 14.8 %, from (21.16×10^6\$) to (19.61×10^6\$) with the full BF and to (18.03×10^6\$) with partial BF. (6) The partial BF gives a 33.3% reduction in the capital cost compared with full BF process. Meanwhile, the process coefficient of performance increases by 40%.

Table 7.13 – Cost data of the process without heat pump, partial and full BF heat pump

BF Heat pump	no	partial	full
Q_C /MW	13.51	6.44	2.88
Q_R /MW	14.24	5.68	0
Q_{HE} /MW	0	8.27	13.61
A_C /m^2	1043	575	59
A_R /m^2	722	288	0
A_{HE} /MW	0	1401	2998
Compressor work/MW	no	1.489	3.413
COP	-	5.6	4.0
Capital cost of compressor /10^6\$	0	5.024	9.866
Energy cost per year /10^6\$	1.692	0.828	0.404
Capital cost /10^6\$	4.244	9.682	14.532
CO_2 emissions /kg/h	4595.1	2106.8	627.9
TAC at PP = 3 /10^6\$	3.107	4.072	5.265
TAC at PP = 10 /10^6\$	2.116	1.803	1.961

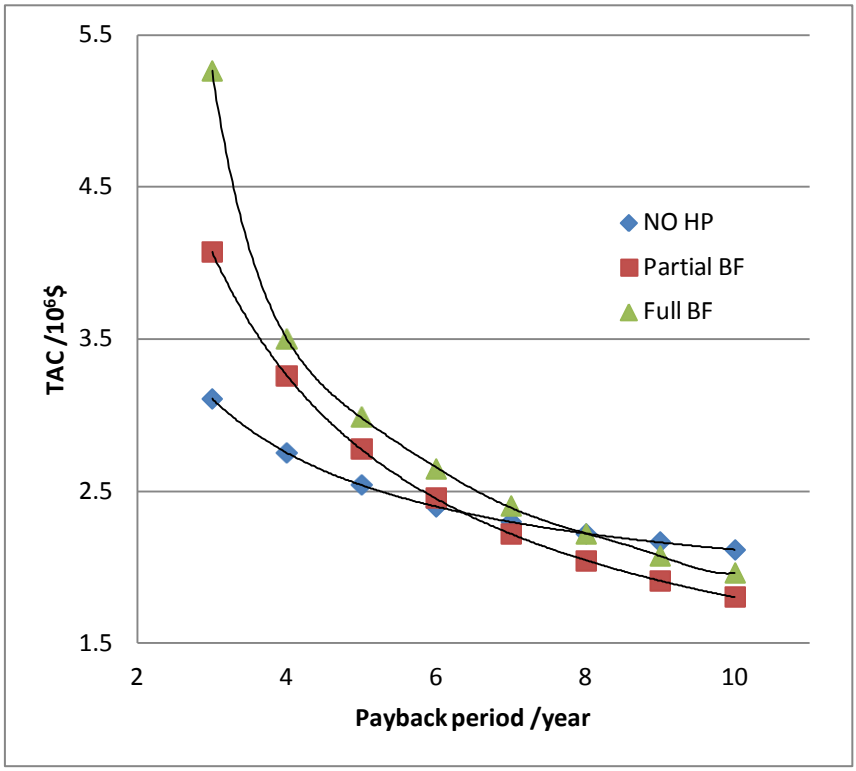

Figure 7.11 – Total annual cost of basic case, full and partial BF heat pump processes following payback period

In summary, from the view of economics, the partial BF heat pump process is better than the full BF heat pump process, but from the environmental aspect, the full BF heat pump process is better than the partial BF process as the CO_2 emissions is reduced by 3.3 times from 2106.8 to 627.9 kg/h.

7.7.5.Summary of mechanical heat pump

In general, compared with the traditional process, the full heat pump assisted extractive distillation process demonstrates a strong advantage in both economical and environmental aspects. The full VRC heat pump shows a better performance than the full BF heat pump since the 10 year total cost is further reduced by 14.5%, but and CO_2 emissions increase by 6.7%. The partial VRC heat pump process proposed in this study has 1.7×10^5\$ reduction in 10 year total cost and 3.8% CO_2 emissions reduction comparing with the proposed partial BF heat pump process. The CO_2 emissions in partial VRC heat pump process is only 44.1% of that in traditional process though it is 3 times compared with full VRC heat pump process. The proposed partial heat pump (partial VRC and partial BF) processes based on the character of extractive distillation can effectively decrease the initial capital cost and increase the process coefficient of performance. In summary, from the economical view, the partial VRC heat pump process is the best choice in mechanical heap pump process, but from the environmental aspect, the full BF heat pump process is better than other alternatives.

7.8.Comparison of OPHI and partial VRC

As shown before, OPHI is the best choice in double-effect heat integration, whereas partial VRC gives the lowest TAC. Thus, we show the comparison of OPHI process and partial VRC heat pump process in Figure 7.12 and Table 7.14.

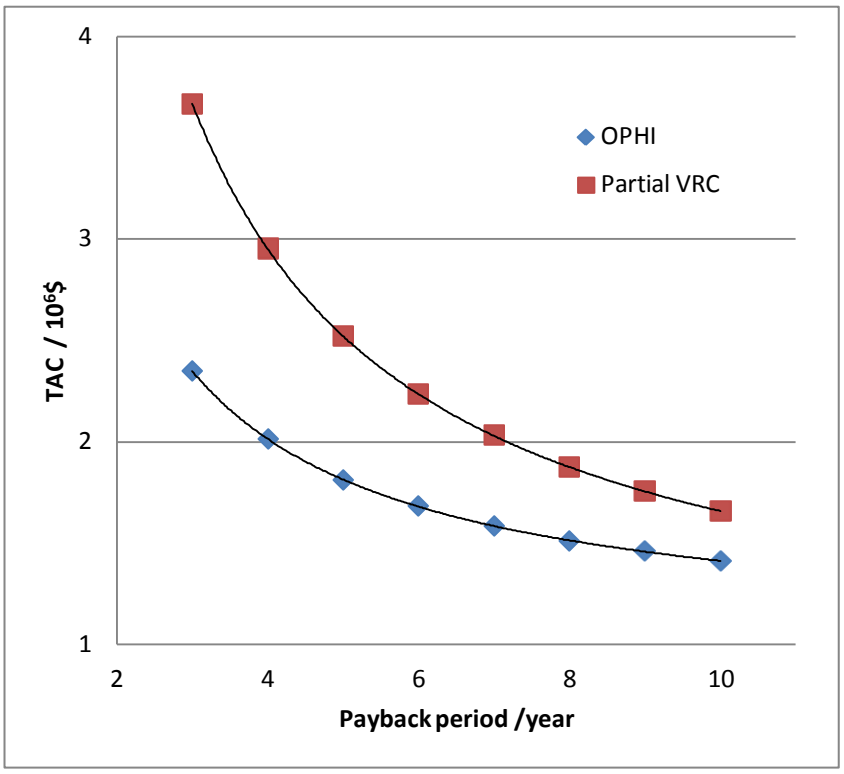

Figure 7.12 – Total annual cost of optimal partial HI and partial VRC process following payback period

Table 7.14 – Comparison of optimal partial HI, partial VRC processes

Process	OPHI	PVRC
Initial investment/10^6\$	4.013	8.612
CO_2 emissions /kg/h	3117.2	2025.7
TAC at PP = 3 /10^6\$	2.349	3.670
TAC at PP = 10 /10^6\$	1.414	1.660

From Table 7.14 and Figure 7.12, we remark that (1) the optimal partial heat integration process is preferable from the economical point of view. It gives a 2.46×10^6\$ and a 7.02×10^6\$ total process cost saving over a 10 year period compared with partial VRC and base case, respectively. The optimal partial heat integration process overwhelms the partial VRC heat pump process because the temperature differences between the extractive and regeneration columns are higher, leading to relatively poor coefficient of performance of heat pump process. (2) On the contrary, CO_2 emissions are reduced by more than 35% in partial VRC heat pump process comparing to optimal partial heat integration process. The potential of heat pump process in reducing CO_2 emissions contributes its interest.

7.9.Conclusions

In order to save the total cost and increase the environmental performance (CO_2 emissions) of traditional extractive distillation process for the separation of minimum azeotropic mixture acetone-methanol with heavy entrainer water, double-effect heat integration and mechanical heat pump are extensively investigated.

Firstly, three kinds of double-effect heat integrations are studied. The direct partial heat integration and full heat integration are the most studied two situations. We propose a novel optimal partial heat integration process aiming at achieving the most energy saving for extractive distillation. A new objective function OF2 describe the energy cost per unit product flow rate is proposed to carry out the optimization of double-effect heat integration by the SQP method in Aspen plus software. The direct partial and optimal full heat integration are regarded as the extremely conditions where (Qr1-Qc2) in OF2 taking the maximal value or the minimal value zero. The results show that double-effect heat integrations give the massive reduction in TAC, energy cost and CO_2 emissions. The optimal partial heat integration has the lowest TAC instead of the optimal full heat integration process as intuition, and it gives a little lower CO_2 emissions. This demonstrates that before rigorous simulation and optimization, the double-effect heat integration can't be used arbitrarily.

Secondly, in order to reduce the CO_2 emissions and initial capital cost, the mechanical heat pump (VRC and BF) is evaluated and both economical and environmental aspects are taken into account. The outlet pressure of compressors is regarded as the main variable for VRC process while the outlet pressure of throttle valves is used for BF process. The partial VRC and partial BF heat pump are proposed based on the character of extractive distillation process that the temperature difference between the bottom of the extractive column and the top of the regeneration column is usually small, and the process coefficient of performance increase by 60.7% and 40.0% compared with the full VRC and full BF heat pump process. The results show that

partial VRC process has both lower TAC and CO_2 emissions than partial BF process. The full VRC process shows lower TAC but higher CO_2 emissions than full BF process. Partial VRC process gives better performance from economical view while full BF process leads better performance in environmental aspect.

In summary, the lowest TAC process is the proposed optimal partial heat integration and the lowest CO_2 emissions process is the full BF process. Partial VRC process gives a trade-off between TAC and CO_2 emissions comparing to full VRC process, and it also significantly reduces the initial investment.

Chapter 8. Conclusions and perspectives

8.Conclusions and perspectives

8.1.Conclusions

A systematic approach in saving energy consumption and improving the energy efficiency of industrial processes is the onion-model developed in industrial (Bruinsma and Spoelstra, 2010). Following the onion-model, based on the knowledge of thermodynamic insight of extractive distillation process, we try to find the opportunity to saving energy cost and capital cost in process itself, double-effect heat integration, heat pump and utilities.

In the field of the extractive distillation process, process feasibility study and process optimal design are always the hot issues. In this manuscript, we use the general feasibility criterion reported by our team as guideline for the process optimization and give a better understanding of the complex process. The results of the optimization which is important for industry give feedbacks to the process feasibility.

We developed a two step optimization strategy for extractive distillation to find suitable values of the entrainer feed flowrate, entrainer feed and azeotropic mixture feed locations, total number of trays, reflux ratio, heat duty and condenser duty in both the extractive column and the entrainer regeneration column. The first strategy relies upon the use of a multi-objective genetic algorithm (GA) with four objective functions: OF, TAC, E_{ext} and e_{ext}. Secondly, results taken from the GA Pareto front are further optimized focusing on decreasing the energy cost by using the four steps procedure: Aspen plus simulator built-in SQP method is used for the optimization of the continuous variables: column refluxes R_1, R_2 and the entrainer flow rate F_E with the energy consumption OF as objective function (step 1). A sensitivity analysis is performed to find optimal values of the two distillates D_1, D_2 (step 2) and the feed tray locations N_{FE}, N_{FAB}, N_{FReg} (step 3) while step 1 is done for each set of discrete variable values. Step 4 is to find the final design through minimizing OF value, corroborate in closed loop flowsheet, and calculate TAC and thermodynamic efficiency indicators.

Chapter 3 concerns the formation and use of four steps procedure for extractive distillation, and the effects of the process variables on each other and on the process. We have obtained optimal parameters for an extractive distillation process for separating the minimum boiling azeotropic mixture acetone-methanol with water (class 1.0-1a) as entrainer, taking into account the both extractive distillation and the entrainer regeneration columns and compared it with Luyben's design under the constraint of 0.995 mole fraction acetone and methanol products. We have combined SQP optimization for the continuous variables F_E, R_1, R_2, and sensitivity analysis for D_1, D_2, N_{FE}, N_{FF}, N_{FReg}. A new objective function accounting for all the energy consumption of per product flow rate value is proposed. Compared with Luyben's design in literature, the total annual cost and energy consumption are reduced by 12.0 % and 14.5 % respectively based on the same column stage numbers. Significant savings in both energy cost and TAC are achieved.

Chapter 4 and 5 concerns finding the possible way to save energy cost in extractive distillation process based on the knowledges of thermodynamic insight.

In chapter4, we have studied the improving design of extractive distillation process for the separation of the acetone – methanol minimum boiling azeotrope with water. By using thermodynamic insight from the analysis of the ternary residue curve map and isovolatility curves, we have noticed the beneficial effect of lowering the pressure in the extractive distillation column. A lower pressure will not only reduces the minimal amount of entrainer, but also increases the relative volatility of acetone – methanol for the composition in the distillation region where the extractive column operates. The 0.6 atm pressure was selected to enable the use of cheap cooling water in the condenser.

Then we have run an optimization aiming at minimizing the total energy consumption per product unit as objective function OF. OF includes both products and both columns energy demands at boiler and condenser and accounts for the price difference in heating and cooling energy and for the price difference in product sales. Rigorous simulations in closed loop flow sheet were done in all cases. For the sake of comparison and process optimal retrofitting, we have kept the total number of trays as literatures. Other variables have been optimized: entrainer flow rate, reflux ratios, entrainer feed location and main feed location.

Double digit savings in energy consumption and in TAC have been achieved compared to literature values thanks to the optimization scheme helped with thermodynamic insight analysis. Two important issues have emerged. First the reduction of pressure is beneficial to the separation. Second, we have proposed a novel function expressing the efficiency of the extractive section and found it correlated with the best design. We have shown that a high E_{ext} is correlated to a well-designed extractive distillation process. We have noticed that a suitable shift of the feed trays locations improves the efficiency of the separation, even when less entrainer is used and related that to thermodynamic insight gained from the ternary diagram analysis. Comparison with literature design confirms that the total extractive efficiency and the extractive efficiency per tray functions are a relevant criterion to assess the performance of an extractive distillation process design.

In chapter 5, We have optimized the design of a homogeneous extractive distillation process for the separation of the DIPE – IPA minimum boiling azeotrope with heavy entrainer 2-methoxyethanol aiming at further demonstrate our methodology used in chapter 4 in finding the possible way to saving energy cost and total annual cost., we have noticed again that lowering the pressure is beneficial to the process separation by using the thermodynamic insight from the analysis of the ternary residue curve map and isovolatility curves. A lower pressure reduces the usage of entrainer and increases the relative volatility of DIPE – IPA for the same entrainer content in the distillation region where the extractive column operates. A 0.4 atm pressure was selected to enable the use of cheap cooling water in the condenser and for further optimization. The energy consumption OF is used again for optimizing the variables of two distillates, entrainer flow rate,

reflux ratios, entrainer feed location and main feed location, and rigorous simulations in closed loop flow sheet were done in all cases. The TAC was calculated for all cases.

Thanks to the optimization scheme helped with thermodynamic insight analysis, significant savings in energy consumption has been achieved while TAC is also reduced. The decrease of energy cost OF following the increase of distillate has been explained by the relationship of two distillates through mass balance. We have shown that pressure reduction is a possible way to save energy cost and total annual cost based on the thermodynamic insight gained from the ternary diagram analysis. The total extractive efficiency indicator and the extractive efficiency indicator per tray are relevant criterions to assess the performance of an extractive distillation process design.

Chapter 6 focuses on two step optimization strategy demonstrated for acetone-methanol with water (class 1.0-1a) extractive distillation process. The advantage of both methods are taken into account: NSGA method can avoid the local optimal and supply a good initial design for SQP method meanwhile the optimal design can be obtained more quickly.

First, aiming at investigating the influences of the thermodynamic efficiency indicators to find an optimal design, we run the optimization by using multi-objective NSGA method since it is not not needing good initial value and allowing the optimization of both continuous (reflux ratio, entrainer and distillates flowrates) and discrete (column tray number and feed locations) variables. It is coded in Excel by our teammates and we linked it with Aspen plus software through programming in VBA. Four objective functions: extractive efficiency indicator E_{ext} and e_{ext} are maximized meanwhile TAC (economic view) and OF (energy cost per unit product) are minimized while 99.5% products purities in the distillates are set as constraints. Through the analysis of Pareto front, the effects of main variables entrainer-to-feed ratio and reflux ratio on TAC and efficiency indicator are shown. There is a maximum E_{ext} for a given reflux ratio, and there is a minimum R_1 for a given E_{ext}. There exist the optimal efficiency indicator $E_{ext,opt}$ which corresponds the optimal design defined as the one with the lowest TAC and $E_{ext,opt}$ can be used as a criterion for the evaluating of different design for the same system. For acetone-methanol with water system, $E_{ext,opt}$ locates at 0.161±3% at 0.6 atm. Indeed we have to conclude that although the thermodynamic efficiency indicators can't be used as an optimization criterion alone, it is worth combining it with usual criteria such as TAC and OF. Through the analysis of extractive profile map, we explain the reasons that efficiency indicator increase following the decrease of entrainer flow rate and the increase of reflux ratio.

Second, the four steps procedure is used to further improve the design following the decrease of OF with the good initial values from NSGA method, and a competitive design is shown. Based on the combination of extractive profile map and the final design, we prove that NSGA optimization with maximizing E_{ext} is doable even that the optimal design is not the one with maximum E_{ext}.

Chapter 7 solves the problems of double-effect heat integration and heat pump technique in order to save the total cost and increase the environmental performance (CO_2 emissions) of traditional extractive distillation process for the separation of minimum azeotropic mixture acetone-methanol with heavy entrainer water.

In double-effect heat integration, three kinds of double-effect heat integrations are studied. The direct partial heat integration and full heat integration are the most two situations in the open references. We propose a novel optimal partial heat integration process aiming at the most energy saving for extractive distillation. A new objective function OF2 is proposed to carry out the optimization of double-effect heat integration with the four steps procedure. The direct partial and optimal full heat integration are regarded as the extremely conditions where (Qr1-Qc2) in OF2 taking the maximal value or the minimal value zero. The results show that double-effect heat integrations give the massive reduction in TAC, energy cost and CO_2 emissions compared with traditional one. The optimal partial heat integration has the lowest TAC instead of the optimal full heat integration process as intuition as well as a little lower CO_2 emissions.

In heat pump technique, the mechanical heat pump (VRC and BF) is evaluated and both economical and environmental aspects are taken into account in order to further saving TAC and initial capital cost. The outlet pressure of compressors is regarded as the main variable for VRC process while the outlet pressure of throttle valves is used for BF process. Based on the character of extractive distillation process, the partial VRC and partial BF heat pump are proposed, and the process coefficient of performance increase by 60.7% and 40.0% compared with the full VRC and full BF heat pump process. Partial VRC process gives better performance from economical view while full BF process leads better performance in environmental aspect.

In summary, the lowest TAC process is the proposed optimal partial heat integration and the lowest CO_2 emissions process is the full BF process. Partial VRC process gives a trade-off between TAC and CO_2 emissions comparing to full VRC process, and it also significantly reduces the initial investment.

8.2. Perspectives

A future work in the area of the optimization of extractive distillation may treat some of the following topic:

1. The optimization method in this manuscript with acetone-methanol with water as entrainer can be used for the optimization of other mixtures for example ethanol-water since it is also pressure sensitive azeotrope.
2. With two step optimization strategy, other class of azeotropic mixture (0.0-1, 1.0-1b, 1.0-2) can be conducted based on the knowledge of thermodynamic insight. Notice that the maximum azeotropic mixtures with a heavy entrainer class 1.0-2 have done.
3. The two step optimization strategy can also be extended to the pressure-swing distillation or azeotropic distillation with the knowledges of the process feasibility.

4. The dividing wall column for extractive distillation can be optimized using two step optimization strategy. The difficulties lie at the convergence of the circle of interstream in DWC and the circle of entrainer at the same time.

Chapter 9. Appendix

9.Appendix

9.1. Cost data

Correlation model:

Purchased cost = (base cost)(F_c)(Index), Installed cost = (base cost) (Index) (IF + F_c -1)

Where F_C is correction factors for materials, pressure, IF = installation factor, Index = the correction factor for inflation

(A) Heat exchangers

$$\text{purchased cost, \$} = \left(\frac{M\&S}{280}\right)(101.3A^{0.65}F_C)$$

Where A = area ft^2, 200<A<5000, $F_c = (F_d+F_p)F_m$

F_C= correction factor, such as pressure, materials, F_m = materials factor, F_p= pressure factor, F_d= design-type correction factor

M&S = Marshall and Swift inflation index, which is published each month in *chemical engineering*

year	2005	2006	2007	2008	2009	2010	2011
M&S index	1244.5	1302.3	1373.3	1449.3	1468.6	1457.4	1518.1

From journal *chemical engineering* 04/ 2012

$$\text{installed cost, \$} = \left(\frac{M\&S}{280}\right)(101.3A^{0.65})(2.29 + F_C)$$

$= (1518.1/280)\ 101.3\ A^{0.65}\ (2.29+1.35)$

$=1999.2\ A^{0.65}$ unit of A: ft^2

$=9367.8\ A^{0.65}$ unit of A: m^2

For reboiler and condenser, F_d=1.35; material: carbon steel, F_m = 1; pressure: at 1 atm, F_p =0, thus F_C = 1.35

- **Correction Factors for Heat Exchangers**

Design type	F_d	Design pressure/psi	F_p
Kettle, reboiler	1.35	Up to 150	0
Floating head	1.00	300	0.10
U-tube	0.85	400	0.25
Fixed-tube sheet	0.8	800	0.52
		1000	0.55

- **Shell-and-Tube Material = F_m**

Surface area, ft^2,	CS/CS	CS/ BRASS	CS/MO	CS/ SS	SS/ SS	CS/ Monel	Monel/ Monel	CS/T_i	T_i/T_i
1000 to 5000	1.00	1.30	2.15	2.81	3.75	3.10	4.25	8.95	13.05

(B) Column shell

$$\text{purchased cost, \$} = \left(\frac{M\&S}{280}\right)(101.9D^{1.066}H^{0.802})F_C$$

$$\text{installed cost, \$} = \left(\frac{M\&S}{280}\right)(101.9D^{1.066}H^{0.802})(2.18 + F_C)$$

$= (1518.1/280)(101.9D^{1.066}H^{0.802})(2.18+2.25)$

$=2447.5\ D^{1.066}H^{0.802}$ D, H unit: ft

$=22522.8\ D^{1.066}H^{0.802}$ D, H unit: m

Where $F_C=F_mF_p$. In this work, $F_p=1$, $F_m=2.25$, material: stainless steel, so $F_C=2.25$

Pressure Factor= F_p

Pressure/psi	Up to 50	100	200	300	400	500
F_P	1.00	1.05	1.15	1.20	1.35	1.45
	600	700	800	900	1000	
	1.60	1.80	1.90	2.30	2.50	

- **Correction Factors for Pressure Vessels**

Shell material	CS	SS	Monel	Titanium
F_m, clad	1.00	2.25	3.89	4.25
F_m, solid	1.00	3.67	6.34	7.89

(C) **Distillation column trays and tower internals**

$$\text{installed cost, \$} = \left(\frac{M\&S}{280}\right)4.7D^{1.55}HF_C$$

$= (1518.1/280) *4.7D^{1.55}H*2.7$

$=68.8D^{1.55}H$ unit of D, H: ft

$=1423.7\ D^{1.55}H$ unit of D, H: m

Where $F_c=F_s+F_t+F_m$, H = tray stack height, ft (24- in. spacing)

In this work, tray spacing =24 in =0.6096 m, so $F_s=1$, $F_t=0$ (sieve), $F_m=1.7$(SS), $F_C=1+0+1.7=2.7$

- **Correction Factors for Column Trays**

Tray spacing, /in.	24	18	12			
F_S	1.0	1.4	2.2			
Tray type	Grid(no down-comer)	plate	Sieve	Trough or valve	Bubble cap	Koch cascade
F_t	0.0	0.0	0.0	0.4	1.8	3.9
Tray material	CS	SS	Monel			
F_m	0.0	1.7	8.9			

9.2. Nomenclature

A	light original component
ABE	Volatility orders, A is possible distillate
A_c	condenser heat transfer area [m^2]
AD	azeotropic distillation
A_R	reboiler heat transfer area [m^2]
B	heavy original Component
BF	bottom flash (heat pump)
C	the third parameter C of the relationship of Antoine [mmHg ° C]
CAMD	computer aided molecular design
COP	coefficient of performance (heat pump process)
COPc	The critical (upper) theoretical value of COP
COSMO-RS	The conductor-like screening model for realistic salvation
$Cost_{cap}$	capital cost [10^6\$]
$Cost_{cap}$	operating cost [10^6\$]
$Cost_{CA}$	column annual cost [10^6\$]
$Cost_{HA}$	cost of heater for cooling recycling entrainer [10^6\$]
D	distillate flow [kmol / h]
D_1	distillate flow of extractive column
D_2	distillate flow of regeneration column
Diameter	diameter of column
DIPE	diisopropyl ether
DMSO	Dimethyl sulfoxide
DMF	N,N-dimethylformamide
DPHI	direct partial heat integration
DWC	Dividing-wall column
E	entrainer
ED	extractive distillation
E_{ext}	efficiency indicator of extractive section

e_{ext}	efficiency indicator of per tray in extractive section
F	feed flow rate [kmol / h]
F_{AB}	original azeotropic mixtures feed flow rate [kmol / h]
F_E	entrainer feed flow rate [kmol / h]
F_E/F	feed ratio, continuous process
F_E/V	feed ratio, batch process
$(F_E/V)_{min}$	minimum feed ratio, batch process
$(F_E/V)_{max}$	maximum feed ratio, batch process
$Fuel_{factor}$	the fuel factor, reflecting the types of the fuels
GA	genetic algorithm
H^v	vapor enthalpy
h^l	liquid enthalpy
h_{proc}	the enthalpy of steam delivered to the process [kJ/kg]
Height	height of column
HTU	height of transfer units
HIDiC	highly integrated distillation columns
ILs	ionic liquids
I_{cs}	column shell investment cost [10^6\$]
I_{HE}	heat exchanger investment cost [10^6\$]
IPA	isopropyl alcohol
k	product price factor for A vs B,
K_i	distribution coefficient
L	liquid flow rate [mol / h]
L_e	extractive section liquid flow rate
L_s	stripping extractive section liquid flow rate
L_T	boiling liquid at top vessel
M	energy price difference factor for condenser vs reboiler
MHP	mechanical heat pump
MESH	material, equilibrium, summation and enthalpy equation
MINLP	mixed integer non-linear programming
N	number of theoretical stages
N_{Ext}	number of theoretical stages of extractive column
N_{FE}	entrainer feed stages
N_{FF}	original mixture feed stages
N_{FReg}	number of theoretical stages of regeneration column
NSGA	Non-Sorted Genetic Algorithm
NTU	number of transfer units

NHV	the net heating value of a fuel with a carbon content (kJ/kg)
OF	objective function (the energy consumption per product flow rate)
OPC_1	outlet pressure of compressor for extractive column [atm]
OPC_2	outlet pressure of compressor for regeneration column [atm]
OPHI	optimal partial heat integration
OPFI	optimal full heat integration
OPT_1	outlet pressures of throttle for extractive column [atm]
OPT_2	outlet pressures of throttle for regeneration column [atm]
p	pressure [Hgmm] [atm]
PSD	pressure-swing distillation
PV	Pervaporation
Q_{c1}	condenser heat duty of extractive column [MW]
Q_{c1}	condenser heat duty of regeneration column [MW]
Q_{fuel}	the amount of fuel burnt [MW]
Q_{HA}	heat duty of heater for cooling recycling entrainer [MW]
Q_{r1}	reboiler heat duty of extractive column [MW]
Q_{r2}	reboiler heat duty of regeneration column [MW]
R	reflux ratio
R_{max}	maximum reflux ratio
R_{min}	minimum reflux ratio
RBM	rectifying body methond
RCM	residue curve map
RD	reactive distillation
$[SN_{extr}]$	extractivefeasible region
S	reboil ratio
S_1	saddle originating at the “product” vertex
S_2	saddle originating at the “nonproduct” vertex
SN	stable node originating at the azeotrope
SN’	stable node originating outside the composition simplex
SQP	Sequential quadratic programming
Str	stripping section
T	temperature [K]
T_C	top temperature of column [K]
TD	temperature difference [K]
T_{FTB}	the flame temperature [^OC]
T_R	bottom temperature of column [K]
T_0	the ambient temperature [^OC]

T_{stack}	the stack temperature [^{O}C]
TAC	total annual cost
UN	unstable node originating at the entrainer vertex
UN'	unstable node originating outside the composition simplex
V	vapor flows [kmol h-1]
VRC	vapor recompression
W	bottom product flow rate [mol / h]
x_D	distillate fraction
x_i	liquid mole fraction of component i
x_F	original mixture liquid mole fraction
x_E	entrainer liquid mole fraction
x_F+x_E	original mixture and entrainer mass balance point
x_p	intersection point between univolatility curve and residue curve passing through the distillate product
x_W	residue mole fraction
y*	vapor phase composition in equilibrium with x
y_i	vapor mole fraction of component i

Greek letters

α	the molar masses content of carbon in CO_2
α_{ij}	volatility of component i relative to component j
γ_i	activity coefficient of component i
λ_{proc}	the latent heat of steam delivered to the process [kJ/kg]
τ	binary interaction parameter in NRTL model
η	the Carnot efficiency

Subscripts

j	component index
min	minimum value
T	top (decanter) vessel
m	middle section or middle section map
r	rectifying section or rectifying map
s	stripping section or stripping map
Heavy	heavy (least volatile) component
light	light (most volatile) component

Explanation of Figures

●	stable node of the distillation line map
O	unstable node of the distillation line map
Δ	saddle point of the distillation line map

composition profile

continuous feasible line

batch feasible line

simulated rectifying composition profile

simulated extractive composition profile

simulated stripping composition profile

extractive and stripping separatrix

residue curve map separatrix

univolatility line

9.3. References

A

Andersen, H.W., Laroche, L., Morari, M., 1991. Dynamics of homogeneous azeotropic distillation columns. Ind. Eng. Chem. Res. 30, 1846–1855.

Arifin, S., Chien, I.-L., 2008. Design and Control of an Isopropyl Alcohol Dehydration Process via Extractive Distillation Using Dimethyl Sulfoxide as an Entrainer. Ind. Eng. Chem. Res. 47, 790–803.

Arlt, W., 2014. Chapter 7. Extractive distillation, in: Gorak, A., Olujic, Z. (Eds.), Distillation: Equipment and Processes. Elsevier, Oxford, GB, pp. 247–259.

B

Baker, L.C.W., Anderson, T.F., 1957. Some Phase Relationships in the Three-component Liquid System CO2-H2O-C2H5OH at High Pressures. J. Am. Chem. Soc. 79, 2071–2074.

Banat, F.A., Simandl, J., 1999. Membrane distillation for dilute ethanol: Separation from aqueous streams. J. Membr. Sci. 163, 333–348.

Bausa, J., Watzdorf, R. v., Marquardt, W., 1998. Shortcut methods for nonideal multicomponent distillation: I. Simple columns. AIChE J. 44, 2181–2198.

Benali, T., Tondeur, D., Jaubert, J.N., 2012. An improved crude oil atmospheric distillation process for energy integration: Part I: Energy and exergy analyses of the process when a flash is installed in the preheating train. Appl. Therm. Eng. 32, 125–131.

Bernon, C., Doherty, M.F., Malone, M.F., 1990. Patterns of composition change in multicomponent batch distillation. Chem. Eng. Sci. 45, 1207–1221.

Botía, D.C., Riveros, D.C., Ortiz, P., Gil, I.D., Sánchez, O.F., 2010. Vapor−Liquid Equilibrium in Extractive Distillation of the Acetone/Methanol System Using Water as Entrainer and Pressure Reduction. Ind. Eng. Chem. Res. 49, 6176–6183.

Bravo-Bravo, C., Segovia-Hernández, J.G., Gutiérrez-Antonio, C., Durán, A.L., Bonilla-Petriciolet, A., Briones-Ramírez, A., 2010. Extractive Dividing Wall Column: Design and Optimization. Ind. Eng. Chem. Res. 49, 3672–3688.

Brehelin, M., Forner, F., Rouzineau, D., Repke, J.-U., Meyer, X., Meyer, M., Wozny, G., 2007. Production of n-Propyl Acetate by Reactive Distillation: Experimental and Theoretical Study. Chem. Eng. Res. Des. 85, 109–117.

Breure, B., Peters, E.A.J.F., Kerkhof, P.J.A.M., 2008. Separation of azeotropic mixtures of alcohols and water with FricDiff. Sep. Purif. Technol. 62, 349–362.

Brüggemann, S., Marquardt, W., 2004. Shortcut methods for nonideal multicomponent distillation: 3. Extractive distillation columns. AIChE J. 50, 1129–1149.

Bruinsma, O.S.L., Spoelstra, S., 2010. Heat pumps in distillation, in: Presented at the Distillation & Absorption Conference. p. 15.

C

Caballero, J.A., Milán-Yañez, D., Grossmann, I.E., 2005. Rigorous Design of Distillation Columns: Integration of Disjunctive Programming and Process Simulators. Ind. Eng. Chem. Res. 44, 6760–6775.

Chua, K.J., Chou, S.K., Yang, W.M., 2010. Advances in heat pump systems: A review. Appl. Energy 87, 3611–3624.

D

Dejanović, I., Matijašević, L., Olujić, Ž., 2010. Dividing wall column—A breakthrough towards sustainable distilling. Chem. Eng. Process. Process Intensif. 49, 559–580.

Dhanalakshmi, J., Sai, P.S.T., Balakrishnan, A.R., 2014. Effect of bivalent cation inorganic salts on isobaric vapor–liquid equilibrium of methyl acetate–methanol system. Fluid Phase Equilibria 379, 112–119.

Dhanalakshmi, J., Sai, P.S.T., Balakrishnan, A.R., 2013. Study of Ionic Liquids as Entrainers for the Separation of Methyl Acetate–Methanol and Ethyl Acetate–Ethanol Systems Using the COSMO-RS Model. Ind. Eng. Chem. Res. 52, 16396–16405.

Díez, E., Langston, P., Ovejero, G., Romero, M.D., 2009. Economic feasibility of heat pumps in distillation to reduce energy use. Appl. Therm. Eng. 29, 1216–1223.

Doherty, M.F., Knapp, J.P., 1993. Distillation, Azeotropic, and Extractive, in: Kirk-Othmer Encyclopedia of Chemical Technology. John Wiley & Sons, Inc.

Doherty, M.F., Malone, M.F., 2001. Conceptual design of distillation systems. McGraw-Hill Science/Engineering/Math.

Doherty, M.F., Perkins, J.D., 1978. On the dynamics of distillation processes—I: The simple distillation of multicomponent non-reacting, homogeneous liquid mixtures. Chem. Eng. Sci. 33, 281–301.

Douglas, J.M., 1988. Conceptual design of chemical processes. McGraw-Hill New York.

E

Earle, M.J., Esperança, J.M., Gilea, M.A., Lopes, J.N.C., Rebelo, L.P., Magee, J.W., Seddon, K.R., Widegren, J.A., 2006. The distillation and volatility of ionic liquids. Nature 439, 831–834.

Elliott, J.R., Rainwater, J.C., 2000. The Bancroft point and vapor–liquid equilibria in the system benzene + isopropanol. Fluid Phase Equilibria 175, 229–236.

Engelien, H.K., Skogestad, S., 2004. Selecting appropriate control variables for a heat-integrated distillation system with prefractionator. Comput. Chem. Eng., ESCAPE 13 28, 683–691.

F

Fernandez, M.F., Barroso, B., Meyer, X.-M., Meyer, M., Le Lann, M.-V., Le Roux, G.C., Brehelin, M., 2013. Experiments and dynamic modeling of a reactive distillation column for the production of ethyl acetate by considering the heterogeneous catalyst pilot complexities. Chem. Eng. Res. Des. 91, 2309–2322.

Figueirêdo, M.F., Guedes, B.P., de Araújo, J.M.M., Vasconcelos, L.G.S., Brito, R.P., 2011a. Optimal design of extractive distillation columns—A systematic procedure using a process simulator. Chem. Eng. Res. Des. 89, 341–346.

Figueiredo, M.F. de, Brito, K.D., Ramos, W.B., Vasconcelos, L.G.S., Brito, R.P., 2014. Effect of Solvent Content on the Separation and the Energy Consumption of Extractive Distillation Columns. Chem. Eng. Commun. 0, null. doi:10.1080/00986445.2014.900053

Filipe, R.M., Turnberg, S., Hauan, S., Matos, H.A., Novais, A.Q., 2008. Multiobjective Design of Reactive Distillation with Feasible Regions. Ind. Eng. Chem. Res. 47, 7284–7293.

Fonyo, Z., Benkö, N., 1998. Comparison of Various Heat Pump Assisted Distillation Configurations. Chem. Eng. Res. Des., Techno-Economic Analysis 76, 348–360.

Fonyo, Z., Mizsey, P., 1994. Economic application of heat pumps in integrated distillation systems. Heat Recovery Syst. CHP 14, 249–263.

Foucher, E.R., Doherty, M.F., Malone, M.F., 1991. Automatic screening of entrainers for homogeneous azeotropic distillation. Ind. Eng. Chem. Res. 30, 760–772.

Francisco, M., González, A.S.B., Dios, S.L.G. de, Weggemans, W., Kroon, M.C., 2013. Comparison of a low transition temperature mixture (LTTM) formed by lactic acid and choline chloride with choline lactate ionic liquid and the choline chloride salt: physical properties and vapour–liquid equilibria of mixtures containing water and ethanol. RSC Adv. 3, 23553–23561.

Frits, E.R., Lelkes, Z., Fonyó, Z., Rév, E., Markót, M.C., Csendes, T., 2006. Finding limiting flows of batch extractive distillation with interval arithmetic. AIChE J. 52, 3100–3108.

G

Gadalla, M.A., Olujic, Z., Jansens, P.J., Jobson, M., Smith, R., 2005. Reducing CO2 Emissions and Energy Consumption of Heat-Integrated Distillation Systems. Environ. Sci. Technol. 39, 6860–6870.

Gadalla, M., Jobson, M., Smith, R., 2003. Shortcut Models for Retrofit Design of Distillation Columns. Chem. Eng. Res. Des., Particle Technology 81, 971–986.

Gao, X., Chen, J., Tan, J., Wang, Y., Ma, Z., Yang, L., 2015. Application of Mechanical Vapor Recompression Heat Pump to Double-Effect Distillation for Separating N,N-Dimethylacetamide/Water Mixture. Ind. Eng. Chem. Res. 54, 3200–3204.

Gao, X., Li, X., Zhang, J., Sun, J., Li, H., 2013. Influence of a microwave irradiation field on vapor–liquid equilibrium. Chem. Eng. Sci. 90, 213–220.

Gao, X., Ma, Z., Yang, L., Ma, J., 2013. Simulation and Optimization of Distillation Processes for Separating the Methanol–Chlorobenzene Mixture with Separate Heat-Pump Distillation. Ind. Eng. Chem. Res. 52, 11695–11701.

García-Herreros, P., Gómez, J.M., Gil, I.D., Rodríguez, G., 2011. Optimization of the Design and Operation of an Extractive Distillation System for the Production of Fuel Grade Ethanol Using Glycerol as Entrainer. Ind. Eng. Chem. Res. 50, 3977–3985.

Gerbaud, V., Rodriguez-Donis, I., 2014. Chapter 6. Extractive distillation, in: Gorak, A., Olujic, Z. (Eds.), Distillation: Equipment and Processes. Elsevier, Oxford, GB, pp. pp. 201–246.

Gharaie, M., Panjeshahi, M.H., Kim, J.-K., Jobson, M., Smith, R., 2015. Retrofit strategy for the site-wide mitigation of CO2 emissions in the process industries. Chem. Eng. Res. Des. 94, 213–241.

Gil, I.D., Botía, D.C., Ortiz, P., Sánchez, O.F., 2009. Extractive Distillation of Acetone/Methanol Mixture Using Water as Entrainer. Ind. Eng. Chem. Res. 48, 4858–4865.

Gil, I.D., Uyazán, A.M., Aguilar, J.L., Rodríguez, G., Caicedo, L.A., 2008. Separation of ethanol and water by extractive distillation with salt and solvent as entrainer: process simulation. Braz. J. Chem. Eng. 25, 207–215.

Gmehling, J., Bölts, R., 1996. Azeotropic Data for Binary and Ternary Systems at Moderate Pressures. J. Chem. Eng. Data 41, 202–209.

Gmehling, J., Onken, U., 1977. VAPOR-LIQUID EQUILIBRIUM DATA COLLECTION. DECHEMA.

Gomez, A., Pibouleau, L., Azzaro-Pantel, C., Domenech, S., Latgé, C., Haubensack, D., 2010. Multiobjective genetic algorithm strategies for electricity production from generation IV nuclear technology. Energy Convers. Manag. 51, 859–871.

Guo, Z., Chin, J., Lee, J.W., 2004. Feasibility of Continuous Reactive Distillation with Azeotropic Mixtures. Ind. Eng. Chem. Res. 43, 3758–3769.

Guo, Z., Lee, J.W., 2004. Feasible products in batch reactive extractive distillation. AIChE J. 50, 1484–1492.

Gutérrez-Antonio, C., Briones-Ramírez, A., Jiménez-Gutiérrez, A., 2011. Optimization of Petlyuk sequences using a multi objective genetic algorithm with constraints. Comput. Chem. Eng. 35, 236–244.

Gutiérrez-Guerra, R., Segovia-Hernández, J.G., Hernández, S., 2009. Reducing energy consumption and CO2 emissions in extractive distillation. Chem. Eng. Res. Des. 87, 145–152.

H

Harmsen, G.J., 2007. Reactive distillation: The front-runner of industrial process intensification: A full review of commercial applications, research, scale-up, design and operation. Chem. Eng. Process. Process Intensif., Selected Papers from the European Process Intensification Conference (EPIC), Copenhagen, Denmark, September 19-20, 2007 46, 774–780.

Harwardt, A., Marquardt, W., 2012. Heat-integrated distillation columns: Vapor recompression or internal heat integration? AIChE J. 58, 3740–3750.

Hilal, N., Yousef, G., Langston, P., 2002. The reduction of extractive agent in extractive distillation and auto-extractive distillation. Chem. Eng. Process. Process Intensif. 41, 673–679.

Hilmen, E.K., 2000. Separation of azeotropic mixtures: tools for analysis and studies on batch distillation operation. Nor. Univ. Sci. Technol. PhD Thesis.

Hilmen, E., Kiva, V., Skogestad, S., 2002. Topology of ternary VLE diagrams: elementary cells. AIChE J. 48, 752–759.

Hiwale, R.S., Bhate, N.V., Mahajan, Y.S., Mahajani, S.M., 2004. Industrial applications of reactive distillation: recent trends. Int. J. Chem. React. Eng. 2.

J

Jana, A.K., 2010. Heat integrated distillation operation. Appl. Energy 87, 1477–1494. doi:10.1016/j.apenergy.2009.10.014

Jork, C., Kristen, C., Pieraccini, D., Stark, A., Chiappe, C., Beste, Y.A., Arlt, W., 2005. Tailor-made ionic liquids. J. Chem. Thermodyn., Ionic Liquids 37, 537–558.

K

Kamath, G., Georgiev, G., Potoff, J.J., 2005. Molecular Modeling of Phase Behavior and Microstructure of Acetone−Chloroform−Methanol Binary Mixtures. J. Phys. Chem. B 109, 19463–19473.

Keller, T., 2014. Chapter 8. Extractive distillation, in: Gorak, A., Olujic, Z. (Eds.), Distillation: Equipment and Processes. Elsevier, Oxford, GB, pp. 261–294.

Kim, K.J., Diwekar, U.M., Tomazi, K.G., 2004. Entrainer Selection and Solvent Recycling in Complex Batch Distillation. Chem. Eng. Commun. 191, 1606–1633.

Kiss, A.A., Flores Landaeta, S.J., Infante Ferreira, C.A., 2012a. Towards energy efficient distillation technologies – Making the right choice. Energy, Asia-Pacific Forum on Renewable Energy 2011 47, 531–542.

Kiss, A.A., Landaeta, S.J.F., Ferreira, C.A.I., 2012b. Mastering heat pumps selection for energy efficient distillation. Chem. Eng. 29.

Kiss, A.A., Suszwalak, D.J.-. P.C., 2012. Enhanced bioethanol dehydration by extractive and azeotropic distillation in dividing-wall columns. Sep. Purif. Technol. 86, 70–78.

Kiva, V., Hilmen, E., Skogestad, S., 2003. Azeotropic phase equilibrium diagrams: a survey. Chem. Eng. Sci. 58, 1903–1953.

Knapp, J.P., Doherty, M.F., 1994. Minimum entrainer flows for extractive distillation: A bifurcation theoretic approach. AIChE J. 40, 243–268.

Knapp, J.P., Doherty, M.F., 1992. A new pressure-swing-distillation process for separating homogeneous azeotropic mixtures. Ind. Eng. Chem. Res. 31, 346–357.

Knapp, J.P., Doherty, M.F., 1990. Thermal integration of homogeneous azeotropic distillation sequences. AIChE J. 36, 969–984.

Kossack, S., Kraemer, K., Gani, R., Marquardt, W., 2008. A systematic synthesis framework for extractive distillation processes. Chem. Eng. Res. Des., ECCE-6 86, 781–792.

Kossack, S., Kraemer, K., Gani, R., Marquardt, W., 2007. A Systematic Synthesis Framework for Extractive Distillation Processes, in: ECCE-6 Book of Abstracts. pp. 557–558.

Kravanja, P., Modarresi, A., Friedl, A., 2013. Heat integration of biochemical ethanol production from straw – A case study. Appl. Energy, Special Issue on Advances in sustainable biofuel production and use - XIX International Symposium on Alcohol Fuels - ISAF 102, 32–43.

L

Lang, P., 1992. Computation of Multicomponent, Multistage Separation Processes, in: Pallai, I., Fonyo, Z. (Eds.), Studies in Computer-Aided Modelling, Design and Operation: Unit Operations. Elsevier, Budapest, p. pp. 256.

Lang, P., Lelkes, Z., Otterbein, M., Benadda, B., Modla, G., 1999. Feasibility studies for batch extractive distillation with a light entrainer. Comput. Chem. Eng., European Symposium on Computer Aided Process Engineering Proceedings of the European Symposium 23, Supplement, S93–S96.

Langston, P., Hilal, N., Shingfield, S., Webb, S., 2005. Simulation and optimisation of extractive distillation with water as solvent. Chem. Eng. Process. Process Intensif. 44, 345–351.

Laroche, L., Andersen, H.W., Morari, M., Bekiaris, N., 1991. Homogeneous azeotropic distillation: Comparing entrainers. Can. J. Chem. Eng. 69, 1302–1319.

Laroche, L., Bekiaris, N., Andersen, H.W., Morari, M., 1992. The curious behavior of homogeneous azeotropic distillation—implications for entrainer selection. AIChE J. 38, 1309–1328.

Laroche, L., Bekiaris, N., Andersen, H.W., Morari, M., 1992. Homogeneous azeotropic distillation: separability and flowsheet synthesis. Ind. Eng. Chem. Res. 31, 2190–2209.

Leboreiro, J., Acevedo, J., 2004. Processes synthesis and design of distillation sequences using modular simulators: a genetic algorithm framework. Comput. Chem. Eng. 28, 1223–1236.

Lei, Z., Chen, B., Ding, Z., 2005. Special Distillation Processes. Elsevier.

Lei, Z., Li, C., Chen, B., 2003. Extractive Distillation: A Review. Sep. Purif. Rev. 32, 121–213.

Lei, Z., Zhou, R., Duan, Z., 2002. Application of scaled particle theory in extractive distillation with salt. Fluid Phase Equilibria 200, 187–201.

Lelkes, Z., Lang, P., Benadda, B., Moszkowicz, P., 1998a. Feasibility of extractive distillation in a batch rectifier. AIChE J. 44, 810–822.

Lelkes, Z., Lang, P., Moszkowicz, P., Benadda, B., Otterbein, M., 1998b. Batch extractive distillation: the process and the operational policies. Chem. Eng. Sci. 53, 1331–1348.

Levy, S.G., Doherty, M.F., 1986. Design and synthesis of homogeneous azeotropic distillations. 4. Minimum reflux calculations for multiple-feed columns. Ind. Eng. Chem. Fundam. 25, 269–279.

Levy, S.G., Van Dongen, D.B., Doherty, M.F., 1985. Design and synthesis of homogeneous azeotropic distillations. 2. Minimum reflux calculations for nonideal and azeotropic columns. Ind. Eng. Chem. Fundam. 24, 463–474.

Liang, K., Li, W., Luo, H., Xia, M., Xu, C., 2014. Energy-Efficient Extractive Distillation Process by Combining Preconcentration Column and Entrainer Recovery Column. Ind. Eng. Chem. Res. 53, 7121–7131.

Li, G., Bai, P., 2012. New Operation Strategy for Separation of Ethanol–Water by Extractive Distillation. Ind. Eng. Chem. Res. 51, 2723–2729.

Linnhoff, B., Dunford, H., Smith, R., 1983. Heat integration of distillation columns into overall processes. Chem. Eng. Sci. 38, 1175–1188.

Li, W., Shi, L., Yu, B., Xia, M., Luo, J., Shi, H., Xu, C., 2013. New Pressure-Swing Distillation for Separating Pressure-Insensitive Maximum Boiling Azeotrope via Introducing a Heavy Entrainer: Design and Control. Ind. Eng. Chem. Res. 52, 7836–7853.

Lladosa, E., Montón, J.B., Burguet, M[a]c., Muñoz, R., 2007. Effect of pressure and the capability of 2-methoxyethanol as a solvent in the behaviour of a diisopropyl ether–isopropyl alcohol azeotropic mixture. Fluid Phase Equilibria 262, 271–279.

Lladosa, E., Montón, J.B., Burguet, M., de la Torre, J., 2008. Isobaric (vapour + liquid + liquid) equilibrium data for (di-n-propyl ether + n-propyl alcohol + water) and (diisopropyl ether + isopropyl alcohol + water) systems at 100 kPa. J. Chem. Thermodyn. 40, 867–873.

Logsdon, J.E., Loke, R.A., 2000. Isopropyl Alcohol, in: Kirk-Othmer Encyclopedia of Chemical Technology. John Wiley & Sons, Inc.

Lucia, A., Amale, A., Taylor, R., 2008. Distillation pinch points and more. Comput. Chem. Eng. 32, 1342–1364.

Luo, H., Bildea, C.S., Kiss, A.A., 2015. Novel Heat-Pump-Assisted Extractive Distillation for Bioethanol Purification. Ind. Eng. Chem. Res. 54, 2208–2213.

Luo, H., Liang, K., Li, W., Li, Y., Xia, M., Xu, C., 2014. Comparison of Pressure-Swing Distillation and Extractive Distillation Methods for Isopropyl Alcohol/Diisopropyl Ether Separation. Ind. Eng. Chem. Res. 53, 15167–15182.

Luyben, W.L., 2012. Pressure-Swing Distillation for Minimum- and Maximum-Boiling Homogeneous Azeotropes. Ind. Eng. Chem. Res. 51, 10881–10886.

Luyben, W.L., 2008. Comparison of Extractive Distillation and Pressure-Swing Distillation for Acetone−Methanol Separation. Ind. Eng. Chem. Res. 47, 2696–2707.

Luyben, W.L., 2006. Distillation Design and Control Using Aspen Simulation. John Wiley & Sons.

Luyben, W.L., Chien, I.-L., 2010. Design and Control of Distillation Systems for Separating Azeotropes. John Wiley & Sons.

Luyben, W.L., Yu, C.-C., 2009. Reactive Distillation Design and Control. John Wiley & Sons.

M

Mahdi, T., Ahmad, A., Nasef, M.M., Ripin, A., 2015. State-of-the-Art Technologies for Separation of Azeotropic Mixtures. Sep. Purif. Rev. 44, 308–330.

Mahmoud, A., Shuhaimi, M., Abdel Samed, M., 2009. A combined process integration and fuel switching strategy for emissions reduction in chemical process plants. Energy 34, 190–195.

Malone, M.F., Doherty, M.F., 2000. Reactive distillation. Ind. Eng. Chem. Res. 39, 3953–3957.

Marrero, J., Gani, R., 2001. Group-contribution based estimation of pure component properties. Fluid Phase Equilibria, Proceedings of the fourteenth symposium on thermophysical properties 183–184, 183–208.

Marshall & Swift, 2011. Average M & S index for year 2011. Chem. Eng. 119, 84.

Matsuyama H;Nishimura, H., 1977. Topological and thermodynamic classification of ternary vapor-liquid equilibria. J. Chem. Eng. Jpn. 10. doi:10.1252/jcej.10.181

McCabe, W., Smith, J., Harriott, P., 2004. Unit Operations of Chemical Engineering, 7 edition. ed. McGraw-Hill Science/Engineering/Math, Boston.

Modla, G., Lang, P., 2013. Heat pump systems with mechanical compression for batch distillation. Energy 62, 403–417.

Modla, G., Lang, P., 2010. Separation of an Acetone−Methanol Mixture by Pressure-Swing Batch Distillation in a Double-Column System with and without Thermal Integration. Ind. Eng. Chem. Res. 49, 3785–3793.

Modla, G., Lang, P., Denes, F., 2010. Feasibility of separation of ternary mixtures by pressure swing batch distillation. Chem. Eng. Sci. 65, 870–881.

Mo, L., Shao-Tong, J., Li-Jun, P., Zhi, Z., Shui-Zhong, L., 2011. Design and control of reactive distillation for hydrolysis of methyl lactate. Chem. Eng. Res. Des. 89, 2199–2206.

O

Oliveira, F.S., Pereiro, A.B., Rebelo, L.P.N., Marrucho, I.M., 2013. Deep eutectic solvents as extraction media for azeotropic mixtures. Green Chem. 15, 1326–1330.

Olujić, Ž., Jödecke, M., Shilkin, A., Schuch, G., Kaibel, B., 2009. Equipment improvement trends in distillation. Chem. Eng. Process. Process Intensif. 48, 1089–1104.

Onsekizoglu, P., 2012. Membrane Distillation: Principle, Advances, Limitations and Future Prospects in Food Industry. INTECH Open Access Publisher.

Orchillés, A.V., Miguel, P.J., González-Alfaro, V., Vercher, E., Martínez-Andreu, A., 2012. 1-Ethyl-3-methylimidazolium Dicyanamide as a Very Efficient Entrainer for the Extractive Distillation of the Acetone + Methanol System. J. Chem. Eng. Data 57, 394–399.

P

Palacios-Bereche, R., Ensinas, A.V., Modesto, M., Nebra, S.A., 2015. Double-effect distillation and thermal integration applied to the ethanol production process. Energy 82, 512–523.

Pereiro, A.B., Araújo, J.M.M., Esperança, J.M.S.S., Marrucho, I.M., Rebelo, L.P.N., 2012. Ionic liquids in separations of azeotropic systems – A review. J. Chem. Thermodyn., Thermodynamics of Sustainable Processes 46, 2–28.

Petlyuk, F.B., 2004. Distillation Theory and its Application to Optimal Design of Separation Units. Cambridge University Press.

Petlyuk, F., Danilov, R., Burger, J., 2015. A novel method for the search and identification of feasible splits of extractive distillations in ternary mixtures. Chem. Eng. Res. Des.

Phimister, J.R., Seider, W.D., 2000. Semicontinuous, Pressure-Swing Distillation. Ind. Eng. Chem. Res. 39, 122–130.

Pierotti, G.J., 1944. Extractive distillation process. US2455803 A.

Pinto, R.T.P., Wolf-Maciel, M.R., Lintomen, L., 2000. Saline extractive distillation process for ethanol purification. Comput. Chem. Eng. 24, 1689–1694.

Pleşu, V., Bonet Ruiz, A.E., Bonet, J., Llorens, J., 2014. Simple Equation for Suitability of Heat Pump Use in Distillation, in: Computer Aided Chemical Engineering. Elsevier, pp. 1327–1332.

Poling, B.E., Prausnitz, J.M., O'connell, J.P., 2001. The properties of gases and liquids. McGraw-Hill New York.

Pretel, E.J., López, P.A., Bottini, S.B., Brignole, E.A., 1994. Computer-aided molecular design of solvents for separation processes. AIChE J. 40, 1349–1360.

R

Ramírez-Corona, N., Ek, N., Jiménez-Gutiérrez, A., 2015. A method for the design of distillation systems aided by ionic liquids. Chem. Eng. Process. Process Intensif. 87, 1–8.

Renon, H., Prausnitz, J.M., 1968. Local compositions in thermodynamic excess functions for liquid mixtures. AIChE J. 14, 135–144.

Reshetov, S.A., Kravchenko, S.V., 2007. Statistics of liquid-vapor phase equilibrium diagrams for various ternary zeotropic mixtures. Theor. Found. Chem. Eng. 41, 451–453.

Ripin, A., Mudalip, S.K.A., Sukaimi, Z., Yunus, R.M., Manan, Z.A., 2009. Effects of Ultrasonic Waves on Vapor-Liquid Equilibrium of an Azeotropic Mixture. Sep. Sci. Technol. 44, 2707–2719.

Rodriguez-Donis, I., Gerbaud, V., Joulia, X., 2012a. Thermodynamic Insights on the Feasibility of Homogeneous Batch Extractive Distillation. 3. Azeotropic Mixtures with Light Entrainer. Ind. Eng. Chem. Res. 51, 4643–4660.

Rodriguez-Donis, I., Gerbaud, V., Joulia, X., 2012b. Thermodynamic Insights on the Feasibility of Homogeneous Batch Extractive Distillation. 4. Azeotropic Mixtures with Intermediate Boiling Entrainer. Ind. Eng. Chem. Res. 51, 6489–6501.

Rodriguez-Donis, I., Gerbaud, V., Joulia, X., 2009a. Thermodynamic Insights on the Feasibility of Homogeneous Batch Extractive Distillation, 1. Azeotropic Mixtures with a Heavy Entrainer. Ind. Eng. Chem. Res. 48, 3544–3559.

Rodríguez-Donis, I., Gerbaud, V., Joulia, X., 2009b. Thermodynamic Insights on the Feasibility of Homogeneous Batch Extractive Distillation, 2. Low-Relative-Volatility Binary Mixtures with a Heavy Entrainer. Ind. Eng. Chem. Res. 48, 3560–3572.

Rodríguez-Donis, I., Gerbaud, V., Joulia, X., 2001. Entrainer Selection Rules for the Separation of Azeotropic and Close-Boiling-Temperature Mixtures by Homogeneous Batch Distillation Process. Ind. Eng. Chem. Res. 40, 2729–2741.

Rodriguez-Donis, I., Papp, K., Rev, E., Lelkes, Z., Gerbaud, V., Joulia, X., 2007. Column configurations of continuous heterogeneous extractive distillation. AIChE J. 53, 1982–1993.

Rodríguez, N.R., González, A.S.B., Tijssen, P.M.A., Kroon, M.C., 2015. Low transition temperature mixtures (LTTMs) as novel entrainers in extractive distillation. Fluid Phase Equilibria 385, 72–78.

Rodriguez, N.R., Kroon, M.C., 2015. Isopropanol dehydration via extractive distillation using low transition temperature mixtures as entrainers. J. Chem. Thermodyn. 85, 216–221.

S

Seader, J.D., Henley, E.J., Roper, D.K., 2010. Separation Process Principles: Chemical and Biochemical Operations, 3 edition. ed. Wiley, Hoboken, NJ.

Seiler, M., Jork, C., Kavarnou, A., Arlt, W., Hirsch, R., 2004. Separation of azeotropic mixtures using hyperbranched polymers or ionic liquids. AIChE J. 50, 2439–2454.

Seiler, M., Köhler, D., Arlt, W., 2003. Hyperbranched polymers: new selective solvents for extractive distillation and solvent extraction. Sep. Purif. Technol. 30, 179–197.

Selvi, A., Breure, B., Gross, J., de Graauw, J., Jansens, P.J., 2007. Basic parameter study for the separation of a isopropanol–water mixture by using FricDiff technology. Chem. Eng. Process. Process Intensif., Selected Papers from the European Process Intensification Conference (EPIC), Copenhagen, Denmark, September 19-20, 2007 46, 810–817.

Shen, W., 2012. Extension of thermodynamic insights on batch extractive distillation to continuous operation [WWW Document]. URL http://ethesis.inp-toulouse.fr/archive/00002137/ (accessed 4.13.15).

Shen, W., Benyounes, H., Gerbaud, V., 2013. Extension of Thermodynamic Insights on Batch Extractive Distillation to Continuous Operation. 1. Azeotropic Mixtures with a Heavy Entrainer. Ind. Eng. Chem. Res. 52, 4606–4622.

Shen, W., Gerbaud, V., 2013. Extension of Thermodynamic Insights on Batch Extractive Distillation to Continuous Operation. 2. Azeotropic Mixtures with a Light Entrainer. Ind. Eng. Chem. Res. 52, 4623–4637.

Smith, R., Delaby, O., 1991. Targeting flue gas emissions. Chem. Eng. Res. Des. 69, 492–505.

Stéger, C., Varga, V., Horváth, L., Rév, E., Fonyó, Z., Meyer, M., Lelkes, Z., 2005. Feasibility of extractive distillation process variants in batch rectifier column. Chem. Eng. Process. Process Intensif. 44, 1237–1256.

T

Teh, Y.S., Rangaiah, G.P., 2003. Tabu search for global optimization of continuous functions with application to phase equilibrium calculations. Comput. Chem. Eng. 27, 1665–1679.

V

Van de Bor, D.M., Ferreira, C.A.I., 2013. Quick selection of industrial heat pump types including the impact of thermodynamic losses. Energy 53, 312–322.

Van Dongen, D.B., Doherty, M.F., 1985. Design and synthesis of homogeneous azeotropic distillations. 1. Problem formulation for a single column. Ind. Eng. Chem. Fundam. 24, 454–463.

Van Duc Long, N., Lee, M., 2013. Optimal retrofit design of extractive distillation to energy efficient thermally coupled distillation scheme. AIChE J. 59, 1175–1182.

Van Dyk, B., Nieuwoudt, I., 2000. Design of Solvents for Extractive Distillation. Ind. Eng. Chem. Res. 39, 1423–1429.

Vázquez-Ojeda, M., Segovia-Hernández, J.G., Hernández, S., Hernández-Aguirre, A., Kiss, A.A., 2013. Design and optimization of an ethanol dehydration process using stochastic methods. Sep. Purif. Technol. 105, 90–97.

W

Waheed, M.A., Oni, A.O., Adejuyigbe, S.B., Adewumi, B.A., Fadare, D.A., 2014. Performance enhancement of vapor recompression heat pump. Appl. Energy 114, 69–79.

Wang, Q., Yu, B., Xu, C., 2012. Design and Control of Distillation System for Methylal/Methanol Separation. Part 1: Extractive Distillation Using DMF as an Entrainer. Ind. Eng. Chem. Res. 51, 1281–1292.

Wang, S.-J., Wong, D.S.H., Yu, S.-W., 2008. Effect of Entrainer Loss on Plant-Wide Design and Control of an Isopropanol Dehydration Process. Ind. Eng. Chem. Res. 47, 6672–6684.

Wang, Y.-C., Teng, M.-Y., Lee, K.-R., Lai, J.-Y., 2005. Comparison between the pervaporation and vapor permeation performances of polycarbonate membranes. Eur. Polym. J. 41, 1667–1673.

Weis, D.C., Visco, D.P., 2010. Computer-aided molecular design using the Signature molecular descriptor: Application to solvent selection. Comput. Chem. Eng., Process Modeling and Control in Drug Development and Manufacturing 34, 1018–1029.

Widagdo, S., Seider, W.D., 1996. Journal review Azeotropic distillation. AIChE J. 42, 96–130.

Y

Yang, X., Song, H., 2006. Computer Aided Molecular Design of Solvents for Separation Processes. Chem. Eng. Technol. 29, 33–43.

Ye, K., Freund, H., Sundmacher, K., 2013. A New Process for Azeotropic Mixture Separation by Phase Behavior Tuning Using Pressurized Carbon Dioxide. Ind. Eng. Chem. Res. 52, 15154–15164.

You, X., Rodriguez-Donis, I., Gerbaud, V., 2015. Improved Design and Efficiency of the Extractive Distillation Process for Acetone–Methanol with Water. Ind. Eng. Chem. Res. 54, 491–501.

You, X., Rodriguez-Donis, I., Gerbaud, V., 2014. Extractive Distillation Process Optimisation of the 1.0-1a Class System, Acetone - methanol with Water, in: Computer Aided Chemical Engineering. Elsevier, pp. 1315–1320.

RÉSUMÉ

La distillation extractive continue avec ajout d'un entraineur lourd est nécessaire pour régénérer les solvants dans des mélanges azéotropiques à température de bulle minimale. L'optimisation multiobjectif du procédé conduit à minimiser la demande énergétique et le coût et à maximiser l'efficacité de séparation E_{ext} qui décrit la capacité à séparer le produit entre le haut et le bas de la section extractive.

Nous optimisons le débit d'entraineur F_E, les positions des alimentations, les taux de reflux R_1, R_2 et les débits de distillat de chaque colonne. L'analyse thermodynamique montre que réduire la pression dans la colonne extractive favorise la séparation et diminue F_E, R_1 et l'énergie nécessaire. Le procédé optimisé est 20% moins cher et énergivore.

Les valeurs minimale et maximale de E_{ext} et R_1 sont interprétées avec la thermodynamique. L'intégration énergétique partielle PHI réduit encore le coût mais c'est la recompression totale des vapeurs qui est la moins énergivore.

Mots clés : Distillation extractive – analyse thermodynamique – pression réduite – intégration énergétique – optimisation multiobjectif – indicateur thermodynamique d'efficacité de séparation.

ABSTRACT

Extractive distillation process with addition of a heavy entrainer is required to regenerate solvent mixtures with minimum boiling azeotropes. We run a multiobjective optimization aiming at minimizing the energy demand and total annualized cost and maximizing an extractive thermodynamic efficiency indicator E_{ext} describing the ability to discriminate the product between the extractive section top and bottom.

The entrainer flowrate F_E, feed locations, reflux ratios R_1, R_2 both distillates and both column tray numbers are optimized. Thermodynamics insight shows that a lower operating pressure increases the relative volatility and reduces F_E, R_1 and the energy consumption for 1.0-1a class separations. Double digit savings in cost and energy are achieved while there is an optimal E_{ext}.

Minimum and maximum E_{ext} and R_1 are discussed with respect to thermodynamics. The partial heat integration process is the cheapest but full vapor recompression achieves the lowest energy demand.

Keywords: Extractive distillation – thermodynamic insight – reduced pressure – energy integration – multiobjective optimization – thermodynamic separation efficiency